



Cerro Chivo



Laguna Azul



Laguna Potrok Aike

3IMC - ARGENTINA



Badacsony



Tihany



Filakovo

2IMC - HUNGARY - SLOVAKIA - GERMANY



Abstract Volume

of the

Fourth International Maar Conference

A Multidisciplinary Congress on Monogenetic Volcanism

Edited by
Kate Arentsen, Károly Németh, Elaine Smid



Pulvermaar



Dauner Maare



Eichholzmaar

1IMC - GERMANY

Auckland, New Zealand
20-24 February 2012





Fourth International Maar Conference
a multidisciplinary congress on monogenetic volcanism

Auckland, New Zealand

20 – 24 February 2012

ABSTRACTS VOLUME

Edited by

Kate Arentsen, Károly Németh, Elaine Smid

Geoscience Society of New Zealand Miscellaneous Publication 131A

ISBN 978-1-877480-15-7

ISSN Online 2230-4495

ISSN Print 2230-4487

Previous IMCs

International Maar Conference
Daun, Germany, 2000

Second International Maar Conference
Lajosmizse, Hungary, 2004

Third International Maar Conference
Malargüe, Argentina, 2009

Conference Supporters

International Association of Volcanology and Chemistry of the Earth's Interior

International Association of Sedimentologists

Geoscience Society of New Zealand

The University of Auckland

Massey University

Institute of Earth Science and Engineering

Earthquake Commission

Elsevier

Springer

Villa Maria Estate

Epic Beer



Organizing Committee

Károly Németh and Ian EM Smith (Co-Chairs)

Members: Kate Arentsen, Shane Cronin, Jan Lindsay, Janet Simes, Elaine Smid

Scientific Advisory Group

Georg Buechel, Kathy Cashman, Shane Cronin, Gonca Gençalioğlu Kuşcu,
Guido Giordano, Stephan Kurszlaukis, Jan Lindsay, Volker Lorenz,
Joan Marti, Károly Németh, Corina Risso, Hetu Sheth, Claus Siebe, Ian EM Smith,
Young Kwan Sohn, Greg Valentine, James White,
Bernd Zimanowski, Bernd Zolitschka

Preface

We extend our warmest welcome to delegates of the Fourth International Maar Conference (4IMC) and look forward to hosting you in Auckland, New Zealand. We anticipate an exciting week of scientific exchanges, renewing friendships and making new friends.

The original idea of organizing a scientific workshop-type meeting focusing on the great variety of geological processes shown in maar volcanoes arose in the type locality of maar volcanism: the Vulkaneifel Mountains of western Germany. Professors Volker Lorenz and Georg Buechel conceived of a meeting that concentrated on the formation of maar volcanoes in which experts could share their views of the origin of this type of volcanism in their type locality. Daun in western Germany hosted the first International Maar Conference (1IMC) in the year 2000, providing a snapshot of the wealth of knowledge underpinning our understanding of maar volcanoes. 1IMC also highlighted the overarching aspects of volcanism, sedimentation, economic significance and geomorphic problems that maar volcanoes offer anyone who wishes to study them. The location of 1IMC naturally determined that the main focus of the conference was young, intact maar volcanoes, their sedimentary environments, ecological sites and hazard aspects.

Four years later the concept of a maar conference was taken to a new level, garnering support from IAVCEI and IAS to produce the second International Maar Conference (2IMC). 2IMC was hosted in Hungary and organized by a tri-nation committee (Hungary – Slovakia – Germany), arranging strongly linked scientific events in each of these three countries. 2IMC was held in the “puszta” (flat lowland) in the small town of Lajosmizse from where field trips went to the western Pannonian Basin and to southern Slovakia to study deeply eroded maar volcanoes. This setting dictated that the main subject of 2IMC had a strong focus on diatremes, the root zones of maar volcanoes.

In 2009, for the third International Maar Conference (3IMC), the venue shifted to the Southern Hemisphere. Argentina hosted 3IMC in Malargue, a small desert town in the eastern foothills of the Andes. The location of 3IMC also determined the main focus of the meeting. Malargue is located at the edge of a major monogenetic volcanic field containing over 800 Pliocene to Recent volcanoes. Among this large number of monogenetic volcanoes only a few have been recognized as having a phreatomagmatic eruption history, highlighting the important message that such volcanoes may carry for paleoenvironmental reconstruction as well as for the elevated hazard such eruptions may pose in an otherwise “dry” explosive eruptive centre-dominated field. 3IMC clearly demonstrated the development and global progress of research into small scale magmatic systems commonly referred to monogenetic volcanic fields.

Maar volcanoes are recognized as the “wet” equivalents of scoria cones and their eruption history, length, and erupted magma volume show great similarity; maars are strongly

influenced by external, while scoria cones by internal, controlling parameters. Shortly after 3IMC a small commemorative workshop was held to celebrate the birth of Jorullo scoria cone in Mexico (Jorullo 250) in 2009 and marked a merging of research groups and research efforts to address the broader aspects of monogenetic volcanism. This led to the establishment of the IAVCEI Commission on Monogenetic Volcanism (https://vhub.org/groups/iavcei_cmv) that supported the Special Issue of Journal of Volcanology and Geothermal Research that published results from the 3IMC and Jorullo 250 conferences [From Maars to Scoria Cones: the Enigma of Monogenetic Volcanic Fields - JVGR 2011 vol. 201(1-4): 1-412.].

The Fourth International Maar Conference (4IMC) is the first in the IMC series in which the main scope of the conference has been specifically expanded to provide a forum to present research results on all aspects of monogenetic (small-volume) volcanism. The study of small volume magmatic systems has received increasing attention in recent times with the realization that, although their surficial expression is as very small volcanoes, they display a remarkable diversity of geochemical and volcanological features that provides a remarkable insight into the processes of magma generation, differentiation, transport and eruption. Naturally maar volcanoes are a central part of this research and 4IMC continues the tradition established by Volker Lorenz and Georg Buechel.

4IMC is hosted by The University of Auckland and supported by Massey University of Palmerston North. Auckland is the largest city of New Zealand with a population of about 1.5 million, living on an active monogenetic volcanic field of at least 54 individual volcanoes that have erupted during the last 250 ka. Each of these volcanoes had at least a brief phreatomagmatic phase in their initial eruptions, while about 34 volcanoes clearly have well developed tuff rings and shallow maars, putting Auckland among regions facing potentially significant volcanic hazard in the future. 4IMC will surely provide a new view of monogenetic volcanic fields to the participants and will help to bring the sometimes life-and-death questions resulting from our research into the real world. Our basic research is the fundamental platform for decision makers and planners responsible for the well-being and safety of a third of New Zealand's population.

4IMC is a scientific event supported directly by IAVCEI and IAS. The scientific program and quality is assured by the sponsorship and backing of 4IMC by the IAVCEI Commission on Monogenetic Volcanism and Commission on Volcanogenic Sediments. We hope you will find 4IMC a memorable event and the Abstract Volume a useful collection.

Welcome to Auckland, a City of Volcanoes.

Conference Chairs

Ian EM Smith, Auckland, New Zealand

Károly Németh, Palmerston North, New Zealand

Contents

*Abstracts are listed in alphabetical order of first author. The presenting author is underlined in the Contents and bolded in the abstract. * denotes an invited Keynote Lecture.*

Oral Presentations

<u>Agustin-Flores, J., K. Németh, S. Cronin, J. Lindsay, G. Kereszturi</u> : Insights into the controls on the formation of contrasting tuff rings vs. cones in the Auckland Volcanic Field, New Zealand	1
<u>Andrews, R., J.D.L. White, M. Rosenberg</u> : Making craters: a review and approach to thermodynamic analysis of the 1886 Rotomahana eruption	3
<u>Bebbington, M., S. Cronin</u> : Paleomagnetic and geological updates to an event-order model for the Auckland Volcanic Field	5
<u>Bishop, M.A.</u> : Volcanic Shield Fields, Newer Volcanic Province, Australia	*7
<u>Blaikie, T., L. Ailleres, P. Betts, R. Cas</u> : A geophysical comparison of simple and complex maar volcanoes from the Cainozoic Newer Volcanics Province, Southeastern Australia	9
<u>Bosshard, S.A., H.B. Mattsson, J.F. Berghuijs</u> : Origin of fluidal pyroclast morphologies in melilititic monogenetic cones: Insights from the recent explosive eruption of Oldoinyo Lengai, Tanzania	11
<u>Boyce, J., I. Nicholls, R. Keays, P. Hayman</u> : The multiple magma batches of Mt. Rouse, Newer Volcanics Province, Victoria, Australia	13
<u>Brenna, M., S. Cronin, I.E.M. Smith, Y-K. Sohn</u> : A genetic model for basaltic volcanic fields, Jeju Island, Korea	15
<u>Briggs, R., A. Pittari, M. Rosenberg</u> : The influence of subsurface hydrogeology on the nature and localisation of volcanism in the South Auckland Volcanic Field	17
<u>Caffe, P.J., G. Maro, J.F. Presta, P.I. Flores, Y. Peralta</u> : Neogene monogenetic volcanoes from the northern Puna of Argentina, Central Andean plateau	19
<u>Carrasco-Núñez, G., M.H. Ort</u> : Rhyolitic and basaltic maar volcanoes, a perspective from Mexican volcanism	*21
<u>Cas, R., J. van Otterloo, S.C. Jordan, J. Boyce, T. Blaikie, G. Prata, D. Uehara, J. van den Hove</u> : Influences on the location of the basaltic, continental Newer Volcanics Province, southeastern Australia, its diverse monogenetic volcanoes, and the highly variable eruption styles	23
<u>Chu, G., Q. Sun, X. Wang, M. Liu, Y. Lin, M. Xie, W. Shang, J. Liu</u> : Seasonal temperature variability during the past 1600 years recorded in the varved sediment from maar lake Sihailongwan and profiles from northeastern China	25
<u>Cronin, S., Y-K. Sohn, I.E.M. Smith, K. Németh, M. Brenna, M. Bebbington, G. Kereszturi, J. Agustin Flores, L. McGee, C-W. Kwon, J. Lindsay, G. Jolly</u> : Insights into monogenetic volcanism from paired studies of two contrasting Quaternary continental volcanic fields – Auckland (New Zealand) and Jeju (Republic of Korea)	27
<u>Espinasa-Pereña, R., M.P. Jácome Paz, H. Delgado Granados</u> : A study of the diffuse emissions of CO ₂ in the Michoacan-Guanajuato monogenetic volcanic field (Mexico)	28

<u>Fox, B., M. Haworth, G. Wilson, D. Lee, J-A. Wartho, J. Bannister, D. Jones, U. Kaulfuss, J. Lindqvist:</u> Greenhouse gases and deglaciation at the Oligocene/Miocene boundary: palaeoclimate evidence from a New Zealand maar lake	29
<u>Gençaliöglu Kuşcu, G., K. Németh, R.B. Stewart:</u> Morphological and chemical diversity of maars in Central Anatolian Volcanic Province (Turkey)	31
<u>Gruber, G.:</u> The Messel Maar, Germany – Correlation of fossil contents on the basis of marker horizons	33
<u>Haller, M.J., F.E. Nullo, C. Risso:</u> Phreatomagmatism related to trachyte dome explosions	35
<u>Harangi, S.:</u> Petrogenesis of the Late Miocene-Quaternary alkaline basalts in the Pannonian Basin, eastern-central Europe	37
<u>Jordan, S.C., R. Cas:</u> Vesicle texture analysis of juvenile pyroclasts from the Pleistocene Lake Purrumbete Maar, Newer Volcanics Province, southern Australia	39
<u>Kämpf, H., K. Bräuer, T. Nickschick, I. Schüller, A. Schmidt, C. Flechsig, T. Jahr:</u> Earthquake swarms, a sign of active magmatic processes in the Regensburg – Leipzig – Rostock zone, Central Europe?	41
<u>Kaulfuss, U., J. Lindqvist, D. Jones, B. Fox, G. Wilson, D. Lee:</u> Post-eruptive maar crater sedimentation inferred from outcrop, drill cores and geophysics – Foulden Maar, Early Miocene, Waipiata Volcanic Field, New Zealand	43
<u>Kenedi, C.L., J. Lindsay, C.L. Ashenden, S. Sherburn:</u> Challenges of monitoring a potentially active volcanic field in a large urban area: Auckland Volcanic Field, New Zealand	45
<u>Kereszturi, G., K. Németh, M. Bebbington, S. Cronin, J. Agustín-Flores, J. Procter, J. Lindsay:</u> Magma-output rates of the Auckland Volcanic Field (New Zealand)	47
<u>Kshirsagar, P.V., H.C. Sheth, B. Shaikh:</u> Mafic alkalic magmatism in central Kachchh, India: a monogenetic volcanic field in the northwestern Deccan Traps	49
<u>Le Corvec, N., M. Bebbington, B.W. Hayward, J. Lindsay, J.V. Rowland:</u> The Auckland Volcanic Field – a basaltic field showing random behaviour?	51
<u>Lefebvre, N., J.D.L. White, B. Kjarsgaard, P-S. Ross:</u> Macro- and micro-characterization of multiple lower diatreme conduit remnants: Implications for maar-diatreme formation	54
<u>Lindsay, J., G. Jolly:</u> Determining volcanic risk in the Auckland Volcanic Field: a multidisciplinary approach	56
<u>Lorenz, V., P. Suhr:</u> On differences and similarities between maar-diatreme volcanoes and explosive collapse calderas	*58
<u>Lutz, H., T. Engel, F. Häfner, J. Haneke, V. Lorenz:</u> The Kisselwörth Diatreme and the Nierstein - Astheim Volcanic System. Phreatomagmatic Paleocene / Eocene volcanism on the western main fault of the Upper Rhine Graben (Germany)	60
<u>Lutz, H., V. Lorenz:</u> Early volcanological research in the Vulkaneifel, Germany. The years 1774 – 1865	62
<u>May, M.D., J.D.L. White:</u> 126 years of changing maar morphology at Rotomahana, North Island, New Zealand	64
<u>McGee, L.E., I.E.M. Smith, M-A. Millet, C. Beier, J. Lindsay, H. Handley:</u> Fine scale mantle heterogeneity revealed in monogenetic eruptions in the Auckland Volcanic Field	66

<u>Németh, K., M. Brenna, S. Cronin, Y-K. Sohn, I.E.M. Smith:</u> A nested polymagmatic and polycyclic tuff ring and scoria cone complex at Chaguido (Jeju Island), South Korea	68
<u>Pittari, A., R. Briggs, T. Ilanko, A. Gibson, M. Rosenberg, K. Németh:</u> Variation in deposit characteristics and eruption processes across the lifetime of a monogenetic field, the South Auckland volcanic field	70
<u>Sheth, H.C.:</u> Evolution of the polygenetic cinder cone of Barren Island, an explosive-effusive mafic arc volcano in the Andaman Sea (NE Indian Ocean)	72
<u>Siebe, C., M-N. Guilbaud, S. Salinas, C. Chédeville-Monzo:</u> Eruption of Alberca de los Espinos tuff cone causes transgression of Zacapu lake ca. 25,000 yr BP in Michoacán, México	*74
<u>Smid, E.R., A. Mazot, G. Jolly, J. Lindsay:</u> Soil Gas CO ₂ Fluxes and Concentrations in the Auckland Volcanic Field, New Zealand: A Pilot Study	76
<u>Smith, I.E.M.:</u> Mantle Flow and the Origin of Tiny Igneous Provinces: an Example from the Late Cenozoic of Northern New Zealand	78
<u>Son, M., J.S. Kim, S. Jung, J.S. Ki, M-C. Kim, Y-K. Sohn:</u> Sedimentary and volcanotectonic evolution of a basaltic diatreme in a nonmarine backarc-margin basin (the Miocene Janggi Basin, SE Korea)	82
<u>Stewart, R.B., K. Németh:</u> Evidence for sporadic Eocene to Pliocene effusive and explosive subaqueous volcanism in northern Chatham Island, SW-Pacific	84
<u>Suhr, P., V. Lorenz, K. Goth:</u> Maar-Diatreme Volcanism and its post-eruptive Subsidence	86
<u>Sulpizio, R., D. Sarocchi, R. Bartali, L.Á. Rodriguez-Sedano:</u> Insights on behaviour of granular flows from field analysis and laboratory experiments	*88
<u>Tămaş, C.G., A. Minuţ:</u> Cetate Breccia, Roşia Montana, Romania – a Dacite Related Au-Ag Mineralized Maar-Diatreme Structure	89
<u>van Otterloo, J., R. Cas:</u> Understanding the dynamics of complex magma-water interaction of a system with alternating magmatic and phreatomagmatic eruption styles, Mt. Gambier, Australia	91
<u>Wallace, P., D. Ruscitto, S. Weaver, E. Johnson, R. Weber, D. Johnston, K. Cashman:</u> Cinder cone fields associated with warm-slab subduction zones: Magma generation and shallow volcanic processes in the Cascades and Central Mexico as revealed by melt inclusions and experimental phase equilibria	*93
<u>Weinstein, Y., R. Weinberger, A. Calvert:</u> The impact of drainage basin dynamics on volcanic activity style: a detailed Ar-Ar dating of a dry-wet transition	95
<u>White, J.D.L.:</u> Fragments within fragments: are composite pyroclasts hints of weakness or sustained violence?	96
<u>Wu, J., Q. Liu, L. Wang, G. Chu:</u> Pollen analysis of a Late Glacial and Holocene sediment core from Moon Lake, Northeast China	98
<u>Zawalna-Geer, A., P. Shane, S. Davies, P. Augustinus:</u> History of ash fall events trapped in maar lake sediments	100
<u>Zhang, Y.:</u> Eruptibility of Gas-driven Eruptions	102

Zolitschka, B., A.C. Gebhardt, C. Ohlendorf, J-P. Buylaert, P. Kliem, C. Mayr, S. Wastegård, PASADO Science Team: Sedimentological responses to hydrological variability for the last 50 ka as recorded in the maar lake Laguna Potrok Aike (Pali Aike Volcanic Field, Argentina) *104

Poster Presentations

Berghuijs, J.F., H.B. Mattsson, S.A. Bosshard: Eruptive and depositional characteristics of the Loolmurwak and Eledoi maar volcanoes, Lake Natron – Engaruka monogenetic volcanic field, northern Tanzania 106

Cronin, S., K. Németh, M. Bebbington, I.E.M. Smith, J. Lindsay, G. Jolly: Developing probabilistic eruption scenarios for distributed volcanism in the Auckland Volcanic Field, New Zealand 108

Gebhardt, A.C., C. Ohlendorf, F. Niessen, M. De Batist, F.S. Anselmetti, D. Ariztegui, P. Kliem, S. Wastegård, B. Zolitschka: Up to 200 m lake-level change since MIS4 recorded in maar lake Laguna Potrok Aike, Southern Patagonia 110

Harangi, S., R. Lukács: Volcano park, geoparks and outreach activities on volcanoes in Hungary 112

Kaufuss, U., D. Lee, J. Bannister, J. Conran, J. Lindqvist, D. Mildenhall, E. Kennedy: Fossil microorganisms, plants and animals from the Early Miocene Foulden Maar, Otago, New Zealand 113

Kereszturi, G., K. Németh, S. Cronin, M. Bebbington: Spatial distribution of monogenetic volcanoes on volcanic islands 115

Kereszturi, G., J. Procter, K. Németh, M. Bebbington, S. Cronin, J. Lindsay: Lava flows and related hazards at the Auckland Volcanic Field (New Zealand) 117

Kim, G.B., Y-K. Sohn: Holocene explosive eruptions of Ulleung Island, a potentially active volcano and a source of marine tephra in the East Sea 119

Kósik, S., T. Nagy, M. Kaproncai, D. Karátson, K. Németh: Geomorphology and paleogeography of lava-capped buttes in Tapolca Basin (Hungary) as reflected by 3D elevation models 121

Lara, L.E.: Tuff cones and maars along the Liquiñe-Ofqui Fault Zone (Southern Andes, Chile): tectonic control of magma-water interactions? 123

Lexa, J., K. Pošteková: Eruptive styles of rhyolite volcanoes in the sedimentary basin setting: the case of the Jastrabá Formation in Central Slovakia 124

Lutz, H., U. Kaufuss, T. Wappler, W. Löhnertz, V. Wilde, D.F. Mertz, J. Mingram, J.L. Franzen, H. Frankenhäuser, M. Koziol: Eckfeld Maar: Window into an Eocene Terrestrial Habitat in Central Europe 126

Mattsson, H.B., S.A. Bosshard, J.F. Berghuijs: Rapid magma ascent and short eruption durations in the Lake Natron - Engaruka monogenetic volcanic field (northern Tanzania): Evidence from the Pello Hill scoria cone 128

Németh, K., J. Lexa, V. Konečný, Z. Pécskay, G. Kereszturi: On the variety of root zones of monogenetic volcanoes 130

Nickschick, T., H. Kämpf, T. Jahr: The Triasscholle near Greiz, E Thuringia - a volcanic based origin? 132

<u>Pardo, N., J.L. Macías, D.R. Avellán, T. Scolamacchia, G. Giordano, P. Cianfarra, F. Bellatreccia</u> : The ~1245 yr BP Asososca maar eruption: the youngest phreatomagmatic event on the western outskirts of Managua, Nicaragua	134
<u>Prata, G., R. Cas, P. Hayman</u> : Cyclicity in fluctuating phreatomagmatic and magmatic eruptive styles at the 35 ka Tower Hill Volcanic Complex, southeast Australia	136
<u>Schmidt, A., N. Nowaczyk, H. Kämpf, I. Schüller, C. Flechsig, T. Jahr</u> : Possible causes for the magnetic anomalies in the volcanoclastic units of the Ebersbrunn diatreme (W Saxony, Germany)	137
<u>Schüller, I., H. Kämpf, A. Schmidt, C. Flechsig, T. Jahr</u> : Petrographic and thermochronometric investigation of the diatreme breccia of the Ebersbrunn Diatreme – W Saxony, Germany	139
<u>van den Hove, J., R. Cas, L. Ailleres</u> : Geophysical and volcanological investigation into subsurface morphologies of maar and nested maar-scoria cone diatremes of the Newer Volcanics Province, Southeastern Australia	141
<u>van Otterloo, J., R. Cas, M. Raveggi</u> : Unraveling the eruption dynamics of the complex volcanology at the 5 ka Mt. Gambier Volcanic Complex, south-eastern Australia	143

The bibliographic reference for the abstracts is:

Author, A.N., 2012. Title of abstract. In: Arentsen, K., Németh, K., Smid, E. (Eds): Abstract Volume of the Fourth International Maar Conference: A Multidisciplinary Congress on Monogenetic Volcanism. Auckland, New Zealand 20-24 February 2012. Geoscience Society of New Zealand Miscellaneous Publication 131A: p. x.

ISBN 978-1-877480-15-7



The content of the abstracts is the responsibility of the authors. The Organizing Committee accept no responsibility for errors or omissions.

Insights into the controls on the formation of contrasting tuff rings vs. cones in the Auckland Volcanic Field, New Zealand

Javier Agustin-Flores¹, Károly Németh¹, Shane Cronin¹, Jan Lindsay², and Gábor Kereszturi¹

¹ Volcanic Risk Solutions, Massey University, Palmerston North, New Zealand – j.agustinflores@massey.ac.nz

² School of Environment, The University of Auckland, Private Bag 92019, Auckland, New Zealand

Keywords: hydromagmatic, water-magma ratio, accidental fragments.

The mixing ratio of magma to water has been proposed by some authors as the main factor that contributes to the explosive eruptive style that leads to the formation of hydromagmatic volcanoes such as maars, tuff rings, and tuff cones (e.g. Sheridan and Wohletz, 1983; Wohletz, 1986; Kokelaar, 1986). However, more recent studies suggest that this assumption oversimplifies the role played by other factors on the processes that create these distinct volcanoes when magma interacts explosively with water (White, 1996). Thus, two different landforms, namely a tuff ring and a tuff cone, could be created by eruptions related to explosive water-magma interactions at similar magma/water ratios. Other factors, such as lithological and hydrogeological characteristics of aquifers, groundwater/surface water characteristics, confinement pressure, magma properties, country rock physical properties, should be taken into account in order to understand the manifestations of phreatomagmatic eruptions and the landforms that result.

A paired qualitative and quantitative approach to better constrain the role of these parameters, can be accomplished by studying the stratigraphy and sedimentology of hydromagmatic deposits, as well as the physical and chemical nature of their components (e.g. Houghton et al. 1999; White 1991).

Maungataketake (Elletts Mountain) and North Head (Maungaika) are small basaltic volcanoes located within the <250 ka Auckland Volcanic Field (AVF), whose initial eruptions were characterized by dominantly hydromagmatic phases, forming a tuff ring and tuff cone, respectively. Both volcanoes later evolved towards a “drier” magmatic style of fragmentation and eruption.

In general, the Maungataketake hydromagmatic sequences are moderately sorted tuffs and lapilli tuffs and display mostly parallel to sub-parallel bedding throughout the ~1km long coastal exposures (Fig. 1), although the lowest units of the distal deposits show distinct irregular, low amplitude undulations in bed thickness. The most proximal exposures are affected by post-eruptive vertical displacements and faulting, but lack the typical

massive, vent clearing breccias seen at other AVF volcanoes (e.g. Orakei Basin). Accidental lithics and minerals derived from country rocks (quartz, feldspar and clays) constitute ~80 vol.% of the fine ash/tuff assemblages; however, lapilli to block size (up to 40 cm) accidental fragments are recognized along some horizons. Juvenile pyroclasts (~20%) are characterized mainly by sub-angular to angular, poorly vesicular, glassy lapilli; forming single trails, grouped trails, or distinct juvenile-rich clast supported beds.



Fig. 1 – Outcrop ~150 m SE to the inferred crater rim showing the parallel to sub-parallel bedding. Circle A highlights an alternation of lapilli tuff and ash tuff. Circle B shows a lapilli rich bed. Arrow points towards a large accidental block that impacted on highly plastic beds.

North Head volcano’s lowermost pyroclastic units are composed of sub-angular to angular, poorly to moderately vesicular, fine to coarse lapilli size, juvenile pyroclasts (>90%) that form crude parallel to massive bedding. These beds are moderately sorted, and firmly cemented. Some magmatic clasts encapsulate or are coated by fine grained country rock materials. Also, some accidental lithic fragments are coated by chilled magma. Towards the upper units, however, the pyroclastic succession becomes an alternating sequence of clast- and matrix-supported, poorly consolidated, medium to coarse lapilli tuff and thin layers of moderately indurated, crudely bedded ash tuff (Fig. 2). There are abundant juvenile bombs (up

to 25 cm) and some accidental lithic blocks (up to 40 cm) along some horizons (Fig. 2).

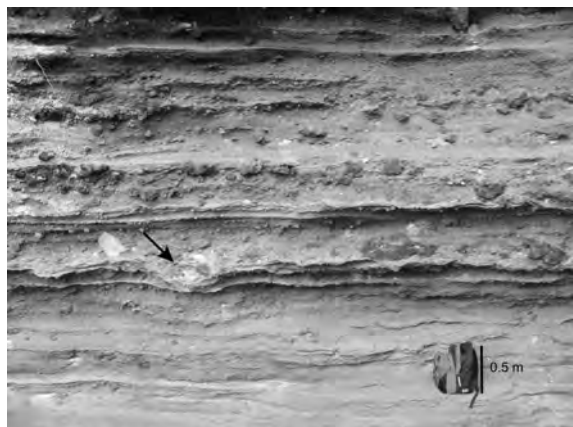


Fig. 2 – North Head volcano's upper hydromagmatic successions. The arrow points to an accidental block forming an impact sag. Note the presence of some thin beds composed of fine ash alternating with juvenile lapilli/bomb-rich sequences.

In most parts of the AVF, including North Head, the volcanic deposits of the AVF are underlain by the ~1000 to 2000 m thick, early Miocene Waitemata Group, which consists in most parts of inter-bedded turbiditic sandstone and pelagic siltstone (Ballance, 1974). The hydraulic parameters as well as the amount of jointing and fractures of the Waitemata Group's rocks vary widely across the area (Crowcroft and Smaill, 2001), and usually form low yield, confined aquifers. Within the Maungataketake area the Waitemata Group is overlain by the shallow-marine Kawa Formation that is possibly meters to tens of meters-thick of siliciclastic sediments of a more permeable, poorly consolidated nature.

From the morphological, stratigraphic, and sedimentological characteristics of the pyroclastic successions studied, and from the pyroclastic morphologies, it is inferred that the formation of Maungataketake tuff ring involved a smaller water-magma ratio compared to that related to the creation of North Head tuff cone. Yet some observations arise when the deposits and their components are examined in detail, questioning the water-magma ratio alone for their formation. For example, the fine fragmented Maungataketake ash tuff deposits show strong evidence of high water involvement (accretionary lapilli, vesicular tuff, and strong plastic bed deformation); was it created at higher magma-ratios than usual highly energetic fragmentation? Alternatively, was the deposit structure due completely to its depositional mechanisms? Does the upward presence of fine grain ash layers in North Head correspond to an activity showing a decrease in water-magma ratios exclusively? Could it be that the shift to a finer fragmented phase was more the

result of the change in the physical properties of water, its access to the fragmentation site and/or changes to the conduit geometry as stated by White (1996)?

The above elucidates into the complexity of the fundamental controls on hydromagmatic eruptions. Apparently, groundwater availability and circulation was more optimal beneath Maungataketake than below North Head, then why was a tuff cone not formed at Maungataketake? Undoubtedly, the geometry, hydraulic conditions, water volume, and rock properties of the aquifer will create a distinct water-magma surface contact and vent geometry conditions, which in turn, together with variations in magma properties, will promote characteristic explosions with their unique fragmentations forming different types of pyroclastic density currents and/or falls that will be deposited accordingly to other number of additional controls (like topography). Therefore two seemingly "simple" hydromagmatic volcanoes pose more questions than answers that need to be assessed in order to envisage any possible future hydromagmatic event in the Auckland area.

Acknowledgements

This research is supported through grants by the Volcanic Risk Solutions (Massey) and part of the research supported by the NZ FRST-IIOF Grant "Facing the challenge of Auckland's Volcanism" (MAUX0808). Also many thanks for the support from the University of Auckland through School of Environment and the Institute of Earth Sciences and Engineering, and the DEVORA project.

References

- Balance, P.F. 1974. An Inter-Arc Flysch Basin in Northern New Zealand: Waitemata Group (Upper Oligocene to Lower Miocene). *The Journal of Geology* 82: 439-471.
- Crowcroft, G., Smaill, A. 2001. Auckland, in *Groundwaters of New Zealand*, Rosen, M.R., and White, P.A., eds., New Zealand Hydrological Society Inc., Wellington, Chapter 13: 303-313.
- Houghton, B.F., Wilson, C.J.N., Smith, I.E.M. 1999. Shallow-seated controls on styles of explosive basaltic volcanism: a case study from New Zealand. *Journal of Volcanology and Geothermal Research*, 91: 97-120.
- Kokelaar, P. 1986. Magma-water interactions in subaqueous and emergent basaltic volcanism. *Bulletin of Volcanology* 48: 275-289.
- Sheridan, M.F., Wohletz, K.H. 1983. Hydrovolcanism: Basic considerations and review, in Sheridan, M.F., and Barberi, F., eds., *Explosive volcanism: Journal of Volcanology and Geothermal Research* 17, 1-29.
- White, J.D.L. 1996. Impure coolants and interaction dynamics of phreatomagmatic eruptions. *Journal of Volcanology and Geothermal Research* 74: 155-170.
- Wohletz, K.H. 1986. Explosive magma-water interactions: Thermodynamics, explosion mechanics, and field studies. *Bulletin of Volcanology* 48: 245-264.

Making craters: a review and approach to thermodynamic analysis of the 1886 Rotomahana eruption

Robin Andrews¹, James White¹ and Michael Rosenberg²

¹ Dept. Geology, University of Otago, Dunedin, New Zealand - r.c.andrews@btinternet.com

² Wairakei Research Ctr., GNS Science, Taupo, New Zealand

Keywords: Rotomahana, maar, cratering.

This presentation reviews inferred eruption mechanisms and known elements of the magmatic and groundwater/geothermal thermodynamic system, with the aim of gaining an understanding of crater formation dynamics of the 1886 Rotomahana eruption and other maar-forming eruptions.

Published research on the event is summarised and assessed, along with the background underpinning the main theories that may explain the highly explosive nature of the eruption. Proposed future research is outlined.

It begins with laboratory-scale cratering experiments to investigate the nature of multiple phase explosive diatreme-forming events. These contrast with single phase explosions already widely studied, and with mechanisms of cratering accompanying sustained uprush. We intend to follow this with a series of similar, field-scale experiments.

New laboratory work will involve the microanalysis of volatiles in glass, work with microlites, and some petrological modelling. By combining (1) characterisation of the pre-eruption geothermal and hydrological system, and (2) results from as-yet unpublished work by JB Rosseel and M May that characterises crater and deposit features, componentry, granulometry, and qualitative and quantitative 2-D and 3-D vesicle textures, our approach should allow inference of relationships between magma supply, cratering intensity, and other eruptive process during the Rotomahana eruption.

Recent reviews (White and Ross, 2011) into the formation of maars indicate that, whilst phreatomagmatism is the key process responsible for their formation, the lithological intricacies of individual field examples are difficult to corroborate with each other: thus, it is important to constrain a) the nature of the thermodynamic system operating during the phreatomagmatic episodes, and b) the

relative significance of the role of the substrate, including its degree of consolidation and permeability.

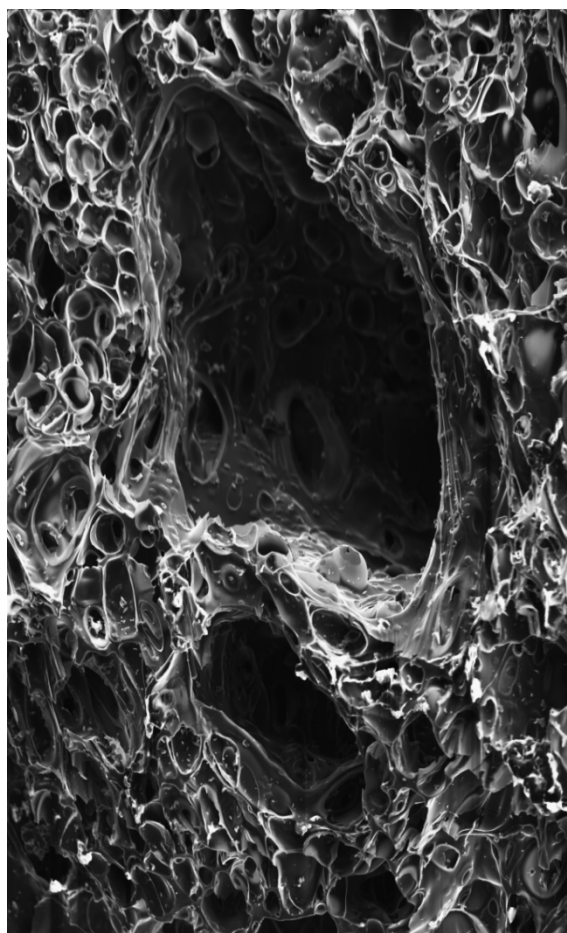


Fig. 1 – An SEM image of part of a Rotomahana 1886 pyroclast.

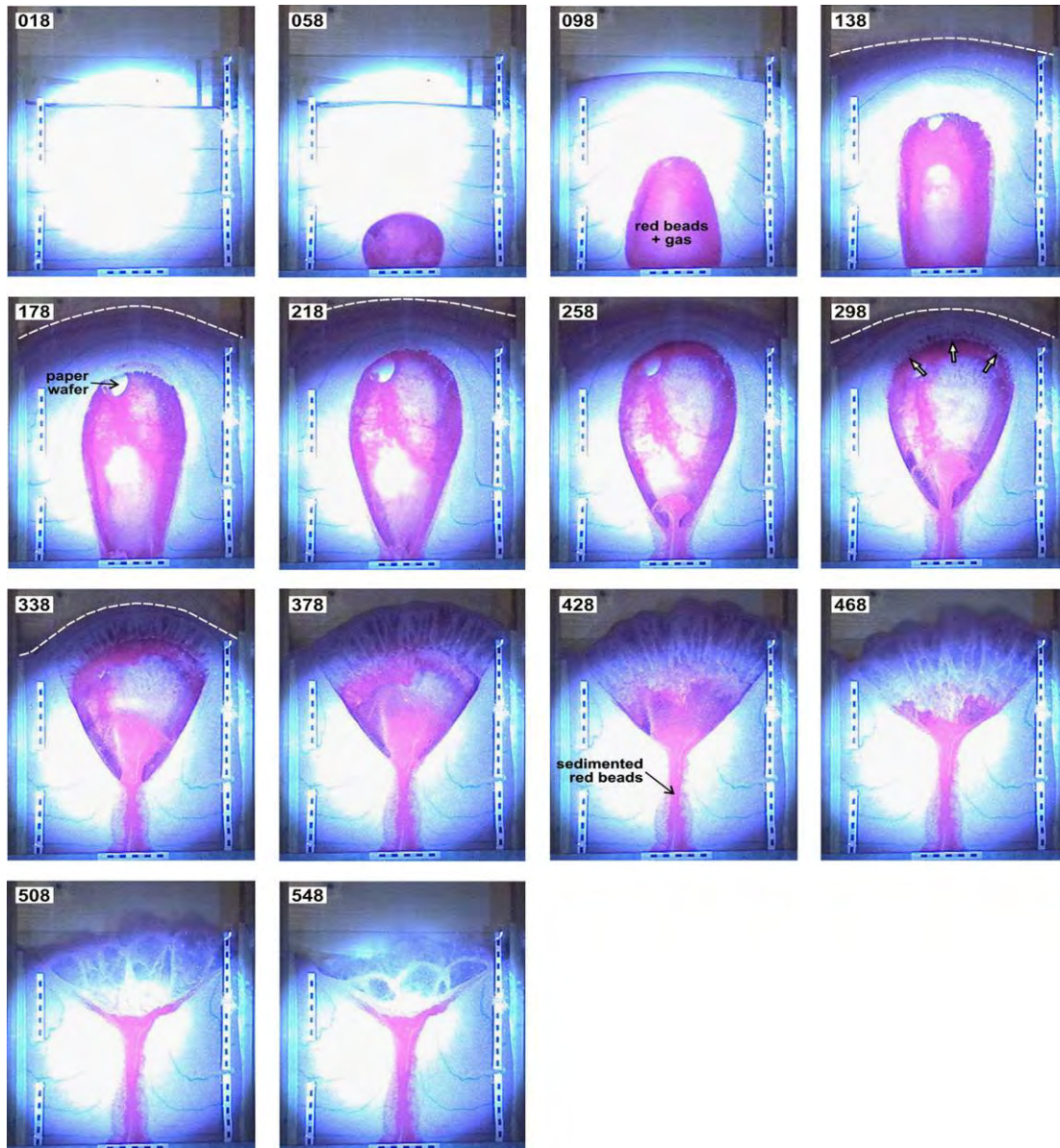


Fig. 2 – A sequence of grabbed video frames from a laboratory-scale cratering experiment run conducted showing an erupting run, akin to those inferred to have occurred at Rotomahana during the 1886 event, (Ross and White, 2006). After Ross et al. (2008).

References

- Ross, P., White, J.D.L. 2006. Debris jets in continental phreatomagmatic volcanoes: A field study of their subterranean deposits in the Coombs Hills vent complex, Antarctica. *Journal of Volcanology and Geothermal Research* 149: 62-84.
- Ross, P., White, J.D.L., Zimanowski, B., Büttner, R. 2008. Multiphase flow above explosion sites in debris-filled volcanic vents: Insights from analogue experiments. *Journal of Volcanology and Geothermal Research* 178: 104-112.
- White, J.D.L., Ross, P. 2011. Maar-diatreme volcanoes: A review. *Journal of Volcanology and Geothermal Research* 201: 1-29.

Paleomagnetic and geological updates to an event-order model for the Auckland Volcanic Field

Mark Bebbington^{1,2} and Shane Cronin¹

¹ Volcanic Risk Solutions, Massey University, Palmerston North, New Zealand – m.bebbington@massey.ac.nz

² IFS-Statistics, Massey University, Palmerston North, New Zealand

Keywords: Age determinations, tephrostratigraphy, temporal hazard rate

The Auckland Volcanic Field (AVF) has c. 49 eruptive centres formed in the last c. 250 ka. Stratigraphy constrains up to 33 of the centres in at least one direction. Other available age determinations, in order of reliability, include C¹⁴ dates (13 centres), Ar-Ar dates (4 centres) and thermoluminescence dates (2 centres). Past K-Ar dating in this field is considered unreliable due to excess Ar. Indirect sources of age information include interpolated C¹⁴ ages in lake-sediment cores recovered from 5 maars in the field, and magnetic anomalies from lavas. The later indicate that a number of the centres erupted during the c. 1000 year-long Mono Lake excursion at 32.4 ± 0.3 ka (Singer, 2007), and possibly others during the Laschamp excursion at 40.4 ± 1.1 ka (Guillou et al, 2004). Moreover, other centres with strong measured magnetic anomalies cannot have occurred during these excursions.

Cassidy and Locke (2010) provide a number of specific constraints based on palaeomagnetism:

- A. Mt Richmond, Crater Hill, Wiri Mountain, Puketutu and Taylor's Hill occurred during the Mono Lake excursion. Taylor's Hill may have occurred at a slightly different time to the others (Cassidy and Hill, 2009).
- B. McLennan Hills occurred during the Laschamp excursion.
- C. Otaru Hill and Hampton Park are contemporaneous (within 0.1 ka), as are Otuaataua and Maungataketake.
- D. Apart from those listed in A and B, only Tank Farm, Onepoto, St Heliers, Orakei Basin, Hopua, Pukaki, Little Rangitoto and Pukeiti can be within an excursion (Cassidy, personal communication).

For the purposes of this exercise, we will accept all the constraints above, and further suppose that they are the second-most reliable source of age data (behind stratigraphy), superseding C¹⁴ ages where present. Certain C¹⁴ ages are reassigned to other sources, consistent with Lindsay and Leonard (2009). An additional geological constraint is also available:

- E. Orakei Basin was not breached by the sea during last interglacial high stand of 5-6 m

above present, thus age must be <120 ka (Hayward, personal communication).

We can now revisit the exercise of matching vents to maar tephras identified by Molloy et al. (2009). The requirement is to allocate *all* tephra, in a *feasible* manner, without assuming that closeness in space translates to closeness in time. Otherwise the assumption determines the hazard estimate (Magill et al., 2005). While tephras AV6-9 possibly match the Mono Lake excursion, none appear to match the Laschamp. The procedure in Bebbington and Cronin (2011), pp. 62-63 is now modified in the following respects: AV9 (Pupuke and Orakei) is assigned to Panmure Basin, while AV9 (Pukaki) matches Crater Hill. AV6 (Pukaki) is now best fitted to Kohuora. As the stratigraphy has Waitomokoia > Pukeiti > Otuaataua, AV16 is assigned to Matarakua. AV11 is assigned to Robertson Hill, AV15 to Little Rangitoto, AV17 to Pigeon Mountain and AV22 to Styaks Swamp. Although some of the latter matches may appear unlikely, they are the only possibilities remaining. Hence the tephra assignment is quite a tight one. A suitable modification of the Monte Carlo simulation algorithm, respecting the constraints A-E above results in the updated age model in Table 1 (1000 repetitions). Hopua Basin falls within the Mono Lake excursion approximately half of the time. No other centres apart from those in A and B fall within either of the excursions.

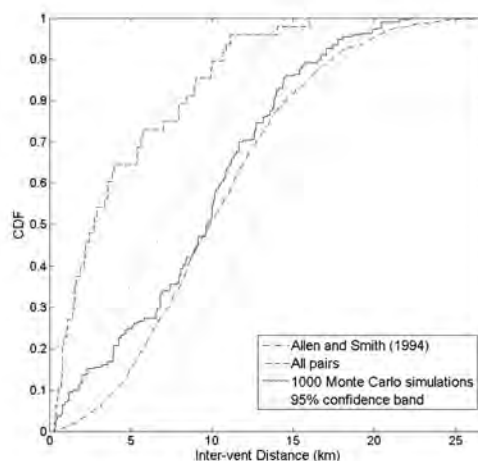


Fig. 1 - Successive event clustering in the AVF.

Table 1 - Monte Carlo ages and ordering from 1000 simulations of the AVF age-order model with paleomagnetic constraints. Bold indicates Mono Lake and Laschamp events. Near contemporaneous events are italicise. Other significant differences from Bebbington and Cronin (2011) are underlined.

Name	Mean Age (ka)	Age Error (ka)	Min Order	Max Order
Onepoto Basin	248.8	29.2	1	7
Albert Park	228.2	41.5	1	7
Lake Pupuke	200.1	7.1	1	8
Pukekiwiriki	199.3	42.2	1	8
<u>Waitomokia</u>	195.4	55.9	1	12
St Heliers	181.9	54.1	2	9
Te Pouhawaiki	153.1	71.0	1	36
Pukeiti	119.3	55.5	2	14
<u>Orakei Basin</u>	102.7	10.2	5	10
Pukaki	83.5	5.4	7	11
Tank Farm	75.0	5.4	8	13
Domain	69.0	4.9	8	12
Mt St John	54.7	4.4	10	13
<i>Maungataketake</i>	41.5	0.4	13	15
<i>Otuataua</i>	41.4	0.4	14	16
McLennan Hills	40.1	1.1	13	16
One Tree Hill	35.0	0.6	16	18
Kohuora	34.0	0.3	16	21
Motukorea	33.7	0.8	17	22
Mt Albert	32.8	0.5	17	22
Ash Hill	32.3	0.1	20	23
Hopua Basin	32.3	0.4	19	26
Puketutu	31.9	0.3	22	27
Wiri Mountain	31.9	0.3	21	28
Mt Richmond	31.7	0.3	22	28
Taylor's Hill	31.7	0.4	21	28
Crater Hill	31.6	0.3	24	28
North Head	31.2	0.1	27	30
Panmure Basin	31.2	0.1	28	31
Mt Victoria	31.1	0.1	29	32
Mt Cambria	31.1	0.1	29	34
<u>Robertson Hill</u>	31.1	0.1	30	33
Mt Roskill	30.4	1.2	19	34
Three Kings	28.8	0.3	33	35
Mt Hobson	28.6	0.3	34	37
Mt Eden	28.4	0.3	36	38
<u>Little Rangitoto</u>	27.8	0.4	37	39
<u>Matakarua</u>	27.0	0.6	35	40
Pigeon Mt	26.8	0.5	38	40
Mangere Lagoon	26.2	0.4	40	41
<i>Hampton Park</i>	25.3	0.7	41	42
<i>Otara Hill</i>	25.2	0.7	42	43
Green Hill	23.5	3.8	28	45
Mt Mangere	22.0	0.4	43	45
Mt Smart	21.7	0.8	43	45
Styaks Swamp	17.0	1.0	46	46
Purchas Hill	10.8	0.1	47	47
Mt Wellington	10.5	0.1	48	48
Mt Wellington 2	10.1	0.1	49	49
Rangitoto	0.6	0.0	50	50
Rangitoto 2	0.5	0.0	51	51

Figure 1 shows that there is still no observable spatio-temporal clustering in the event model, and hence the best model for the temporal hazard is that

in Bebbington and Cronin (2011), with updated parameter estimates are $\mu = 0.000076 \pm 0.000012$ per year, $\nu = 0.62 \pm 0.06$ and $\sigma = 1687 \pm 913$ years. The updated hazard estimates are shown in Figure 2.

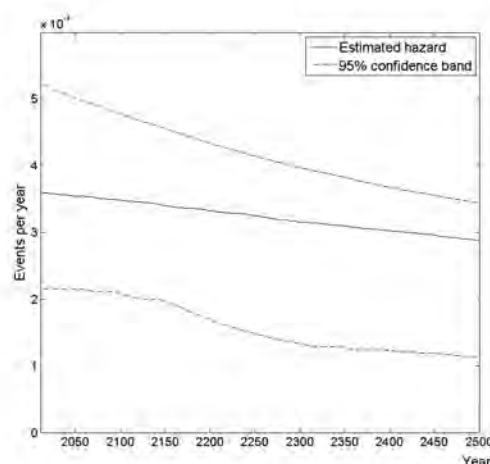


Fig. 2 - Temporal hazard in the AVF.

References

- Allen, S.R., Smith, I.E.M. 1994. Eruption styles and volcanic hazard in the Auckland Volcanic Field, New Zealand. *Geoscience Reports Shizuoka University* 20: 5-14.
- Bebbington, M., Cronin, S.J. 2011. Spatio-temporal hazard estimation in the Auckland Volcanic Field, New Zealand, with a new event-order model. *Bulletin of Volcanology* 73: 55-72.
- Cassidy, J., Hill, M.J. 2009. Absolute palaeointensity study of the Mono Lake excursion recorded by New Zealand basalts, *Physics of the Earth and Planetary Interiors* 172: 225-234.
- Cassidy, J., Locke, C.A. 2010. The Auckland volcanic field, New Zealand: Geophysical evidence for structural and spatio-temporal relationships. *Journal of Volcanology and Geothermal Research* 195: 127-137.
- Guillou, H., Singer, B.S., Laj, C., Kissel, C., Scaillet, S., Jicha, B.R. 2004. On the age of the Laschamp geomagnetic excursion, *Earth and Planetary Science Letters* 227: 331-343.
- Lindsay, J., Leonard, G. 2009. Age of the Auckland Volcanic Field. *IESE Report* 1-2009.02
- Magill, C.R., McAneney, K.J., Smith, I.E.M. 2005. Probabilistic assessment of vent locations for the next Auckland volcanic field event. *Mathematical Geology* 37: 227-242.
- Molloy, C., Shane, P., Augustinus, P. 2009. Eruption recurrence rates in a basaltic volcanic field based on tephra layers in maar sediments: implications for hazards in the Auckland volcanic field. *GSA Bulletin* 121: 1666-1677.
- Singer, B.S. 2007. Polarity transitions: radioisotopic dating. In: E.H. Bervera and D. Gubbins, Editors, *Encyclopedia of Geomagnetism and Paleomagnetism*, Springer-Verlag, pp. 834-839.

Volcanic Shield Fields, Newer Volcanic Province, Australia

Mark A. Bishop

Planetary Science Institute, Tucson, Arizona, USA – bishop@psi.edu

Keywords: shield volcano, volcanic fields, Newer Volcanic Province.

Volcanic shield fields are ubiquitous across planetary surfaces and have recently received significant attention in the geographic and geological mapping of Moon (Shockey and Gregg, 2009), Mars (Baptista et al. 2008) and Venus (Miller and Gregg, 2011). In comparison, the spatial recognition and description of terrestrial shield fields has been limited. Fields of low, diminutive shield shaped structures can occur as parasitic forms on larger composite edifices, for example, Kilauea in Hawaii, but can be commonplace also in many monogenetic volcanic landscapes such as the central Snake River Plain, USA, and the Newer Volcanic Province of southeastern Australia. For monogenetic provinces such as that in Australia, low shields may demonstrate the most significant output of magma and areal coverage relative to any other volcanic construct of Quaternary-to-late Neogene age. They also represent a landform in which the transport of lava can occur over many tens of kilometers through a complex array of tubes and channels.

Seminal studies on the shields of the Faroe Islands (Noe-Nygaard, 1968), Mauna Iki of Kilauea (Macdonald, 1972) and Snake River Plain (Greeley, 1977) realized the necessity for a sub-category of shield volcano that was neither classic Hawaiian- or Icelandic-type. Macdonald acknowledged these volcanoes as *lava cones*, Noe-Nygaard used the description *shield volcano of scutulum type* and Greeley proposed the term *low shield* to best describe this category of volcano. The term, low shield, is that which also best describes the structures of the Newer Volcanic Province.

In this paper, it is reported how the morphology of low shields for the Newer Volcanic Province has significant variation across the field, and that their organization is indicative of a shield field. Using Shuttle Radar Topography Mission (SRTM) DEM data and landscape analysis within a GIS, the metric of circularity¹ was determined for successive natural breaks in slope to demonstrate the morphological variation of low shields. In this instance, circularity values are the quotients of shield areas and perimeters. From these measures, it is shown that shields demonstrate a range of values that lie

between 0.07 and 0.63 (Table 1). In all instances, the degree of circularity is low across the field and recognizes the involvement of topographic control and post-eruptive erosional modification of lava flows for each of the centers.

Volcano Name	Circularity (min)	Circularity (max)
Mount Gellibrand	0.07	0.10
Mount Porndon	0.07	0.22
The Sisters	0.07	0.11
Mount Eccles	0.12	0.17
Mount Rouse	0.09	0.27
Mount Napier	0.21	0.51
Stockyard Hill	0.09	0.22
Mount Widderin	0.21	0.33
Mount Elephant	0.20	0.63
Mount Hamilton	0.11	0.16
Mount Fyans	0.16	0.24

Table 1 – Circularity metrics for low shields

Although less obvious than either cinder (scoria) cones or maars topographically (Fig. 1), low shields are landforms that often organize into fields that have notable geomorphic involvement in the long-term evolution of landscape (Fig. 2).

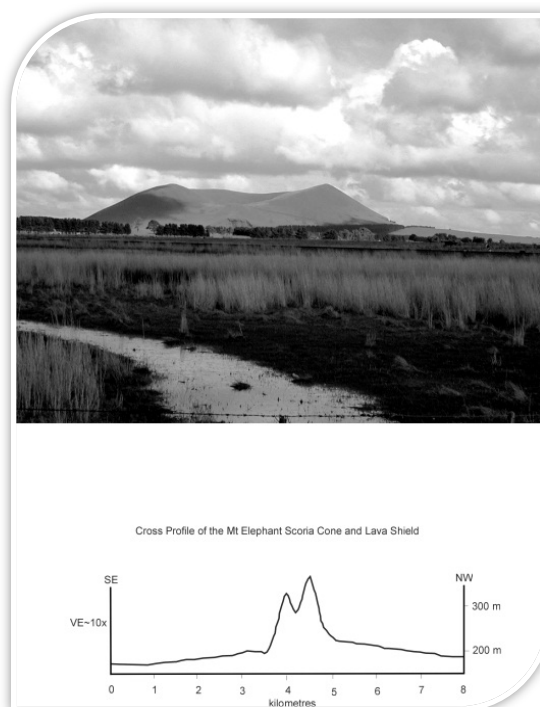


Fig. 1 – Mount Elephant scoria cone and low shield

¹ Circularity is a measure of the compactness of a shape. A circle has a value of 1 with less circular objects having values that approach 0.

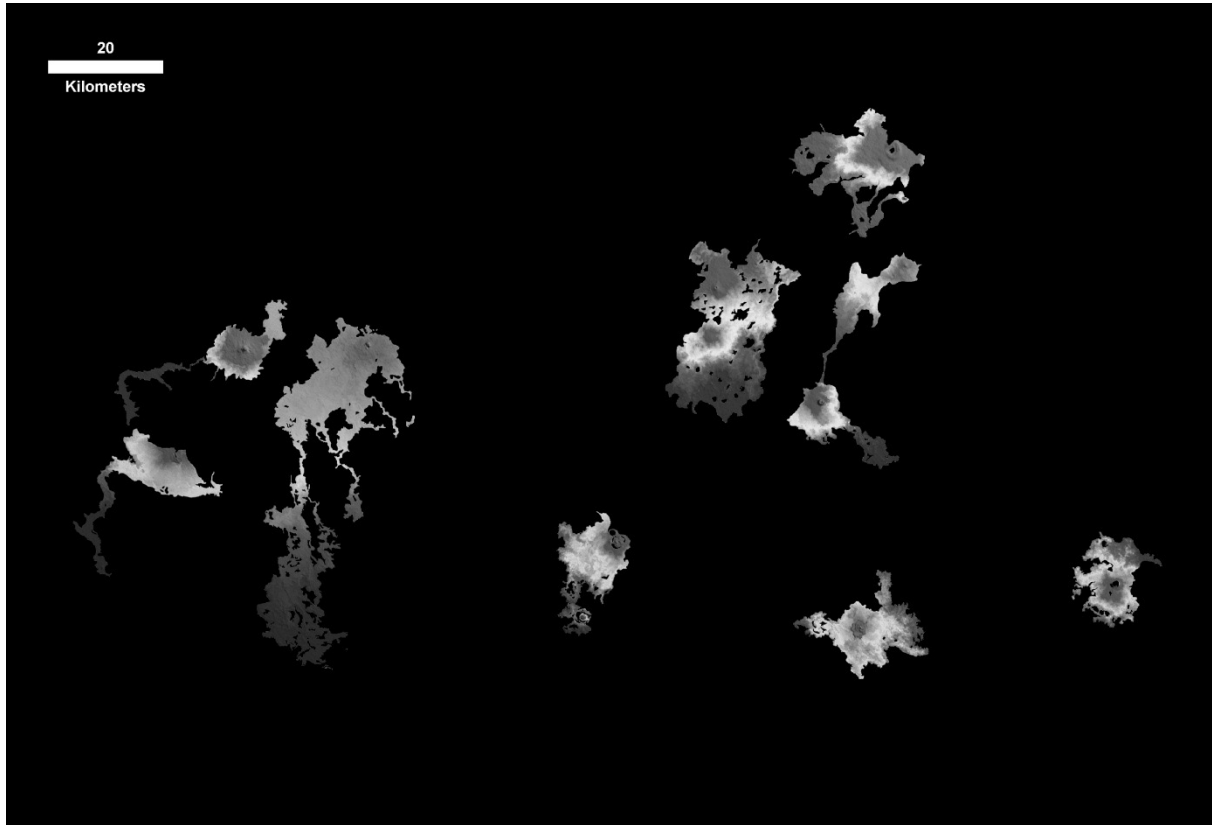


Fig. 2 – Part of the Quaternary-late Neogene age low-shield field of the Newer Volcanic Province of southeastern Australia. The image is derived from an SRTM 3-sec DEM in which a Jenks' natural breaks algorithm classifies the data into a choropleth map. Low-shield centers are prevalently identified with the darker grey colors, many with cinder cones and/or maar craters marking these locations. In many instances lava flows have pirated stream courses to extend many tens-of-kilometers from the eruption center. Maps of this type are ideal for both general and specific geomorphometric analysis of land form. North is towards the top. Image credit: NASA/JPL/USGS/PSI

For example, the geography of shields and their associated lava flows across the Newer Volcanic Province have aided in arranging regional drainage patterns and the shape of the landscape, and subsequently the geomorphic boundary conditions that control surface processes following the volcanic episode.

Furthermore, the pattern(s) of distribution, or surface signatures, are also indicative of the magmatic architecture of volcanic systems. Shield development displays a transitional setting of latitudinal change from south-to-north, and a distinctive adjustment in eruption style across the field (Bishop, 2009).

The comparative study of planetary volcanism using a geographic perspective has changed the perception of volcanic landforms and processes, and offers to better interpret volcanic landscapes and land form.

Acknowledgements

In memory of Ron Greeley (1939-2011): pioneer, teacher, mentor and inspiration to planetary geology.

References

- Baptista, A.R., Mangold, N., Ansan, V., Baratoux, D., Lognonne, P., Alves, E.I., Williams, D.A., Bleacher, J.E., Masson, P., Neukum, G. 2008. A swarm of small shield volcanoes on Syria Planum, Mars. *Journal of Geophysical Research* 113: E09010.
- Bishop, M.A. 2009. A generic classification for the morphological and spatial complexity of volcanic (and other) landforms. *Geomorphology* 111:104-109.
- Greeley, R. 1977. Basaltic "Plains" Volcanism, in Greeley, R., King, J.S. eds., *Volcanism of the Eastern Snake River Plain, Idaho: A Comparative Planetary Geology Guidebook NASA CR-154621*: 24-44.
- Macdonald, G.A. 1972. *Volcanoes*. Prentice-Hall, New Jersey 510 pp.
- Miller, D.M., Gregg, T.K.P. 2011. Characteristics and geologic relationships of shield fields versus shield plains on Venus. 42nd Lunar and Planetary Science Conference, Abstract #1550.
- Noe-Nygaard, A. 1968. On extrusion forms in plateau basalts. *Visindafelag Islendinga, Reykjavik*: 10-13.
- Shockey, K.M., Gregg, T.K.P. 2009. The spatial relationship within fields of shield volcanoes. 40th Lunar and Planetary Science Conference, Abstract #2056.

A geophysical comparison of simple and complex maar volcanoes from the Cainozoic Newer Volcanics Province, Southeastern Australia

Teagan Blaikie, Laurent Ailleres, Peter Betts and Ray Cas

School of Geosciences, Monash University, Clayton, Victoria, 3800, Australia – Teagan.Blaikie@monash.edu

Keywords: geophysics, diatreme, Newer Volcanics Province.

Potential field geophysical modeling can be used to image subsurface geologic features and its application to volcanology may contribute to a better understanding of the internal structure and evolution of a volcanic centre. The internal structures of maar volcanoes are rarely exposed and as a result are often inferred by studying the surrounding pyroclastic deposits. Understanding the relationships between the eruptive styles of maar volcanoes, their deposits and the geometry of its diatreme and feeder vents are important for an improved understanding of how these types of volcanoes erupt.

Maar volcanoes are ideal for geophysical modeling as the volcanic nature of the maar diatreme and its feeder vents will generally result in a high petrophysical contrast with the host rock (Cassidy et al. 2007). When the data is appropriately constrained, the internal structure of a maar, including the geometry of its diatreme and the distribution of rock properties such as density and magnetic susceptibility can be determined using two and three dimensional forward and inverse modeling. Several maar volcanoes, both simple and complex, located within the Cainozoic Newer Volcanics Province (NVP) of southeastern Australia are the focus of detailed geophysical investigations.

The maar volcanoes under investigation include several maars within the Red Rock Volcanic Complex (RRVC), Ecklin maar and the Mount Leura Volcanic Complex (MLVC). These maars are hosted in the weakly lithified sedimentary sequences of the Otway Basin, with soft-sediment behavior likely influencing their evolution. Ecklin maar is a small, simple maar volcano, showing dominantly phreatomagmatic eruptive styles. The MLVC consists of a large maar crater and overlapping tuff rings, with up to 16 scoria cones contained within the centre. The RRVC is one of the most complex volcanic centers within the NVP, host to over 40 eruption points. The complex consists of numerous poly-lobate maars and a scoria cone complex.

High resolution gravity and magnetic data was acquired across each of these maars in a series of cross-cutting traverses. The data was subsequently modeled in two and three dimensions to understand the morphology of the diatreme. Models of the maars subsurface structures are constrained by the

regional geology, pyroclastic deposits, petrophysical properties and the interpretation of gridded geophysical data. Gridded data is selectively filtered in order to emphasise different features and aid in the interpretation. Vertical derivatives, high and low pass filters are applied to highlight wavelengths in the data associated with deep and shallow sources (Fig. 1).

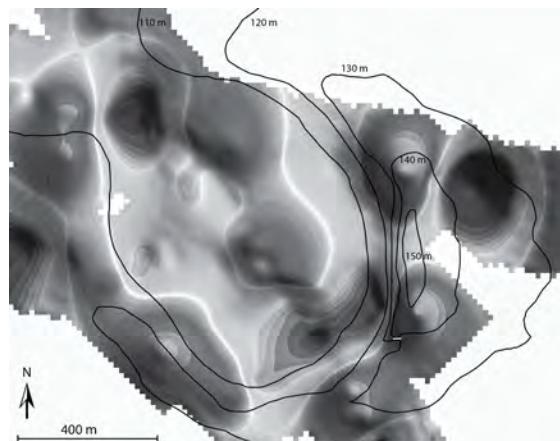


Fig. 1 – High Pass filter (800m cutoff wavelength) of the Bouguer gravity data over Ecklin maar applied to remove a strong regional gradient. Two weak gravity highs can be observed in the centre of the maar and correlate with two magnetic anomalies.

Varied geophysical responses are observed across each of the maars surveyed, indicating the complex and variable nature of the subsurface volcanic vent, even when they are similar in surface morphology.

Ecklin maar consists of two corresponding gravity and magnetic highs in the centre of the crater, surrounded by a gravity and magnetic low (Fig. 1). The MLVC has a large gravity high within the centre of the maar crater with a corresponding magnetic anomaly, related to the larger scoria cones. Magnetic anomalies are variable across this complex due to the dispersed scoria cones within the maar crater. Magnetic highs are observed over the cones, however they do not always have a corresponding gravity anomaly.

Geophysical signatures across the RRVC are highly variable, with some maars displaying

corresponding gravity and magnetic highs, others corresponding lows, and some with magnetic anomalies but no gravity anomalies.

Where corresponding gravity and magnetic lows are detected across a maar crater, it is suggested that all the available magma was erupted and the maar diatreme was not intruded by any dykes. The gravity low arises because of lower density lake sediments and pyroclastic debris infilling the diatreme. The lack of any intrusive dykes or remnant vents within the diatreme suggests that plenty of groundwater was available for phreatomagmatic explosions, preventing the ascent of magma through the diatreme.

Maars with corresponding gravity and magnetic highs indicate a large volume of subsurface basalt is present, possibly in the form of a dyke or sill or resulting from the ponding of magma at the surface of the vent. This results from a lack of groundwater for magma to interact with during the eruption, which facilitates magma rising upwards through the diatreme.

The variable subsurface structures of the RRVC and the Ecklin maar were revealed by two-dimensional forward modeling of potential field data. The Ecklin maar consists of a shallow, broad diatreme, a structure typical of a maar hosted in soft-sediment. The centre of the maar is denser and has a higher magnetic susceptibility, representing the higher volume volcanic debris contained within the vent. The margins have a lower density and magnetic susceptibility due to higher volumes of host rock debris, which subside into the crater during the eruption.

Modeling of several maars across the RRVC have revealed complex diatreme geometries (Fig. 2 and 3), suggesting that the maars formed from multiple coalesced craters (Blaikie et al. in preparation). Local gravity and magnetic anomalies within the centre of a number of maars indicate the presence of remnant basaltic feeder vents and intrusive dykes within the diatremes (Fig 2). The diatremes are shallow and bowl-shaped, indicating that the soft sediment behavior of the host rock influenced its final geometry.

The 2D forward models are used to construct a 3D reference model for potential field property and geometry inversions. Inversions are performed to reduce the geophysical misfit of the model by optimizing the geometry and petrophysical property distribution within the model. Property inversions have the advantage of being able to model variations in density or magnetic susceptibility within a specific unit of the model, whereas properties are kept homogenous during 2D forward modeling.

Heterogeneous property inversions of the RRVC have identified different geophysical domains and structures within the maar diatremes that were not

apparent during 2D modeling. Higher density domains have been identified within the centre of the diatreme while the margins are lower in density. Several narrow intrusive dykes contained within one of the larger maar diatremes of the complex were identified from inversion results.

This study highlights the usefulness of combining geophysical methods with volcanology. Such complex subsurface structures and could not be detected simply by studying the limited outcrops in the maar rims and was only revealed after geophysical modeling.

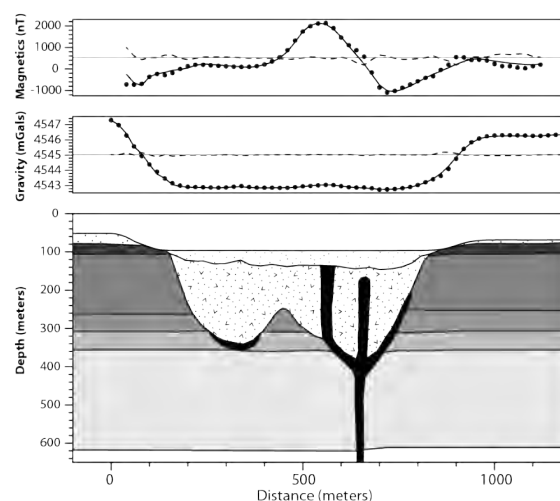


Fig. 2 – 2D forward model of a maar within the RRVC showing two coalesced diatremes and several feeder dykes (Blaikie et al. in preparation).

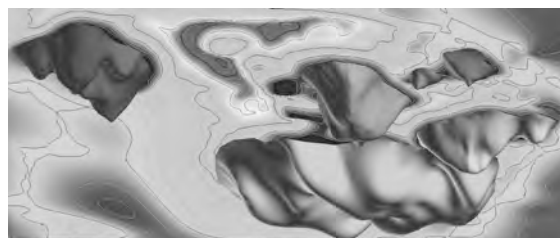


Fig. 3 – 3D model of the maar diatremes underlying the RRVC. The complex diatreme geometries indicate multiple eruption points within each maar.

Acknowledgements

This research has been partly supported by the AusIMM Bicentennial Gold Endowment Fund.

References

- Blaikie, T., Ailleres, L., Cas, R., Betts, P. in preparation. Three-dimensional modeling of a multi-vent maar diatreme – the Lake Coragulac maar, Newer Volcanics Province, South Eastern Australia
- Cassidy, J., Frances, S.J., Locke, C. 2007. Gravity and magnetic investigation of maar volcanoes, Auckland volcanic field, New Zealand. *Journal of Volcanology and Geothermal Research* 159: 153-163.

Origin of fluidal pyroclast morphologies in melilititic monogenetic cones: Insights from the recent explosive eruption of Oldoinyo Lengai, Tanzania

Sonja A. Bosshard, Hannes B. Mattsson and Jaap F. Berghuijs

Institute of Geochemistry and Petrology, Swiss Federal Institute of Technology (ETH Zürich), Zürich, Switzerland – sonja.bosshard@erdw.ethz.ch

Keywords: cannonball lapilli, CO₂, melilitite.

Melilititic eruption products within the Lake Natron - Engaruka monogenetic volcanic field (LNE-MVF) in northern Tanzania show distinct spherical pyroclast morphologies. In some cones, such as Mianmoja Hill and Essoite, cannonball bombs and lapilli are dominating the deposits. In fact, the entire edifice at Mianmoja Hill appears to be constructed by cannonball lapilli (with layering being the result of variations in grain-size; Fig. 1).

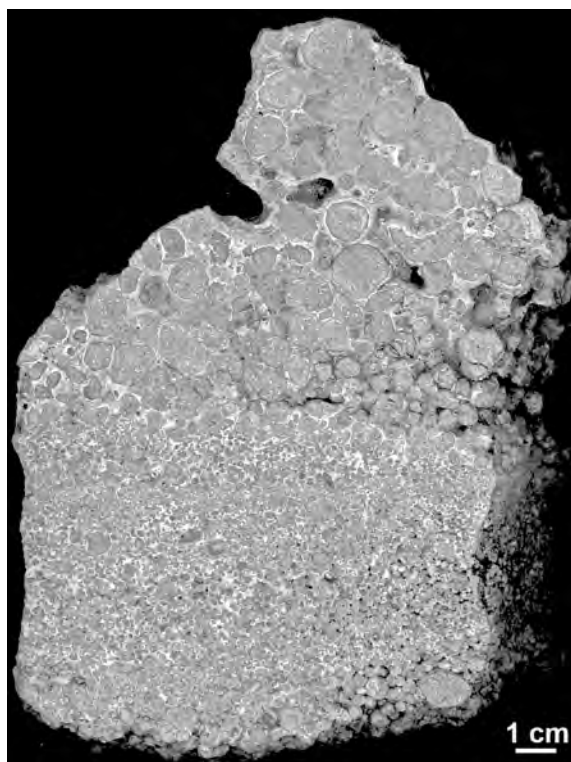


Fig. 1 – Hand specimen from the melilititic Mianmoja Hill edifice in Tanzania. Note that all lapilli are near-spherical in shape (only occasionally broken on impact). Secondary carbonates cement the groundmass and infilling vesicles.

In a recent paper, Alvarado et al. (2011) reported cannonball lapilli and bombs from a basaltic scoria cone in Costa Rica. They suggest that this type of dense pyroclasts forms as ballistic ejecta derived from a degassed magma and that the round shape is

a result of the ejecta rolling down the slopes of the edifice at high speed. In contrast to the Costa Rican lapilli described by Alvarado et al. (2011), the individual pyroclasts from Tanzania are vesicular and frequently contain one, or more, large crystals near the centre of the pyroclast (Fig. 2). Thus an alternative explanation for their origin must be sought.

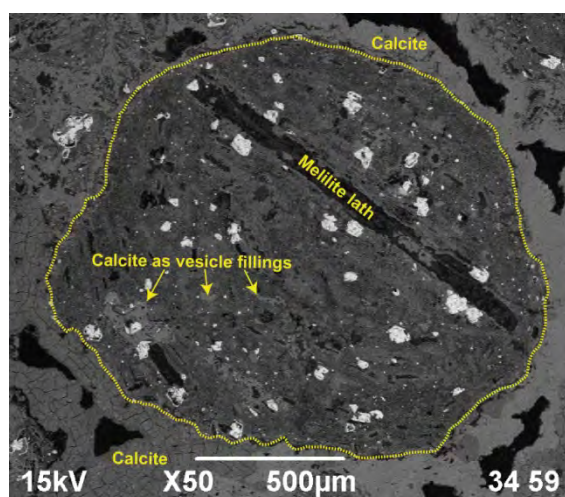


Fig. 2 – Backscattered SEM image of a spherical pyroclast from Mianmoja Hill. Note the large melilitite lath near the centre and the infilling of secondary calcite in vesicles.

The key to the origin of the spherical bombs and lapilli may come from a rather unexpected source. In 2007-2008 the Oldoinyo Lengai volcano (OL) erupted explosively with little precursory activity. This eruption was surprisingly vigorous, with an eruption plume that occasionally rose more than 15 km high above the volcano (Kervyn et al., 2010). The eruption deposited wide-spread tephra falls and built a ~50 m high cone inside the summit crater of the volcano. We collected samples of these explosive deposits during a field campaign in 2011. The OL pyroclasts show strong similarities in their morphology to the spherical lapilli of the melilititic monogenetic cones.

The tephra from Oldoinyo Lengai is predominantly composed of fine ash to fine lapilli,

and distinct spherical shapes dominate the surface morphologies (Fig. 3). About 60% of the lapilli from Oldoinyo Lengai have one, or more, euhedral silicate crystals in their center of the lapilli with an outer coating of highly vesiculated magma (Fig. 3). Early in the eruption the tephra was composed of silicate and carbonatite droplets indicating incomplete mixing of two magmas (cf. Mattsson and Reusser 2010). As the eruption progressed, the composition of the tephra changed towards being dominated by the nephelinitic component. Petrologically, the samples from different stages of the eruption plot on a mixing line between natrocarbonatitic and nephelinitic magmas.

As the Oldoinyo Lengai pyroclasts show distinct fluidal features (and droplet shapes) we interpret these morphologies to be formed in a dry magmatic eruption. In the case of OL the spherical shapes are probably a direct result of the gas-rich environment in the eruption. When the natrocarbonatitic and nephelinitic magmas mix at depth beneath the volcano, the carbonate minerals start to thermally decompose (Norton and Pinkerton, 1997). Decomposition occurs contemporaneously with magma moving closer to the surface. This allows for significant expansion of the CO₂ inside the conduit. The surprising vigor of the eruption may thus be a result of thermal decomposition of carbonates, in combination with decompression of a gas-rich nephelinitic magma.

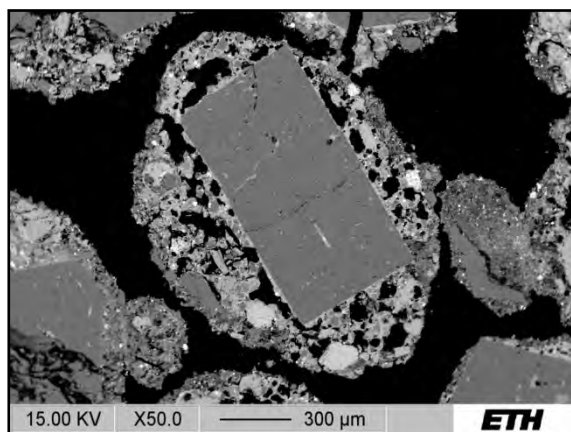


Fig. 3 – Backscattered image of a lapillus from the 2007-2008 eruption of Oldoinyo Lengai. Nepheline crystal cored with melt. Note the high abundance of vesicles in the melt.

We interpret the spherical lapilli that formed in the explosive event of Oldoinyo Lengai to represent vesiculating droplets of low-viscosity magma carried by a gas-stream (i.e., in a similar fashion as aerosol sprays). This hypothesis, requiring variable

amounts of mixing between carbonatite and silicate magma, is also supported by the petrological data.

The strong similarities in pyroclast shape (as well as internal textures) between lapilli from Oldoinyo Lengai, Mianmoja Hill and the Essoite cone suggest a similar origin for the pyroclasts. Geochemically, there is no direct evidence that decomposition of carbonatite melts was involved in the Mianmoja and Essoite eruptions. However, from experimental petrology it has been known for a long time that melilititic magmas are CO₂-rich (Brey, 1978). This is also supported by the abundant inclusions found in silicate phases such as clinopyroxene and olivine from the melilititic rocks from northern Tanzania. Rapid decompression of such CO₂-rich, low-viscosity, melts may thus be sufficient to produce magma droplets carried by a gas stream (i.e., aerosol-mode transport). Because of the low viscosity of the magma, in combination with the transport-mode (gas-stream), the resulting pyroclasts can be expected to be highly vesicular.

Thus, we conclude that the spherical cannonball lapilli at Mianmoja Hill and Essoite cone, as well as at Oldoinyo Lengai can be related to unusually CO₂-rich eruptions. Although there are no evidence for magma mixing and thermal decomposition of carbonates at Mianmoja Hill and Essoite cone, the strong similarities between the pyroclasts suggest the formation in a gas-rich environment.

References

- Alvarado, G.E., Pérez, W., Vogel, T.A., Gröger, H., Patiño, L. 2011. The Cerro Chopo basaltic cone (Costa Rica): An unusual completely reversed graded pyroclastic cone with abundant low vesiculated cannonball juvenile fragments. *Journal of Volcanology and Geothermal Research* 201: 163-177.
- Brey, G. 1978. Origin of olivine melilitites — chemical and experimental constraints. *Journal of Volcanology and Geothermal Research* 3: 61-88.
- Kervyn, M., Ernst, G., Keller, J., Vaughan, R., Klaudius, J., Pradal, E., Belton, F., Mattsson, H.B., Mbede, E., Jacobs, P. 2010. Fundamental changes in the activity of the natrocarbonatite volcano Oldoinyo Lengai, Tanzania. II. Eruptive behaviour during the 2007-2008 explosive eruptions. *Bulletin of Volcanology* 72: 913-931.
- Mattsson, H.B., Reusser, E. 2010. Mineralogical and geochemical characterization of ashes from an early phase of the explosive September 2007 eruption of Oldoinyo Lengai (Tanzania). *Journal of African Earth Sciences* 58: 752-763.
- Norton, G.E., Pinkerton, H. 1997. Rheological properties of natrocarbonatite lavas from Oldoinyo Lengai, Tanzania. *European Journal of Mineralogy* 9: 351-364.

The multiple magma batches of Mt. Rouse, Newer Volcanics Province, Victoria, Australia

Julie Boyce, Ian Nicholls, Reid Keays and Patrick Hayman

School of Geosciences Monash University, Australia – Julie.Boyce@monash.edu

Keywords: intraplate, monogenetic, magma batches

Intraplate basaltic volcanism in eastern Australia has a history stretching back at least to Jurassic times. One of the two most recent groups of occurrences is the Newer Volcanics Province (NVP) in the state of Victoria, active from 4.5 Ma to approximately 4000 BP.

The NVP was thought to be composed of short-lived monogenetic centres featuring single magma batches and simple evolutions (Joyce, 1975). However, recent research indicates that at least some of the centres have undergone more complex evolution. Centres such as Mt. Rouse (Boyce et al., in prep), Mt. Gambier (van Otterloo, in prep) and Red Rock (Piganis, unpublished) are all polymagmatic in the sense of containing multiple magma batches within complex deposits.

Situated in the Western Plains sub-province at Peshurst, Victoria, Mt. Rouse is a complex volcano of lava and pyroclastic deposits, rising 120 m above the surrounding lava plains, measuring approximately 1.2 km N-S and 0.75 km E-W. The volcanic complex features at least six eruption points (Fig.1).

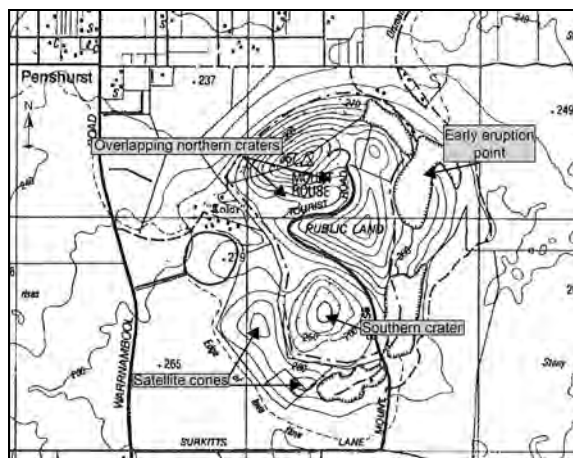


Fig. 1 – Map of Mt. Rouse (Rosengren, 1994) showing eruption points.

The main crater is composed of two overlapping craters running E-W, breached to the west. An early eruption centre is exposed to the north-east of the main crater, and to the south of the main peak is another crater containing a low scoria cone and two

satellite cones. The volume of magma erupted from Mt. Rouse is triple the volume of that erupted from other volcanic centres. The Mt. Rouse lava field extends 60 km to the coast at Port Fairy (Sutalo & Joyce, 2004), and covers >535 km² (Boyce et al., in prep.). Eruption styles vary from alternating magmatic (fire fountaining to strombolian) to phreatomagmatic, particularly during later stages.

Systematic sampling and detailed geochemistry were used to trace petrogenetic evolution and provide mantle source constraints. All lavas are weakly alkaline basalts whereas pyroclastics range from basanites through to trachy-basalts.

Rare earth element patterns (Fig. 2) show that the products of Mt. Rouse were generated from multiple magma batches. All lavas define Batch 1 (including the final products of the southern crater); southern cone pyroclastics and the two satellite cones of the southern crater define Batch 2, and a third batch is postulated from preliminary studies of the early eruption centre and the spatter rampart of the northern cone.

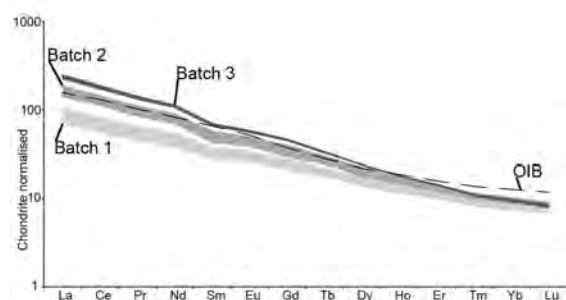


Fig. 2 – Chondrite normalised rare earth element data for Mt. Rouse. Batch 1 consists of 20 samples, Batch 2 of 15 samples and Batch 3 of 3 samples.

Mt. Rouse has had a complex eruption history, with probable simultaneous eruption of distinct magma batches, attested to by the overlapping relationships between successive constructional edifices as the eruption points shifted in time, and the fact that lava from Batch 1 is found interbedded in the products from Batch 2. Additionally, a surge deposit is found containing Pele's tears and hair from Batch 1, and scoria from Batch 2.

Petrogenetic modelling of the most primitive samples of each batch using equations from Lee et al (2009) indicates formation of magma batches at different depths (Fig. 3). Batch 1 was sourced from a depth of 68 km (2.09 ± 0.2 GPa) at a temperature of $1455 \pm 44^\circ\text{C}$, Batch 2 from 91 km (2.85 ± 0.2 GPa) and $1496 \pm 45^\circ\text{C}$ and Batch 3 from 103 km (3.22 ± 0.2 GPa) and $1514 \pm 45^\circ\text{C}$. For melting to occur, the mantle must also have contained water. This would have reduced the melting point, especially at elevated pressures. The occurrence of small lherzolite xenoliths (< 2 cm) in the products of Batches 1 and 3 is compatible with their origin near the spinel garnet lherzolite transition zone.

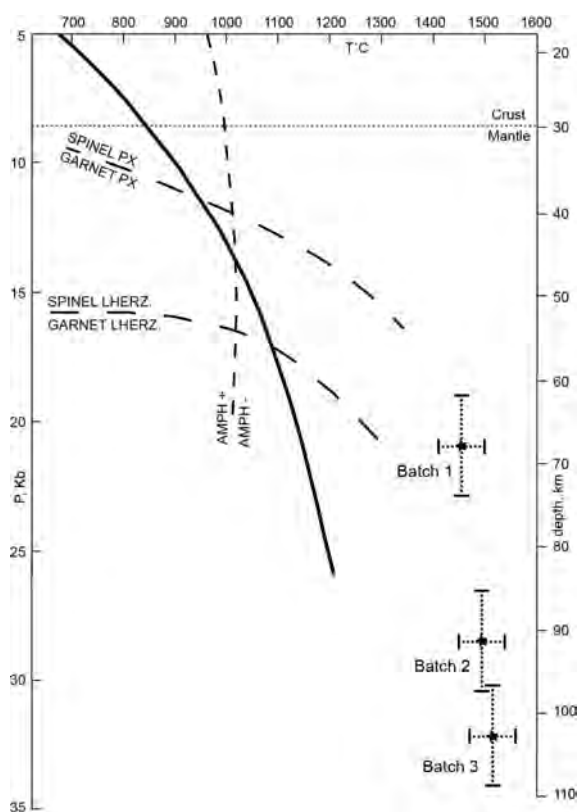


Fig. 3 – Southeast Australian geotherm (O'Reilly and Griffin, 1985) showing the estimated temperatures and depths of origin of the most primitive magmas of Mt. Rouse.

References

- Boyce, J.A., I.A. Nicholls, R. Keays, P. Hayman. in preparation. Composition and volatile contents of parental magmas of Mt. Rouse, a polymagmatic volcano in the Newer Volcanics intraplate basaltic province, SE Australia.
- Joyce, E.B. 1975. Quaternary volcanism and tectonics in Southeastern Australia. In: Suggate, R.P., Cresswell, M.M. (eds). Quaternary Studies. Royal Society of New Zealand Bulletin 13: 169-176.
- Lee, C.A., Luffi, P., Plank, T., Dalton, H., Leeman, W.P. 2009. Constraints on the depth and temperatures of basaltic magma generation on Earth and other terrestrial planets using new thermobarometers for mafic magmas. *Earth and Planetary Science Letters* 279: 20-33.
- O'Reilly, S.Y., Griffin, W.L. 1985. A xenolith-derived geotherm for southeastern Australia and its geophysical implications. *Tectonophysics* 111: 41-63.
- Piganis, F. 2011. A volcanological investigation of the polymagmatic Red Rock Volcanic Complex and a 3D geophysical interpretation of the subsurface structure and geology of the poly-lobate Lake Purdigulac maar, Newer Volcanics Province, southeastern Australia. Unpublished Masters thesis, Monash University, Australia.
- Rosengren, N. 1994. Eruption points of the Newer Volcanics Province of Victoria – an inventory and evaluation of scientific significance. National Trust of Australia (Victoria) and the Geological Society of Australia (Victoria Division), Melbourne.
- Sutalo, F., Joyce, E.B. 2004. Long basaltic lava flows of the Mt. Rouse volcano in the Newer Volcanic Province of Southeastern Australia. *Proceedings of the Royal Society of Victoria* 116(1): 37-49.
- van Otterloo, J., Raveggi, M., Cas, R. in preparation. Mantle-derived polymagmatic activity at a monogenetic volcanic complex in the intraplate Newer Volcanics Province, S.E. Australia: new insights in the occurrence of intraplate volcanic activity in Australia.

A genetic model for basaltic volcanic fields, Jeju Island, Korea

Marco Brenna¹, Shane J. Cronin¹, Ian E.M. Smith² and Young Kwan Sohn³

¹ Volcanic Risk Solutions, Massey University, Palmerston North, New Zealand – m.brenna@massey.ac.nz

² School of Environment, The University of Auckland, Private Bag 92019, Auckland, New Zealand

³ Department of Earth and Environmental Sciences and Research Institute of Natural Sciences, Gyeongsang National University, Jinju, Republic of Korea

Keywords: intraplate alkali basalt, field evolution, trachyte.

Jeju Island (Fig. 1) is the sub aerial representation of a basaltic volcanic field, developed over continental crust and has formed over the last ~1.8 Ma. Initial volcanism was submarine, comprising dispersed, small-volume (<<1 km³) basaltic eruptive centres that built up a phreatomagmatic tuff pile, which was capped by lavas from continuing monogenetic volcanism, and since ~0.5 Ma voluminous (>1 km³) lavas, building a composite shield (Mount Halla).

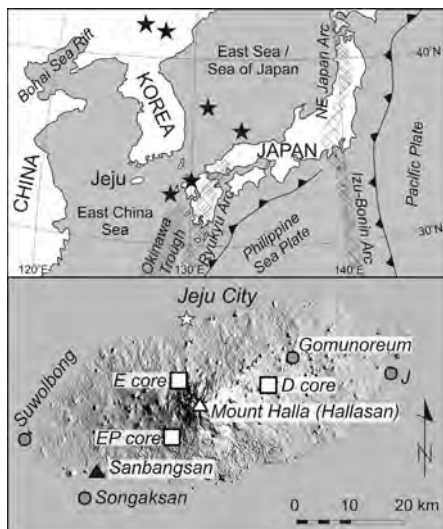


Fig. 1 – Tectonic setting and sampling localities.

Three magma suites: Early Pleistocene High-Al alkali (HAA), Late Pleistocene and Holocene Low-Al alkali (LAA) and Subalkali (SA) fed both small-volume and large-volume eruptions. The chemical similarity between small-volume and primitive large-volume eruptions suggests analogous parent magmas and fractionation histories independent of erupted volumes (Fig. 2). The large-volume magmas evolved to trachyte erupted in two distinct temporal episodes: the HAA Sanbongsan suite erupted c. 750 ka and the LAA Hallasan suite erupted c. 25 ka.

Major and trace element and isotope data (Fig. 2) suggest a common, shallower source for older monogenetic magmas and SA lavas, in contrast to a deeper source for younger monogenetic magmas. We propose that mantle melting was initiated near the garnet to spinel transition at pressures of ~2.5

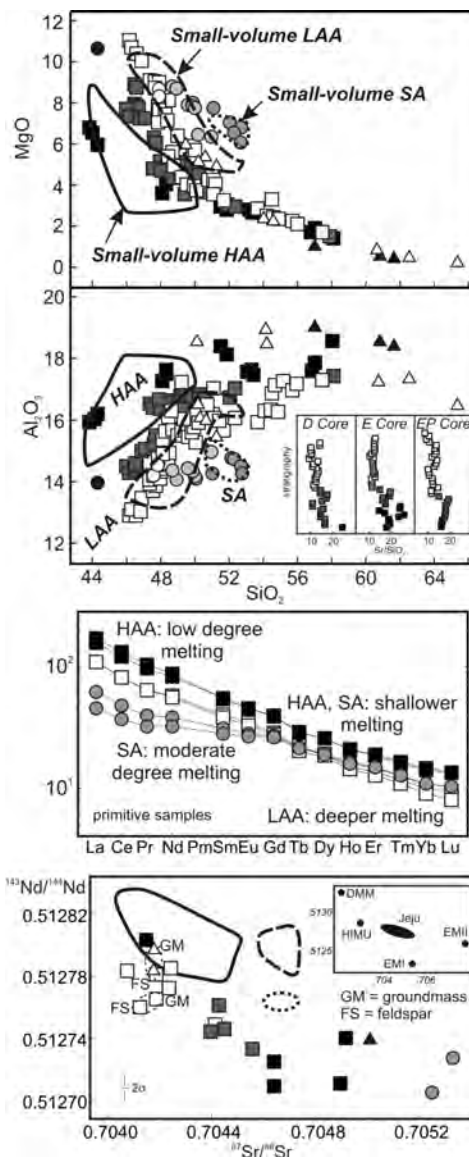


Fig. 2 – Chemical classification of Jeju large-volume samples and comparison with small-volume magma suites.

GPa. Later, as higher volumes of melt were produced from this zone the melting also extended deeper, reaching 3-3.5 GPa (Fig. 3). Samples transitional between HAA and LAA, and between LAA and SA indicate that melting occurred in discrete but adjacent mantle domains. Increasing

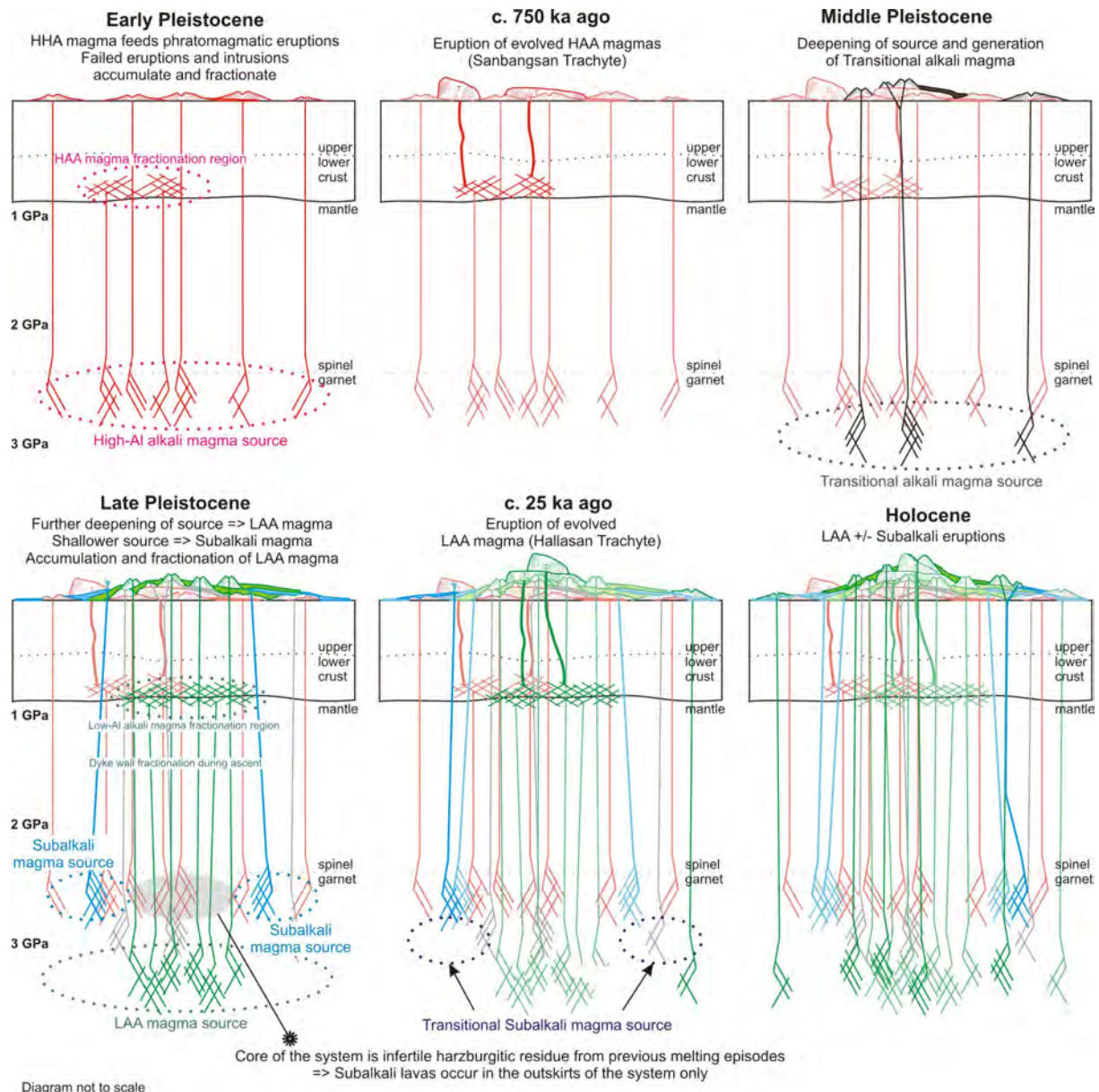


Fig. 3 – Conceptualized genetic model for the Jeju Island volcanic field.

melt production may have been related to the melting zone deepening process, or it may reflect higher rates of convective mantle upwelling. While not a classical plume, mantle upwelling in sheets or lenses below this volcano was probably focused along weak, sheared zones in the mantle created during the opening of the Sea of Japan/East Sea at around 15 Ma. These were probably reactivated as rotation of the subduction vector of the Philippine Sea plate occurred ~2 Ma ago.

The implication of this model (Fig. 3) is that the volume, proportion and depth of magma produced in the mantle are the dominant factors in determining the course of magmatic activity. Each magma batch subsequently acts as a monogenetic entity feeding an

independent, spatially distinct eruption. Therefore Mount Halla is not a classical polygenetic volcano, but rather, a “cumulative volcanic field”.

At Jeju, mantle upwelling appears to have been greater in the core of the system giving rise to an accumulation of monogenetic eruptions creating the central composite shield. Lower rates in distal parts of the field are reflected only by a continuation of small-volume monogenetic volcanism. These results imply that eruptions situated in the centre of long-lived monogenetic fields are more likely to produce larger volume, potentially more evolved and explosive lava outpourings, compared to those at the outer margins, and that eruptive activity in the field may be related to distal plate subduction activity.

The influence of subsurface hydrogeology on the nature and localisation of volcanism in the South Auckland Volcanic Field

Roger Briggs¹, Adrian Pittari¹ and Michael Rosenberg²

¹ Department of Earth & Ocean Sciences, University of Waikato, Hamilton, New Zealand – r.briggs@waikato.ac.nz

² GNS Science, Wairakei Research Centre, Private Bag 2000, Taupo, New Zealand

Keywords: South Auckland volcanic field, maars, basalt.

The Quaternary South Auckland volcanic field (SAVF) comprises at least 82 monogenetic basaltic volcanic centres, represented as either isolated volcanoes or grouped together if tuff rings/maars and scoria cones overlap. The SAVF covers an area of about 300 km², and is situated about 40 km south of the active Auckland Volcanic Field (100 km²; ca. 0.25 to 0.06 Ma; Edbrooke, 2001). K-Ar dating of basaltic crystalline groundmass from 43 of the centres in the SAVF produced ages ranging from 1.59 to 0.51 Ma, and the field is considered to be extinct. There are two peaks of activity at 1.3 and 0.6 Ma, although volcanic activity appears to be intermittent over the broad 1 Ma duration span of the field (Briggs et al. 1994). There are 38 tuff rings and maars formed from phreatomagmatic eruptions, and 17 scoria cones and 40 lava shields/cones produced from magmatic Hawaiian-Strombolian mainly effusive eruptions. In the central part of the field extensive basaltic lava flows from multiple centres overlap and intercalate with Quaternary sedimentary rocks, and have constructed broad shields, whereas on the periphery of the field the volcanic centres are isolated and generally smaller in volume.

The basalts of the South Auckland field can be divided into two broad groups (A and B) based on their petrography, mineralogy and geochemistry (Rafferty and Heming 1979; Briggs et al. 1994; Cook et al. 2005). Group A comprises silica-undersaturated hy-normative, transitional basalts, hawaiites, ol-tholeiitic basalts and alkali basalts. Group B comprises strongly silica-undersaturated ne-normative basanites, nephelinites, ne-hawaiites, mugearites and alkali ol-basalts. Ultramafic xenoliths of dunite, lherzolite, harzburgite and wehrlite are hosted in several basanite and ne-hawaiite lavas and tuff rings in the SAVF (Sanders 1994), and indicate rapid magma ascent. This is supported by the composition of the basaltic magmas, many of which have Mg numbers > 60 (Cook et al. 2005), implying little time for fractional crystallisation en route to the surface.

In this paper we have divided the SAVF into 4 areas based on the subsurface geology, which can be

demonstrated to play a major role in influencing the nature and localisation of volcanism.

Area 1 is situated in the northeast sector and is characterised by a block-faulted region of uplifted Mesozoic basement greywacke (Waipapa composite terrane, Edbrooke, 2001). Area 1 is bounded by the Drury Fault to the west and the Pokeno Fault to the south. These indurated sandstones have low porosity and host only fracture-controlled aquifers, properties that we infer to have limited the volcanism to predominantly magmatic or effusive styles. All 23 centres in Area 1 are strongly localised along block faults. The Mangatawhiri and Maketu tuff rings are the only exceptions and occur along Mesozoic/Quaternary boundary faults where groundwater would have been relatively available in hydraulically-active fault zones or in Quaternary alluvium.

Area 2 is situated in the northwestern sector in the structurally down-faulted block of the Manukau Lowlands, north of Waikato Fault and west of Drury Fault. This area is underlain by Pliocene, shallow marine and estuarine Kaawa Formation sandstone which overlies the Miocene Waitemata Group. The Kaawa Formation is known from numerous (>200) drillholes in the Manukau Lowlands to be highly porous (20-50%, average 35%) and permeable, well sorted thick sandstone (up to 250 m thick around Pukekohe and Tuakau). The Formation has high transmissivity (30-500 cm/s) and forms a high-quality aquifer in South Auckland (Greig et al. 1989). 26 out of a total of 38 tuff rings and maars in the SAVF occur in Area 2, and the Kaawa Formation is considered to have been the principal source of external water for phreatomagmatic eruptions. Further evidence for this is the presence of intact Kaawa Formation fossils and fossil fragments at discrete horizons within the tuffs in the Barriball Road tuff ring. Local drillhole data have shown Kaawa Formation fossiliferous shell beds 170-190 m below the surface (Ilanko 2010), so this could provide depths of fragmentation from magma-water interaction.

Area 3 covers the very low-lying sections of the Waikato River valley. A number of tuff rings and maars are situated in the valley now occupied by the

Waikato River where magma once rose into water-saturated Quaternary alluvium. The Onepoto scoria cone and lava field is a notable exception to the mostly phreatomagmatic styles, but there, high flux and volume of magma is assumed to have allowed progression to dry eruption styles.

The southwestern Area 4 sector is an uplifted block of Late Triassic to Early Cretaceous basement rocks south of the Waikato Fault. The basement rocks are indurated volcanogenic sandstones and siltstones of the Murihiku terrane, separated by a regional unconformity from Oligocene Te Kuiti Group calcareous siltstones, sandstones and limestones, overlain irregularly by the Miocene Waitemata Group. Volcanism in Area 4 was predominantly effusive and these vent locations were strongly controlled by regional-scale faults. The Mesozoic basement and overlying Te Kuiti and Waitemata groups all have low transmissivities and contain no known aquifers, so it is surprising that the largest tuff ring/maar (2.7 km diameter) in the SAVF (Onewhero, dated at 0.88 Ma) should occur in this area. However, Gibson (2011) noted the presence of foreign crystals of orthopyroxene, quartz, and plagioclase in Onewhero tuffs which do not occur as large crystals in any of the underlying formations but are common crystals in Quaternary alluvium. This block of Area 4 is known to have been tectonically uplifted during the Quaternary (Hochstein and Nunns 1976) along the Waikato Fault, and so the large volume of external water required for phreatomagmatic activity may have been derived from when Onewhero was situated in the low-lying Waikato River valley prior to 0.88 million years.

Many SAVF volcanoes are aligned along faults, with at least 10 along the Drury Fault and many along the Waikato Fault, Waiuku Fault and faults in the uplifted Hunua block or intersections of faults, e.g. the Maketu tuff ring. Ascent of magma may also have occurred along the intersection of faults with joints or bedding structures to form dike-sill

complexes, as shown in well-exposed coastal sections in the older intraplate fields of Ngatutura and Okete, and may explain why some centres are offset slightly from known faults.

References

- Briggs, R.M., Okada, T., Itaya, T., Shibuya, H., Smith, I. E.M. 1994. K-Ar ages, paleomagnetism, and geochemistry of the South Auckland volcanic field, North Island, New Zealand. *New Zealand Journal of Geology and Geophysics* 37: 143-153.
- Cook, C., Briggs, R. M., Smith, I. E. M., Maas, R. 2005. Petrology and geochemistry of intraplate basalts in the South Auckland volcanic field, New Zealand: Evidence for two coeval magma suites from distinct sources. *Journal of Petrology* 46: 473-503.
- Edbrooke, S.W. (compiler) 2001. *Geology of the Auckland area*. Institute of Geological & Nuclear Sciences 1:250 000 geological map 3. 1 sheet + 74 p. Lower Hutt, New Zealand: Institute of Geological & Nuclear Sciences Limited.
- Gibson, A.C. 2011. *Volcanology of tuff rings at Kellyville, Onewhero and Bombay, South Auckland volcanic field*. Unpublished MSc thesis, University of Waikato, Hamilton, New Zealand.
- Greig, D.A. 1989. *A study of the Kaawa Formation aquifer system in the Manukau Lowlands*, Technical Publication No. 85, Auckland Regional Water Board, Auckland.
- Hochstein, M.P., Nunns, A.G. 1976. Gravity measurements across the Waikato Fault, North Island, New Zealand. *New Zealand Journal of Geology and Geophysics* 19: 347-358.
- Ilanco, T. 2010. *Eruption and emplacement of the Barribal Road Tuff Ring, South Auckland*. Unpublished BSc(Hons) thesis, University of Waikato, Hamilton, New Zealand.
- Rafferty, W.J., Heming, R.F. 1979. Quaternary alkalic and sub-alkalic volcanism in South Auckland, New Zealand. *Contributions to Mineralogy and Petrology* 71: 139-150.
- Sanders, R.J. 1994. *Ultramafic and mafic xenoliths from the Okete, Ngatutura, and South Auckland volcanics*. Unpublished MSc thesis, University of Waikato, Hamilton, New Zealand.

Neogene monogenetic volcanoes from the northern Puna of Argentina, Central Andean plateau.

Pablo J. Caffè¹, Guadalupe Maro¹, Juan F. Presta², Patrocinio I. Flores¹ and Yesica Peralta³

¹ CONICET and Instituto de Geología y Minería, Universidad Nacional de Jujuy, Av. Bolivia 1661, CP 4600 San Salvador de Jujuy, Jujuy, Argentina – pabcaffè@idgym.unju.edu.ar

² CICTERRA – CONICET, Universidad Nacional de Córdoba, Córdoba, Argentina

³ Facultad de Ingeniería, Universidad Nacional de Jujuy, Jujuy, Argentina.

Keywords: Strombolian eruptions, northern Puna, andesites.

Mafic (basaltic andesite to andesite) volcanic rocks are rare in the Neogene volcanic record of the northern Puna (Fig. 1), an area dominated by voluminous silicic (dacite to rhyolite) ignimbrites and lavas sourced from large calderas or composite volcanoes (Coira et al., 1993) erupted during the Miocene to Pleistocene.

Most mafic volcanic rocks in the northern Puna were sourced from small scoria cones that are scattered across a 115 x 185 km area (Fig. 1) near the boundaries between Argentina, Chile and Bolivia (~70 km east of the current arc). Although scarce, understanding the eruption style of these volcanoes is relevant, because they behave in a similar way as basaltic volcanic centers that are the most common eruptive structures on Earth (Walker, 2000). Additionally, as the mafic rocks from Puna are coeval with the extensive dacitic ignimbrites, and the latter are considered as a mixture of 50:50 crustal/mantle magmas (Kay et al., 2010), the record of compositional variations in the mafic magmatism is also important for defining the mantle end-member in the dacitic Puna mix.

Fourteen scoria cones and related mafic lava flows were studied to define facies architecture and compositional variations. These centers comprise either small isolated edifices (e.g., Pabellón) with no relation to other volcanoes, or may be related to large composite volcanoes (e.g., Tropapete), but most frequently form amalgamated clusters of different size (15 km² – 120 km²) and complexity. Main mafic volcanic fields are aligned in the NNE-SSW direction (Fig. 1), coincident with the orientation of the principal Andean thrusts. Transverse, NW-SE and E-W faults that usually act as transfer structures (Petrinovic et al., 2006) also seem to have participated in the eruptions.

Almost all centers involve pyroclastic as well as lava flow units. Scoria cone remnants preserve their original shape, but are rather low in altitude (mean height ~70 m; mean height/basal diameter ~0.07), with external maximum slopes <16°. These parameters are consistent with moderate erosion due to arid climate, considering the Late Miocene-Early Pliocene ages of most edifices. Some cones (El

Toro, Campo Negro, Bitiche) show horse-shoe morphologies due to partial collapse caused by rafting during lava outpours.

Petrographic and geochemical composition is very variable, ranging between crystal-poor (3-10%) rocks with skeletal microphenocrysts of olivine and/or pyroxene, to well-crystallized and crystal-rich (~20-30%) plagioclase-pyroxene ± amphibole ± olivine phyric andesites.

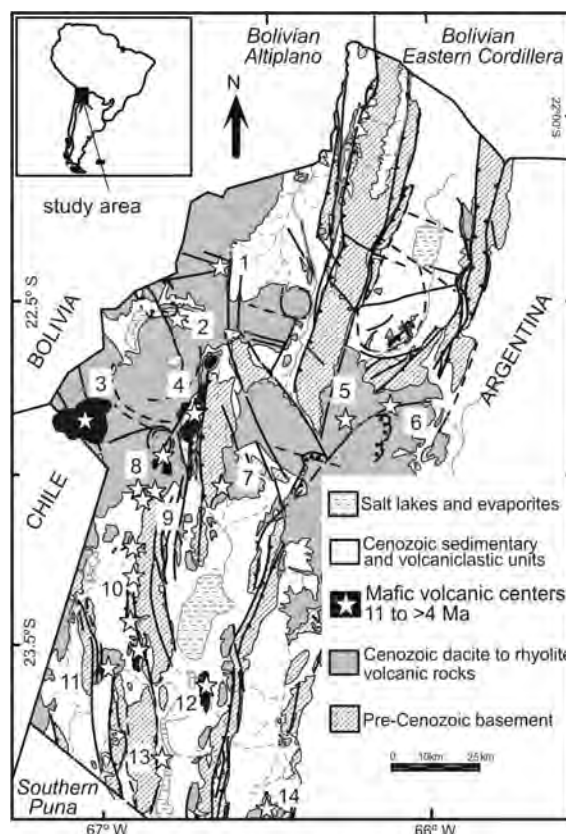


Fig. 1 – Geological map from the Argentine northern Puna and location of the mafic (basaltic andesite to andesite) volcanic rocks studied. 1-Pabellón, 2-Pululus, 3-Bitiche, 4-Cerro Morado, 5-Barro Negro, 6-Rachaite, 7-Campo Negro, 8-Patahuasi, 9-El Toro, 10-Jama, 11-Tropapete, 12-Cerro Negro, 13-Porvenir, 14-Tuzgle.

Geochemical compositions range between calc-alkaline basaltic andesite to andesite, with a few

centers (Rachaite, Barro Negro) transitionally trending to trachyandesite or shoshonite. Most of these rocks have SiO₂ contents (54-63 %) and Mg# values (>45) typical of high-Mg andesites (Kelemen et al., 2004). The most mafic samples fall in the Mg# range 60-67, overlapping with values shown by the scarce (pre-Neogene) Cenozoic basalts erupted in the Central Andes.

Lavas have slabby or massive aspects, some of them showing meso- to macro-scale sheath-like flow folding in flow fronts (e.g., Cerro Morado, Jama, El Toro), or compressional ridges in the top (e.g., Campo Negro). Blocky lavas are scarce, but remnants of *aa* surfaces are conserved occasionally (e.g., Cerro Negro) on top of massive lavas. In the contrary, blocky lavas are ubiquitous only in the Quaternary Tuzgle center. Stacking of flows and presence of partly eroded or well preserved rafted pyroclastic deposits dragged during eruption are common features. Rare pseudofiamme in a few lavas (Cerro Morado, El Toro) suggest origins by clastogenesis (Cabrera and Caffe, 2009). Only in Patahuasi, intrusive andesite bodies develop fluidal peperite margins or dispersion of fragments as small (<1 m) rounded pillows with blocky peperite margins that indicate in-situ brecciation during injection of magma in wet silicic volcanoclastic sequences.

Scoria cones exhibit typical facies of Strombolian edifices elsewhere (e.g., Vespermann and Schmincke, 2000). Recognized facies include: a) rare massive and cross bedded beds, interpreted as hydrovolcanic deposits formed during explosive encountering of magma and ground-water; b) unwelded spindle-shaped bomb and scoria deposits that dip away from the vent, typical of the external wall facies of the cone; c) minor beds of better sorted and finer material (ash or fine lapilli) interstratified with the coarser facies; d) interstratified beds of weakly welded scoria and moderately to strongly welded spatter in many rafts, and especially in layers that dip towards the interior of the edifice, interpreted as the internal wall and crater facies of the cone (e.g., El Toro, Cerro Morado, Jama); d) vertical to inclined lava dykes, as well as lava filling breaks in the cone, interpreted as the representant of the complex plumbing system that cut different parts of the cones.

From cone facies and morphology, as well as compositional correlation between deposits of several cones and lava flows, it is possible to infer that pyroclastic and effusive eruptions were probably concurrent, as is confirmed by abundant rafts of welded (internal) to unwelded (external) cone deposits on the top of lava flows. Eruptions had

a typical Strombolian style, with brief periods of fountaining and/or development of short-lived eruptive columns that alternated with the predominantly pulsatory Strombolian dynamics.

Estimated discharge rates (to 10-20 m³/s) deduced from lava flow lengths (Walker, 1973) and the absence of interruptions in the volcanic activity evidenced by the lack of paleosoils or interstratification of other volcanic rocks are consistent with a short eruptive life-span, as observed in monogenetic fields elsewhere.

Acknowledgements

Roberto Liquín, Agustín Cabrera, Marcelo Claros and Romina López Steinmetz are thanked for their help. This work was financed with grants from SeCTER-UNJU (08/E028) and CONICET (PIP 2010-2012 N° 204).

References

- Cabrera, A.P., Caffe, P.J. 2009. The Cerro Morado Andesites: Volcanic history and eruptive styles of a mafic volcanic field from northern Puna, Argentina. *Journal of South American Earth Sciences* 28 (2): 113-131.
- Coira, B., Kay, S.M., Viramonte, J.G. 1993. Upper Cenozoic magmatic evolution of the Argentine Puna. A model for changing subduction geometry. *International Geology Review* 35: 677-720.
- Kay, S.M., Coira, B., Caffe, P.J., Chen, C-H. 2010. Regional chemical diversity, crustal and mantle sources and evolution of central Andean Puna Plateau Ignimbrites. *Journal of Volcanology and Geothermal Research* 198: 81-111.
- Kelemen, P.B., Hanghoj, K., Greene, A.R. 2004. One view of the geochemistry of subduction-related magmatic arcs, with emphasis on primitive andesite and lower crust. In: Rudnick, R.L. (Ed.), *The Crust, Treatise on Geochemistry*, vol. 3. Elsevier, Netherlands, pp. 593-659.
- Petrinovic, I.A., Riller, U., Brod, J.A., Alvarado, G., Arnosio, M. 2006. Bimodal volcanism in a tectonic transfer zone: Evidence for a tectonically controlled magmatism in the Southern Andes, NW Argentina. *Journal of Volcanology and Geothermal Research* 152: 240-252.
- Vespermann, D., Schmincke, H.U. 2000. Scoria cones and tuff rings. En: Sigurdsson, H., Houghton, B., McNutt, S.R., Rymer, H., Stix, J. (Eds.), *Encyclopedia of Volcanoes*. Academic Press, San Diego, 683-694.
- Walker, G.P.L. 1973. Lengths of lava flows. *Philosophical Transactions of the Royal Society of London, Series A* 274: 107-118.
- Walker, G.P.L. 2000. Basaltic volcanoes and volcanic systems. In: Sigurdsson, H., Houghton, B., McNutt, S.R., Rymer, H., Stix, J. (Eds.) *Encyclopedia of Volcanoes*, pp. 283-290. Academic Press. San Diego.

Rhyolitic and basaltic maar volcanoes, a perspective from Mexican volcanism

Gerardo Carrasco-Núñez¹ and Michael H. Ort²

¹ Centro de Geociencias, Universidad Nacional Autónoma de México, Campus Juriquilla, Querétaro, Qro. 76230, México – gerardoc@geociencias.unam.mx

² SESES, Northern Arizona University, Flagstaff, Arizona, 86011, USA

Keywords: maar, rhyolite, basalt, volcano evolution.

Maar volcanoes result from the strong interaction of water, typically phreatic, and a rising magma. Variation in the explosivity and eruptive style is controlled by several parameters. General features observed in maar volcanoes of contrasting compositions indicate that the composition of magma plays an important role in the origin and evolution of these volcanoes. We explore those differences through the study of Mexican maar volcanoes.

In central Mexico, the three major maar volcano fields include San Luis Potosí, Valle de Santiago and Serdán-Oriental Basin (SOB). The latter two fields are part of the Neogene-Quaternary Mexican Volcanic Belt province, in contrast with the first one, which is Pliocene. Basaltic magmas are by the far the dominant type, except in the SOB.

The monogenetic volcanism that characterizes the SOB is dominated by basaltic and rhyolitic maar volcanoes and rhyolitic domes, with a minor occurrence of cinder cones. About a dozen maar volcanoes occur in the area (Gasca-Durán, 1981). Some (e.g. Alchichica; Aljojuca; Tecuitlapa, Ort and Carrasco-Núñez, 2009; Atexcac, Carrasco-Núñez et al., 2007) have a basaltic composition while others (e.g. Tepexitl, Austin-Erickson et al., 2011; Cerro Pinto, Zimmer, 2007, Zimmer et al., 2010) have a rhyolitic composition. There are, in general, strong morphological differences between the SOB's maar volcanoes depending on the composition of magma involved. For instance, basaltic maar volcanoes such as Tecuitlapa (Fig. 1) or Atexcac exhibit craters that extend much deeper into the pre-eruptive substrate than those related to rhyolitic magmas such as C. Pinto or Tepexitl (Fig. 2). The basaltic eruptions reached the local water table, causing the formation of a permanent lake in their crater's interior, in contrast to the rhyolitic volcanoes, which are shallower and never have a lake inside. Thus, basaltic volcanoes tend to form maars *sensu stricto*, exposing the country rock at the crater's basal interiors, or tuff cones, while the rhyolitic ones form tuff rings. Also, the basaltic maars generally form a more elongated crater, which in at least two cases (Tecuitlapa and Atexcac) seems to be related to clear

migration of the locus of the explosions. This is particularly evident at Tecuitlapa (Ort and Carrasco-Núñez, 2007).

These conditions may have some effects on the eruptive style and type of deposits for each case. Deposits of the basaltic maar volcanoes are generally surge-dominated and have more evidence of wet conditions, in contrast to the studied rhyolitic deposits, where deposits are fall-dominated sequences.



Fig. 1 – The Tecuitlapa basaltic crater is a typical example of a basaltic maar volcano in which a clear migration of the locus of explosivity is evident. The inner part of the crater is occupied by an E-W trending alignment of cinder and lava cones showing a younging trend to the east.

Most basaltic magma rises as dikes through the crust, and different conditions may exist along the dike during an eruption, leading to phreatomagmatic behavior concentrating in one part. Relatively narrow fractures can be used by basaltic magmas during their ascent. In contrast, the injection of highly viscous magmas to the upper crust may require wider conduits in order to avoid freezing and stopping their ascent. In the SOB area, several large rhyolitic domes (e.g. Cerro Pizarro, Las Derrumbadas and Cerro Pinto) had phreatomagmatic eruptions, but only in the case of Cerro Pinto were maar volcanic structures formed.

Molten fuel-coolant interaction (MFCI) is commonly thought to cause the repetitive water-

magma interaction in phreatomagmatic eruptions, particularly at basaltic magmas. Based upon field work at Tepexitl (Austin-Erickson et al., 2011) and laboratory experiments (Austin-Erickson et al., 2008), a viable mechanism for rhyolitic MFCI requires that water or fluidized sediments intrude marginal fractures in the rhyolite magma, creating enough interfacial surface area to initiate phreatomagmatic explosions from within the interior of a rising plug or dome. Tepexitl is situated in an area with a high water table, high sediment flux, basement faulting, and a recent history of high-silica dome intrusions that are periodically destroyed by successive explosive eruptions. The lack of lakes in the rhyolitic maars may be related to the need for a plug or dome to form, which raises the level of the magma surface. A temporary 'doming' of the water table caused by the intrusion of the magma may have created temporary lakes that could then inundate the domes and lead to phreatomagmatism. After the eruption, the water returned to its regional level, leaving no lake. In basaltic maars, the thin dike may not drive as much water out, so that the magma-water interaction occurs at or below the regional water table.

A feeder dike is a response of the regional state of stress that controls the distribution and orientation of weakness structures. It is possible that the nature of the country rock (hard rock versus soft sediments) and the structural configuration of the area involving the geometric patterns and intensity of fracturing are important factors controlling the volcanism and may be responsible of the migration of the locus of phreatomagmatic activity.



Fig. 2 – Tepexitl tuff ring is a typical rhyolitic maar volcano showing a shallow crater without an interior lake. These volcanoes are named in Mexico xalapaxcos. In the background is Las Derrumbadas rhyolitic twin domes, which are typically associated with the evolution of these rhyolitic maar volcanoes (Austin-Erickson et al., 2011).

Acknowledgements

This work is supported by both PAPIIT grant No. IN106810-3 and CONACYT grant (“solicitud”) No. 150900. Logistical support was provided by Centro de Geociencias (UNAM).

References

- Abrams, M., Siebe, C. 1994. Cerro Xalapaxco: an unusual tuff cone with multiple explosion craters, in central Mexico (Puebla). *Journal Of Volcanology and Geothermal Research* 63: 183–199.
- Austin-Erickson, A., Büttner, R., Dellino, P., Ort, M.H., Zimanowski, B. 2008. Phreatomagmatic explosions of rhyolitic magma: Experimental and field evidence. *Journal of Geophysical Research* 113: B11201, doi:10.1029/2008JB005731.
- Austin-Erickson, A., Ort, M., Carrasco-Núñez, G. 2011. Rhyolitic phreatomagmatism explored: Tepexitl tuff ring (Eastern Mexican Volcanic Belt). *Journal of Volcanology and Geothermal Research* 201: 325-341. doi:10.1016/j.volgeores.2010.09.007.
- Carrasco-Núñez, G., Riggs, N. 2008. Polygenetic nature of a rhyolitic dome and implications for hazard assessment: Cerro Pizarro volcano, Mexico. *Journal of Volcanology and Geothermal Research* 171: 307-315.
- Carrasco-Núñez, G., Ort, M.H., Romero, C. 2007. Evolution and hydrological conditions of a maar volcano (Atexcac crater, Eastern Mexico). “Maar-diatreme volcanism and associated processes”(Ed. Martin, U., Németh, K., Lorenz, V., White, J.) *Journal of Volcanology and Geothermal Research* 159: 179-197.
- Gasca-Durán, A. 1981. Génesis de los lagos-cráter de la cuenca de Oriental. *Colecc. Cient. Prehist.* 98 57 pp.
- Ort, M.H., Carrasco-Núñez, G. 2009. Lateral Vent Migration during Phreatomagmatic and Magmatic Eruptions at Tecuitlapa Maar, East-Central Mexico. *Journal of Volcanology and Geothermal Research* 181: 67-77.
- Riggs, N., Carrasco-Núñez, G. 2004. Evolution of a complex, isolated dome system, Cerro Pizarro, central Mexico. *Bulletin of Volcanology* 66: 322–335.
- Siebe, C., Macías, J.L., Abrams, M., Rodríguez, S., Castro, R., Delgado, H. 1995. Quaternary explosive volcanism and pyroclastic deposits in east central Mexico: implications for future hazards. *Geological Society of America Field Trip Guidebook*, 1–47.
- Zimmer, B.W. 2007. Eruptive variations during the emplacement of Cerro Pinto dome complex, Puebla, Mexico. MS thesis, Northern Arizona University, 119 pp.
- Zimmer, B., Riggs, N.R., Carrasco-Núñez, G. 2010. Evolution of tuff ring-dome complex: the case study of Cerro Pinto, eastern Trans-Mexican Volcanic Belt. *Bulletin of Volcanology*, 72, 1233-1240.

Influences on the location of the basaltic, continental Newer Volcanics Province, southeastern Australia, its diverse monogenetic volcanoes, and the highly variable eruption styles

Ray Cas, Joshua van Otterloo, Simone Jordan, Julie Boyce, Teagan Blaikie, Gemma Prata, Dan Uehara and Jackson van den Hove

MONVOLC, School of Geosciences, P.O. Box 28, Monash University, Victoria 3800, Australia.

Keywords: tectonic setting, aquifer distribution, crustal fracture conduits, magma ascent rates, aquifer recharge rates

The intraplate basaltic Newer Volcanics Province of western Victoria and southeastern South Australia, has an area of >25,000 km², is dominated by relatively small volume plains lavas, and preserves more than 400 volcanoes, including scoria cones, maars, shield volcanoes and complexes of the preceding (Figure 1). The NVP has an east-west orientation, parallel to the tectonic trend of the Otway Basin, a Gondwana break-up basin. The southern half of the NVP on-laps the northern margin of the Otway Basin, whereas the northern margin of the NVP on-laps the Palaeozoic metasedimentary basement, which has a north-northwest tectonic trend. Phreatomagmatic volcanoes are prominent in the southern half of the NVP where it overlies Tertiary aquifers of the Otway Basin. Volcanism commenced about 6 Ma, counter-intuitively, at a time when the crust of southeastern Australia experienced the onset of regional compression, probably originating from far-field stresses at the New Zealand margin of the Australia-India plate, which caused basin inversion of the Otway Basin and other break-up basins. It is speculated that volcanism may have been triggered by the interaction of east-southeast to west-northwest directed compressional stresses acting on pre-existing structural north-south and east-west crustal elements in the crust so initiating local trans-tensional domains that triggered decompressional melting of the upper mantle, and facilitated magma uprise. The NVP also lies in the region of the onland projection of the Tasman Fracture Zone, a major oceanic transform fault extending from Australia to Antarctica. It is unclear if the on-land projection of this major lithospheric structure at all influenced the location of the NVP.

Volcanoes are often aligned along lineaments and consist of clusters of eruption points forming linear alignments, indicating that crustal faults acted as conduits for magmas at both regional and local scales.

Volcanoes vary from simple scoria cones (e.g. Mt. Elephant), lava shields (Bald Hill, Mt Pollock, Warrion Hill) flow fields, and maar volcanoes (e.g. Purrumbete, Keilambete, Ecklin) to complex

volcanoes involving phases of both magmatic and phreatomagmatic explosive activity, multiple vents, and multiple coalesced maars and cones.

Many of these complex volcanoes are elongate in plan view, and vents are aligned along one or more linear trends, interpreted to represent the trace of feeder dyke fissure magma conduits in the sub-surface (e.g. Mts Schank, Gambier). In some cases, more than one such linear alignment of vents occurs (e.g. Tower Hill). Detailed ground geophysics, inversions and 3D forward modelling has allowed us to image the subsurface structure of some of these complex conduits, highlighting coalescence of maar craters (e.g. Red Rock, Mt Leura, Mt Noorat, Ecklin maar).

Detailed mapping of some volcanoes has allowed an eruption chronology and order of vent activity to be established. Stratigraphic relationships demonstrate that vents have migrated through time, and in some cases the opening of new vents has involved a change in eruption style (e.g. Mt Schank, Mt Gambier).

Establishing detailed stratigraphy and chronology of eruptive phases at individual volcanoes has allowed careful, stratigraphically controlled sampling for geochemistry to be undertaken. Although some multi-vent volcanoes were monogenetic and monomagmatic (e.g. Tower Hill, Mt Leura), others were monogenetic and polymagmatic, with at least two compositionally distinctive magma batches erupting contemporaneously (e.g. Mt Gambier, Red Rock, Mt Rouse). None of these show any evidence for a geologically significant time break within their stratigraphic successions.

In addition, in some of these complex volcanoes, there is an overall simple trend from phreatomagmatic maar forming eruption phase to magmatic scoria and spatter cone explosive eruption style (Mt Leura, Mt Noorat), or vice-versa (Mt Schank). In others, although there was an overall change from phreatomagmatic to magmatic, even during the phreatomagmatic stage, there were short-lived intervals of magmatic explosive interspersed

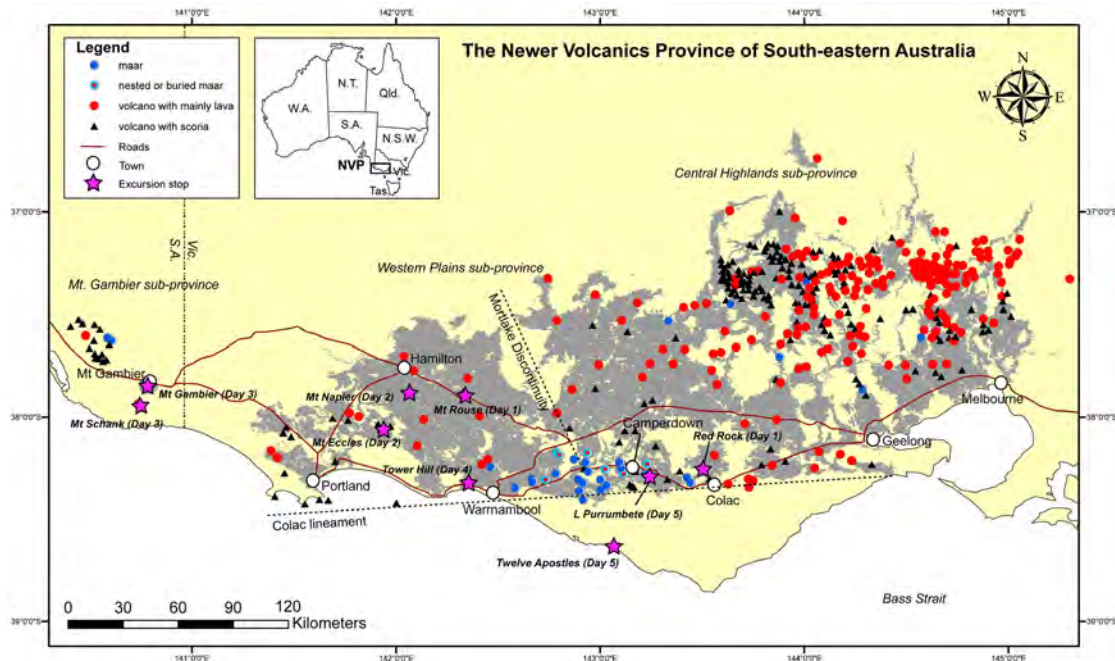


Fig. 1 - Map of the Newer Volcanics Province of southeastern Australia, showing the distribution of different volcano types.

with phreatomagmatic intervals, represented by scoria fallout deposits within the phreatomagmatic maar rim succession (e.g. Tower Hill Volcanic Complex). And even in simple maar volcano rim successions there are horizons of more vesiculated scoriaceous fallout deposits, reflecting variations in the degree of water:magma explosive interaction (e.g. Purrumbete and Ecklin maars).

The possible causes of these fluctuations in eruption style include:

1. Migration of vents along a fissure dyke from a location where an aquifer has high yield to a location where aquifer yield is low. That is, there are significant lateral changes in aquifer quality, which cause eruptions to be more magmatic in dry aquifer localities, and more phreatomagmatic in wet aquifer locations along the same fissure vent.
2. Changing magma discharge or ascent rates, causing a changing time scale for effective explosive magma-water interaction. Fast ascent rates minimize effective magma-water interaction leading to more magmatic explosive phases, whereas slow ascent rates optimize opportunities for efficient magma-water interaction.
3. Fuel-Coolant interaction cycles, causing fluctuations between efficient phreatomagmatic interaction and drier, perhaps even short-lived magmatic explosive activity on time scales of seconds.
4. Development of chilled basalt lining the conduit and limiting aquifer water access into the conduit. This could have a short term occlusion effect before such a lining fractures or fails so

allowing water access the vent again, or longer term effects eventually occluding water completely and causing a long term change to magmatic eruptive activity.

5. The existence of limited water aquifers, so leading to drying of the aquifer during the eruption as all water around the conduit is used up, causing a transition from phreatomagmatic to magmatic eruptive activity.
6. Aquifers with low permeability and water recharge rate into the magma conduit, leading to regular short-term fluctuations between magmatic and phreatomagmatic activity.
7. Episodic damage to aquifers by subsurface explosions that pulverize the aquifer host rock at the level of the fragmentation surface, which leads to at least temporary occlusion of porosity and severely reduced permeability. This would lead to reduced explosive magma-water interaction, represented by more magmatic phases of activity
8. Episodic repair and recovery of damaged aquifers, caused by build-up of aquifer pore water pressure, and flushing of pore blockages, so allowing explosive magma-water interaction to recommence.
9. Changing depth of the fragmentation surface as a maar diatreme is progressively excavated deeper during an eruption, leading to changing degrees of explosive magma-water interaction, depending on the aquifer/aquitard characteristics of the immediate country rock host.

A number of these causes may operate at any volcano.

Seasonal temperature variability during the past 1600 years recorded in the varved sediment from maar lake Sihailongwan and profiles from northeastern China

Guoqiang Chu¹, Qing Sun², Xiaohua Wang¹, Meimei Liu^{2,3}, Yuan Lin², Manman Xie¹, Wenyu Shang⁴ and Jiaqi Liu¹

¹ Key Laboratory of Cenozoic Geology and Environment, Institute of Geology and Geophysics, Chinese Academy of Sciences, Beijing 100029, China - chuguoqiang@mail.igcas.ac.cn

² National Research Center of Geoanalysis, Beijing 100037, China

³ Shanxi Experimental Institute of Geology and Mineral resources, Xian 710054, China

⁴ China University of Geosciences, Beijing 100083, China.

Keywords: Varved sediments, alkenone unsaturation index, documentary evidence.

Lake Sihailongwan, a closed maar lake, is located in northeastern China. Annually laminated sediments have been reported in earlier studies and provide a reliable time scale for paleoclimatic research in this data-sparse area (Mingram et al., 2004; Chu et al., 2005a; 2009; Schettler et al., 2006a, b).

Long chain alkenone (LCA) unsaturation index is well known for its use in marine paleotemperature reconstructions (Prah and Wakeham, 1987). The data from monthly sediment trap in maar Lake Sihailongwan indicated that there is little of alga during the ice-cover period for heavy snow limiting light into water (Chu et al., 2005a). So, the alkenone-based temperature should represent the water temperature in the growing season (ice-out period).

Based on the alkenone-based temperature reconstruction for growing season, the most notable cold spells occurred during the periods AD480-860, AD1260-1300, AD1510-1570 and AD1800-1900 with a temperature decrease of about 1 °C compared to the 20th century over the past 1600 years. Besides natural forcing factors (solar irradiance and explosive volcanism), the Pacific Decadal Oscillation (PDO) may play an important role in regulating the temperature for growing season in the studied area.

In the winter season, the lake was closed by heavy ice and snow. It is hard to get temperature. Based on the clear evidence such as “snow or frost in the summertime” and “no ice during the wintertime” in the historical documents, we compile extreme cold summer events and warm winter events over the past 1600 years. The Little Ice Age suffered more extreme cold summer/warm winter events, the Medieval Warm Period with milder winter. The winter extreme cold /warm events could be linked with the Arctic Oscillation (AO). The physical link between the AO and winter temperature may be link to changes in the frequency

and tracks of cold surge. In the negative phase of the AO, the higher pressure over the pole and weaker westerlies (southward) may induce an increasing of baroclinic waves along westerly zone and southward descent of the polar jet stream, which is in favor of the cold wave and snow occurrence in China.

We also compile seasonal temperature anomaly from historical documents over the past 1600 years. With this research, we hope to gain an overall view of the regional temperature variations from independent data.

Acknowledgements

This study was supported by the CAS Strategic Priority Research Program (Grant No. XDA05080400), Research Program of China (973 Program, 2010CB950201) and the National Natural Science Foundation of China (Grant no. 40972121).

References

- Prah, F.G., Wakeham, S.G. 1987. Calibration of unsaturation patterns in long-chain ketone compositions for palaeotemperature assessment. *Nature* 330: 367-369.
- Chu, G.Q., Liu, J.Q., Schettler, G., Li, J.Y., Sun, Q., Gu, Z.G., Lu, H.Y., Liu, Q., Liu, T.S. 2005a. Sediment fluxes and varve formation in Sihailongwan, a maar lake from northeastern China. *Journal of Paleolimnology* 34: 311–324.
- Chu, G.Q., Sun, Q., Li, S.Q., Zheng, M.P., Jia, X.X., Lu, C.F., Liu, J.Q., Liu, T.S. 2005b. Long-chain alkenone distributions and temperature dependence in lacustrine surface sediments from China. *Geochimica et Cosmochimica Acta* 69: 4985–5003.
- Mingram, J., Allen, J.R.M., Brüchmann, C., Liu, J., Luo, X., Negendank, J.F.W., Nowaczyk, N., Schettler, G. 2004. Maar- and crater lakes of the Long Gang Volcanic Field (N.E. China) – overview, laminated sediments, and vegetation history of the last 900 years. *Quaternary International* 123-125: 135-147.
- Schettler, G., Liu, Q., Mingram, J., Negendank J.F.W. 2006a. Palaeovariations in the East-Asian monsoon

regime geochemically recorded in varved sediments of Lake Sihailongwan (Northeast China, Jilin province). Part 1: Hydrological conditions and dust flux. *Journal of Paleolimnology* 35: 239-270.

Schettler, G., Liu, Q., Mingram, J., Stebich, M., Dulski, P. 2006b. East-Asian monsoon variability between 15000 and 2000 cal. yr BP recorded in varved sediments of Lake Sihailongwan (northeastern China, Long Gang volcanic field). *The Holocene* 16: 1043-1057.

Insights into monogenetic volcanism from paired studies of two contrasting Quaternary continental volcanic fields – Auckland (New Zealand) and Jeju (Republic of Korea)

Shane Cronin¹, Young-Kwan Sohn², Ian Smith³, Karoly Nemeth¹, Marco Brenna¹, Mark Bebbington¹, Gabor Kereszturi¹, Javier Agustin Flores¹, Lucy McGee³, Chang-Woo Kwon², Jan Lindsay³ and Gill Jolly⁴

¹ *Volcanic Risk Solutions, Massey University, Palmerston North, New Zealand – s.j.cronin@massey.ac.nz*

² *Geyongsang National University, Jinju, Republic of Korea*

³ *School of Environment, University of Auckland, Auckland, New Zealand*

⁴ *GNS Science, Wairakei Research Centre, Taupo, New Zealand*

Keywords: hazard, Auckland, Jeju, monogenetic volcanism

A three-year collaborative partnership project between researchers from the Republic of Korea and New Zealand, funded by paired government research grants, is moving toward completion in 2012. This project set out to achieve, via comparing and contrasting background knowledge and targeted new multidisciplinary studies, an integrated understanding of: (1) the evolution of the magmatic feeding systems of small-volume monogenetic volcanism; (2) magmatic and environmental factors controlling eruption types and processes; (3) probabilistic models for forecasting spatio-temporal eruption hazards; and (4) integration of geological information into models of economic impact for future monogenetic volcanism in urbanised areas.

These two volcanic areas have predominantly involved alkali basaltic-series magmatism, with the longer-lived Jeju (1.6 Ma to the present) having produced a greater range in volcanic compositions (extending to trachytes and sub-alkali basalts) and a polygenetic-like composite shield structure with the largest-volume eruptions in its central part. By contrast, the Auckland field (0.25 Ma to present) has only around 50 eruptive centres, with a tight range in erupted volumes and compositions, although notably including also sub-alkaline lavas in its most recent eruption. The older sibling, Jeju, has been drilled many hundreds of times, and during this project around 10 new drill cores were completed, allowing access to high-quality samples in stratigraphic sequences extending up to 600 m through the volcanic pile and into the sediments below.

In general terms, the Jeju example shows how following the onset of extraction of deep mantle (3.5 GPa) magmas in small isolated batches, the melting column increased in length, extending to shallower levels in the mantle, and producing consequently larger-volume magmas to feed lava flow-producing eruptions. Some of these larger magmas were able to stall and fractionate toward trachytic compositions. As this process continued, sub-alkalic basalts were also generated in the still-fertile mantle surrounding the central melting

anomaly. At Auckland, while this range in compositional evolution is not seen, the general tendency is for the larger alkali-series eruptions to occur in the centre of the field, causing several partly overlapping volcanoes. The latest sub-alkali magma was erupted from the outer limits of the Auckland field, mirroring the pattern seen on Jeju.

In the case of both Jeju and Auckland, the volcanism appears to relate to localized mantle upwelling along sheared zones developed in relation to rotation of distal subduction zones (600-1000 km distant). These distal plate-boundary processes may also play a role in influencing this intraplate volcanism, such as with the triggering and onset of an isolated burst of activity at Auckland between 40-25 ka, for example, corresponding in timing to plate-boundary related processes, including increases in subduction related volcanism in NZ.

Via extremely detailed geochemical sampling at fine intervals vertically through tuff cone/scoria cone and lava sequences at Jeju, we have derived new models for the feeding systems for individual monogenetic eruptions. It appears that many monogenetic eruptions sample small batches of magma pre-existing in the mantle. A triggering event may engender the rise of multiple magma batches that either follow a single conduit system or develop separate upper-level pathways to produce complex multiple, closely-spaced vents. These magmas may be produced from different depths within the mantle, but can be distinguished by exhibiting individual chemistries and separate fractionation trends. Transitions between one magma type and the next can be marked by transitions in behaviour from phreatomagmatic to magmatic (tuff to scoria), or from unconformities marking short (hours) to long (weeks) breaks in the eruption progression. In Auckland, where the volcanoes are generally smaller in volume than the Jeju examples, typically only single magma batches are erupted with limited compositional variation. The largest of Auckland eruptives show the greatest chemical variation, with the latest showing the presence of two magma batches.

A study of the diffuse emissions of CO₂ in the Michoacan-Guanajuato monogenetic volcanic field (Mexico)

Ramón Espinasa-Pereña¹, Mariana Patricia Jácome Paz² and Hugo Delgado Granados¹

¹ Instituto de Geofísica, UNAM, Ciudad Universitaria, 04510, México City, México – hugo@geofisica.unam.mx

² Facultad de Ciencias, UNAM, Ciudad Universitaria, 04510, México City, México

Keywords: CO₂, degassing, Michoacan-Guanajuato volcanic field.

Monogenetic volcanism is commonly characterized by relatively short-lived, isolated eruptions of basaltic or basaltic-andesite magma, producing tephra cones and lava flows that rarely reactivate. Magma degassing has frequently been used in monitoring active volcanoes with the intention of predicting possible eruptions (Chiodini, 1997; Inguaggiato, 2011; Carapezza, 2004, Varley and Taran, 2003) or for field evidence of faults and fractures, showing those as high concentration CO₂ points (Giammanco, 1997; Chiodini, 1997).

At mafic monogenetic volcanoes degassing of volatiles from magma has been studied for ascent, crystallization and eruption (e.g. Johnson et al., 2010), but rarely has been used for prediction of the next eruption in the entire field or for degassing after

eruption been considered. However, emissions of gas associated with monogenetic volcanoes can be surprisingly large and long-lived (Evans et al., 2009), and can even produce changes in the solidified lava composition (Kuritani & Nakamura, 2006).

We present here a new methodology, aiming to forecast the next weakness zone in the entire field using the diffuse degassing as main indicator, using a portable instrument with accumulation chamber and IR spectrometer for the CO₂ soil flux.

We present results of measurements of passive degassing at the youngest cone of the monogenetic field: Parícutin volcano, 60 years after the end of eruption; the Jorullo volcano and other locations monitored for the last three years.

Greenhouse gases and deglaciation at the Oligocene/Miocene boundary: palaeoclimate evidence from a New Zealand maar lake

Bethany Fox^{1,2}, Matthew Haworth³, Gary Wilson^{2,1}, Daphne Lee¹, Jo-Anne Wartho⁴, Jennifer Bannister⁵, Daniel Jones¹, Uwe Kaulfuss¹ and Jon Lindqvist¹

¹ Department of Geology, University of Otago, PO Box 56, Dunedin, New Zealand – bethany.fox@otago.ac.nz

² Department of Marine Science, University of Otago, PO Box 56, Dunedin, New Zealand

³ CNR - Istituto di Biometeorologia (IBIMET), Florence, Italy

⁴ School of Earth and Space Exploration, Arizona State University, Tempe, Arizona, USA

⁵ Department of Botany, University of Otago, PO Box 56, Dunedin, New Zealand

Keywords: palaeoclimate, Miocene, deglaciation

Foulden Maar is an annually-resolved maar lake deposit dating from the Oligocene/Miocene (O/M) boundary. The deposit, from the South Island of New Zealand, is the first high-resolution terrestrial record of the O/M boundary and the rapid deglaciation of Antarctica that occurred during the second half of the Mi-1 event (Wilson 2008). A ~180 m core from the centre of the lake bed comprises ~60 m of basal graded breccias, sands and muds overlain by ~120 m of diatomite punctuated by volcanogenic horizons. The basal siliciclastic sediments contain clasts of basalt and country rock and are interpreted as diatreme breccias coeval with the formation of the maar (Jones et al., in prep.).

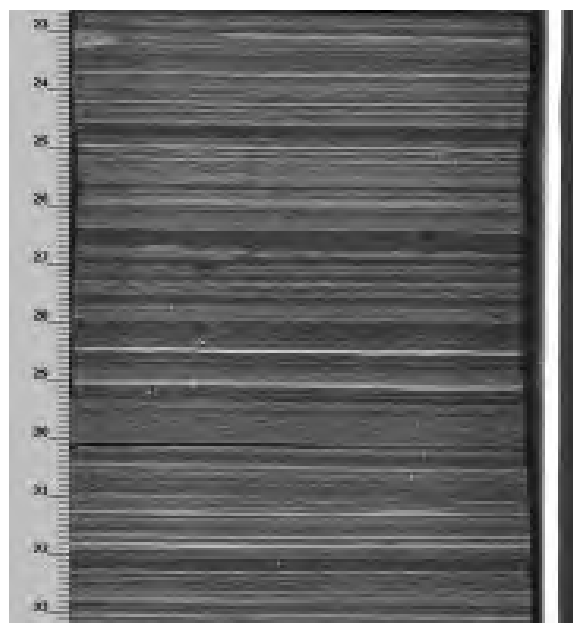


Fig. 1 – A 10-cm section of the diatomaceous section of the Foulden Maar core. Note the finely-laminated background sedimentation and mm-scale turbidite beds.

⁴⁰Ar/³⁹Ar laser step-heated whole rock dates were obtained from basaltic clasts found at ~110 m depth (close to the base of the diatomite succession) in a slump deposit of crater wall material. These

give ages of 23.38 ± 0.24 Ma (2σ including J value error, Mean Square of Weighted Deviation (MSWD) = 0.68, probability = 0.74, containing 69.8% of the ³⁹Ar) and 24.51 ± 0.24 Ma (2σ including J value error, MSWD = 0.58, probability = 0.82, containing 57.7% of the ³⁹Ar). A nearby basaltic dyke formed during the same episode of volcanism as the maar crater gives a date of 23.17 ± 0.17 Ma (Lindqvist and Lee 2009). A magnetic reversal occurs at ~106 m depth in the core, constraining the age of this point to 23.35 Ma (the base of chron C6Cn.3n) or 23.03 Ma (the base of chron C6Cn.2n) (Billups et al. 2004). Spectral analysis of physical properties measurements of the diatomite section of the core reveals obliquity and precessional frequencies. An age model based on these frequencies shows that individual light-dark couplets of diatomite represent annual varves and that the normally magnetised section from ~106 m depth to the top of the core covers ~100,000 years. This rules out C6Cn.3n, which is only 50,000 years long, placing the base of the diatomite succession at 23.03 Ma, the Oligocene-Miocene boundary and the peak of the Mi-1 event.

The diatomite succession consists of mm- to sub-mm-scale light-dark couplets and diatomaceous turbidites. The light layers consist almost entirely of diatom frustules and are interpreted as representing diatom blooms. The dark layers are still largely diatomaceous, but also contain some organic matter, sponge spicules and resting spores. Throughout most of the succession, light layers are thicker than dark layers and vary in colour from yellow to cream. However, in some intervals, light layers are less variable and much darker, ranging from brown to almost black. These intervals have higher terrigenous content and last for a few thousand years. They are interpreted as periods of poor growing conditions within the lake, suggestive of climatic deterioration. The proportion of the succession represented by these dark intervals decreases upcore, suggesting a general trend towards more favourable conditions, which may be

connected to the global warming associated with the end of the Mi-1 event.

Wavelet analysis of high-resolution RGB data shows that 2-8 year ENSO-scale cycles are present throughout the diatomite succession. These cycles are modulated by a 2000-year signal, similar to that found in present-day ENSO records (Moy et al. 2002). Millennial-scale cycles are also present and may be related to glacial advance and retreat.

The diatomite succession preserves a large number of fossil leaves with cuticles intact. We have collected stomatal index values from *Litsea* and *Podocarpus* leaves found in the succession. The *Podocarpus* values are calibrated using *Podocarpus* plants grown at atmospheric carbon dioxide levels of 380 ppmv at 1500 ppmv. The *Litsea* values are calibrated using published SI values for various *Litsea* species of similar morphology and inferred ecology (the NLE approach, McElwain and Chaloner 1996). Our results show an atmospheric carbon dioxide level of ~400 ppmv at ~23.01 Ma (77 m depth below the top of the core), with concentration increasing to ~800-1200 ppmv at ~22.98 Ma (55 m) and dropping back to ~400-600 ppmv at ~22.9 Ma (0 m, the present-day surface outcrop). This short-lived, rapid increase in atmospheric carbon dioxide concentration coincides with the initiation of the deglaciation phase of the Mi-1 event and implies that CO₂ was the driver of this deglaciation.

Acknowledgements

Funding for this project was provided by the Marsden Fund of the Royal Society of New Zealand. We are grateful for the assistance of Featherstone Resources, Webster Drilling and the Gibson and MacRae families.

References

- Billups, K., Pälike, H., Channel, J.E.T., Zachos, J.C., Shackleton, N.J. 2004. Astronomic calibration of the late Oligocene through early Miocene geomagnetic polarity time scale. *Earth and Planetary Science Letters* 224: 33–44.
- Jones, D., Wilson, G.S., Gorman, A.R. In prep. Geophysical characterisation of the Foulden Maar, Waipiata Volcanic Field, southern New Zealand.
- Lindqvist, J.K., Lee, D.E. 2009. High-frequency paleoclimate signals from Foulden Maar, Waipiata Volcanic Field, southern New Zealand: An Early Miocene varved lacustrine diatomite deposit. *Sedimentary Geology* 222: 98–100.
- McElwain, J.C., Chaloner, W.G. 1996. The Fossil Cuticle as a skeletal record of environmental change. *Palaios* 11: 376–388.
- Moy, C.M., Seltzer, G.O., Rodbell, D.T., Anderson, D.M. 2002. Variability of El Niño/Southern Oscillation activity at millennial timescales during the Holocene epoch. *Nature* 420: 162–165.
- Wilson, G.S., Pekar, S.F., Naish, T.R., Passchier, S., DeConto, R. 2008. The Oligocene–Miocene Boundary – Antarctic Climate Response to Orbital Forcing, in Florindo, F., and Siegert, M., eds., *Antarctic Climate Evolution. Developments in Earth and Environmental Sciences* 8: 369–400.

Morphological and chemical diversity of maars in Central Anatolian Volcanic Province (Turkey)

Gonca Gençalioğlu Kuşcu¹, Karoly Nemeth² and Robert B. Stewart²

¹ Department of Geological Engineering, Muğla University, Kötekli, Muğla, Turkey – gkuscu@mu.edu.tr

² Volcanic Risk Solutions, Massey University, Palmerston North, New Zealand

Keywords: Turkey, Cappadocia, monogenetic volcanism

Neogene-Quaternary Central Anatolian Volcanic Province (CAVP) (also known as the Cappadocian Volcanic Province) hosts around 800 monogenetic volcanoes. Majority of these are scoria cones, while maars and domes are subordinate in number. These small-volume volcanoes are mainly clustered in five locations (Toprak, 1998) (Fig. 1).

There are at least eleven maars identified within the CAVP (Fig. 1). Majority of the maar volcanoes are concentrated in the southwestern part of the CAVP, namely in Karapınar region and Eğrikuyu region between Karacadağ and Hasandağ.

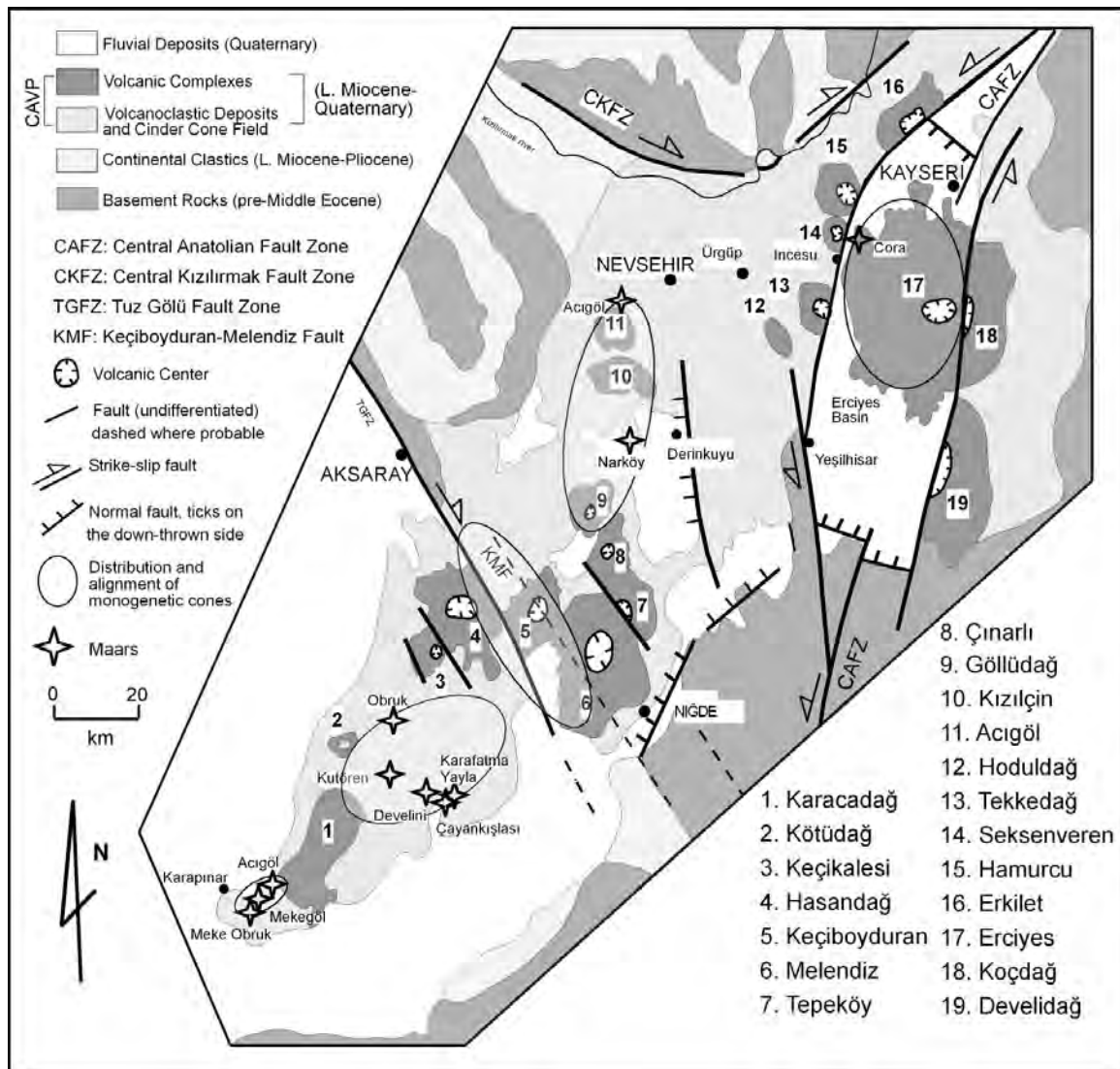


Fig. 1 – Map of the Central Anatolian Volcanic Province (from Toprak, 1998) showing the distribution of monogenetic volcanoes and location of maar volcanoes.

Maars of the CAVP and their tephra deposits are usually well-preserved and display some interesting depositional features (e.g., Cora Maar in the Erciyes Volcanic Complex, Gençalioğlu Kuşcu et al. 2007). Some of the maars reflect a complex origin with clear evidence for time breaks during eruption (e.g., Mekegölü Maar), while others show evidence for a single eruption (e.g., Mekeobruk Maar). Some of the maars presently have a lake (e.g., Acıgöl-Karapınar and Narköy Maars), yet others do not have a lake (e.g., Kutören and Obruk Maars). The close association of maars and scoria cones (as in Mekegölü, Mekeobruk, Kutören, and Obruk Maars), or domes (as in Acıgöl Maar-Nevşehir) reflects the interplay between phreatomagmatic and magmatic fragmentation mechanisms (Fig. 2).

Depending on the lithology they cut through, CAVP maars are two types. Broad and shallow maars which erupted through a soft substrate include Kutören, Obruk and Karafatma Yayla Maars in the Eğrikuyu region, and Acıgöl Maar in Nevşehir region. Cora Maar in the Erciyes Volcanic Complex and Narköy Maar in the Derinkuyu region are examples to steep-sided and deep maars which erupted through solid rock.

Although the CAVP maars are well-preserved and display some interesting characteristics, there is

generally a lack of detailed information on their formation and eruption style.

There is no complete data set on the composition of most CAVP maars, either. Based on the available studies so far, they are generally mafic in composition. The only exception is the Acıgöl Maar in Nevşehir region which is rhyolitic.

According to Keller (1974) maars in the Karapınar region are alkaline basalts. Although the Quaternary monogenetic volcanoes in the CAVP are generally considered to be alkaline, Cora Maar scoria is basaltic andesitic (Gençalioğlu-Kuşcu, 2011). Gençalioğlu-Kuşcu (2011) suggests that Cora Maar scoria is geochemically comparable to other CAVP monogenetic basalts, and display geochemical evidence for derivation from a shallow, garnet-free source, i.e. the lithospheric, not the asthenospheric mantle.

The morphological diversity of the maars, variety of magma compositions involved, polygenetic nature of some maars, well preserved maar tephra sequences, close association of maars and scoria cones make the CAVP an ideal place to study monogenetic volcanism. Therefore detailed research on physical volcanology and petrogenesis of the maars in this natural laboratory can contribute to better understanding of monogenetic volcanism.



Fig. 2 – General view of the Kutören Maar and scoria cone

References

- Gençalioğlu-Kuşcu, G. 2011. Geochemical characterization of a Quaternary monogenetic volcano in Erciyes Volcanic Complex: Cora Maar (Central Anatolian Volcanic Province, Turkey). *International Journal of Earth Sciences* 100: 1967-1985.
- Gençalioğlu-Kuşcu, G., Atilla, C., Cas, R.A.F., Kuşcu, I. 2007. Eruption History, Vent Development and Depositional Processes of a Wet Phreatomagmatic Volcano in Central Anatolia (Cora Maar). *Journal of Volcanology and Geothermal Research* 159: 198-209.
- Keller, J. 1974. Quaternary maar volcanism near Karapınar in central Anatolia. *Bulletin of Volcanology* 38: 378-396.
- Toprak, V. 1998. Vent distribution and its relation to regional tectonics, Cappadocian volcanics, Turkey. *Journal of Volcanology and Geothermal Research* 85: 55-67.

The Messel Maar, Germany – Correlation of fossil contents on the basis of marker horizons

Gabriele Gruber

Hessisches Landesmuseum Darmstadt, Friedensplatz 1, 64283 Darmstadt, Germany - gabriele.gruber@hlmd.de

Keywords: paleontology, sedimentology, Eocene

The Messel Maar near Darmstadt, since 1995 UNESCO World Natural Heritage site, is famous for its perfectly preserved and highly diverse fossil record. Since the first discovery of fossils in 1875, the Hessisches Landesmuseum Darmstadt (HLMD) built up a large Messel collection. Biostratigraphically the Messel Formation represents the European Land Mammal Age (ELMA) Geiseltalium, mammal level MP 11 (Middle Eocene; Franzen and Haubold 1986). In 2001 a drilling project (“Forschungsbohrung Messel 2001”; e.g., Felder and Harms 2004) reached a depth of 433 m and revealed that the Messel Formation was deposited in an ancient maar lake. Radiometric dating of juvenile volcanics from the diatreme tuff yielded an age of 47.8 ± 0.2 Ma (Mertz and Renne 2005). The sediments filling the diatreme correlate well with the maar lithozones introduced by Pirrung (e.g. Pirrung et al. 2003) for the Eckfeld and the Döttingen Maar in the Eifel.

Despite the fact that thousands of fossils have been excavated and studied, taphonomical research aiming at both, a general correlation of facies and fossil contents and on correlations among the fossils themselves is still at its beginning. First studies have already been published by Franzen (1978, 1979) and Franzen, Weber and Wuttke (1982). However, besides these only a few more studies have been published e.g. concerning arthropods (Lutz 1991) and fish (e.g., Micklich 2002).

Besides authigenic minerals like Messelite which occurs only irregularly forming small nodules (< 5 mm) and Montgomeryite which builds up the conspicuous marker horizon (“M”), Siderite is most common. It is not equally distributed over the oilshale but primarily forms discrete laminae which may build up thicker siderite rich sequences. Thus, the question arises if in Messel correlations between siderite-facies and the vertical distribution of fossils can be shown like this has been done for the Eckfeld Maar (e.g., Lutz 2000, Lutz and Kaulfuss 2006) and how it is described by Franzen (2007).

In the core drilled in 2001 near the centre of the pit three of the marker horizons known from the excavations (α , β) have been observed. This allowed the construction of a “standard profile” which we are now using for a correlation of sedi-

mentological and taphonomical data from different excavation sites. However, we have to keep in mind that – due to the rather large lateral distances between our excavation sites – we cannot exclude lateral variations in thickness of turbidites. In consequence our results have to be discussed with care, always considering that we are working with average values.

From our field work paleontological information is available for the upper 40 meters of the “standard profile”. Due to excavating techniques in many cases we have to use mean values for the stratigraphic position of fossil finds within oilshale slabs up to 20 cm thick. Taxa used for the correlation are fish, amphibians, reptiles, bats, birds and mammals, which not only have different lifestyles but also different biostratonomical characteristics.

The relative abundances and occurrences of fossil groups above and below the reference layers do not significantly differ from each other. Furthermore, profile sections with many fish also yielded comparatively frequent records of other groups. This, however, can also be an artifact of the excavation procedure. In the main frequencies intensively excavated profile sections generally also the most of all fossil taxa can be expected. On the other hand, gaps can also result from peculiar oilshale sections which were not as easily accessible as others. Looking in detail, the faunal diversity above “M” is larger than below this horizon. It is unclear whether this is also an artifact of the excavation activities. The area which was available for the excavation below “M” was considerably smaller than the one above. Nevertheless, we mainly focus on the distribution patterns below “m” because these were excavated very accurate in a special excavation project (Micklich and Drobek 2007). Here it can be noticed that the aquatic taxa like fish mainly occur in the upper and in the lower profile sections and are comparatively sparse in the middle part. Disregarding the general low frequency of all fossils below “M” it can be stated that the reptiles (mainly crocodylian teeth) only occur in the uppermost part (where fish were abundant) and that birds dominate the bats. This distribution pattern might indicate that the living conditions for aquatic organisms were less favorable in the middle part of the profile (22.15 to

21.20 m). Regarding bats it may be concluded that there were no steady negative events which may have caused increased mortality for longer periods of time (10 cm correspond to c. 1000 years). The fact that the fossil distributions do not significantly differ above or below the marker horizons indicates that their chemical precipitation or sedimentation did not have a significant influence on the lake's hydrology and the living conditions of aquatic taxa, respectively. Unfortunately, up to now for this sediment sequence there is no information available concerning the quantitative vertical distribution of siderite like it is the case for greater parts of the Eckfeld Maar profile. There siderite formation obviously strongly influenced both life in the lake and the taphonomical processes (e.g. Lutz and Kaulfuss 2006).

The oilshale sections which are excavated at the so-called "turtle hill" (grid square HI7, Schaal 2004, Fig. 1), are close to marker horizon γ (Harms et al. 2005). Here records of turtles seem to be more frequent than at other excavation sites. Further peculiarities are the comparatively high frequency of percoids (*Palaeoperca proxima* and the small-sized of *Rhenanoperca minuta*) which both are rare or absent at other sites. By contrast to other excavation sites the bowfin *Cyclurus kehreri* and the gar *Atractosteus trausi* are also represented by comparatively small individuals. This may indicate that the sediments cropping out at this place have been deposited in a developmental stage of the ancient lake which was characterized by peculiar environmental conditions for at least the fish fauna (Franzen 1979, Micklich 2005). Unfortunately, this stratigraphic level is not accessible at other locations within the pit. To provide further quantitative evidence at this site we started to collect detailed stratigraphical data since three years ago. These data will be correlated with microfacies analyses with special focus on authigenic minerals like siderite.

Acknowledgements

My thanks go to my colleagues Norbert Micklich and Sabine Gwosdek, HLMD, for information on the excavations and critical discussions. Herbert Lutz, Mainz, I thank for fruitful discussions and his comments concerning the manuscript.

References

- Felder, M. and Harms, F.-J. 2004. Lithologie und genetische Interpretation der vulkano-sedimentären Ablagerungen aus der Grube Messel anhand der Forschungsbohrung Messel 2001 und weiterer Bohrungen. Courier Forschungsinstitut Senckenberg 252: 151-203.
- Franzen, J.L. 1978. Senckenberg-Grabungen in der Grube Messel bei Darmstadt. 1. Probleme, Methoden, Ergebnisse 1976-1977. Courier Forschungsinstitut Senckenberg 27: 135 pp.
- Franzen, J.L. 1979. Senckenberg-Grabungen in der Grube Messel bei Darmstadt. 2. Ergebnisse 1978. Courier Forschungsinstitut Senckenberg 36: 144pp.
- Franzen, J.L. 2007. Eozäne Equoidea (Mammalian, Perissodactyla) aus der Grube Messel bei Darmstadt (Deutschland). Funde der Jahre 1969-2000. Schweizer paläontologische Abhandlungen: 1-254.
- Franzen, J.L., Haubold, H. 1986. The Middle Eocene of European mammalian stratigraphy. Modern Geology 19: 159-170.
- Franzen, J.L., Weber, J., Wuttke, M. 1982. Senckenberg-Grabungen in der Grube Messel bei Darmstadt. 3. Ergebnisse 1979-1981. Courier Forschungsinstitut Senckenberg 54: 118 pp.
- Harms, F.-J., Hottenrott, M., Micklich, N. 2005. The Messel Pit. Kaupia 14: 107-112.
- Lutz, H. 1991. Qualitative und quantitative Verteilung von Kleinfossilien im Bereich des Nordwesthangs der Fundstätte Messel (Mittel-Eozän). Courier Forschungsinstitut Senckenberg 139: 83-97.
- Lutz, H. 2000. Correlation of facies and fossil contents in meromictic lakes - the example Eckfeld Maar. In: International Maar Conference, August 2000, Daun/-Eifel. Terra Nostra, 2000/6: 301-308.
- Lutz, H., Kaulfuss, U. 2006. A dynamic model for the meromictic lake Eckfelder Maar (Middle Eocene, Germany). Zeitschrift der Deutschen Gesellschaft für Geowissenschaften 157: 433-450.
- Mertz, D.F., Renne, P.R. 2005. A numerical age for the Messel fossil deposit (UNESCO World Heritage Site) derived from $^{40}\text{Ar}/^{39}\text{Ar}$ dating on a basaltic rock fragment. Courier Forschungsinstitut Senckenberg 255: 67-75.
- Micklich, N. 2002. The fishfauna of the Messel-Pit: A nursery school? Courier Forschungsinstitut Senckenberg 255: 97-125.
- Micklich, N., Drobek, M. 2007. Mining, Excavations and Preparation. In: Gruber, G. and Micklich, N. (eds.). Messel - Treasures of the Eocene: 15-22.
- Pirrung, M., Fischer, C., Büchel, G., Gaupp, R., Lutz, H., Neuffer, F.O. 2003. Lithofacies succession of maar crater deposits in the Eifel area (Germany). - Terra Nova 15: 125-132.
- Schaal, S. 2004. Aktuelle Übersichtskarte zur Betriebs- und Grabungsplanung in der Fossilfundstätte Grube Messel. Courier Forschungsinstitut Senckenberg 252: 207-210.

Phreatomagmatism related to trachyte dome explosions

Miguel J. Haller¹, Francisco E. Nullo² and Corina Risso³

¹ Universidad Nacional de la Patagonia San Juan Bosco & Centro Nacional Patagónico-CONICET, Argentina - haller@cenpat.edu.ar

² Consejo Nacional de Investigaciones Científicas y Técnicas & SEGEMAR, Argentina

³ Departamento de Ciencias Geológicas, Universidad de Buenos Aires, Argentina

Keywords: thrachyte phreatomagmatism, Somuncura plateau, dome explosions

An important trachyte volcanism developed on the periphery of the Somuncura basalt plateau in Patagonia, Argentina, during Miocene time. Two calderas and their volcanic products are the records of this explosive episode. Talagapa Chico caldera is 3.25 x 3.12 km, with a cavity volume of 2.1 km³. Talagapa Grande caldera is 4 x 5.4 km in size, with a cavity volume of ca. 5.4 km³ (Fig. 1). Field evidence shows that a basal trachyte lava flow is covered by a thick pyroclastic succession. An intercalated non consanguineous basalt flow yielded isotopic (K-Ar) ages from 19 to 20 Ma and helps to date the trachytic event. The pyroclasts are covered by a 15 m thick trachyte lava flow. A good exposure of tephra located half way between the two Talagapa calderas gives a good insight to understand the development of one of the several episodes of Talagapa complex eruptive history.

The succession of light gray tephra layers 98 m thick can be divided into three rock units (Fig. 1) on the base of the dominant facies, bedding style and clast size. The lower section is massive with a faint layering shown by poorly defined levels of larger blocks. The intermediate section is evenly bedded, laminated, extensively cross bedded and with scour channels. The upper section is medium light gray and evenly layered in parallel beds. Juvenile material throughout the Talagapa pyroclasts is trachyte. Juvenile material is dominantly vitrophyric and, less commonly, porphyritic (5–10 vol. % phenocrysts). Phenocrysts are dominated by sanidine, with sparse biotite. Juvenile clast textures include pumiceous, vitrophyric and spherulitic. Lithic clasts occur in different proportions throughout the Talagapa deposits. Lithic clast compositions are predominantly trachyte, pumice, and colorless and brown glass. Xenocrysts include sanidine and very scarce pyroxene.

The lower unit is a pale pinkish gray, massive to thinly bedded, non-welded ignimbrite. Measured thickness is 32 m and the base is unexposed. The unit contains 2–25 cm large, pumice, basalt and trachyte angular blocks immersed in a fine ash groundmass. Pumice blocks show in general low vesiculation. Silicified wood fragments are common. The base of the succession is not visible, and the measured thickness is 56.60 m.

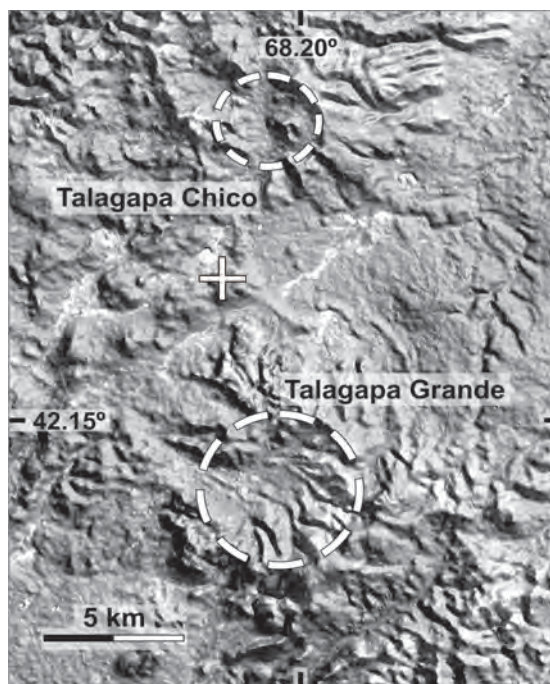
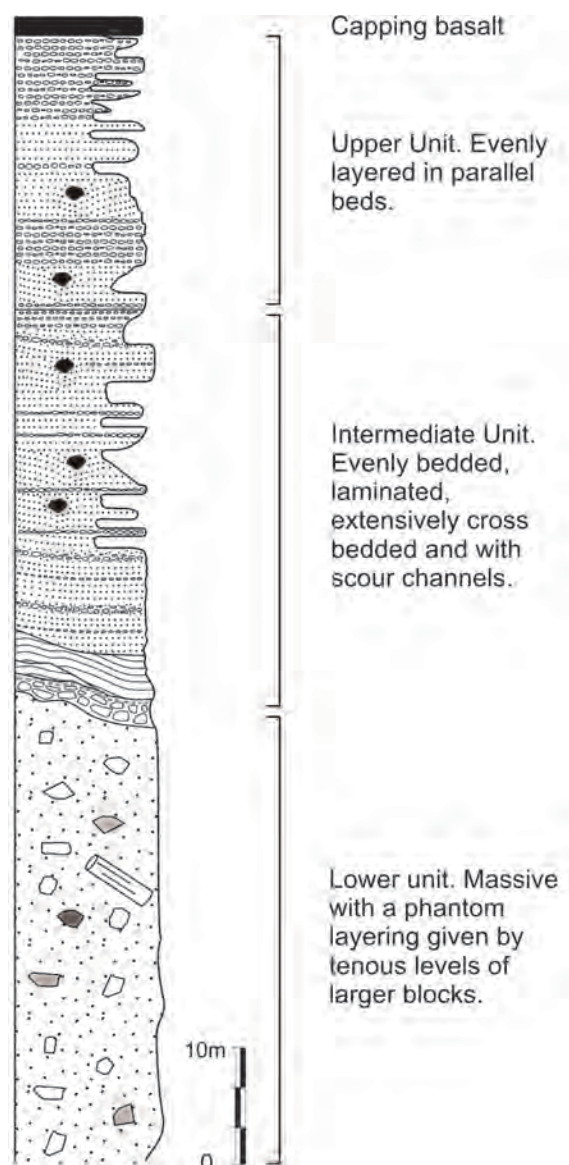


Fig. 1 – Google image+DEM of Talagapa Calderas. White cross indicates location of the studied pyroclastic profile.

The intermediate unit disconformably overlies the lower unit. The succession starts with a thin horizon (10 cm) of white pumice clasts. Upward pyroclasts are bedded with an average thickness of 10 cm, alternating between lapilli and ash beds. Ash beds show parallel lamination. The lapilli are normally bedded and, some of the beds are normally graded. It contains black trachytic and white pumice lithoclasts up to 2.5 cm. Centimetre-sized accretionary lapilli are found in some beds. A few thin lapilli levels show intense iron-alteration of both matrix and lithic clasts. Truncated contact surfaces and scour channels are common. Frequent volcanic bombs and ballistic blocks produce impact sags. The upper beds of the intermediate unit are clast-supported, with abundant white pumice and trachyte lithoclasts, up to 1.5 cm. The thickness of this unit is 31.05 m.



The upper unit begins with fine laminated sub-parallel matrix-supported beds. They show isolated lapilli, white pumice and dark trachyte lithoclasts of 0.5-3 mm in diameter. The matrix contains pumice and trachyte lithoclasts, sanidine and alkaline plagioclase crystaloclasts, accretionary lapilli and glass fragments. Scour channels, truncation surfaces and undulate bedding are common. Rare ballistic blocks cause 10 to 17 cm-deep impact sags in the deposits. This level holds several large ballistic trachytic vitrophyre (up to 0.80 m) boulders. Above, continue stratified clast-supported pyroclastic beds 3-5 cm thick, alternating with matrix-supported beds of finer ash with isolated lapilli. The lapilli, 2.5 cm, are mostly accompanied by white pumice trachyte. The matrix is composed by trachyte and pumice lithoclasts, crystaloclasts of sanidine, very fine ash aggregates, and fragments of brown and colorless volcanic glass. Upwards continue matrix-supported beds containing lithoclasts (average size 0.5-1 cm)

of rounded trachyte and angular pumice. Some levels contain accretionary lapilli. Ballistic blocks of basalt and vitrophyre- and porphyritic trachyte are common. The uppermost section consists of tabular beds with plane-parallel base and top of fine-poor lapilli lithoclast breccia normally graded in banks of 5-10 cm. Ballistic basalt and trachyte vitrophyre blocks disrupt the pyroclastic layers. The thickness of the upper unit is 10.35 m.

The presence of abundant bomb sags, accretionary lapilli, scour channels, undulatory bedding, and iron alteration of lapilli indicates the participation of water in the eruptive system. On the other hand, trachyte vitrophyre indicates a quickly cooled rock which may be consistent with a rapidly quenched magma plug in a water-rich environment. Such viscous lava would form a dome in the crater. The presence of common large trachyte vitrophyre ballistic blocks and boulders in the upper unit of the pyroclastic succession is interpreted to result from a destructive explosion of the dome accompanied by emission of phreatomagmatically-fragmented material.

The base ignimbrite could be formed by a low energy volcanic column. The intermediate unit was formed by base surges indicated by the scour channels and alternations of ash-fall deposits with wet and dry surges, as suggested by the accretionary lapilli, truncated contact surfaces and clast-supported levels. In the upper unit wet surges and ash-fall occurred during the deposition of the lower levels while hyperconcentrated flows took an important role during the deposition of the upper beds, as indicated by the well bedded fine-poor lapilli flat beds.

The pyroclastic succession is capped by a non-consanguineous basalt lava. The fact that erupted products were dominantly trachyte throughout the eruption and the abundance and large size of trachyte vitrophyre ballistic block suggests that the pyroclastic deposits are related to dome explosions in the nearby trachyte calderas.



Fig. 2 – Ballistic trachyte vitrophyre block and impact sag developed in lapilli beds of the upper unit.

Petrogenesis of the Late Miocene-Quaternary alkaline basalts in the Pannonian Basin, eastern-central Europe

Szabolcs Harangi

Volcanology Group, Department of Petrology and Geochemistry, Eötvös University, Budapest, Hungary – szabolcs.harangi@geology.elte.hu

Keywords: Pannonian basin, magma generation, spinel.

Formation and evolution of the Pannonian Basin has been accompanied by a variety of volcanic activities. Among them, the origin of the Late Miocene to Quaternary alkaline basaltic volcanism is still unresolved. The basaltic volcanism resulted in monogenetic volcanic fields as well as single volcanic events in different parts of this region. In this work a general outline of the main features of this volcanism is presented, focusing primarily on the origin of the mafic magmas.

The basaltic volcanic activity in the Pannonian basin covered almost all the major characteristics of eruption of mafic magmas. It includes formation of shield volcanoes and lava plateaus as well as volcanic edifices (scoria cones, maars and tuff rings) related to magmatic and phreatomagmatic explosive events. Many of these volcanoes have been severely eroded and as a result, their root zones (diatremes) have been exposed. Therefore, this region can be regarded as a natural laboratory, where evolution of basaltic volcanoes can be investigated in detail.

The alkaline basaltic volcanism was taking place during the post-rift thermal subsidence and the tectonic inversion phases of the Pannonian basin from 11.5 to 0.1 Ma. In the Stíavnica-Nógrád-Gömör and the Bakony-Balaton Upland volcanic fields, the volcanism was relatively long-lived (7-0.4 Ma and 7.9-2.6 Ma, respectively), involving distinct active phases and several 100's ka long quiescence periods. In the Styrian Basin only one active phase can be detected from 4.9 to 1.9 Ma, whereas the youngest volcanic field (Persány) in the southeastern part of this region is characterized by two active volcanic stages (1.2-1.4 Ma and 0.5-0.6 Ma) so far. Two areas can be considered as still potentially active (Stíavnica-Nógrád-Gömör and Persány) and further volcanic events at the southern Hungarian Plain also cannot be excluded.

The basaltic volcanic fields in the Pannonian basin show a remarkable spatial distribution. They are situated mostly at the west-northwestern periphery of the Pannonian basin and not in the region which underwent significant thinning and thus characterized by thin lithosphere. This peripheral area is underlain by a lithosphere/asthenosphere boundary with a steep

gradient (from 110 to 70 km depths). In contrast, the Persány volcanic field is found just the opposite parts of this region, close to the Vrancea seismically active area. Here, the deep hypocenters of the earthquakes indicate a near-vertical cold, dense slab, regarded as the trace of final stage of subduction or a delaminated part of the lower lithosphere.

The composition of the basaltic rocks is in a wide range from nephelinites to trachybasalts, however, no subalkaline types exist. Large compositional variety can be often found even within the volcanic fields. In single monogenetic volcanoes, we have not found significant change in the composition of the erupted magmas, although this kind of studies is just in the initial stage.

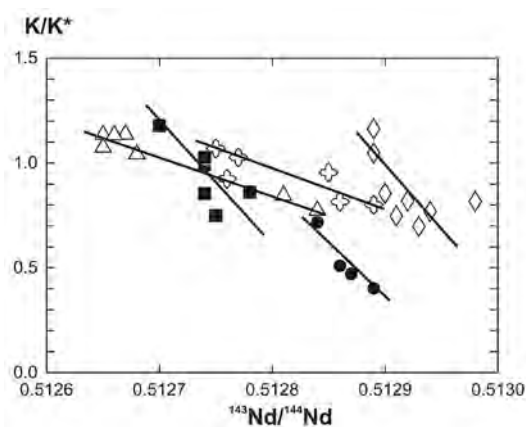


Fig. 1 – Correlation between the $^{143}\text{Nd}/^{144}\text{Nd}$ isotope ratio and the degree of negative K-anomaly (K/K^*) in individual basalt volcanic fields could indicate heterogeneous mantle source regions.

The chemical composition of the mafic rocks indicates that melt generation could have occurred mostly in the sublithospheric mantle, within the garnet-peridotite stability zone, i.e. > 60-80 km depth by 1-4% of melting. Partial melting at such depths could take place only if the potential temperature of the upper mantle is higher than the average (i.e. upwelling plume) or there are materials with lower solidus than the peridotite. This could be either peridotite with hydrous phases (amphibole or phlogopite) or existence of pyroxenite/eclogite.

Indeed, trace element patterns of many basalts show a negative K-anomaly, which could be consistent with low-degree melting of an amphibole- or phlogopite-bearing garnet-peridotite. However, this geochemical feature could be explained also by the fingerprint of the source region, i.e. melting of inherently K-depleted rocks. Pyroxenites and eclogites representing dehydrated oceanic crustal material could be reasonable candidates for this. The negative correlation between the $^{143}\text{Nd}/^{144}\text{Nd}$ isotope ratio and the degree of negative K-anomaly (K/K^*) within individual basalt volcanic fields (Fig. 1) may indicate the latter scenario and melting of heterogeneous mantle source regions. The sublithospheric mantle beneath the Pannonian basin could be heterogeneous on a relatively small-scale (possibly in a scale of 10^2 - 10^3 m), where the erupted magmas represent often a mixture of mafic melts occasionally coming from very different mantle source domains (e.g., pyroxenitic/eclogitic and peridotitic sources). Involvement of pyroxenitic material could be implied also by the relatively low CaO contents of the basalts.

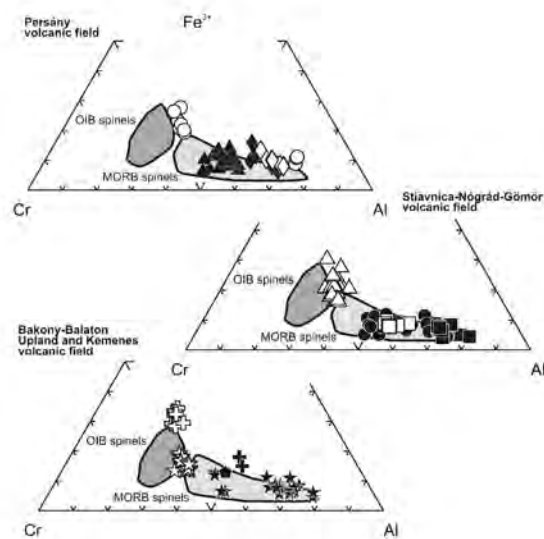


Fig. 2 – Compositional variation of spinels found as inclusions in olivine of the basalts from different volcanic fields. Symbols denote individual localities. OIB and MORB spinel fields are after Roeder (1994).

Additional implications for a small-scale heterogeneous mantle source come from an ongoing detailed study of the chemistry of spinels. Spinels are among the first phases to crystallize from basaltic magma and their compositions strongly depend on the magma- and source compositions. They are fairly common as inclusions enclosed by olivine phenocrysts in basalts of each volcanic field. Selecting only those spinels, which occur in

forsteritic olivine and are not undergone in differentiation process, we can find a remarkable variation in the Cr-Fe³⁺-Al plot (Fig. 2). The spinel compositions are in the range from typical OIB to MORB spinel characteristics even within single volcanic fields. This could suggest melting of variously enriched mantle material.

The reason of melt generation following well the main extensional phase of the Pannonian basin has been a subject of debate. The lack of broad topographic updoming, a high velocity body in the mantle transitional zone, the sporadic distribution of the mafic volcanic fields and the fairly low magma production rate are all inconsistent with an upwelling mantle plume. Instead, the distribution of the basaltic volcanic fields could have significance. The magma generation occurred mostly in the peripheral areas of the Pannonian basin that are underlain by a lithosphere/asthenosphere boundary with a steep gradient. The Pannonian basin could act as a thin-spot providing suction in the sublithospheric mantle and generating mantle flow from below the thick lithospheric roots. This mantle flow would have a near-vertical component along the steep lithosphere/asthenosphere boundary that could lead to decompression melting in the strongly heterogeneous upper mantle. On the other hand, a different scenario is necessary for the mafic magmas at the southeastern part of this region. The single basaltic eruption event at Lucaret could be related to the differential crustal movements (it occurs at the boundary of subsiding and uplifting blocks) in the present tectonic inversion phase, whereas the formation of the youngest volcanic field in the Persány area could be due to a combined result of a major reorganization in the upper mantle and stretching of the lithosphere as a cold, dense material is descending beneath the Vrancea zone. Since this is a still ongoing process, further volcanic eruptions could be still expected here.

Acknowledgements

The results presented here have come from beneficial discussions with many of my colleagues for years, and these studies are continuously inspired by the enthusiastic research works of the MSc and PhD students of the Volcanology Group of the Eötvös University.

References

- Roeder, P.L. 1994. Chromite: from the fiery rain of chondrules to the Kilauea Iki lava lake. *Canadian Mineralogist* 32: 729–746.

Vesicle texture analysis of juvenile pyroclasts from the Pleistocene Lake Purrumbete Maar, Newer Volcanics Province, southern Australia

Simone C. Jordan and Ray A.F. Cas

School of Geosciences, Monash University, Australia – simone.jordan@monash.edu

Keywords: vesicularity, fine ash, phreatomagmatic

The record of the 50-60 ka Lake Purrumbete maar deposits shows several changes in the eruption style. The facies range from thin dry magmatic scoria layers, to scoriaceous lapilli layers to dry phreatomagmatic lapilli ash and wet phreatomagmatic ash layers. Furthermore abundant basaltic bombs occur within the sequence. This study aims to investigate the role of volatiles and vesicularity of the magma in the phreatomagmatic eruption style, therefore we evaluate the vesicularity, Bubble Number densities and shape parameter for the different facies and try to understand through comparison with each other the role of vesiculation in phreatomagmatic eruptions.

Phreatomagmatic deposits are generally characterised by fine ash fragments ($< 65\mu\text{m}$), Wohletz (1983), therefore we concentrate on particles smaller than $65\mu\text{m}$. Juvenile clasts in BSE images of polished thin sections of fine ash were analysed in terms of vesicularity, and bubble structures. The problem that occurred is that the bubbles were often larger than the preserved juvenile fragments, as a result only parts of the former bubbles are preserved in the cusped outline of the fragments.

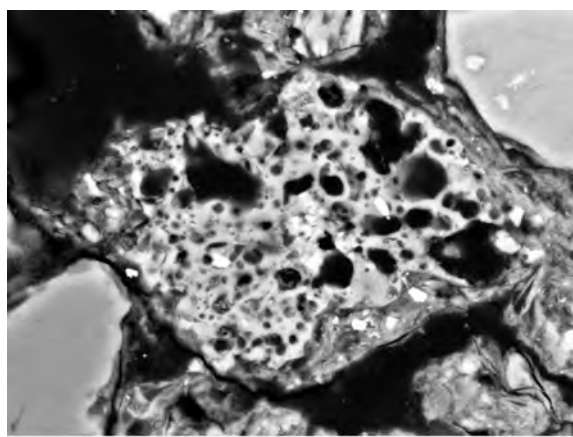


Fig. 1 - Back scattered image of a fine ash particles in a polished thin section of wet phreatomagmatic pyroclastic ash. The clast in the middle has a relatively high vesicularity in contrast to the surrounding dense clast.

To evaluate if the analysis of these bubble fragments reflect the correct shape parameters,

vesicularities and Bubble Number Density (BND) values, these parameters were calculated for the fine ash particles and compared to the values of larger clasts within the fine ash samples. Furthermore the shape and size of the bubbles were compared as well, to be certain that the bubbles in all clast sizes within one sample were generated prior to fragmentation. Bubble number density (BND) values, vesicularity and shape parameters were calculated after the method of Shea et al (2010), using the program ImageJ 1.43. These parameters were also calculated for juvenile clasts of the more magmatic deposits. The preliminary results show, that the clast vesicularity of the phreatomagmatic samples vary in a wide range from 4 to 60% in the same sample, whereas the vesicularity of the scoriaceous clasts is in a more narrow range of 30 to 60%.

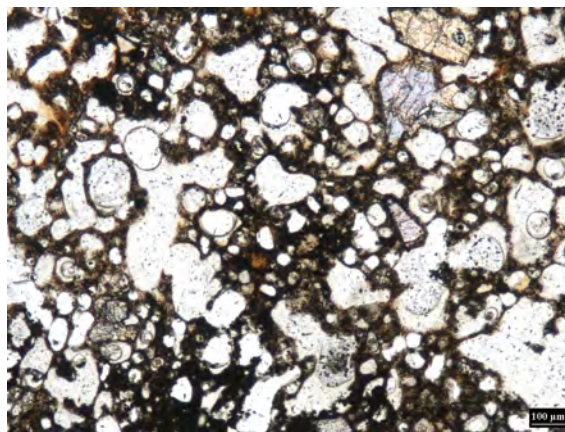


Fig. 2 - Micrograph of a juvenile clast from a scoriaceous lapilli deposit. The majority of bubbles are connected with each other, which indicates coalescence.

The clasts show both stretched and round vesicles, often both in different parts of the same clast, indicating that these bubbles were entrapped in the rising magma and were sheared immediately prior to fragmentation. However the clasts of both the dry phreatomagmatic and scoriaceous lapilli facies show more often features of coalescence such as lobate shape and connected vesicles, than the clasts of the fine ash facies. Furthermore the BND

values of the fine ash facies are 2 orders of magnitude higher ($5 \times 10^{12} \text{ m}^{-3}$) than the BND values of the lapilli facies ($5 \times 10^{10} \text{ m}^{-3}$).

Lithic fragments from the underlying stratigraphy show that the fragmentation level for the phreatomagmatic units was shallow with less than 50m below surface. The lithic clast distribution gives no evidence for a deepening of the fragmentation level during the eruption. Therefore we conclude that the differences in bubble coalescence and BND values are due to conduit processes. These changes seem to have influenced

the mixing process of magma and water and hence the efficiency of the fragmentation.

References

- Shea, T., Houghton, B.F., Gurioli, L., Cashman, K.V., Hammer, J.E., Hobden, B.J. 2010. Textural studies of vesicles in volcanic rocks: An integrated methodology. *Journal of Volcanology and Geothermal Research* 190: 271-289.
- Wohletz, K.H. 1983. Mechanics of hydrovolcanic pyroclast formation: grain-size, scanning microscopy, and experimental studies. *Journal of Volcanology and Geothermal Research* 17: 31-63.

Earthquake swarms, a sign of active magmatic processes in the Regensburg – Leipzig – Rostock zone, Central Europe?

Horst Kämpf¹, Karin Bräuer², Tobias Nickschick¹, Irka Schüller¹, Alina Schmidt³, Christina Flechsig³ and Thomas Jahr⁴

¹ GeoForschungsZentrum, Potsdam, Germany– kaempf@gfz-potsdam.de

² UFZ-Helmholtz Centre for Environmental Research, Halle, Germany

³ Universität Leipzig, Institute for Geophysics and Geology, Leipzig, Germany

⁴ Friedrich Schiller University, Jena, Germany

Keywords: earthquake swarms, magma/fluid conduits, maar-diatreme-volcano

Earthquake swarms (ES) correspond to a special type of seismic activity that is concentrated in time and space without an outstanding principal earthquake event. In general, the occurrence of ES is typically in space and time related to magmatic activity, e.g. in volcanoes (eruptions and magma movements; Hill, 1977). Apart from active volcanoes, swarms also occur in intraplate environments, like the middle part of the Regensburg-Leipzig-Rostock zone (RLRZ) in Germany (Fig. 1; Spicak et al., 2000; Bankwitz et al., 2003; Neunhöfer and Hemmann, 2005; Ibs-von Seht et al., 2008; Korn et al., 2008).

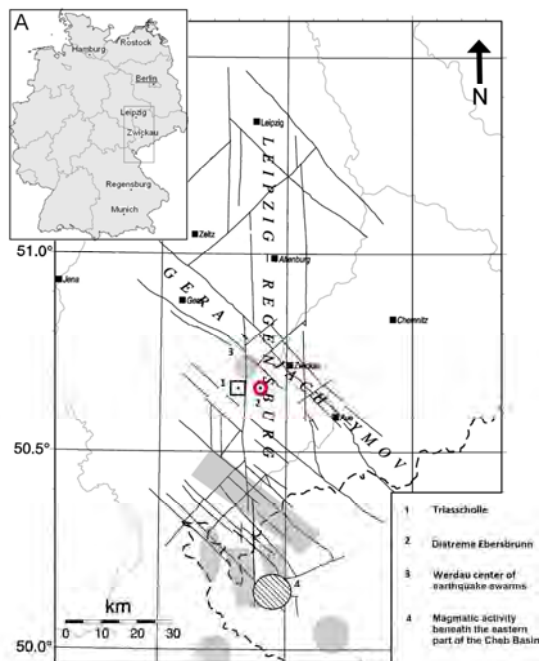


Fig. 1 – Central part of the RLRZ with earthquake swarm activity (grey shaded) modified after Korn et al. 2008. Dashed: magmatic activity in the eastern part of the Cheb Basin after Bräuer et al. (2009, 2011).

The investigations aim is to compare two areas where earthquake swarms occur (Werdau focal zone, west of Zwickau; 3 in Fig. 1, and the eastern part of

the Cheb Basin, including the Nový Kostel focal zone; 4 in Fig. 1). Whereas earthquake swarm activity occurs in both areas, magmatic activity was detected only in the eastern part of the Cheb Basin so far.

The most active earthquake swarm area in Central and Western Europe is the Nový Kostel focal zone with four intense earthquake swarm periods up to magnitude 4.6 since 1985 (1985/86, 2000, 2008, 2011). This observation is consistent with structural and degassing anomalies of the lithosphere: the upwelling of the Moho and the Lithosphere Asthenosphere Boundary (LAB) (Heuer et al., 2006) as well as the progressive increase of the mantle-derived helium at locations in the eastern part of the Cheb Basin (Bräuer, 2009; 2011). The repeated occurrence of earthquake swarms takes place at the intersection of two NW-SE (Mariánské Lázně fault - MLF) and N-S (Počátky-Plesná fault zone - PPZ) striking fault zones. Presently the PPZ is the main seismically active fault zone. Bräuer et al. (2009) interpreted a three-month lasting increase in the $^3\text{He}/^4\text{He}$ ratios in spring 2006 as indication for a hidden magma intrusion process from the upper mantle into the lower crust. They assume that the strong earthquake swarm in October 2008 was initiated by this magma intrusion.

We have used the soil carbon dioxide concentration and soil gas flow as well as the gas flow of mofettes for tracing PPZ fault segments of an area of ca. 6 km². As a result two isolated highly permeable Diffuse Degassing Structures (DDS) could be distinguished within the PPZ, ca. 1 km in length and 300 m in width, each. The $^3\text{He}/^4\text{He}$ ratios of free mofette gases cover the subcontinental mantle range as defined by Gautheron et al. (2005) from measurements at mantle xenoliths. One surprising was that also at soil gas within the DDS the $^3\text{He}/^4\text{He}$ ratios were close to the subcontinental mantle signature. As a whole the isotopic signature ($^{13}\text{C}_{\text{CO}_2}$, $^3\text{He}/^4\text{He}$) of both mofette gas as well as soil gas in combination with the high CO_2 flow within the DDS point to conduit-like structures that act as

deep-reaching mantle–fluid injection zones inside of the PPZ.

The Werdau focal zone is located at the intersection of RLRZ and the Gera-Jachymov fault zone (GJZ), (Fig. 1). As reported by Korn et al. (2008) the Werdau focal zone is the northernmost location where swarm-like seismicity occurs. Small to middle earthquake swarm activity was observed in December 1997/January 1998 and in August/September 2006 (Hemmann and Kämpf, 2002; Hemmann et al., 2003; Korn et al., 2008). The seismic activity of 1997/98 took place close to the intersection of faults of the RLRZ and the GJZ. The swarm period started with single events at 18.5 km depths rising progressively with time up to 13.5 km and followed by swarm activities in about 13 km at the RLRZ and the GJZ. The migration of the focal zones from lower to mid-crustal depths, points to hidden magma/fluid intrusion.

However, active degassing as well as Quarternary volcanic activity is unknown in the Werdau area. Recently, we started investigations due to Cenozoic volcanism of the area to look for indications of interaction between fault tectonics, magmatic intrusion processes and volcanic activity: see poster of Nickschick et al. (2012), Schüller et al. (2012) and Schmidt et al. (2012), this volume.

Acknowledgements

This research is supported by the German Science Foundation (KA 902/9, 16-1 and 17-1, JA 542/21-1) and the GFZ Potsdam.

References

- Bankwitz, P., Schneider, G., Kämpf, H., Bankwitz, E. 2003. Structural characteristics of epicentral areas in Central Europe: study case Cheb Basin (Czech Republic) 35: 5-32.
- Bräuer, K., Kämpf, H., Strauch, G. 2009. Earthquake swarms in non-volcanic regions: What fluids have to say. *Geophysical Research Letters* 36: L17309, doi:10.1029/2009GL039615, 2009.
- Bräuer, K., Kämpf, H., Koch, U., Strauch, G. 2011. Monthly monitoring of gas and isotope compositions in the free gas phase at degassing locations close to the Nový Kostel focal zone in the western Eger rift, Czech Republic. *Chemical Geology* 290: 163-176.
- Gautheron, C., Moreira, M., Allegre, C. 2005. He, Ne and Ar composition of the European lithospheric mantle. *Chemical Geology* 217: 97-112.
- Hemmann, A., Kämpf, H. 2002. Seismicity in the central part of the Naab-Pritzwalk-Rostock Lineament, related to mantle fluid activity? EGS XXVII General Assembly, Nice, 21-26 April 2002, abstract 5193.
- Hemmann A., Meier T., Jentzsch G., Ziegert A. 2003. Similarity of waveforms and relative relocalisation of the earthquake swarm 1997/1998 near Werdau. *Journal of Geodynamics* 35: 191-208.
- Heuer, B., Geissler, W.H., Kind, R., Kämpf, H. 2006. Seismic evidence for asthenospheric updoming beneath the western Bohemian Massif, central Europe. *Geophysical Research Letters* 33: L05311, doi: 10.1029/2005GL025158, 2006.
- Hill, D.P. 1977. A model for earthquake swarms. *Journal of Geophysical Research* 82: 1347-1352.
- Kämpf, H., Geissler, W., Bräuer, K. 2007. Combined gasgeochemical and receiver function studies of the Vogtland/ NW Bohemia intraplate mantle degassing field, in *Mantle Plumes — A Multidisciplinary Approach*, edited by U.R. Christensen and J.R.R. Ritter, pp. 127–158, Springer, Berlin.
- Ibs-von Seht, M., Plenefisch, T., Klinge, K. 2008. Earthquake swarms in continental rifts – A comparison of selected cases in America, Africa and Europe. *Tectonophysics* 452: 66-77.
- Korn, M., Funke, S., Wendt, S. 2008. Seismicity and seismotectonics of West Saxony, Germany - New Insights from recent seismicity observed with the Saxonian Seismic Network. *Studia Geophysica et Geodaetica* 52: 479-492.
- Neunhöfer, H., Hemmann, A. 2005. Earthquake swarms in the Vogtland/ Western Bohemia region: Spatial distribution and magnitude-frequency distribution as an indication of genesis of swarms? *Journal of Geodynamics* 39: 361-385.
- Nickschick, T., Kämpf, H., Jahr, T. 2012. The Triasscholle near Greiz, E Thuringia – a volcanic based origin? IAVCEI, CMV/CVS, IAS 4IMC Conference Auckland, New Zealand, this volume.
- Schüller, I., Kämpf, H., Schmidt, A., Flechsig, C., Jahr, T. 2012. Petrographic and thermochronometric investigation of the diatreme breccia of the Ebersbrunn Diatreme – W Saxony, Germany. IAVCEI, CMV/CVS, IAS 4IMC Conference Auckland, New Zealand, this volume.
- Schmidt, A., Nowaczyk, N., Kämpf, H., Flechsig, C., Jahr, T. 2012. Possible causes for magnetic anomalies in the volcanoclastic units of the Ebersbrunn diatreme (W Saxony, Germany). IAVCEI, CMV/CVS, IAS 4IMC Conference Auckland, New Zealand, this volume.
- Špičák, A. 2000. Earthquake swarms and accompanying phenomena in intraplate regions: a review. *Studia Geophysica et Geodaetica* 44: 89–106.

Post-eruptive maar crater sedimentation inferred from outcrop, drill cores and geophysics – Foulden Maar, Early Miocene, Waipiata Volcanic Field, New Zealand

Uwe Kaulfuss¹, Jon Lindqvist¹, Daniel Jones¹, Bethany Fox^{1,2}, Gary Wilson^{1,2} and Daphne Lee¹

¹ Department of Geology, University of Otago, PO Box 56, Dunedin, New Zealand – kauuw275@student.otago.ac.nz

² Department of Marine Science, University of Otago, PO Box 56, Dunedin, New Zealand

Keywords: maar lake, crater sediments, Foulden Maar.

Foulden Maar is a partly eroded maar-diatreme volcano located at the western fringe of the Miocene monogenetic Waipiata Volcanic Field (WVF) in Otago. It comprises a semicircular depression ~1500m in diameter surrounded by Otago Schist basement and several erosion remnants of basaltic dykes, plugs and flows (Lindqvist & Lee 2009). Limited outcrops within the depression expose 15 m thick laminated diatomite. Isolated blocks of silicified sandstone and quartz and schist pebble conglomerate in the vicinity of the maar are inferred to be remnants of pre-eruptive sediment cover (Pakaha Group, Late Cretaceous–Paleogene) (Lindqvist & Lee 2009). Pyroclastic deposits are not preserved around the periphery. Erosion depths calculated for nearby volcanic vents of similar age amount to up to 400 m (Németh 2001).

Information about the lithology, thickness and the vertical and lateral distribution of crater-infilling sediments at Foulden Maar is available from seismic, magnetic and gravity surveys (Jones 2011), and two drill cores (120 and 184 m long) from central parts of the maar crater, which have been analyzed with a GEOTEK Multi-Sensor Core Logger. Four lithozones can be distinguished (from top to base) for the post-eruptive sedimentary succession based on lithological and geophysical properties (Fig. 1).

Lithozone 1 (120 m thick), the uppermost unit preserved, consists predominantly of two depositional facies: 1) thinly laminated diatomite of alternating pale and dark couplets averaging 0.5 mm thick, and 2) massive to graded beds of laminated diatomite clasts in a fine-grained diatomaceous matrix. Pale laminae consist of frustules of pennate diatoms and are interpreted as biogenic fall-out from the water column of a deep, meromictic maar lake in summer season. Dark laminae of fine organic debris, pennate and centric diatoms, chrysophycean stomatocysts and spicules of freshwater sponges were deposited in colder, presumably wet and windy seasons. In outcrops, individual laminae are laterally continuous for at least 300 m. The uniform composition of this 120 m thick interval indicates long-lasting stable and calm limnological conditions.

Well-preserved fossils in this facies provide valuable information about the early Miocene biota (Kaulfuss et al. 2012, this volume). Mainly massive to graded diatomaceous beds lacking erosional bases constitute ~50% of sediment in LZ 1, become less frequent up-core, are mm to m thick and may contain variable amounts of schist-derived sand and volcanic ash and/or lapilli. They are the result of sub-aqueous turbidity currents and debris flows that originated in profundal, littoral or sub-aerial zones.

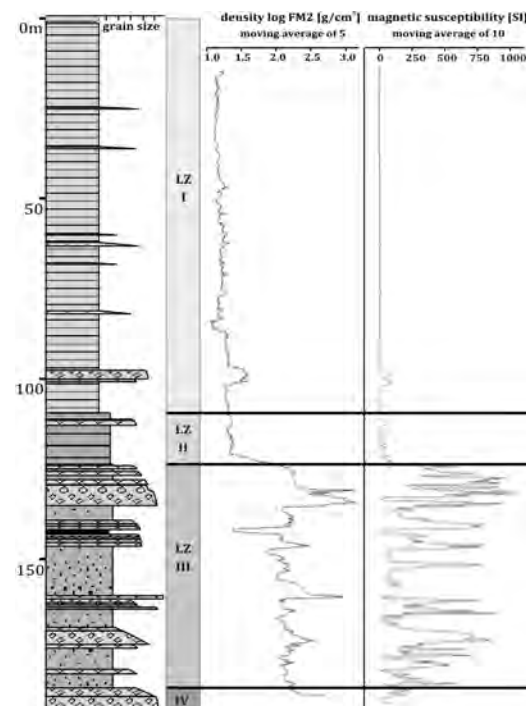


Fig. 1 – Lithology, density log and magnetic susceptibility of post-eruptive central crater sediments at Foulden Maar

Lithozone 2 (13.6 m thick) is characterized by alternating beds of non- to thinly bedded diatomite, sand of schistose and/or volcanogenic pyroclastic composition, and breccias containing pebble to cobble-sized schist or basaltic clasts and rare reworked lapilli. Fluctuating values for magnetic susceptibility and density (1.28 – 1.86 g/cm³) in LZ 2 reflect strongly varying amounts of metamorphic

and volcanic (extra)clasts in individual horizons. LZ 2 is interpreted as lacustrine background sedimentation frequently interrupted by sub-aqueous mass flow events (turbidites, debris or grain flows) from the crater wall and the tephra rim. Rounded quartz and glauconite occasionally present in coarser horizons indicate that a marine sandstone cover existed at the time of the eruption, as has been shown elsewhere in the WVF (Németh & White 2003).

Lithozone 3 (62 m thick) features a general increase in grain-size and comprises homogeneous or stratified mud/sandstone beds, graded gravel to sand horizons, unsorted, lithologically diverse, occasionally carbonate-cemented breccia of fragmented basement rock, pre-eruptive siliciclastic sediment, pyroclastic material and basalt clasts. Diatomaceous sediment has not been encountered. The ratio of accidental lithic clasts/juvenile clasts (reworked) varies between individual breccia horizons but is generally >1. Juvenile material in LZ 3, mainly (altered) non- to incipiently vesicular sideromelane, is regarded as reworked from the tephra rim that surrounded the maar and will provide information about the eruption style and fragmentation processes at Foulden Maar. Lithological composition and textural patterns in LZ 3 suggest initiation as rock falls, debris or granular flows from the steep crater walls and the presumably weakly vegetated (according to palynology) and unstable tephra rim, and sub-aquatic transport and deposition (debris flows and turbidites) following groundwater inflow and successive flooding in central parts of the maar crater. Magnetic susceptibility and density vary considerably in LZ 3, with highest values associated with massive breccia beds.

Massive breccias of *Lithozone 4 (7+ m thick)* contain abundant angular gravel to block-sized (>1.5 m) clasts of Otago Schist in a sandy matrix. Sideromelane clasts, non- to incipiently vesicular, or basaltic clasts are comparatively rare in this lowermost section sampled in cores. Density increases in LZ 4 while magnetic susceptibility decreases to minimal values encountered in LZ 3. LZ 4 represents rock-fall and debris flow breccias (collapse breccia) deposited in an early post-eruptive phase, presumably under sub-aerial conditions in a relatively short period of time. The base of the schist

breccias has not been sampled in drill cores; seismic profiles indicate a thickness of >20 m and an underlying funnel-shaped diatreme structure containing well-bedded, coarse material (Jones 2011).

The sedimentary succession from Foulden Maar is comparable to crater-infilling successions described from other maar craters (e.g. Liebig 2001, Pirrung et al. 2003, Goth & Suhr 2005) and reflects post-eruptive processes that generally accompany this particular volcanic landform. As with many other Cenozoic maar-diatreme structures, direct observations on primary pyroclastic facies are prevented by the level of erosion at Foulden Maar.

Acknowledgements

We thank the Gibson family and Featherston Resources for kindly allowing us access to the site, and the Marsden Fund and the Division of Science, University of Otago, for financial support.

References

- Goth, K., Suhr, P. 2005. Baruths heisse Vergangenheit – Vulkane in der Lausitz. Knopek & Klaus, 107pp.
- Jones, D.A. 2011. The geophysical characterization of the Foulden Maar. MSc thesis, University of Otago, 214pp.
- Kaufuss, U., Lee, D., Bannister, J., Conran, J., Mildenhall, D., Kennedy, L. 2012. Fossil microorganisms, plants and animals from the Early Miocene Foulden Maar (Otago, New Zealand). IAS 4IMC Conference, abstract volume.
- Liebig, V. 2001. Neuaufnahme der Forschungsbohrungen KB 1,2,4,5 und 7 von 1980 aus der Grube Messel (Sprenglinger Horst, Südhessen). *Kaupia* 11: 3–68.
- Lindqvist, J.K., Lee, D.E. 2009. High-frequency paleoclimate signals from Foulden Maar, Waipiata Volcanic Field, southern New Zealand: An Early Miocene varved lacustrine diatomite deposit. *Sedimentary Geology* 222: 98–110.
- Németh, K., White, J.D.L. 2003. Reconstructing eruption processes of a Miocene monogenetic volcanic field from vent remnants: Waipiata Volcanic Field, South Island, New Zealand. *Journal of Volcanology and Geothermal Research* 124: 1–21.
- Pirrung, M., Fischer, C., Büchel, G., Gaupp, R., Lutz, H., Neuffer, F.-O. 2003. Lithofacies succession of maar crater deposits in the Eifel area (Germany). *Terra Nova* 15: 125–132.

Challenges of monitoring a potentially active volcanic field in a large urban area: Auckland Volcanic Field, New Zealand

Catherine L. Kenedi¹, Jan M. Lindsay², Caroline L. Ashenden³ and Steve Sherburn³

¹ Institute of Earth Science and Engineering, The University of Auckland, Private Bag 92019, Auckland, 1142, New Zealand – katelk@auckland.ac.nz

² School of Environment, The University of Auckland, Private Bag 92019, Auckland, 1142, New Zealand

³ GNS Science, Lower Hutt, 5040, New Zealand

Keywords: borehole seismology, Auckland, volcano monitoring.

Introduction

The city of Auckland (population 1.3 million) is built on and around a potentially active basaltic intraplate volcanic system, the Auckland Volcanic Field (AVF). This monogenetic field of ca. 50 small volcanoes covers an area of 360 km² and may have been active for ca. 250 ka. Volcano monitoring can be difficult in small, distributed volcanic fields such as the AVF because the next vent location is not known; traditional techniques such as geochemical and ground deformation monitoring may not be feasible, as there is no obvious target for measurements. In such cases, seismic monitoring may be the only suitable technique. Recent attempts to improve monitoring capability in the AVF include the installation of six borehole seismometers across Auckland.

Borehole Seismology

The advantage of borehole seismometers for an urban environment is the ability to recognize microearthquakes even when there is substantial cultural/city noise (Ashenden et al., 2011). The records in Figure 1, from north Auckland, show two noise contrasts, Daytime vs nighttime cultural noise, and Seismic noise on the surface and in the borehole. The contrast between day and night is more significant on the surface seismometer. However, because the daytime higher noise level is still visible on the borehole seismometer, a deeper instrument would be required in order to identify the smallest earthquakes. In Auckland this was the first station installed, and 3 of 4 subsequent stations have been installed at greater depths.

The contrast between the surface and borehole noise levels is illustrated by a small event recorded on both instruments, circled on Figure 1. While the event is clearly identifiable on the borehole seismogram, it is difficult to identify in the surface data. Much of the noise has as high amplitudes as the seismic signal. This example demonstrates that borehole seismometers improve the ability to detect

small seismic signals. Because the signals are clearer, it becomes easier to identify clear p- and s-wave arrivals (Ashenden et al., 2011). These are critical for calculating accurate earthquake locations.

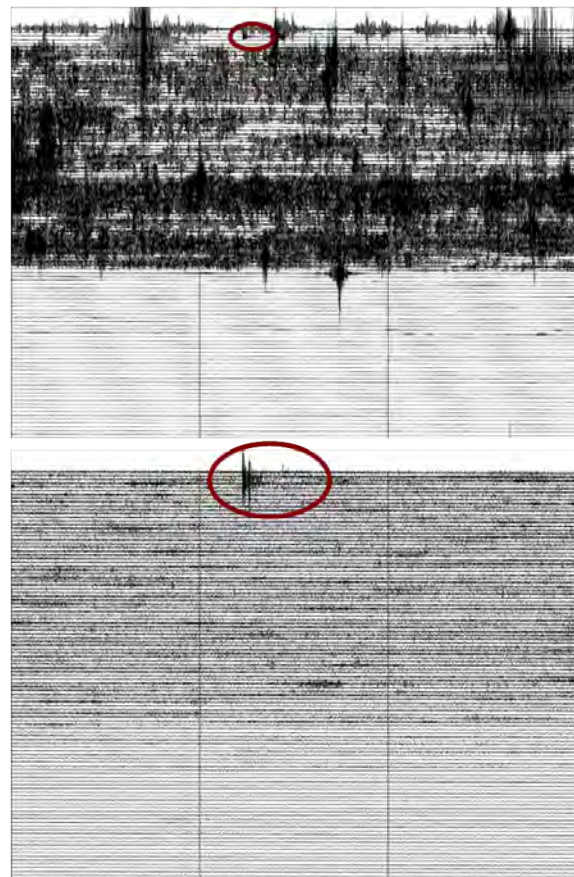


Fig. 1 - Helicorder plots recorded at Riverhead (north Auckland, see map Fig. 3) starting in the morning and going into the night of 11 April 2007. Seismograms are from the surface seismometer (*Top*) and the borehole seismometer at 245 m depth (*Bottom*). Time along the x axis is 3 minutes. The plots are not shown on the same scale due to the high amplitude of the noise. From Ashenden et al. (2011).

Another advantage of borehole seismometers is the improvement of signal to noise ratio and increase

in frequency content that reaches the instrument (Figure 2). If the seismometer can be placed below the surface layer, the signal reflects less attenuation and scattering. With increased depth the signal to noise ratio improves, as does the recording of higher frequencies.

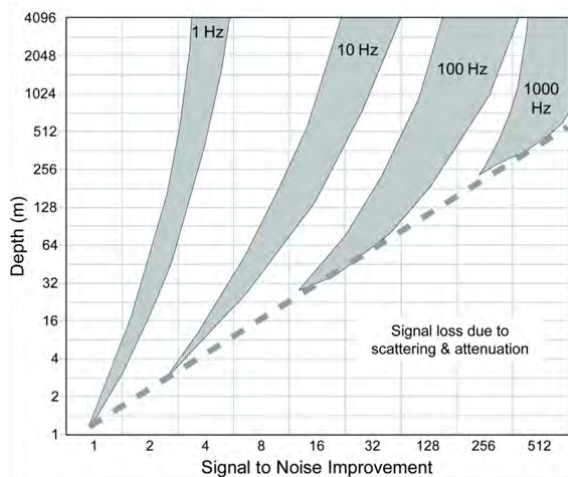


Fig. 2 - Expected improvement of signal to noise ratio with increased seismometer depth. Based on empirical data, Peter Malin and Ashenden et al. (2011).

In order to best take advantage of borehole seismometry there must be multiple instruments in an array; a network is critical in order to achieve triangulation of signals and accurate earthquake locations (Malin et al., in prep) The network needs to be closely enough spaced that multiple seismometers record the same earthquake in order to calculate accurate locations (Malin et al., in prep).

Volcano Monitoring In Auckland

High levels of background (cultural) seismic noise and extremely low levels of historical seismicity make volcano monitoring particularly challenging in the AVF. The monitoring agency GeoNet (GNS Science) has recently supplemented its 5-station surface network with 6 borehole seismometers (Figure 3).

If subsurface magmatic movement occurs, associated with the onset of volcanic activity in Auckland, seismicity would be expected, and it is unclear how big the earthquakes would be (Sherburn et al., 2007). It is possible that earthquakes would be small enough that a borehole network would provide a significant advantage in detecting precursory activity. This is an unknown due to the rare occurrence of eruptions in basaltic fields similar to Auckland (Sherburn et al., 2007) combined with the relatively new arrival of borehole seismometry in volcanic monitoring (Mattioli et al., 2004).

Conclusion

We conclude that borehole instrumentation in a volcano monitoring network allows better detection of local earthquakes, and multiple borehole sensors are required for adequate earthquake location. The advantages of a network of borehole instruments include the following: 1. Reducing cultural noise from the surface, 2. Increasing the signal to noise ratio due to reducing attenuation and scattering in the surface layer, and 3. Improving our ability to locate earthquakes by clearly identifying earthquake phase arrivals. These factors will be discussed in detail in the presentation.

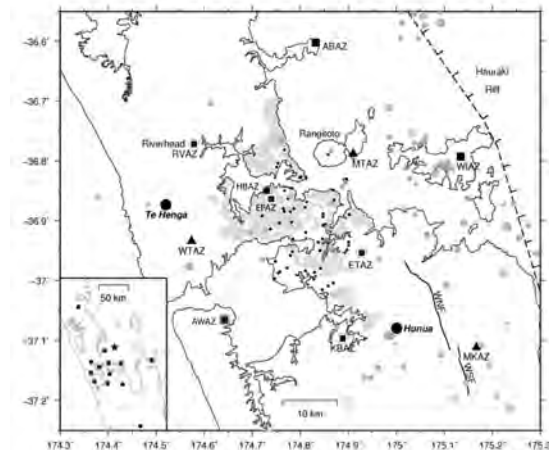


Figure 3. Map of the Auckland region. GeoNet monitors 5 surface seismometers (*black triangles and black squares*) and 6 borehole seismometers (*black rimmed squares*). Earthquakes that occurred between 1980 and 2009 are *grey circles*. Volcanic cones are *small black dots*. Inset shows regional seismic stations (*dots*) and the locations of an earthquake swarm in 2007 (*star*). Modified from Ashenden et al. (2011).

References

- Ashenden, C.L., Lindsay, J.M., Sherburn, S., Smith, I.E.M., Miller, C.A., Malin, P.E. 2011. Some challenges of monitoring a potentially active volcanic field in a large urban area: Auckland volcanic field, New Zealand. *Natural Hazards* 59: 507-528.
- Malin, P.E., Kenedi, C.L., Shalev, E. Chavarria, J. in preparation. Advantages of a borehole seismometer network for improving earthquake location and frequency content: Long Valley, California.
- Mattioli, G., et al. 2004. Prototype PBO instrumentation of CALIPSO Project captures world-record lava dome collapse on Montserrat. *Eos Trans. AGU* 85(34): 317-325.
- Sherburn, S., Scott, B.J., Olsen, J., Miller, C. 2007. Monitoring seismic precursors to an eruption from the Auckland Volcanic Field, New Zealand., New Zealand. *Journal of Geology and Geophysics* 50: 1-11.

Magma-output rates of the Auckland Volcanic Field (New Zealand)

Gábor Kereszturi¹, Károly Németh¹, Mark Bebbington^{1,2}, Shane J. Cronin¹, Javier Agustín-Flores¹, Jonathan Procter¹ and Jan Lindsay³

¹ Volcanic Risk Solutions, Massey University, Palmerston North, New Zealand – kereszturi_g@yahoo.com

² Institute of Fundamental Sciences – Statistics, Massey University, Palmerston North, New Zealand

³ School of Environment, The University of Auckland, Auckland, New Zealand

Keywords: eruptive volume, magma source, monogenetic

A good chronological and eruptive volume record is essential to understand the long-term evolution of a monogenetic volcanic field, determining its stage of development and also identifying whether it erupts with a regular periodicity or with pulses of activity (Connor et al., 2000, Kereszturi et al., 2011). Eruptive volume calculations for small-volume volcanic edifices are often challenging task because of the propensity for rapid erosion, weathering and anthropogenic modification, especially in heavily populated areas. A reconstruction of the dimensions of the original volcanic landforms is needed, applying theoretical models of the architecture typical volcanic cones and tuff rings.

Two end-member types of volcanic fields have been postulated: ‘time’ or ‘volume’ dependent models (Valentine and Perry, 2007). This classification has a significant impact on the methods that are applied for probabilistic volcanic hazards assessments at any particular field. Here we investigate whether the Auckland Volcanic Field, New Zealand, displays either one of these types of behavior (Fig. 1). The age of the volcanoes and the rough event order was previously estimated together with the eruptive volumes (Allen and Smith, 1994). They estimated a strongly asymmetric volume distribution, because more than half (59%) of the eruptive volumes (in Dense Rock Equivalent) were included in the last eruptive event, producing Rangitoto (ca. 553–504 yrs. BP), a scoria cone with surrounding lava flow field, forming a circular island at the northern edge of the field. We revisit the eruptive volume estimates based on a new, high-resolution Digital Elevation Model captured by aerial Light Detection and Ranging (LiDAR) survey and apply an updated temporal eruption order for the field (Bebbington and Cronin, 2011).

A general scheme for estimating magmatic output volume in monogenetic volcanic fields was established and applied to Auckland. A “model” monogenetic volcano was subdivided into up to 6 parts (not always present), including: (1) sub-surface diatreme; (2) crater infill; (3) tephra ring; (4) scoria cone; (5) lava flows and (6) distal tephra blanket. From these, only parts 3, 4 and 5 can be measured

directly using a DEM, the others require geophysical or geological investigation or some degree of reconstruction based on idealized parameters. At Auckland, 39 tuff rings and associated diatremes, 39 scoria cones and 33 lava flows or ponded intra-crater lavas were identified. From these components, the bulk volume is preserved as lava.

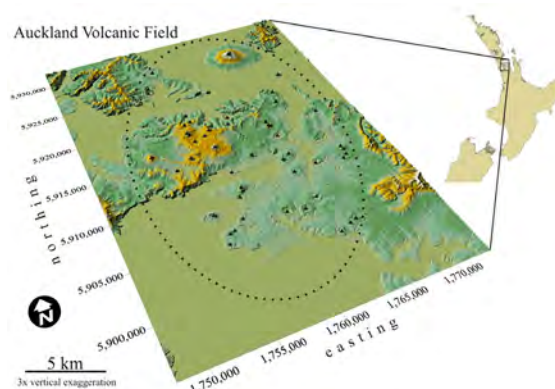


Fig. 1 – Overview DEM of Auckland Volcanic Field in New Zealand with the location of ca. 50 eruption centers (triangles).

Based on the DEM-measurements, the surface magmatic volume (DRE; Fig. 2) of the AVF is newly calculated at 2.17 km^3 , which is around half the previous estimate of ca. 4.2 km^3 (Allen and Smith, 1994). The reconstructed original tuff cone dimensions add $\sim 0.05 \text{ km}^3$ and magmatic crater infills contribute another $\sim 0.13 \text{ km}^3$. The distal tephra volume of each volcano was estimated by using the preserved/reconstructed crater sizes and a relationship introduced by Sato & Taniguchi (1997). While subject to the greatest potential error, the distal tephra adds up to $\sim 2.45 \text{ km}^3$, resulting in a total estimated magma output of 4.82 km^3 . This total volume could rise as high as 5.73 to 7.55 km^3 if theoretical conical or cylindrical sub-surface diatremes were added, based on the model of Lorenz (1986). Collectively, an average AVF eruption size is 0.04 (DEM-based volumes) or 0.15 km^3 (including all elements).

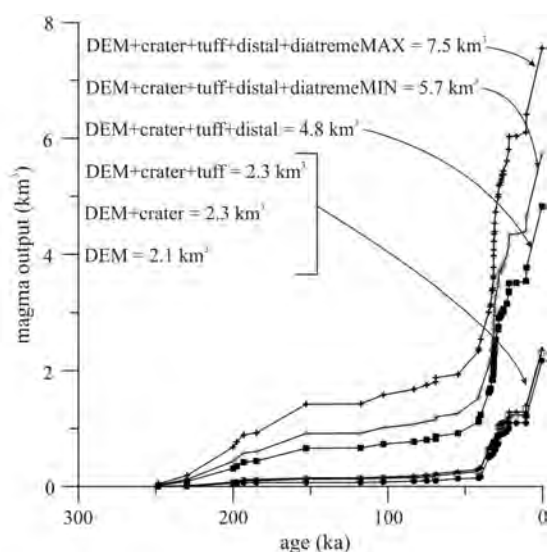


Fig. 2 – The changes of volume output measured. Note: DEM – purely the measurable volume from DEM, crater – magmatic crater infill volume, tuff – volume of circle-based reconstructed tuff ring, distal – volume of distal tephra blanket based minus present tuff ring or scoria cone volume, diatreme MIN and MAX – volumes preserved in the conical and a cylinder-shaped diatreme.

The estimated magma output rates for the entire field range from a minimum of 4.7×10^6 up to 24×10^6 m^3/ka . When examining this rate over time, it is highly apparent that either the age-control on the older part of the field is poor, or since ~ 50 ka there has been a major increase in output rate (Fig. 2). Consequently, the volume output of the field is highly time-inhomogeneous because of the existence of a volumetrically large single edifice, Rangitoto ca. 1 km^3 , and the “flare-up” period between 35 and 20 ka, which formed ca. 30 eruption centres scattered around the field (Cassidy, 2006, Molloy et al., 2009). Initial growth stages of the AVF show magma output rates of between 0.4×10^6 to 9.1×10^6 m^3/ka , with post 40 ka rates being between 37×10^6 to 128×10^6 m^3/ka . These latter magma output rates are the equivalent of one average AVF volcano per 1000 years. Interestingly, the volume based on DEM measurements (incl. crater infills and minimal tephra ring corrections) for Rangitoto and for the “flare-up” period are commensurate, around 0.96 and 1.08 km^3 , which requires further research.

Acknowledgements

This study was supported by the NZ FRST-IIOF Grant “Facing the challenge of Auckland’s Volcanism” (MAUX0808). The authors would like to thank the Auckland City Council for the LiDAR dataset.

References

- Allen, S.R., Smith, I.E.M. 1994. Eruption styles and volcanic hazard in the Auckland Volcanic Field, New Zealand. *Geoscience Reports of Shizuoka University* 20: 5-14.
- Bebbington, M.S., Cronin, S.J. 2011. Spatio-temporal hazard estimation in the Auckland Volcanic Field, New Zealand, with a new event-order model. *Bulletin of Volcanology* 73(1): 55-72.
- Cassidy, J. 2006. Geomagnetic excursion captured by multiple volcanoes in a monogenetic field. *Geophysical Research Letters* 33(L21310): 1-5.
- Connor, C.B., Stamatakos, J.A., Ferrill, D.A., Hill, B.E., Ofoegbu, G., Conway, F.M., Sagar, B., Trapp, J. 2000. Geologic factors controlling patterns of small-volume basaltic volcanism: Application to a volcanic hazards assessment at Yucca Mountain, Nevada. *Journal of Geophysical Research* 105(1): 417-432.
- Grosse, P., van Wyk de Vries, B., Petrinovic, I.A., Euillades, P.A., Alvarado, G.E. 2009. Morphometry and evolution of arc volcanoes. *Geology* 37(7): 651-654.
- Kereszturi, G., Németh, K., Csillag, G., Balogh, K., Kovács, J. 2011. The role of external environmental factors in changing eruption styles of monogenetic volcanoes in a Mio/Pleistocene continental volcanic field in western Hungary. *Journal of Volcanology and Geothermal Research* 201(1-4): 227-240.
- Molloy, C., Shane, P., Augustinus, P. 2009. Eruption recurrence rates in a basaltic volcanic field based on tephra layers in maar sediments: Implications for hazards in the Auckland volcanic field. *Geological Society of America Bulletin* 121(11-12): 1666-1677.
- Németh, K., Risso, C., Nullo, F., Kereszturi, G. 2011. The role of collapsing and rafting of scoria cones on eruption style changes and final cone morphology: Los Morados scoria cone, Mendoza, Argentina. *Central European Journal of Geosciences* 3(2): 102-118.
- Sato, H., Taniguchi, H. 1997. Relationship between crater size and ejecta volume of recent magmatic and phreato-magmatic eruptions: Implications for energy partitioning. *Geophysical Research Letters* 24(3): 205-208.
- Valentine, G.A., Perry, F.V. 2007. Tectonically controlled, time-predictable basaltic volcanism from a lithospheric mantle source (central Basin and Range Province, USA). *Earth and Planetary Science Letters* 261(1-2): 201-216.

Mafic alkalic magmatism in central Kachchh, India: a monogenetic volcanic field in the northwestern Deccan Traps

Pooja V. Kshirsagar, Hetu C. Sheth and Badrealam Shaikh

Department of Earth Sciences, Indian Institute of Technology Bombay, Powai, Mumbai, 400076, India – poojakv@iitb.ac.in

Keywords: Monogenetic volcanic field, maar-diatreme, Deccan Traps.

The Late Cretaceous to Palaeocene Deccan Traps (Fig. 1a) are one of the largest continental flood basalt provinces in the world, with a present-day area extent of 500,000 km² primarily in western and central India. Over much of this area the Traps are dominated by thick, extensive subalkalic basalt and basaltic andesite lava flows. Magmatism in Kachchh, in the northwestern Deccan continental flood basalt province (Fig. 1a,b), is represented not only by typical tholeiitic flows and dikes, but also plug-like bodies, in Mesozoic sandstone, of alkali basalt, basanite, melanephelinite and nephelinite, containing mantle nodules of spinel wehrlite, spinel lherzolite and dunite. They form the base of the local Deccan stratigraphy and their volcanological context was poorly understood. ⁴⁰Ar-³⁹Ar ages of 65-66 Ma (Pande et al., 1988) make them contemporaneous with the bulk of the Deccan Traps to the south. Based on new and published field, petrographic and geochemical data, we have identified the Kachchh central alkalic plugs as an eroded monogenetic volcanic field (Sheth et al., 2010; Kshirsagar et al., 2011). The plugs are shallow-level intrusions (necks, sills, dikes, sheets, laccoliths); one of them is known to have fed a lava flow. We have found local peperites reflecting mingling between magmas and soft sediment, and the remains of a pyroclastic vent (Karinga Dungar) composed of non-bedded lapilli tuff breccia, injected by mafic alkalic dikes (Fig. 2). The lapilli tuff matrix contains basaltic fragments, glass shards, and detrital quartz and microcline, with secondary zeolites, and there are abundant lithic blocks of mafic alkalic rocks. We interpret this deposit as a maar-diatreme, formed due to phreatomagmatic explosions and associated wall rock fragmentation and collapse. This is a one of few known hydrovolcanic vents in the Deccan Traps. The central Kachchh monogenetic volcanic field has >30 individual structures exposed over an area of ~1,800 km² and possibly many more if compositionally identical igneous intrusions in northern Kachchh are proven by future dating work to be contemporaneous.

A close analogue of the central Kachchh monogenetic volcanic field is the Late Miocene to Pleistocene Bakony-Balaton field in the western Pannonian Basin, Hungary (Németh and Martin, 2007) in which a shallow alkali basalt-basanite dike-

sill complex, emplaced in clastic sedimentary rocks, fed some phreatomagmatic volcanoes.

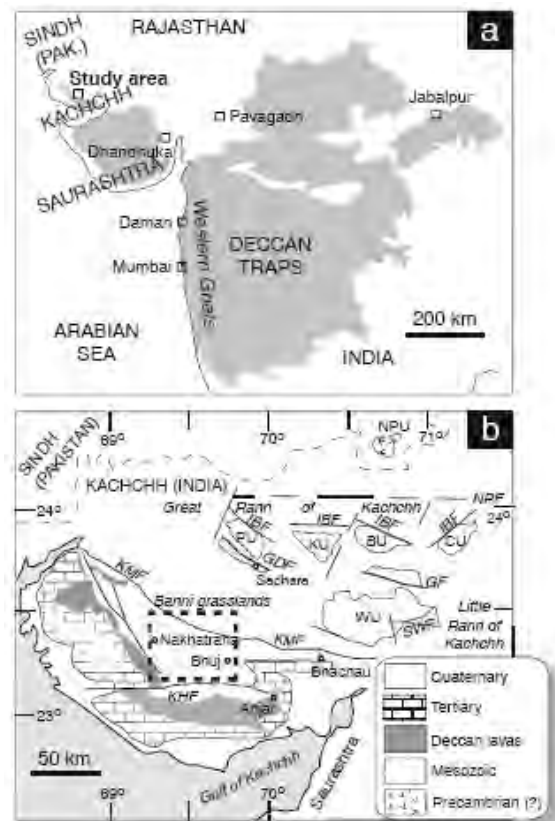


Fig. 1 - (a) Map of the Deccan Traps continental flood basalt province (shaded), showing the study area, the Western Ghats (type section of the Deccan flood basalts), and some localities. (b) Geological map of the Kachchh region, based on Ray et al. (2006), showing the geographic features, distribution of the various stratigraphic units, various structural uplifts (denoted by U's) forming "islands" in the Rann of Kachchh, and major faults (denoted by F's). Box shown with thick dashed line over central Kachchh is the area of the present study.

The central Kachchh field contains the same rock types (alkali basalt, basanite, melanephelinite) that are also abundant in the Honolulu (Hawaii), Bakony-Balaton, Waipiata (South Island, New Zealand) and Eifel (Germany) fields (Fig. 3). These fields are also well known for their mantle nodules, which the central Kachchh rocks also contain.

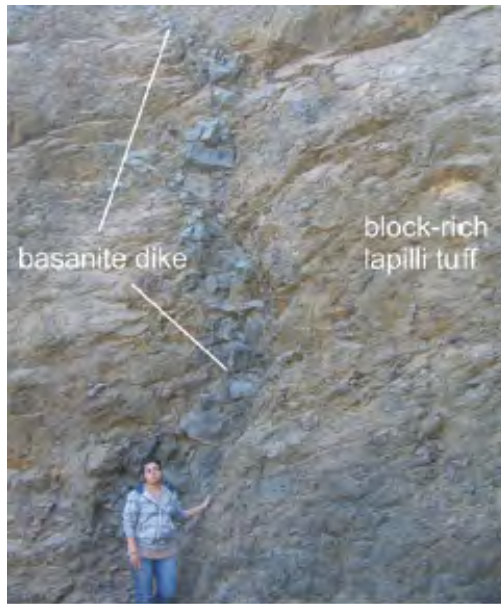


Fig. 2 – Quarry section in the Karinga Dungar maar-diatreme, composed of lithic-block-rich lapilli tuff intruded by basanite dikes (Kshirsagar et al., 2011).

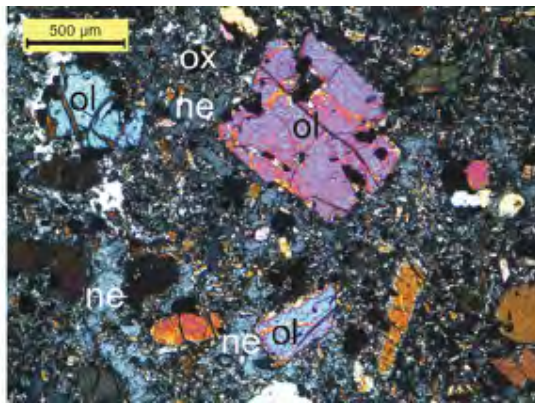


Fig. 3 – Melanephelinite, Aval Devi plug, central Kachchh. ol is olivine, ox is oxide, and ne is nepheline (Kshirsagar et al., 2011).

The central Kachchh field is considerably older than many well-known, young or active, monogenetic volcanic fields of the world, and more deeply eroded than most. Features of the central Kachchh field can thus be a guide to their substructure. The central Kachchh structures are analogues of the Type 1 vents of Németh and White (2003) in the Waipiata field, which are exclusively or largely composed of lava, and of the nature of necks, plugs, laccoliths, sills, dikes, and sheets. Karinga Dungar, a maar-diatreme, corresponds to Type 2 vents of Németh and White (2003) in the Waipiata field which represent substructures of phreatomagmatic tuff rings or maars.

The central Kachchh monogenetic volcanic field implies low-degree mantle melting and limited, periodic magma supply. Regional directed extension was absent or at best insignificant during its

formation, in contrast to the contemporaneous significant directed extension and vigorous mantle melting under the main area of the Deccan flood basalts (Ray et al., 2007). The central Kachchh field demonstrates regional-scale volcanological, compositional, and tectonic variability within flood basalt provinces, and adds the Deccan Traps to the list of such provinces containing monogenetic-and/or hydrovolcanism, namely the Karoo-Ferrar and Emeishan flood basalts, and plateau basalts in Saudi Arabia, Libya, and Patagonia.

Acknowledgements

This work was supported by grants to Sheth from the IRCC, IIT Bombay and Dept. Sci. Tech. (Govt. of India). Kshirsagar and Shaikh were supported by IIT Bombay Ph.D. and M.Tech. Student fellowships, respectively.

References

- Kshirsagar, P. V., Sheth, H. C., Shaikh, B. 2011. Mafic alkalic magmatism in central Kachchh, India: A monogenetic volcanic field in the northwestern Deccan Traps. *Bulletin of Volcanology* 73: 595-612.
- Németh, K., White, J.D.L. 2003. Reconstructing eruption processes of a Miocene monogenetic volcanic field from vent remnants: Waipiata volcanic field, South Island, New Zealand. *Journal of Volcanology and Geothermal Research* 124:1-21.
- Németh, K., Martin, U. 2007. Shallow sill and dyke complex in western Hungary as a possible feeding system of phreatomagmatic volcanoes in “soft-rock” environment. *Journal of Volcanology and Geothermal Research* 159: 138-152.
- Pande, K., Venkatesan, T. R., Gopalan, K., Krishnamurthy, P., Macdougall, J. D. 1988. ^{40}Ar - ^{39}Ar ages of alkali basalts from Kutch, Deccan volcanic province, India. *Geological Society of India Memoir* 10: 145–150.
- Ray, A., Patil, S.K., Paul, D.K., Biswas, S.K., Das, B., Pant, N.C. 2006. Petrology, geochemistry and magnetic properties of Sadara sill: evidence of rift related magmatism from Kutch basin, northwest India. *Journal of Asian Earth Sciences* 27: 907-921.
- Ray, R., Sheth, H.C., Mallik, J. 2007. Structure and emplacement of the Nandurbar-Dhule mafic dike swarm, Deccan Traps, and the tectonomagmatic evolution of flood basalts. *Bulletin of Volcanology* 69: 531-537.
- Sheth, H.C., Kshirsagar, P.V., Shaikh, B. 2010. Mafic alkalic magmatism in central Kachchh: a monogenetic volcano field in the northwestern Deccan Traps. *Geological Society of America Meeting: Tectonic Crossroads: Evolving Orogens of Eurasia-Africa-Arabia*; Ankara: 27-6.

The Auckland Volcanic Field – a basaltic field showing random behaviour?

Nicolas Le Corvec¹, Mark S. Bebbington², Bruce W. Hayward³, Jan M. Lindsay¹ and Julie V. Rowland¹

¹ School of Environment, The University of Auckland, Private Bag 92019, Auckland, New Zealand – n.lecorvec@auckland.ac.nz

² Volcanic Risk Solutions, Massey University, Palmerston North, New Zealand

³ Geomarine Research, 49 Swainston Rd, St Johns, Auckland, New Zealand

Keywords: Auckland Volcanic Field, Nearest Neighbor Analysis, Temporal Evolution.

Basaltic monogenetic volcanism is a worldwide phenomenon typically producing basaltic volcanic fields [Connor and Conway, 2000]. These fields consist of numerous volcanic centers generated by only one or few eruptions [Brenna et al., 2010; Needham, 2009] with each volcanic centre representing the final point at the surface of a magma propagating from its source. The general formation and evolution of basaltic volcanic fields seem to be similar, with their number of volcanic centers increasing with time. However, the evolution process is not constant but punctuated by single eruptions, flare-ups and hiatuses (e.g., Cassata et al., 2008; Molloy et al., 2009).

The analysis of the spatial distribution and temporal evolution of the volcanic centers within basaltic volcanic fields can provide constraints on the physical processes (e.g., magma production, tectonic controls) affecting the evolution of the field. These processes are keys to understand the future development of basaltic volcanic fields [Connor and Hill, 1995; Valentine and Perry, 2007]. The analysis of particular basaltic volcanic fields has shown the relationship between the distribution of their volcanic centers and the structural environment (e.g., Connor et al., 2000; Tinkler, 1971). Volcanic fields, however, are each geometrically different, with different number of volcanic centers, areas and spatial organization of their volcanic centers (with clusters and/or lineaments) [Le Corvec et al., in prep]. Comparing basaltic volcanic fields from different environments can help to classify them depending of the spatial distribution of their vents.

The development of a volcanic field is by definition a time dependent process, which involves mechanisms occurring in the mantle and the transfer of magma from the source to the surface [Valentine and Perry, 2007]; however, most volcanic fields are lacking reliable absolute dates for their volcanic centers. In the Auckland Volcanic Field (AVF), although the lack of reliable absolute dating prevent us to properly study its temporal evolution [Lindsay et al., 2010], a recent study has provided a relative chronology of the sequence of eruption within the AVF [Bebbington and Cronin, 2011]. This temporal

sequence as well as newly reworked versions will be used to study the potential evolution of the AVF.

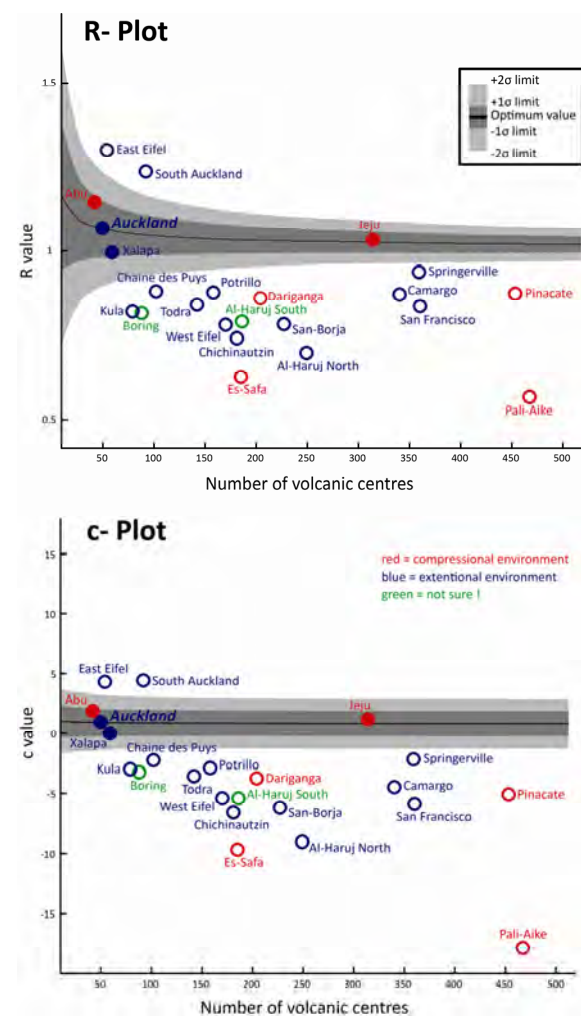


Fig. 1 – Plot of the R- and c- values for a selection of volcanic fields. Most of the volcanic fields show clustering compared to the Poisson distribution ($R < -2\sigma$). Auckland, Xalapa, Abu and Jeju volcanic fields fit the Poisson distribution (R within the $\pm 2\sigma$). The South Auckland and East Eifel volcanic fields show a more dispersed distribution compared to the Poisson distribution ($R > +2\sigma$).

Poisson Nearest Neighbor (PNN) analysis evaluates the spatial distribution of a natural population (also called the observed data) over the spatial distribution of a statistical random model, the Poisson model (also called the expected data), by comparing the mean distance between each NN of the observed data (r_o) with the mean distance between each NN of the expected data (r_e).

$$R = \frac{r_o}{r_e}$$

The resulting ratio (R) quantifies the amount of departure of the observed data from the random model [Clark & Evans 1954]. The relevance of the statistical value R is estimated through the statistical value c :

$$c = \frac{r_o - r_e}{\sigma_e}$$

with σ_e being the standard error of the mean NN for the expected distribution [Clark & Evans 1954].

The statistical analysis was executed through MATLAB using the Geological Image Analysis Software (GIAS; www.geoanalysis.org) [Beggan & Hamilton 2010].

The results of this analysis for a selection volcanic fields show that most of them have a clustered distribution compared to the Poisson distribution and few show either a dispersed distribution, or a distribution fitting the Poisson model, like the AVF.

One might ask what the future evolution of the AVF will be. Could it either follow most of the volcanic fields shown in Fig. 1 and evolve in a clustered distribution, or follow the South AVF and evolve in a dispersed distribution, or will it continue to evolve in a random way which fits the Poisson model. Each of these cases involves different scenarios in term of location of the next volcanic vent, and each also results in a different area for the volcanic field.

To answer these questions, we used the PNN technique to analyze the different temporal sequences of the AVF. We recalculated the R - and c - value for each step in the temporal evolution of the AVF.

The results show that the temporal evolution of the spatial distribution of the AVF stays consistent with the Poisson model (Figure 2). The overall evolution tends to be going toward a more clustered distribution. We can also observe small fluctuations in series 2 and 3. These results, however, cannot be used to extrapolate the future evolution of the volcanic field due to the high uncertainties related to the ordering of each volcanic vent. These results will be upgraded as the age database of the AVF improves over time.

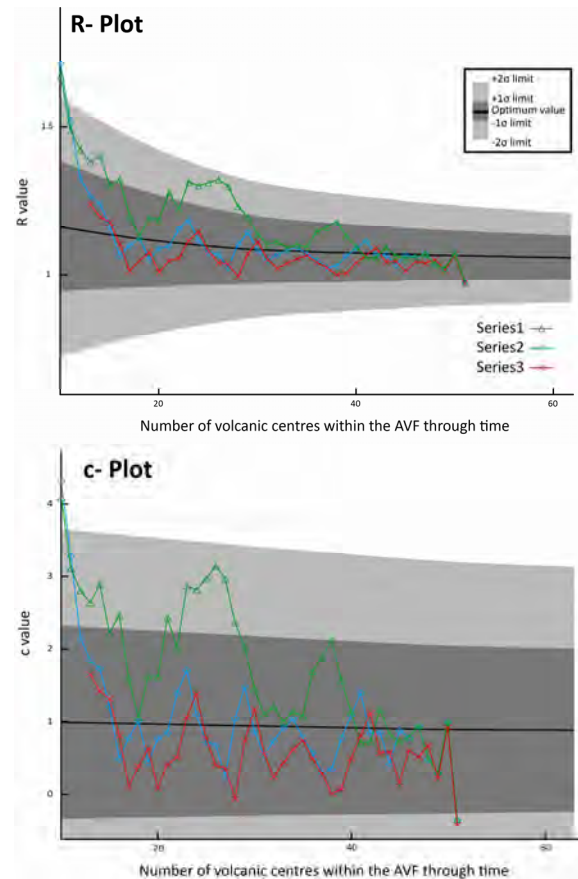


Fig. 2 – Plot of the statistical R - and c - values against the number of volcanic centers within the AVF through time.

Acknowledgements

This work was undertaken through the DEVORA (Determining Volcanic Risk in Auckland) project co-funded by the NZ Earthquake Commission (EQC) and the Auckland Regional Council (now part of the wider Auckland Council).

References

- Bebbington, M., Cronin, S. 2011. Spatio-temporal hazard estimation in the Auckland Volcanic Field, New Zealand, with a new event-order model. *Bulletin of Volcanology* 73(1): 55-72.
- Brenna, M., Cronin, S.J., Smith, I.E.M., Sohn, Y-K., Németh, K. 2010. Mechanisms driving polymagmatic activity at a monogenetic volcano, Udo, Jeju Island, South Korea. *Contributions to Mineralogy and Petrology* 160(6): 931-950.
- Cassata, W.S., Singer, B.S., Cassidy, J. 2008. Laschamp and Mono Lake geomagnetic excursions recorded in New Zealand. *Earth and Planetary Science Letters* 268(1-2): 76-88.
- Connor, C.B., Hill, B.E., 1995. Three nonhomogeneous Poisson models for the probability of basaltic volcanism: application to the Yucca Mountain region, Nevada. *Journal of Geophysical Research* 100(B6): 10,107-110,125.

- Connor, C.B., Conway, F.M. 2000. Basaltic volcanic fields. *Encyclopedia of Volcanoes* 331-343.
- Connor, C.B., Stamatakos, J.A., Ferrill, D.A., Hill, B.E., Ofoegbu, G.I., Conway, F.M., Sagar, B., Trapp, J. 2000. Geologic factors controlling patterns of small-volume basaltic volcanism: Application to a volcanic hazards assessment at Yucca Mountain, Nevada. *Journal of Geophysical Research B: Solid Earth*, 105(B1): 417-432.
- Le Corvec, N., Spörli, K.B., Legrand, D., Rowland, J.V. in prep. Monogenetic volcanic fields: Spatial distribution and volcanic lineaments as indicators for crustal controls.
- Lindsay, J., Marzocchi, W., Jolly, G., Constantinescu, R., Selva, J., Sandri, L. 2010. Towards real-time eruption forecasting in the Auckland Volcanic Field: application of BET_EF during the New Zealand National Disaster Exercise 'Rauumoko'. *Bulletin of Volcanology* 72(2): 185-204.
- Molloy, C., Shane, P., Augustinus, P. 2009. Eruption recurrence rates in a basaltic volcanic field based on tephra layers in maar sediments: Implications for hazards in the Auckland volcanic field. *Geological Society of America Bulletin* 121(11-12): 1666-1677.
- Needham, A.J. 2009. The eruptive history of Rangitoto Island, Auckland Volcanic Field, New Zealand. Thesis (MSc Geology), University of Auckland.
- Tinkler, K.J. 1971. Statistical analysis of tectonic patterns in areal volcanism: The bunyaruguru volcanic field in West Uganda. *Journal of the International Association for Mathematical Geology* 3(4): 335-355.
- Valentine, G.A., Perry, F.V. 2007. Tectonically controlled, time-predictable basaltic volcanism from a lithospheric mantle source (central Basin and Range Province, USA). *Earth and Planetary Science Letters* 261(1-2): 201-216.

Macro- and micro-characterization of multiple lower diatreme conduit remnants: Implications for maar-diatreme formation

Nathalie Lefebvre¹, James D.L. White¹, Bruce Kjarsgaard² and Pierre-Simon Ross³

¹ Department of Geology, University of Otago, P.O. Box 56, Dunedin, New Zealand – lefna448@student.otago.ac.nz

² Geological Survey of Canada, 601 Booth Street, Ottawa, Ontario, Canada

³ Institut national de la recherche scientifique, 490 rue de la Couronne, Québec, Canada

Keywords: lower diatreme, debris-jets, conduit, country rock, xenolith

How maar-diatreme volcanoes excavate the country rock and evolve over the duration of an eruption is still poorly understood. This is because modern eruptions are rare, and study of all volcano-structural levels of one volcano i.e. the conduit and their associated deposits representing the entire eruption is impossible, with the subterranean portions generally inaccessible for study. However, in deeply eroded monogenetic centres we know that the diatreme structures have steep near subvertical walls with sharp external contacts and are infilled by different poorly sorted mixtures of country rock clasts, fragmented magma and cement(s). It is generally agreed upon that this region acts as a conduit where pyroclastic debris is transported towards the surface and deposited, and also where wall rock collapses into thereby increasing the volume of the overall structure (White and Ross, 2011). However, there are several different ideas on what drives country rock excavation (e.g. Sparks et al., 2006; Lorenz and Kurszlauskis, 2007; Porritt et al., 2008; Valentine et al., 2011), specifically are the eruptions sustained or pulsatory, and how much debris remains within the diatreme and how much is deposited onto the surrounding surface.

Diatreme deposits present a partial record of pipe forming and related eruption processes, providing valuable information to better understand maar-diatreme eruptions. The Hopi Buttes Volcanic Field (HBVF) situated on the tectonically stable Colorado Plateau in northeastern Arizona is an ideal locality to study diatremes. This is because it has experienced varying degrees of erosion, revealing superb pseudo-3D exposures of the different volcano-structural levels of a maar-diatreme volcano. Moreover, the well exposed and flat-lying sedimentary host rock strata have unique identifiable characteristics allowing for linking of quantitative measurements of country rock abundances from any volcanological unit to specific country rock formations of known thickness and depth.

West Standing Rocks (WSR) exposed about 300 m below the HBVF pre-eruptive land surface is an excellent vertical section of a lower diatreme (Fig.1; White, 1991).

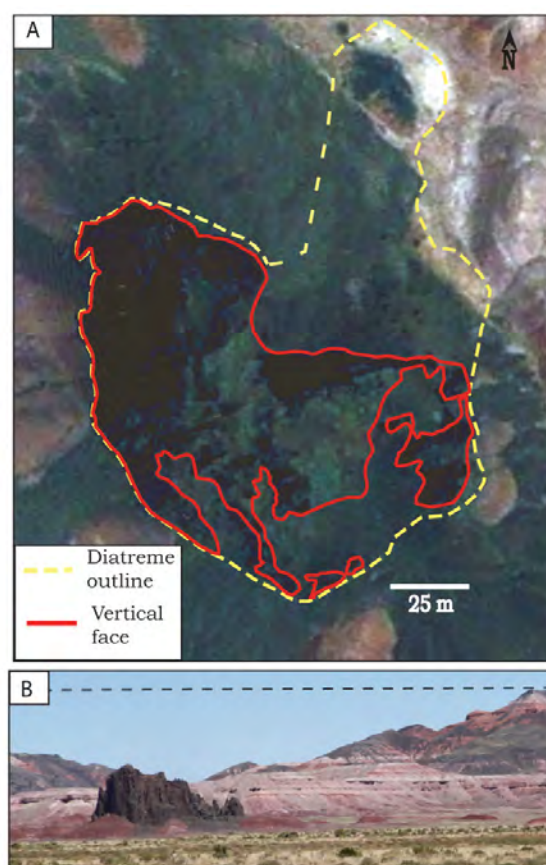


Fig. 1 – WSR diatreme. A. Plan view satellite image showing the extent (8900 m²) of vertical exposure available for mapping. B. Photograph of WSR diatreme showing the excellent exposure of the volcano and surrounding country rock. Stippled line marks the approximate pre-eruptive land surface.

Apart from the north side, it consists of several sub-vertical columns of pyroclastic debris marked by differences in the types and size of volcanic and country rock constituents (Fig.2). These columns are interpreted as the preserved record of multiple individual jets of pyroclastic debris propagating up through the pile of unconsolidated diatreme deposits, and are the vertical equivalent of the plan view domains within the diatreme complex documented in Coombs Hills, Antarctica (Ross and White, 2006). Both these localities show that the

diatreme structure is composed of multiple debris-filled conduits reflecting not one but many eruptive bursts at several different locations and times within the diatreme structure.

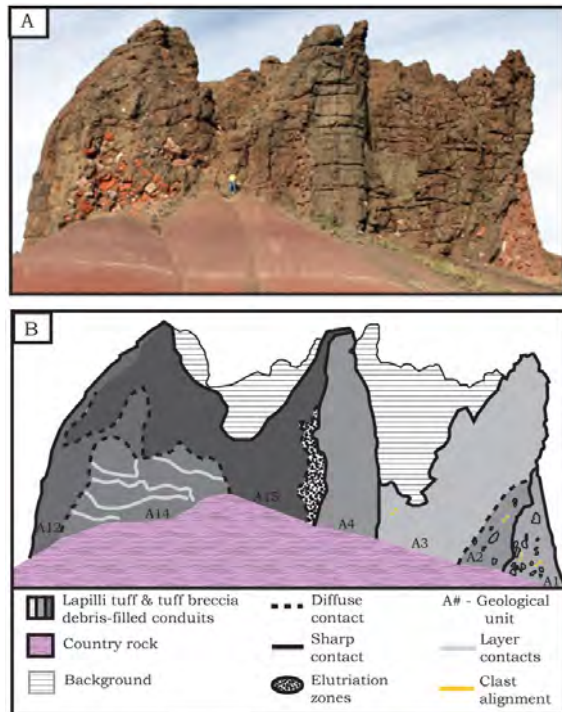


Fig. 2 – East side of WSR lower diatreme showing the subvertical columns interpreted as debris-filled conduits marked by differences in componentry type and abundance. A. Photograph with person for scale. B. Face map of photograph.

The WSR study entails detailed volcanological mapping, quantitative clast size and abundance measurements from image analysis studies and complimentary petrographic examination of the subvertical columns comprising the lower diatreme at WSR. This study provides the first detailed macro-and micro characterization of a well exposed lower diatreme, linking detailed mapping and componentry data from well exposed outcrops to the volume of individual eruptive bursts, well constrained country rock units and of the overall diatreme structure.

Results provide insight into the nature of the fragmentation site (i.e. within the wall rock or pyroclastic debris from an earlier burst), how much country rock debris remains within the diatreme structure over the course of a maar-diatreme eruption, and how much can be inferred to be ejected. The detailed study from WSR shows that the lower diatreme deposits are products of multiple fragmentation bursts which occur at variable lateral and vertical locations within the diatreme structure,

substantiating the work at Coombs Hills (Ross and White, 2006) and analogue debris-jet experiments (Ross et al., 2008a,b).

Acknowledgements

We are grateful to George Billingsley and Bernard Lefebvre for their invaluable assistance in the field. This study was supported by a Society of Economic Geologists Student Grant, Sigma Delta Epsilon Graduate Women in Science Fellowship, Commonwealth PhD Scholarship to N. Lefebvre and GNS Science funding to J.D.L. White. Field work on the Navajo Nation was conducted under a permit from the Navajo Nation Minerals Department.

References

- Lorenz, V., Kurszlaukis, S. 2007. Root zone processes in the phreatomagmatic pipe emplacement model and consequences for the evolution of maar-diatreme volcanoes. *Journal of Volcanology and Geothermal Research* 159: 4-32.
- Porritt, L.A., Cas, R.A.F., Crawford, B.B. 2008. In-vent column collapse as an alternative model for massive volcanoclastic kimberlite emplacement: An example from the Fox kimberlite, Ekati Diamond Mine, NWT, Canada. *Journal of Volcanology and Geothermal Research* 174: 90-102.
- Ross, P.-S., White, J.D.L. 2006. Debris jets in continental phreatomagmatic volcanoes: A field study of their subterranean deposits in the Coombs Hills vent complex, Antarctica. *Journal of Volcanology and Geothermal Research* 149: 62-84.
- Ross, P.-S., White, J.D.L., Zimanowski, B., Buttner, R. 2008a. Rapid injection of particles and gas into non-fluidized material, and some volcanological implications. *Bulletin of Volcanology* 70: 1151-1168
- Ross, P.-S., White, J.D.L., Zimanowski, B., Buttner, R. 2008b. Multiphase flow above explosion sites in debris-filled volcanic vents: Insights from analogue experiments. *Journal of Volcanology and Geothermal Research* 178: 104-112.
- Sparks, R.S.J., Baker, L., Brown, R.J., Field, M., Schumacher, J., Stripp, G., Walters, A. 2006. Dynamical constraints on kimberlite volcanism. *Journal of Volcanology and Geothermal Research* 155: 18-48.
- Valentine, G.A., Shufelt, N.L., Hintz, A.R.L. 2011. Models of maar volcanoes, Lunar Crater (Nevada, USA). *Bulletin of Volcanology* 73: 753-765.
- White, J.D.L., Ross, P.-S. 2011. Maar-diatreme volcanoes: A review. *Journal of Volcanology and Geothermal Research* 201: 1-29.
- White, J.D.L. 1991. Maar-diatreme phreatomagmatism at Hopi Buttes, Navajo Nation (Arizona), USA. *Bulletin of Volcanology* 53: 239-258.

Determining volcanic risk in the Auckland Volcanic Field: a multidisciplinary approach

Jan Lindsay¹ and Gill Jolly²

¹ School of Environment, The University of Auckland, Private Bag 92019, Auckland, New Zealand - j.lindsay@auckland.ac.nz

² GNS Science, Wairakei Research Centre, Taupo, New Zealand

Keywords: Auckland Volcanic Field, volcanic hazard, DEVORA

The potentially active Auckland Volcanic Field (AVF) comprises ca. 50 basaltic ‘monogenetic’ volcanic centres (Fig. 1) and is coincident with New Zealand’s largest city, Auckland. The oldest eruption occurred about 250,000 years ago and the most recent eruption, 550 years ago, was witnessed by early indigenous Maori. Although the volcanoes in Auckland are small and their eruptions have been infrequent, the risk associated with future activity is very high given the high physical and economic vulnerability of Auckland (population 1.3 million; 2006 census). Assessing long term volcanic hazard and associated risk in Auckland is challenging. However, since 2008 there has been a boost in research in this area through the multidisciplinary, multi-agency DETERmining VOLcanic Risk in Auckland (DEVORA) research programme which has led to an improved understanding of both the inner workings of the field and also what we might expect in the event of a future eruption.

The DEVORA project has core funding from the New Zealand Earthquake Commission (EQC), Auckland Council (AC), The University of Auckland and GNS Science and is divided into three themes. The Geological theme aims to integrate structural, petrological and geophysical data into a geological model of the AVF to explain source-to-surface magma migration and dynamics. The Probabilistic Volcanic Hazard theme focuses on creating a realistic volcanic hazard outlook for Auckland, using dating and tephrochronology to assess magnitude-frequency patterns and possible spatio-temporal trends. In the Risk and Social theme, the economic and social effects of an AVF eruption on Auckland and the rest of New Zealand are being investigated, and a quantitative risk assessment and emergency management risk reduction framework for Auckland’s vulnerable groups and structures prepared.

Past eruptions in the AVF have typically initiated with phreatomagmatic explosions and base surges, followed by mildly to moderately explosive strombolian to sub-plinian activity building scoria cones. In many cases the last phase of an eruption has resulted in lava flows. Most of the volcanoes in Auckland are thought to have grown during eruptions lasting a few months or possibly a few

years. Several volcanoes in the field (e.g. Rangitoto) comprise numerous volcanic features and/or satellite cones indicating that several eruptive episodes have occurred during their formation, perhaps with time breaks between eruptions.

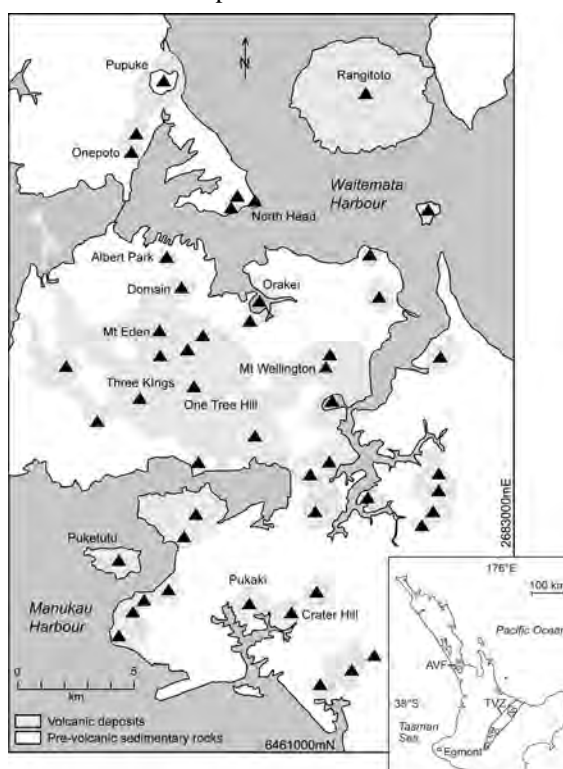


Fig. 1 Map of the Auckland region showing the Auckland Volcanic Field centers (triangles) and deposits. Inset shows the position of the AVF relative to other major volcanic centers, Egmont and the Taupo Volcanic Zone (TVZ), in the North Island of New Zealand.

Over the past decade several AVF craters have been drilled to extract cores containing tephra layers interbedded with laminated lake sediments, and these tephra layers provide great insight into the frequency with which Auckland has been impacted by eruptions in the past. At least 30 local eruptions in the last 80,000 yrs have so far been recognized, at an average frequency over this time period of 1 per 2,600 yrs, although few of these can be correlated to their source volcanoes (Molloy et al. 2009). The tephra record also reveals that activity has been episodic, with a major ‘flare-up’ in volcanism at 32

± 2 ka. A recent review of the seemingly large number (> 180) of age determinations available for individual centres in the AVF concluded that strongly reliable age estimates can only be given for three centres: Rangitoto (0.6 ka), Mt Wellington (10 ka) and Three Kings (28.5 ka) (Lindsay et al. in press). Best-estimate radiometric ages available for the AVF display a marked clustering of possible ages between 28 and 33 ka, which corresponds well with the clustering of basaltic tephra in the same age range observed in the maar sediment cores as well as a clustering of activity during this timeframe indicated by several centres in the field that display anomalous paleomagnetic signatures (Cassata et al. 2008; Cassidy 2006). To date there have been no reliable spatio-temporal trends identified in the AVF. If any trends are present, they appear to be obscured by a general lack of reliable numeric ages, the fact that past eruptions have been small with restricted deposits that seldom overlap those of neighbouring centres, and little evidence for structural control of vent locations.

Although a future eruption in Auckland would be relatively small, its effects would be devastating to the economy of New Zealand. In Auckland, the evacuation of hundreds of thousands of people and likely closure of the international airport would have a huge impact, possibly resulting in a 47 % and 14% reduction in gross domestic product (GDP) for the Auckland region and New Zealand, respectively (MCDEM 2008).

A recent Disaster Exercise “Ruaumoko”, based on an AVF eruption, highlighted the difficulties in calling a mass evacuation in a situation where the source of the hazard (the eruption vent) is not known until shortly before the outbreak. Auckland emergency managers now have a better appreciation of the trade-off between certainty in eruption location and time available (i.e. the longer you wait the more certain the vent location but the shorter the time available to complete the evacuation). The authorities and scientists are now working together to investigate the possibility of using probabilistic methods of eruption forecasting to aid decision making (Lindsay et al. 2010; Sandri et al. in press).

Currently, volcanic risk in Auckland is estimated qualitatively by Civil Defense personnel as part of legislative requirements for developing a multi-hazard risk profile for Auckland. Through DEVORA, we are moving towards more

quantitative volcanic risk modeling in Auckland through the Regional RiskScape project (Schmidt et al. 2011) carried out by GNS Science and the National Institute of Water and Atmospheric Research Ltd. (NIWA).

Despite the uncertainties associated with a future AVF eruption, scientists, authorities, lifeline organisations and funding agencies are all working together to ensure that New Zealand is well prepared should the volcanic field become restless again.

References

- Cassata, W.S., Singer, B.S., Cassidy, J. 2008. Laschamp and Mono Lake geomagnetic excursions recorded in New Zealand. *Earth and Planetary Science Letters* 268(1-2): 76-88. DOI 10.1016/j.epsl.2008.01.009.
- Cassidy, J. 2006. Geomagnetic excursion captured by multiple volcanoes in a monogenetic field. *Geophysical Research Letters* 33: L21310. DOI 10.1029/2006GL027284.
- Lindsay, J.M., Marzocchi, W., Jolly, G., Constantinescu, R., Selva, J., Sandri, L. 2010. Towards real-time eruption forecasting in the Auckland Volcanic Field: application of BET_EF during the New Zealand National Disaster Exercise 'Ruaumoko'. *Bulletin of Volcanology* 72: 185-204. DOI 10.1007/s00445-009-0311-9.
- Lindsay, J.M., Leonard, G.S., Smid, E.R., Hayward, B.W. in press. Age of the Auckland Volcanic Field: a review of existing data. *New Zealand Journal of Geology and Geophysics*.
- MCDEM 2008. Exercise Ruaumoko '08. Final Exercise Report (2008). Ministry of Civil Defence and Emergency Management.
- Molloy, C., Shane, P., Augustinus, P. 2009. Eruption recurrence rates in a basaltic volcanic field based on tephra layers in maar sediments: implications for hazards in the Auckland Volcanic Field. *Geological Society of America Bulletin* 121(11-12): 1666-1677.
- Sandri, L., Jolly, G., Lindsay, J., Howe, T., Marzocchi, W. in press. Combining long- and short-term probabilistic volcanic hazard assessment with cost-benefit analysis to support decision making in a volcanic crisis from the Auckland Volcanic Field, New Zealand. *Bulletin of Volcanology*.
- Schmidt, J., Matcham, I., Reese, S., King, A., Bell, R., Henderson, R., Smart, G., Cousins, J., Smith, W., Heron, D. 2011. Quantitative multi-risk analysis for natural hazards: a framework for multi-risk modelling. *Natural Hazards* 58: 1169-1192. DOI 10.1007/s11069-011.

On differences and similarities between maar-diatreme volcanoes and explosive collapse calderas

Volker Lorenz¹ and Peter Suhr²

¹ *Physical Volcanological Laboratory, University of Wuerzburg, Pleicherwall 1, D-97070 Wuerzburg, Germany - vlorenz@geologie.uni-wuerzburg.de*

² *Sächsisches Landesamt für Umwelt, Landwirtschaft und Geologie, (LfULG), P.O. Box 54 01 37, D-01311 Dresden, Germany*

Keywords: Maar-diatreme volcano, explosive collapse caldera, caldera substructure

Maar-diatreme volcanoes and explosive collapse calderas represent two volcano types displaying craters that cut into pre-eruptive country rocks. Despite differences in size and other characteristics they display some distinct similarities. For an explosive collapse caldera the term ash-flow caldera has frequently been used as a synonym (e.g. Lipman 1997).

Maar-diatreme volcanoes have a crater of a diameter of perhaps several tens of meters in case of very small and short-lived craters and up to c. 2 or even more km in case of very large and long-lived or intersecting maar craters (Lorenz 2007, Lorenz and Kurszlaukis 2007). The diameter of small explosive collapse caldera craters may be only a few km wide whereas in case of large ones it may reach 40 to c. 100 km.

In addition to their contrast in size, other major differences between these two volcano types are the dominant magma types involved (mafic to ultramafic versus intermediate to acidic), the ejected tephra volume, and the dominant eruption type (phreatomagmatic versus magmatic). In each of their many eruptions, maar-diatreme volcanoes usually eject a rather small tephra volume. The eruption clouds lead to proximal base surge deposits on the tephra ring and outside to distal ash falls. Maar extra-crater tephra deposits have a total volume between much less than or up to c. 0.1-0.2 km³. In contrast, one or only a few ash-flow and associated proximal and distal ash fall deposits characterize the tephra of explosive collapse calderas and add up to a volume of up to several 1000 km³ for very large calderas.

During early post-eruptive time the crater of many maar and subaerial explosive collapse caldera volcanoes are frequently filled by a lake. However, at probably the majority of maar-diatreme volcanoes post-phreatomagmatic activity has led to intra-crater intrusions and magmatic volcanic deposits such as scoria cones, lava flows, lava lakes, or even domes in case of acidic maars. At Ukinrek East Maar scoria was even ejected from a second intra-crater vent between, simultaneously with and even briefly after the phreatomagmatic eruptions that lasted for only 8

days in 1977 (Lorenz 2007). In addition to intrusions leading to ring-dykes or even resurgence, the equivalent post-collapse volcanic features at explosive collapse calderas may be intra-caldera scoria cones, lava flows, domes, and ash flow deposits. Lava flows and domes also get frequently fed from conduits located on caldera ring-fault segments (Lipman 1997).

Both volcano types display a substructure below their crater. A cone-shaped diatreme with an upper diameter of up to several 100 m, rarely exceeding 1000 m, underlies the maar craters (Lorenz and Kurszlaukis 2007). An equivalent large substructure underlies the explosive collapse calderas. Their substructure is possibly funnel-shaped in case of small calderas whereas it is plate-underlain in case of large calderas (Lipman 1997). A large diatreme, up to 2-2.5 km deep, contains (1) up to several 100 or even more than one thousand m thick, finely bedded primary tephra deposits, mostly of base surge origin, and (2) interbedded, usually thicker beds of reworked tephra. These beds demonstrate that the maar crater floor acted as a depot centre: thick primary and reworked tephra (debris flows, lahars) accumulated on the maar crater floor. During syn-eruptive growth of maar-diatreme volcanoes the primary and reworked intra-crater tephra and collapse breccias subside inside the diatreme along its ring-fault (Lorenz and Kurszlaukis 2007, White and Ross 2011) - as is shown by the diatremes, e.g., in the Missouri Breaks in Montana (Hearn 1966), the Midland Valley in Scotland (Francis 1970, Leys 1982), and the Hopi Buttes in Arizona (White 1991). The diatreme fill is cut by narrow tephra feeder conduits. In all probability, their diameter has originally been up to a few tens of meters wide only (Lorenz and Kurszlaukis 2007, White and Ross 2011).

The reworked tephra, that are interbedded with the primary tephra beds in a diatreme, originate from collapse (slumps, slides) of arcuate slices of bedded primary tephra on the inner crater wall of the maar tephra ring. In some diatremes also country rocks, i.e. hard rocks or soft sediments respectively, collapsed from unstable country rocks in the lower

inner crater walls during and soon after the eruptions. These collapsed country rocks became deposited on the crater floor as rock falls, rock slumps or scree or even as sand flows respectively. These collapse processes of tephra and country rocks repeatedly increased the maar crater diameter. They are considered to have been caused by the enlargement of the underlying cone-shaped diatreme (Lorenz and Kurszlauskis 2007). In substructures of explosive collapse calderas, equivalent, primary, mostly welded ash-flow deposits and collapse breccias, the latter syn- and post-eruptively derived from collapsed country rocks from the crater wall, are widely known and may jointly reach several km in thickness (Lipman 1997).

Ring dykes in diatremes (Hearn 1966, Lorenz and Haneke 2004) are the equivalent of dykes along caldera ring-faults. Despite syn-eruptive subsidence of both, the caldera and diatreme fill, the ring dykes imply an extensional stress. This is also indicated by the repeated post-eruptive opening of an arcuate fissure on the floor of Marteles Maar on Gran Canaria (Schmincke and Sumita 2010).

Following syn-eruptive subsidence, post-eruptive subsidence of the unconsolidated water-saturated diatreme fill and post-eruptive sedimentary maar crater fill has been shown for a few maar-diatremes and it lasted for up to several tens of million years (Suhr et al. 2006). Post-eruptive subsidence of intra-caldera ash-flow and collapse breccia deposits that had already synchronously subsided with the caldera subsidence has not been described yet. Such a post-eruptive subsidence could be possible, however, not only for collapse breccias but also for non-welded intra-caldera ash-flow deposits (Walker 1983).

The impressive similarities between the two volcano types have, in principle, a similar origin. The typical shape of a maar-diatreme volcano is the rock-mechanical response to (1) explosive phreatomagmatic, i.e. thermohydraulic fragmentation of magma and relatively large amounts of surrounding country rocks at the top end of an active feeder dyke and (2) the consequent ejection of the tephra from that explosion chamber. The resulting mass deficiency causes subsidence of the overlying crustal rocks and tephra, i.e. the syn-eruptive subsidence and growth of the diatreme and, of course, of the overlying maar crater. Likewise, the explosive collapse caldera is the rock-mechanical response to a very rapid rise and ejection of a large vesiculating magma volume from an even larger magma reservoir. The ensuing mass

deficiency at depth causes syn-eruptive subsidence of the overlying rocks and tephra. At explosive collapse calderas the extra-caldera ash-flow deposits correspond to the base surge deposits of the maar tephra ring. The intra-caldera ash-flow deposits correspond to the intra-diatreme base surge tephra.

Large maar-diatremes may merge with small calderas in geometry and size (Lipman 1997).

References

- Francis, E.H. 1970. Bedding in Scottish (Fifeshire) tuff-pipes and its relevance to maars and calderas. *Bulletin volcanologique* 34: 697-712.
- Hearn, B.C. 1968. Diatremes with kimberlitic affinity in north-central Montana. *Science* 159: 622-625.
- Leys, C.A. 1982. Volcanic and sedimentary processes in phreatomagmatic volcanoes. Unpublished Ph.D. thesis, University of Leeds, 402 pp.
- Lipman, P.W. 1997. Subsidence of ash-flow calderas: relation to caldera size and magma chamber geometry. *Bulletin of Volcanology* 59: 198-218.
- Lorenz, V. 2007. Syn- and post-eruptive hazards of maar-diatreme volcanoes. *Journal of Volcanology and Geothermal Research* 150: 285-312.
- Lorenz, V., Haneke, J. 2004. Relationship between diatremes, dykes, sills, laccoliths, intrusive-extrusive domes, lava flows, and tephra deposits with unconsolidated water-saturated sediments in the late Variscan intermontane Saar-Nahe-Basin, SW Germany, in Bretkreuz, C., Petford, N., eds., *Physical geology of high-level magmatic systems*. Geological Society, London, Special Publications 234: 75-124.
- Lorenz, V., Kurszlauskis, S. 2007. Root zone processes in the phreatomagmatic pipe emplacement model and consequences for the evolution of maar-diatreme volcanoes. *Journal of Volcanology and Geothermal Research* 150: 4-32.
- Schmincke, H.-U., Sumata, M. 2010. Geological evolution of the Canary Islands. 196 pp., Görres Verlag; Koblenz, Neuwied, Germany.
- Suhr, P., Goth, K., Lorenz, V., Suhr, S. 2006. Long lasting subsidence and deformation in and above maar-diatreme volcanoes - a never ending story. *Zeitschrift der deutschen Gesellschaft für Geowissenschaften* 157: 491-511.
- Walker, G.P.L. 1983. Ignimbrite types and ignimbrite problems. *Journal of Volcanology and Geothermal Research* 17: 65-88.
- White, J.D.L. 1991. Maar-diatreme phreato-magmatism at Hopi Buttes, Navajo Nation (Arizona), USA. *Bulletin of Volcanology* 53: 239-258.
- White, J.D.L., Ross P.-S. 2011. Maar-diatreme volcanoes: A review. *Journal of Volcanology and Geothermal Research* 201: 1-29.

The Kisselwörth Diatreme and the Nierstein - Astheim Volcanic System. Phreatomagmatic Paleocene / Eocene volcanism on the western main fault of the Upper Rhine Graben (Germany)

Herbert Lutz¹, Thomas Engel¹, Friedrich Häfner², Jost Haneke² and Volker Lorenz³

¹ Naturhistorisches Museum Mainz / Landessammlung für Naturkunde Rheinland-Pfalz, Reichklarastr. 10, 55116 Mainz, Germany – thomas.engel@stadt.mainz.de

² Landesamt für Geologie und Bergbau Rheinland-Pfalz, Emy-Roeder-Straße 5, 55129 Mainz, Germany

³ Physikalisch Vulkanologisches Labor, Universität Würzburg, Pleicherwall 1, 97070 Würzburg, Germany

Keywords: Phreatomagmatic volcanism, Paleogene, Upper Rhine Graben.

In Western Europe several Cenozoic rifts are known (European Cenozoic Rift System / ECRIS), most of them being associated with intensive volcanic activity (Central European Volcanic Province / CEVP, Dèzes et al. 2004). Among these rifts the Upper Rhine Graben (ORG) in Germany is certainly the morphologically most conspicuous and also best studied one. Especially at its northern end, a great number of Tertiary volcanoes have been recorded. Besides some sparse volcanic activity already in the Late Cretaceous (Maastrichtian, c. 68-70 Ma; e.g., Katzenbuckel) with unsure genetic relationships to the ORG this volcanism reached its climax in the Middle Eocene (47-49 Ma; e.g. Lippolt et al. 1974, Derer et al. 2005, Schmitt et al. 2007, Reischmann 2011). While volcanoes are common along the northern margin and on the eastern shoulder of the northern ORG only a few have been found up to now on its western shoulder and in the Mainz Basin.

When the Rhine River has extreme low water – as it did in May 2011 – one can sample and study a diatreme tuff cropping out in its riverbed between Nackenheim and Nierstein, 12 km south of the state capital of Mainz. As far as we know, this locality has been sampled for the first time in 1985 by Karl Stapf (†), Johannes Gutenberg-University (JGU) Mainz. However, his specimen has never been studied. In 2003 other samples have been collected by colleagues from the Geological Survey of Rhineland-Palatinate (LGB) and also by Dieter Mertz, JGU. These have briefly been studied petrographically and Dieter Mertz has dated a hornblende using the ⁴⁰Ar/³⁹Ar technique. This provided an age of c. 55 Ma (Dieter Mertz, personal comm., 15.07.2011), i.e. the volcano erupted near the Paleocene / Eocene boundary (PETM = 55.8 Ma) well before first signs of rifting can be observed in the southernmost ORG. There, terrestrial sediments are up to 52 Ma old while limnic sedimentation started not until c. 46 Ma ago and first brackish conditions got established even later (45 Ma). In the northern part of the ORG subsidence

started much later: Biostratigraphically limnic sediments are c. 35 Ma old and first brackish sediments are another two Ma younger. Thus, the eruption of the Kisselwörth maar-diatreme volcano (or tuff ring?) predated the start of obvious rifting in the S by c. 10 Ma and in the N even by c. 20 Ma. Since - as far as we know - the Kisselwörth diatreme is the only volcano that erupted exactly on the western main fault its eruptive fissure enabled phreatomagmatic activity long before it became the main fault of the subsiding graben.

What else makes the Kisselwörth diatreme interesting? Tectonics within and along the ORG has intensively been studied since decades [e.g. Illies and Fuchs (Eds.) 1974, Stapf 1988, Dürr and Grimm 2011]. Up to now it has been unclear, why the Rotliegend of the Nierstein Horst cuesta (= Nierstein Horst Formation, = Uppermost Rotliegend, = top of preserved Lower Permian) immediately to the west of the diatreme continues eastward in the so-called Astheim Block which, however, is eroded and covered by a few meters of Quaternary and Holocene Rhine sediments. Despite this, its margins are well documented by boreholes showing three major fault directions. Its south-eastern margin is defined by the western main fault of the ORG. These fault directions we also find as joints within the tuff of the diatreme. Therefore, these joints reflect the regional stress field, but do not result from syn- or post-eruptive subsidence. Near its northern margin, the Astheim Block is hosting a “basalt” vent. Associated with this basalt and the Kisselwörth diatreme two other basaltic dykes or vents and two tuff locations have been located (Schmitt and Steuer 1974). However, except for a “basalt” vent on the top of the Nierstein Horst (“Auf der Schmidt”), these vents are only known from excavating activities in the Rhine River bed. They seem to be aligned along a NNW-SSE trending (“eggish”) structure. Therefore we assume that this indicates a fault which separates the Astheim Block from the Nierstein Horst, as it has already been mapped in a similar way by Karl Stoltz in 1909. Such a fault

would allow understanding why Cenozoic sediments of the Rhine River are covering the spur-like Astheim Block. The Kisselwörth diatreme is positioned on the edge of the Nierstein Horst - the outer bank of the Rhine valley - and thus has been eroded at least by the difference between its own actual top and the preserved top of the nearby Nierstein Horst (c. 75 m). This is of interest for any calculations regarding the former size of the diatreme and the syneruptive landscape respectively.

The horizontally transected diatreme, which is c. 150 m in diameter, shows differences in height a.s.l. of less than 1 m. Nevertheless, the exposed tuff varies to some extent. Most of it appears as a rather dull greyish-brown c. 1:1 mixture of juvenile and country rock clasts with diameters less than 1 cm. Larger clasts are present but rare. A subordinate coarser type of tuff is also exposed containing much larger clasts of both country rock and lapilli (diameters up to 5 cm). These differences might indicate some bedding within this part of the diatreme. In all localities the tuff is matrix supported, the matrix being composed of ash and finely fragmented country rocks (Permian sand-, silt- and claystones).

First petrographic analyses of the juvenile clasts revealed that these are tachylitic and also contain sideromelane. They plot in the basalt field of the TAS diagram (Streckeisen diagram: basalt / andesite field). Many of these lapilli are well rounded and represent spherical lapilli having diameters of mostly less than 1 cm (sometimes up to 5 cm). Others are angular and sharply edged. Usually they are only weakly vesicular and many of them have a core of either a hornblende crystal (-fragment) or of an angular country rock clast respectively. Hornblende (Pargasite) crystals are also common in the tuff matrix, the largest one having a size of 30 x 45 mm.

Country rock xenoliths comprise fragments of red, orange, brown or green sand-, silt- and claystones of Lower Permian age. Mesozoic sediments obviously are missing. This agrees with observations made in the northern ORG itself and in the neighboring Mainz Basin where Tertiary sediments are lying unconformably on Permian ones. Xenoliths older than Permian in age are also missing. Rare clasts of crystalline rocks most likely stem from Lower Permian gravel horizons (total thickness of Rotliegend in this area: c. 1800 m).

Our studies will be continued and include samples from the adjacent volcanic vents which we all regard as belonging to one system, for which we suggest the name Nierstein - Astheim Volcanic System. It includes five vents near Nierstein and Nackenheim and one near Astheim. Our future work aims to contribute to a better understanding of the

pre-rift development of the area at the northern end of the ORG.

Acknowledgements

Our thanks go to the Ministry of the Interior of the State of Rhineland-Palatinate (RLP), to Harald Brock, Water Police RLP, Ingo Braun, Police RLP, Helicopter Squadron Winnigen, Dieter Mertz, JGU Mainz, Michael Krimmel, Winfried Kuhn, both Landesamt für Geologie und Bergbau RLP (= Geological Survey RLP), Georg Meyer, Mainz, and Gabriele Gruber, Hessisches Landesmuseum Darmstadt.

References

- Derer, C.E., Schumacher, M.E., Schäfer, A. 2005. The northern Upper Rhine Graben: basin geometry and early syn-rift tectono-sedimentary evolution. *International Journal of Earth Sciences (Geologische Rundschau)* 94: 640–656.
- Dèzes, P., Schmid, S.M., Ziegler, P.A. 2004: Evolution of the European Cenozoic Rift System: interaction of the Alpine and Pyrenean orogens with their foreland lithosphere. *Tectonophysics* 389: 1-33.
- Dürr, S.H., Grimm, M.C. 2011: Tektonische Übersicht. – In: Deutsche Stratigraphische Kommission (Hrsg.): *Stratigraphie von Deutschland IX. Tertiär, Teil 1. Oberrheingraben und benachbarte Tertiärgebiete. - Schriftenreihe der Deutschen Gesellschaft für Geowissenschaften* 75: 7-15.
- Illies, J.H., Fuchs, K. (Eds.) 1974: *Approaches to Taphrogenesis*. 460 pp.
- Lippolt, H. J., Todt, W., Horn, P. 1974. Volcanism of the Rhinegraben; potassium-argon ages, local setting, petrology, and gravity anomalies. In: Illies, J.H., Fuchs, K. (Eds.): *Approaches to Taphrogenesis*: 213-221.
- Reischmann, T. 2011: Tertiärer Vulkanismus. Mit Beiträgen von: Heinz-Dieter Nesbor, Wolfgang Wimmenauer. In: Deutsche Stratigraphische Kommission (Hrsg.): *Stratigraphie von Deutschland IX. Tertiär, Teil 1. Oberrheingraben und benachbarte Tertiärgebiete. Schriftenreihe der Deutschen Gesellschaft für Geowissenschaften* 75: 16-30.
- Schmitt, A.K., Marks, M.A.W., Nesbor, H.D., Markl, G. 2007. The onset and origin of differentiated Rhinegraben volcanism based on U-Pb ages and oxygen isotopic composition of zircon. *European Journal of Mineralogy* 19: 849-857.
- Schmitt, O., Steuer, A. 1974: Erläuterungen zur Geologischen Karte von Hessen 1:25000. Blatt Nr. 6016 Groß-Gerau. 202 pp.
- Stapf, K.R.G. 1988: Zur Tektonik des westlichen Rheingrabenrandes zwischen Nierstein am Rhein und Wissembourg (Elsaß). *Jahresberichte und Mitteilungen des Oberrheinischen Geologischen Vereins*, N. F. 70: 399-410.
- Stoltz, K. 1909: Geologische Bilder aus dem Grossherzogtum Hessen (Zweiter Teil: Rheinhessen). Beilage zum Jahresbericht des Großherzoglichen Ludwig-Georgs-Gymnasiums und der Vorschule der beiden Gymnasien zu Darmstadt. 39 pp.

Early volcanological research in the Vulkaneifel, Germany. The years 1774 – 1865

Herbert Lutz¹ and Volker Lorenz²

¹ Naturhistorisches Museum Mainz / Landessammlung für Naturkunde Rheinland-Pfalz, Reichklarastr. 10, 55116 Mainz, Germany – dr.herbert.lutz@stadt.mainz.de

² Physikalisch Vulkanologisches Labor, Universitaet Wuerzburg, Pleicherwall 1, 97070 Wuerzburg, Germany

Keywords: history, volcanology, Vulkaneifel

The Vulkaneifel (Volcanic W-Eifel) in the west of the Rhenish Slate Mountains is part of the large Rhenish Shield. Its name derives from nearly 280 monogenetic volcanoes of Quaternary age which are scattered over a NW-SE trending area of approx. 600 km² (Westeifel Volcanic Field, WEVF). Here, the volcano-term maar has been coined by Johann Steininger in 1819. Along its north-eastern margin the WEVF overlaps with the Tertiary Hocheifel Volcanic Field (THV) which comprises more than 400 deeply eroded volcanoes distributed over an area of ca. 1800 km². The oldest and best studied one among these is the Eckfeld Maar (e.g. Mertz et al. 2000, Pirrung et al. 2003, Lutz et al. 2010). East of this THV lies the Quaternary Osteifel Volcanic Field (EEVF) with another approx. 100 monogenetic volcanoes and four phonolitic eruption centres. Most famous among these is the Laacher See Volcano that erupted approx. 10.930 years BC.

Until the late 19th century the central and western parts of the Eifel have been comparatively poorly developed and not well connected to the travel infrastructures along the Rhine River. In addition, due to the harsh climate, the western parts of the Eifel frequently have been even called French or Prussian Siberia respectively. In consequence, they have not been accessible as easy as the regions immediately along the Rhine River and their systematic scientific exploration started – as compared to the situation in the EEVF - rather late.

Nevertheless, the first volcano in the Vulkaneifel was already discovered in 1774 by the Belgian “geologist” Robert de Limbourg (1731-1808). He described the Quaternary Steffelner Kopf, a small scoria cone with spatter and palagonite. His paper was published in 1777 (Limbourg 1777) but remained widely ignored until today.

Our next information we owe to the German physician Carl Wilhelm Nose (1753-1835) who’s “assistant” Johann Heinrich Wilhelm Perz (personal data unknown, a boatman and citizen of Oberwinter S of Bonn) had visited greater parts of the Hocheifel and of the Vulkaneifel before 1789. From there he brought home surprising news about the existence of many scoria cones and basaltic necks. He also had a

great variety of volcanic rocks and minerals in his luggage which very much resembled those in the EEVF or looked even identical.

Then in 1803 the Belgian Laurent-Francois Dethier (1757-1843) published a report on his travels to the Vulkaneifel during the years 1800 – 1802. In this book he mentions a young German physician from Hillesheim, Eifel, named “Smits” (= most likely “Schmitz”, a common name in the Westeifel), who not only showed him scoria cones but who also took for granted that the round and deep lakes in the Vulkaneifel are the craters of extinct volcanoes. Dethier’s friend J.-L. Wolff (personal data unknown) had already in 1801 drawn a coloured “geological map” – the first of this kind for the Eifel – which presumably was engraved in the same year. However, it is still unclear if it has also been printed and distributed as a single sheet that early since Dethier’s book was sold without this map. Maybe that for the first time it came on the market with Dethier’s anonymously published excursion guide for the surroundings of his hometown Spa (Dethier 1814).

After the Eifel had become part of Prussia in 1814 – the Napoleonic Wars ended in 1815 – an increasing number of geologists travelled to the Vulkaneifel and Hocheifel to study their volcanic formations. Among these were men like Christian Keferstein (1784-1866), François Dominique de Reynaud Comte de Montlosier (1755-1838) who had already intensively studied the Auvergne, Johann Steininger (1794-1874), George Poulett Scrope (1797-1876), M. Behr (personal data unknown), the philosopher and famous socialist Jean Ernest Reynaud (1806-1863), Leopold von Buch (1774-1853), Hermann van der Wyck (1769-1843), Alexander von Humboldt (1769-1859) and Heinrich von Dechen (1800-1889) to mention just the best-known. Since their contributions have already been discussed elsewhere we will refer only to a few aspects.

To our opinion, it was A. Stengel, a Prussian administrator of a steel furnace near Adenau in the Hocheifel (further personal data are still unknown to us), who already in 1822 and 1823 published path-

breaking ideas that, unfortunately, have not yet attracted attention as they should have done. During his extensive travels through the Vulkaneifel – he was searching for coal seams – Stengel converted from a Neptunist to a true Vulkanist. He clearly described geological phenomena which could only be explained by “subterranean fire”. Here, his experience from his profession as head of a smelter was of great advantage to him. In the end he published his own theory of volcanic action in which he, e.g., as mechanism for the rise of magma, assumed processes which anticipated modern ideas like “magmatic assimilation” or “syntexis”. As for Nose, Montlosier and others, for him the interaction of magma and groundwater at the base of the sedimentary rocks overlaying the crystalline basement was also of major importance for the start of volcanic eruptions. He thought of processes that, today, we call thermo-hydraulic processes and which are the motor of what we know as highly explosive phreatomagmatic eruptions (Stengel 1822, 1823).

Last but not least we will introduce in some detail the ideas of Eilhard Mitscherlich (1794-1863) which he had presented to the Royal Academy of Sciences in Berlin on their sessions in the years 1848, 1854 and 1858. However, his important contributions became published posthumously as late as 1865 by his colleague Justus Roth (1818-1892).

A short presentation of rare early maps will finally illustrate not only the progress regarding the exploration of the Vulkaneifel and the Eifel but also the improvements with geological mapping in general. Especially noteworthy are the maps of Karl von Raumer (1783-1865) and his companion Moritz von Engelhardt (1779-1842), that of Jean-Baptiste Julien d’Omalius d’Halloy (1783-1875) and the beautiful map of Gustav von Leonhard (1816-1878) that he has drawn for his German edition of Adam Sedgwick’s (1785-1873) and Roderick Murchison’s (1792-1871) paper “On the Palaeozoic Deposits on the North of Germany and Belgium”.

Finally Steininger’s first and last map on that subject which he published in 1822 and 1853 respectively illustrate his personal progress during

these years of pioneering research in the Vulkaneifel (for a comprehensive bibliography compare Lutz and Lorenz 2009).

References

- Dethier, L.-F. 1814. *Le Guide des curieux qui visitent les eaux de Spa, ou Indication des lieux où se trouvent les curiosités de la nature et de l’art, à voir à l’entour de ce Rendez-vous Célèbre et en général, parmi la contrée de Meuse, Moselle et Rhin; avec quelques notices analogues au sujet. Opuscule servant d’explication et de supplément à la Carte géologique et synoptique de l’Ourte et des environs, etc.*, VI + 122 pp., Verviers and Spa.
- Limbourg, R. de 1777. *Mémoire pour servir à l’Histoire naturelle des fossiles des Pays-bas. Lû à la Séance du 7. Février 1774. – Mémoires de l’académie impérial et royale des sciences et belles-lettres de Bruxelles 1: 361-410.*
- Lutz, H., Kaulfuß, U., Wappler, T., Löhnertz, W., Wilde, V., Mertz, D., Mingram, J., Franzen, J., Frankenhäuser, H., Koziol, M. 2010. *Eckfeld Maar: Window into an Eocene Terrestrial Habitat in Central Europe. Acta Geologica Sinica (English Edition) 84 (4): 984-1009.*
- Lutz, H., Lorenz, V. 2009. *Die Vulkaneifel und die Anfänge der modernen Vulkanologie – eine geohistorische Quellensammlung. Mainzer Naturwissenschaftliches Archiv 47 (Festschrift): 193-261.*
- Mertz, D.F., Swisher, C.C., Franzen, J.L., Neuffer, F.O., Lutz, H. 2000. *Numerical dating of the Eckfeld maar fossil site, Eifel, Germany: A calibration mark for the Eocene time scale. Naturwissenschaften 87: 270-274.*
- Pirring, M., Fischer, C., Büchel, G., Gaupp, R., Lutz, H., Neuffer, F.O. 2003. *Lithofacies succession of maar crater deposits in the Eifel area (Germany). Terra Nova 15: 125-132.*
- Stengel, A. 1822. *Geognostische Beobachtungen über die Lagerungen des Sandsteins in der Grauwacke, mit Rücksicht auf die bei Neigen aufgefundenen Steinkohlentheile, so wie über die merkwürdigsten Flötz=Trappegebirge in einem Theile der Eifel. – Das Gebirge in Rheinland-Westphalen 1: 51-78.*
- Stengel, A. 1823. *Ueber die Entstehung des Basalts hinsichtlich seines Vorkommens in der Eifel. – Das Gebirge in Rheinland-Westphalen 2: 189-212.*

126 years of changing maar morphology at Rotomahana, North Island, New Zealand

Michael D. May and James D.L. White

Department of Geology, University of Otago, P.O. Box 56, Dunedin, New Zealand – maymi024@student.otago.ac.nz

Keywords: Rotomahana, maar morphology, density currents

On 10 June 1886 Tarawera and Rotomahana (Okataina Centre, Taupo Volcanic Zone) produced New Zealand's largest, most destructive historic eruption, opening a 17 km fissure across Mt Tarawera and the adjoining Rotomahana basin. The southwesternmost 9 km of the fissure transected marshlands and an intensely active geothermal system, excavating coalesced maar craters now holding modern Lake Rotomahana. Dilute pyroclastic density currents reached 6 km from their crater sources, forming lithic-rich deposits containing basalt pyroclasts sourced from the various Rotomahana vents.

The eruption of Tarawera-Rotomahana is best known for the basaltic Plinian fissure deposits from the rhyolitic massif of Mt Tarawera (Walker et al. 1984, Houghton et al., 2004, Sable et al. 2006, Carey et al. 2007, Sable et al. 2009) with relatively little attention being paid to the more complex, maar forming Rotomahana segment (Nairn, 1979, Rousseel et al. 2006, May et al. in prep).

Using historical photos taken before and shortly after the 1886 eruption we can see much detail about the morphology of the Rotomahana maars which is now hidden by the modern day lake. These details allow us to make better estimates of crater size and volume, the volume of lithic material consumed by the eruption, the deposition characteristics, base surge directions etc. Close inspection of before and after photos reveal several prominent topographical high points that have disappeared into the Great Crater Basin, which is the largest maar and situated at the site of the greatest pre eruption geothermal activity. These topographic massifs have either been destroyed by the phreatomagmatic eruption, or have slumped into the expanding crater.

By comparing these historic photographs with images acquired with Google Earth and with modern digital photographs taken from roughly the same locations it is possible to see how the landscape has changed in the 126 years since the eruption.

Additional information has been compiled from the photos regarding the orientation, form, and spacing of bedforms produced by density currents emitted from the craters. A considerable thickness of Rotomahana mud also was deposited below the



Fig. 1 – A Burton Brothers photograph of the Rotomahana maars shortly after the June 10th eruption. The Northeasternmost maars are beginning to fill with what was then called Rotomakariri and the Southwestern maars still steam due to the remnant geothermal heat in that area. Source: <http://collections.tepapa.govt.nz>.

current water level and may change the overall volume of the deposit.

By combining the information from observable bedforms in photos, from the scale and sites of modifications to pre-eruption topography, and from deposit componentry we are able to produce a more precise interpretation of the directions and magnitude of material transport out of the craters to form the preserved density-current and fall deposits. Textural data from pyroclasts in different deposits surrounding the craters will be linked back to individual craters or crater groups, allowing us to examine how variations in the magmatic system along the rift are related to crater excavation and dispersal of pyroclastic debris by plume and density current transport, and how these changes are related

to known variations in the hydrology along the rift and intensity of geothermal activity.

Acknowledgements

This research was supported by GNS funding. We would like to thank Te Papa museum for the old images, and the Department of Conservation, Kaingaroa Timberlands and local Iwi for access to the land.

References

- Carey, R.J., Houghton, B.F., Sable, J.E., Wilson, C.J.N. 2007. Contrasting grain size and componentry in complex proximal deposits of the 1886 Tarawera basaltic Plinian eruption. *Bulletin of Volcanology* 69: 903-926.
- Houghton, B.F., Wilson, C.J.N., Del Carlo, P., Coltelli, M., Sable, J.E., Carey, R. 2004. The influence of conduit processes on changes in style of basaltic Plinian eruptions: Tarawera 1886 and Etna 122 BC. *Journal of Volcanology and Geothermal Research* 137: 1-14.
- May, M.D., White, J.D.L., Carey, R.J., Houghton, B.F., Rosenberg, M. in prep. Textural characteristics of pyroclasts from the maar forming Rotomahana segment of the 1886 Tarawera eruption, New Zealand.
- Nairn, I.A. 1979. Rotomahana-Waimangu eruption 1886: Base surge and basalt magma. *New Zealand Journal of Geology and Geophysics* 22: 363-378.
- Rousseel, J., White, J.D.L., Houghton, B.F. 2006. Complex bombs of phreatomagmatic eruptions: Role of agglomeration and welding in vents of the 1886 Rotomahana eruption, Tarawera, New Zealand. *Journal of Geophysical Research* 111: B12205
- Sable, J.E., Houghton, B.F., Wilson, C.J.N., Carey, R.J. 2006. Complex proximal sedimentation from Plinian plumes: the example of Tarawera 1886. *Bulletin of Volcanology* 69: 89-103.
- Sable, J.E., Houghton, B.F., Wilson, C.J.N., Carey, R.J. 2009. Eruption mechanisms during the climax of the Tarawera 1886 basaltic Plinian eruption inferred from microtextural characteristics of the deposits. In: Thordarson, T., Self, S., Larsen, G., Rowland, S.K., Hoskuldsson, A., (Eds.), *Studies in Volcanology: The Legacy of George Walker*. Special Publications of IAVCEI 2: 129-154.
- Walker, G.P.L., Self, S., Wilson, L. 1984. Tarawera 1886, New Zealand – A basaltic Plinian fissure eruption. *Journal of Volcanology and Geothermal Research* 21: 61-78.

Fine scale mantle heterogeneity revealed in monogenetic eruptions in the Auckland Volcanic Field

Lucy E McGee¹, Ian E M Smith¹, Marc-Alban Millet², Christoph Beier^{3,4}, Jan M Lindsay¹ and Heather Handley³

¹ School of Environment, The University of Auckland, Private Bag 92019, Auckland, New Zealand - lmcgee@auckland.ac.nz

² SGEES, Victoria University, PO Box 600, Wellington, NZ

³ GEMOC, Macquarie University, Sydney, Australia

⁴ Now at Universität Erlangen-Nürnberg, Germany

Keywords: Mixing, subduction modification, Pb-isotopes

How melts are extracted from their mantle sources and what happens to them *en route* to the surface are fundamental questions in the workings of basaltic volcanic fields. The well-sampled Auckland Volcanic Field (AVF) – an intraplate volcanic system in northern New Zealand – offers excellent opportunities to build up a more detailed picture of the plumbing systems feeding such fields. Here we present major and trace element data along with new Sr-Nd-Pb, in order to investigate the processes involved in the large chemical variety seen in the AVF.

Detailed sampling has shown that individual trends for each centre can be explained by either high-pressure clinopyroxene or shallow olivine

fractionation. Near-primary magmas show a range in degrees of partial melting from ~4% down to <0.5% in the smallest centres. Anomalies in multi-element plots show that at least two sources are implicated in the petrogenesis of the Auckland basalts, and this is supported by Pb isotopic data which show three-component mixing between two FOZO-like sources and a source displaying more radiogenic Pb isotope ratios. Trace element ratios and high (²³⁰Th/²³²Th) ratios (1.16-1.33) show melts are primarily formed within the garnet stability zone, but mixing models indicate that these deep melts are variably modified by interaction with a shallower mantle which has seen small amount of subduction-related modification (Figure 1). The subduction-modified

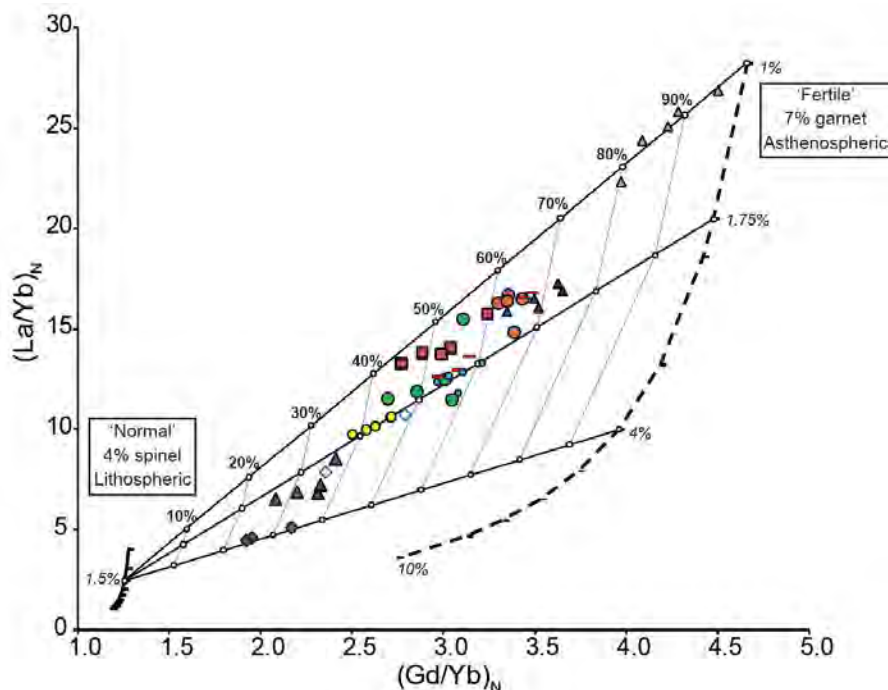


Fig. 1 - (La/Yb)_N vs. (Gd/Yb)_N for primitive compositions in the AVF. Solid curve denotes 0.5-5% melting of a 4% spinel peridotite (1.5% melting marked) using a normal mantle composition (Hofmann 1988), melting in the proportions Ol: 0.1, Cpx: 0.5, Opx: 0.27, Sp: 0.13 (Thirlwall et al., 1994). Dashed curve denotes 1-10% melting of a more fertile (i.e. more cpx-rich) 7% garnet peridotite of a more enriched mantle composition (La/Yb: 1.87, Gd/Yb: 1.59), melting in the proportions Ol: 0.05, Cpx: 0.3, Opx: 0.2, Gt: 0.45 (Thirlwall et al., 1994). Horizontal lines through unfilled circles denote mixing between different degrees of 'asthenospheric' melts (dashed line, melting degrees used in mixing calculations shown in italics) and 1.5% melting of the lithospheric source (solid line). Non-italicised numbers with percentages refer to percentage of asthenospheric melt involved in mixing.

mantle appears to be depleted whereas the more radiogenic mantle is far more fertile. Mixing between end-members is seen at both the single volcano and the field-wide scale.

Together with the lack of any spatial or temporal trend in the chemistry of the field, these results suggest that melt batches evolve in isolation, being subject to differing processes and are able to move at variable speeds and through variable porosities in the mantle, resulting in dispersed plumbing systems for such fields and an erratic pattern of eruptions.

References

- Hofmann, A.W. 1988. Chemical differentiation of the Earth: the relationship between mantle, continental crust, and oceanic crust. *Earth and Planetary Science Letters* 90: 297-314.
- Thirlwall, M.F., Upton, B.G.J., Jenkins, C. 1994. Interaction between Continental Lithosphere and the Iceland Plume—Sr-Nd-Pb Isotope Geochemistry of Tertiary Basalts, NE Greenland. *Journal of Petrology* 35: 839-879.

A nested polymagmatic and polycyclic tuff ring and scoria cone complex at Chaguido (Jeju Island), South Korea

Károly Németh¹, Marco Brenna¹, Shane J Cronin¹, Young Kwan Sohn² and Ian E.M. Smith³

¹ Volcanic Risk Solutions, Massey University, Palmerston North, New Zealand – k.nemeth@massey.ac.nz

² Department of Earth and Environmental Sciences, Gyeongsang National University, Jinju, South Korea

³ School of Environment, The University of Auckland, Private Bag 92019, Auckland, New Zealand

Keywords: sideromelane, phreatomagmatic, dispersed plumbing system.

There is increasing realization of the complexity of monogenetic volcanoes, not only in terms of variations in eruption style and vent geometries, but also the presence of multiple magma sources as well as temporal changes of the chemistry of the rising magmas (e.g. Németh 2010, Brenna et al 2011). Here we present a new example to explore the occurrence of polycyclic volcanism, i.e., repeated “monogenetic” eruptions at the same location separated by long repose intervals. Chaguido is a small east-west elongated volcanic island (~900 by 400 m), 1.2 km from the western coast of Jeju Island (South Korea) showing excellent coastal exposures of complex volcanic sequences. Chaguido is aligned with a small, strongly eroded, scoria cone core and the Upper/Middle (?) Pleistocene phreatomagmatic

Dangsanbong tuff ring (Sohn & Park 2005). The age of Chaguido is unknown but the older portions of it, with well-developed weathered soil cover may correlate with the nearby Dangsanbong volcanism. Chaguido (Fig. 1) consists of a hilly eastern side and a flat topped western zone. The NE part of the island is composed of a pyroclastic succession that dips seaward with a radially changing dip direction, indicating that it is part of a tuff ring. The pyroclastic rocks are dominated by moderately palagonitized ash, with common cauliflower bombs, accidental volcanic lithics and also clasts derived from siliciclastic sediments, indicating that these units were formed by phreatomagmatic explosive eruptions due to interaction of sub-surface and/or surface water and rising magma.

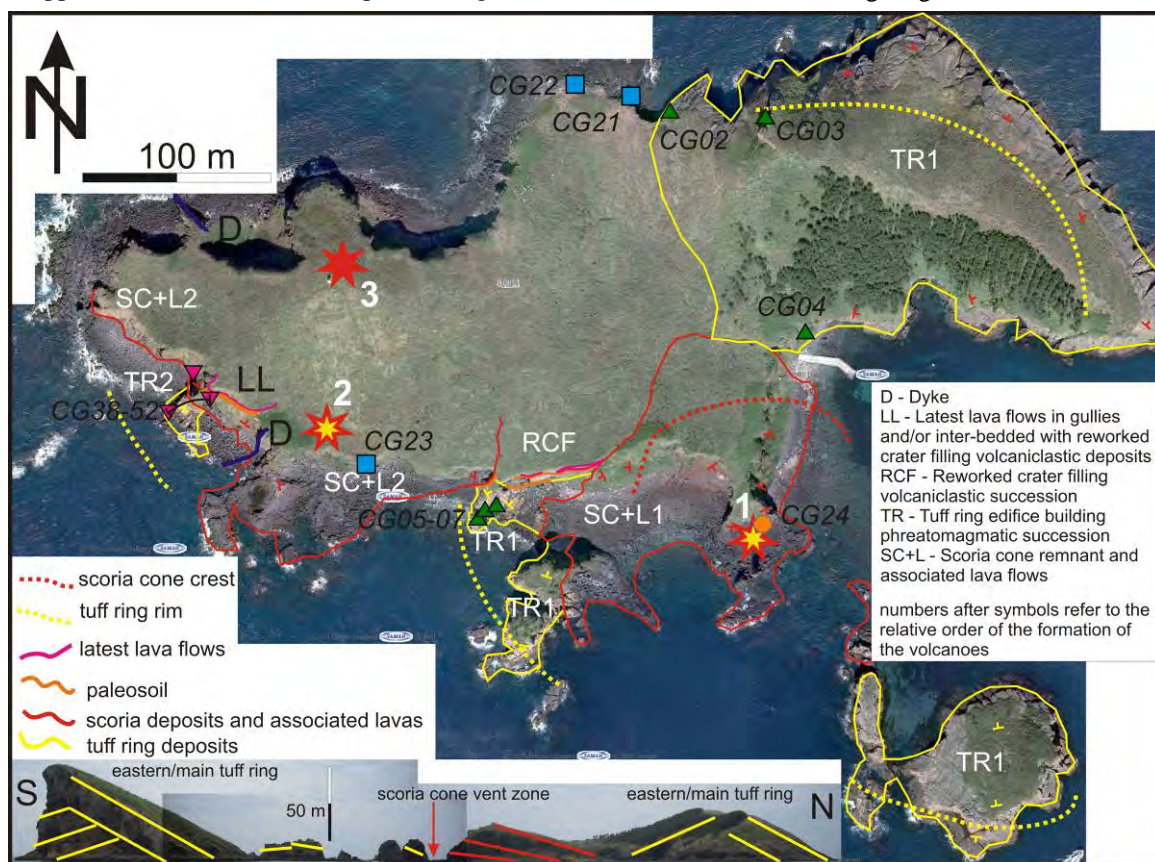


Fig. 1 – Preliminary geological map of Chaguido Island. Stars mark estimated eruptive centre locations: yellow/red indicate phreatomagmatic to magmatic eruptions; red dry-magmatic eruption. Sample locations and coloured symbols refer to Fig. 3.

In the SE part of the island, a major unconformity surface is exposed separating an inward and outward dipping section of a tuff ring composed of pyroclastic rocks similar in texture to those observed in the NE. Between these two segments a strongly welded and dyke-mingled zone occurs, which includes an inward-dipping agglutinate sequence that rapidly grades outward into opposite dipping lava bomb/spatter and scoria lapilli beds. This appears to represent the exhumed core of a scoria cone formerly erupted in the crater of a tuff ring (TR1).

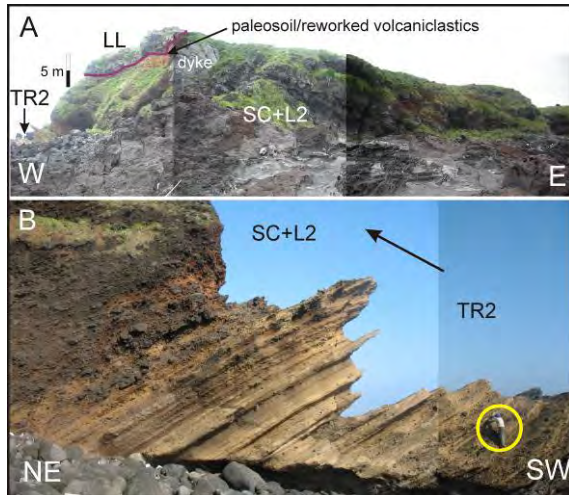


Fig. 2 – Facies relationships of the TR2 tuff ring (A) exposing a gradual transition of phreatomagmatic (TR2) to dry, scoriaceous successions and lava flows (SC+L2).

On the outer margins of the scoria cone remnant, a mature, yellow paleosol is formed, which is in turn covered by younger lavas. The paleosol evidences thousands of years time break, before a stack of lava flows and scoria deposits were erupted to form a thick capping unit that can be traced across to the west of the island (Fig 1). At a site further NW, these capping lavas lie possibly conformably over a wet-dry phreatomagmatic succession (Fig. 2) suggesting a gradual transition from phreatomagmatic to magmatic eruption style cored by a tuff ring.

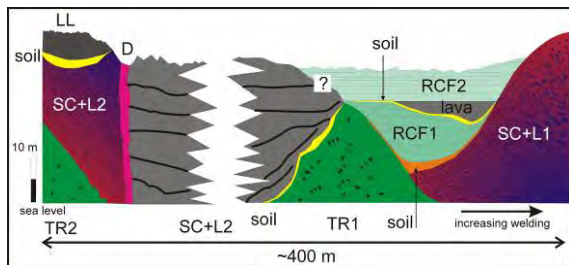


Fig. 3 – Facies relationships of the volcanic rocks exposed in the southern side of Chaguido.

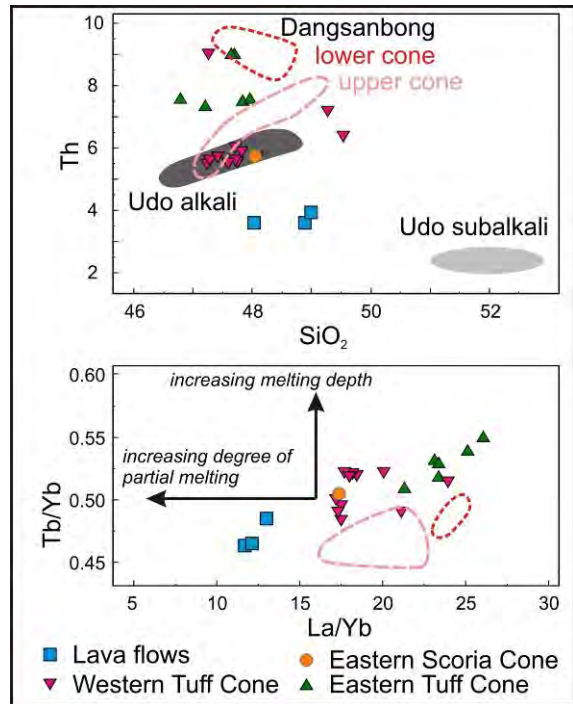


Fig. 4 – Chemical distinction of the magmas involved in the Chaguido eruption and comparison with other Jeju monogenetic volcanoes.

This younger tuff ring (TR2) and scoria cone (SC+L2) is covered by a further paleosol below the youngest lava flow (LL) filling gullies (Fig. 3). The older eastern tuff ring (TR 1) crater is partially filled with a thick reworked volcaniclastic succession that is interrupted by at least one paleosol and invaded by younger lava flows (Figs 1 & 3).

At least three distinct magmas were involved in the eruption (Fig. 4). All three are alkali basalt to trachybasalt, with the lava flows tending to mildly subalkaline compositions. The magma feeding TR1 shows the greatest enrichment in trace elements and LREE over HREE, suggesting a deeper source and a smaller degree of partial melting, as opposed to the magma feeding the lava flows. The magma feeding TR2 was transitional between these two end members. This may indicate melting of a mantle column and extraction from the deeper portion first.

References

- Brenna, M., Cronin, S.J., Németh, K., Smith, I.E.M., Sohn, Y-K. 2011. The influence of magma plumbing complexity on monogenetic eruptions, Jeju Island, Korea. *Terra Nova* 23(2): 70-75.
- Németh, K. 2010. Monogenetic volcanic fields: Origin, sedimentary record, and relationship with polygenetic volcanism. *Geol Soc Am Spec Paper* 470: 43-66.
- Sohn, Y-K., Park, K.H. 2005. Composite tuff ring/cone complexes in Jeju Island, Korea: possible consequences of substrate collapse and vent migration. *Journal of Volcanology and Geothermal Research* 141(1-2): 157-175

Variation in deposit characteristics and eruption processes across the lifetime of a monogenetic field, the South Auckland volcanic field

Adrian Pittari¹, Roger Briggs¹, Tehnuka Ilanko¹, April Gibson¹, Michael Rosenberg² and Karoly Nemeth³

¹ Department of Earth & Ocean Sciences, University of Waikato, Hamilton, New Zealand – apittari@waikato.ac.nz

² GNS Science, Wairakei Research Centre, Private Bag 2000, Taupo, New Zealand

³ Volcanic Risk Solutions, Massey University, Palmerston North, New Zealand

Keywords: South Auckland, tuff ring, scoria cone

To gain insight into the future evolution of an active monogenetic field and possible future eruption styles it is useful to understand the volcanic history of related precursory monogenetic fields. The Quaternary South Auckland Volcanic Field (SAVF) was active for about one million years (1.59-0.51 Ma), and preceded the currently active Auckland Volcanic Field, which is located 40 km to the north. The ideal age bracket has enabled almost half of the 82 volcanic centres to be dated reliably by K/Ar methods (Briggs et al. 1994), whilst the volcanic field is youthful enough to allow preservation of the edifices and their deposits. Hence, the complete history of a young monogenetic field is preserved in the SAVF. This presentation will overview the range of volcanic deposits and processes evident in the SAVF in an effort to provide useful input to understanding the future eruptive potential in the Auckland Volcanic Field.

The SAVF is comprised of 38 tuff rings and maars, 17 scoria cones and 40 lava shields/cones spread over an area of about 300 km². Multiple tuff rings/maars and/or scoria cones often occur as nested or overlapping complexes. Extensive overlapping basalt lavas are most voluminous towards the centre of the field where they amalgamate into several broad shields constructed from multiple closely-spaced centres.

Tuff rings, which encircle broad flat basins, likely to be sediment-filled maar craters, range from 0.5 to 2.7 km in diameter and have successions up to 60 m thick. Tuff ring successions are broadly constructed of alternating facies intervals by either: (a) diffuse- to well-, thin- to medium-bedded vitric lapilli tuff recording periods dominated by near-vent pyroclastic fall, or surge-modified fall processes; or (b) planar-, wavy- and cross-laminated to thin-bedded vitric tuff facies recording periods dominated by pyroclastic surge processes. Several tuff ring successions (e.g. Barriball Road, Kellyville) show an overall upward progression to finer-grained surge-dominated facies. High magma ascent rates relative to the water recharge rate from surrounding aquifers early in these eruptions, and

immediately after their initial vents were excavated, caused mixed magmatic and phreatomagmatic fragmentation, and subsequent complex near-vent surge-fall interactions. The latter phases of these eruptions were characterized by slower magma ascent rates allowing for more efficient interaction of the magma with aquifer waters and subsequent surge-forming phreatomagmatic explosions. Other tuff ring successions are more monotonous. For example, the largest tuff ring, Onewhero, consists predominantly of surge-dominated vitric tuff facies for most of its succession, although coarser-grained intervals of vitric lapilli tuff are more common towards the top (Gibson, 2011).

In detail, however, each tuff ring preserves a unique stratigraphic succession of at least several hundred discrete depositional layers of varying thickness (laminae to medium-sized beds), geometry (continuous or discontinuous across outcrops), structure (planar, wavy and low angle cross beds) and textural characteristics (fine tuff, coarse tuff, lapilli tuff, accretionary lapilli). Basalt and country rock blocks and basalt bombs, some of which have formed bedding sags, are often dispersed through tuff ring successions, but may also be concentrated at distinct stratigraphic intervals. Erosional channels and post-depositional flame structures are preserved locally in several tuff rings.

Juvenile basaltic clasts are the most abundant component of tuff ring deposits and show a wide range of vesicularity (e.g. 1-48% at Barriball Road tuff ring). Country rock-derived lithic clasts (e.g. siltstones, sandstones, greywacke, alluvial pebbles, and fossils) and foreign crystals (e.g. quartz, feldspar, hornblende, glauconite, orthopyroxene) generally constitute <20% of tuff ring deposits, although they can be dominant components in discrete horizons, indicating the influence of aquifers in driving phreatomagmatism. Fossils found in the Barriball Road tuff ring, which were derived from discrete shell horizons in the underlying Kaawa Formation, suggest that the depth of fragmentation for at least part of this eruption, was at 170-190 m below the surface (Ilanko, 2010).

Very little, if any, of the initial phases of these phreatomagmatic eruptions are preserved. Evidence of a post-eruptive lake (i.e. diatomite) within the Kellyville tuff ring and a higher abundance of country rock lithics in the lower part of its succession, suggests that it may have initiated as a maar-forming explosion. However, the abundance of juvenile pyroclasts throughout most of the Kellyville and other tuff rings indicate that these successions were constructed after the initial vent clearing phase.

Most scoria cone successions are only exposed in local quarries and are predominantly composed of either, or both, of hawaiian or strombolian fall deposits, and associated lava flows. The Onepoto scoria cone contains: (a) a lower, greater than 10 m thick succession of massive, medium to very coarse scoria lapilli, representing steady accumulation from a sustained (possibly subplinian) eruption column, although several distinct thick beds and dispersed vesicular bombs occur towards the top; and (b) an upper, greater than 4 m thick, hawaiian succession of massive, very coarse lapilli agglomerate (see also Rosenberg, 1991).

Most of the volume of the SAVF comprises lava flows of several prominent basalt shields (e.g. Pukekohe and Bombay shield complexes). A large section through the Bombay volcanic complex is exposed at the Bombay Quarry. Here there is a 70 m thick ponded succession of columnar-jointed, sheeted and massive basalt lava, with multiple intercalated scoria and spatter cones; and a topographically higher 50 m thick tuff ring succession (Gibson, 2011). Multiple small scoria and/or lava cones are dispersed across the top of the Bombay shield. Intercalated sedimentary deposits between basalt lavas, found in boreholes around the basalt shield volcanoes, suggest that the construction of these edifices was polygenetic.

Individual volcanic successions in the SAVF record the ongoing history of monogenetic eruptions, after their initial vent opening phase. The

presence of significantly thick tuff ring successions with internally variable deposit characteristics around most phreatomagmatic centres in the SAVF highlights the ongoing and highly unpredictable hazard posed by these centres after the initial explosive phase. Although scoria cones are generally less explosive than phreatomagmatic centres, they can generate periods of intense, sustained eruption.

The SAVF also highlights the potential for volcanic centres to cluster and amalgamate into shield complexes. Although probably constructed over several eruptions, these shields are the focus of the largest magma volumes. They pose a significant lava flow hazard and the potential for multiple active vent systems.

Acknowledgements

Holcim Quarries are kindly thanked for providing access to the Bombay Quarry during the MSc research project of A. Gibson.

References

- Briggs, R.M., Okada, T., Itaya, T., Shibuya, H., Smith, I.E.M. 1994. K-Ar ages, paleomagnetism, and geochemistry of the South Auckland volcanic field, North Island, New Zealand. *New Zealand Journal of Geology and Geophysics* 37: 143-153.
- Gibson, A.C. 2011. Volcanology of tuff rings at Kellyville, Onewhero and Bombay, South Auckland volcanic field. Unpublished MSc thesis, University of Waikato, Hamilton, New Zealand.
- Ilanko, T. 2010. Eruption and emplacement of the Barriball Road Tuff Ring, South Auckland. Unpublished BSc(Hons) thesis, University of Waikato, Hamilton, New Zealand.
- Rosenberg, M.D. 1991. The nature and mechanisms of phreatomagmatic volcanism in the South Auckland volcanic field. Unpublished MSc thesis, University of Waikato, Hamilton, New Zealand.

Evolution of the polygenetic cinder cone of Barren Island, an explosive-effusive mafic arc volcano in the Andaman Sea (NE Indian Ocean)

Hetu C. Sheth

Department of Earth Sciences, Indian Institute of Technology Bombay, Powai, Mumbai, 400076, India – hcsbeth@iitb.ac.in

Keywords: Barren Island, arc volcanism, cinder cone.

Barren Island (India) (Fig. 1, 2) is an effusive as well as explosive mafic stratovolcano in the Andaman Sea, northeastern Indian Ocean. It is the northernmost active volcano of the great Indonesian arc. The Andaman Trench, along which the NE-moving Indian Plate currently subducts beneath the Burmese Plate, is 250 km west of the volcano. The tectonic scenario is complicated by the presence of active back-arc spreading in the Andaman Sea ESE of Barren Island. To the north of Barren Island are two important dormant volcanoes: Narcondam (India) and Popa (Myanmar).

Barren Island is 3 km in diameter, has restricted public access, and no regular monitoring. The volcano is known to have been active from 1787 to 1832 (its “historic” eruptions), when it produced basalt and basaltic andesite tephra and lava flows from a cinder cone located in a 2-km-diameter caldera (Fig. 2). Activity older than this (hitherto undated, “prehistoric” eruptions) is represented on the caldera wall. It includes lava flows (of basalt and basaltic andesite, and rare andesite) and volcanoclastic deposits, including lahar deposits, and pyroclastic fall and surge deposits that form a hydrovolcanic tephra ring (Fig. 3, Sheth et al., 2009, 2010). There is evidence in ash layers sampled in a marine sediment core near the volcano that the prehistoric activity goes back to at least 72 ka, and the caldera may have formed at ≤ 10 ka (Awasthi et al., 2010). Four recent eruptions from the same polygenetic cinder cone (1991, 1994-95, 2005-06, and 2008-ongoing) have produced aa and blocky aa lava flows of highly porphyritic basalt and basaltic andesite. Lavas of the former three episodes covered the historic flows and flowed into the sea on the western side through a breach in the caldera wall. The ongoing eruption (2008-) produced an aa flow entering the sea over the cliffs on the northern side as observed in March 2009 (Sheth et al., 2010), though the lava eruption had stopped by December 2010, with Strombolian-type explosions from the cinder cone observed every few minutes (Sheth et al., unpublished data).

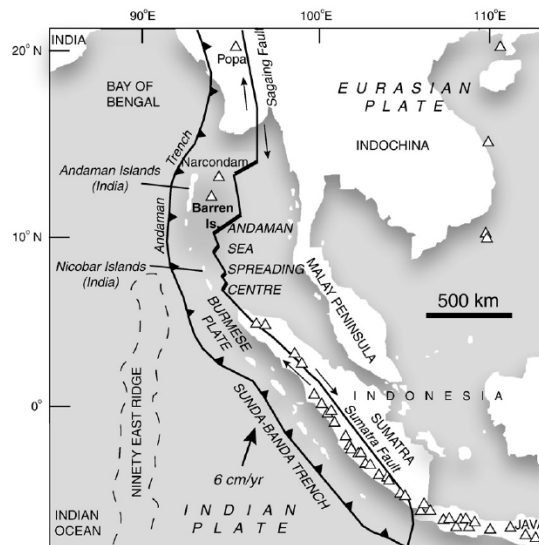


Fig. 1 - Map showing the major geological and tectonic features of the northeastern Indian Ocean and southeastern Asia, along with the locations of the Andaman Islands, Barren Island, and Narcondam, an extinct (possibly dormant) Andaman volcano. White triangles are Holocene volcanoes. Based on Luhr and Haldar (2006) and references therein.

Plagioclase is the most common phenocryst phase in Barren Island’s eruptive products, followed by olivine and clinopyroxene. Amphibole is found in some prehistoric lavas, and is rare. All Barren Island lava flows, prehistoric through the March 2009 flow, are aa flows, and pahoehoe is absent. The flows are distinctly channelized, as is typical of aa flows, and the whole caldera-filling aa flow field is made up of ridges of the flows sloping towards the sea and with an overall surface amplitude of as much as 25 metres. All these aa flows have jagged, very sharp and highly vesicular clinker at the top, and usually have levees made up of coarse aa rubble. They also show massive cores at several places, typical of aa flows. An aa flow near the western coast also shows excellent examples of toothpaste lava, which forms squeeze-ups (Fig. 4). This flow has close similarities to toothpaste lavas previously described from Hawaii, Paricutin, and Etna.



Fig. 2 – View, looking NE, of Barren Island (April 2008). The active cinder cone is at the centre of a caldera (2 km diameter, and now completely covered by historic and recent lava flows, dark in colour). To the north and south (bright, light-coloured areas) are the “prehistoric” deposits of the volcano (Sheth et al., 2009, 2010, 2011). Yellowish white patches on the cinder cone are sublimates.



Fig. 3 – Cross-bedded base surge deposits of fine ash (with some lithic blocks) near the exposed base of the volcano, on the southern caldera wall. Similar deposits on the northern caldera wall lead one to infer a complete hydrovolcanic tephra ring (Sheth et al., 2009).



Fig. 4 – Squeeze-ups (sheets and slabs) of toothpaste lava in a recent Barren Island aa flow (Sheth et al., 2011). Flow direction is from lower left to right centre.

The central cinder cone on Barren Island has existed for the past 220 years at least, and must be described as polygenetic, in contrast to the much more common monogenetic cinder cones that are typically active for a few months to a few years (e.g., Paricutin 1943-1952, Luhr and Simkin 1993) and form “monogenetic volcanic fields”. The interplay of primary eruptive processes and erosion in the development of cinder cones has been addressed by several workers (e.g., Ollier 1959). It is known that during the recent eruptions the height

and shape of the cinder cone have changed greatly. However, in the time between the historic eruptions of 1787-1832 and the first of the recent eruptions in 1991, the cinder cone has managed to survive erosion, testifying to the general rule that cinder cones are well sorted and highly permeable, which means slow erosion because of little surface runoff (Segerstrom, 1950).

The four recent eruptions of Barren Island beginning 1991, and ongoing (as of December 2010) mean much excitement in store for volcanologists. Barren Island, “Lighthouse of the Andaman” (Sheth et al., 2010) is only ~500 km from the Myanmar coast, 135 km from Port Blair, and 70 km from the nearest inhabited island of the Andamans, meaning that its hazard aspects are also important.

Acknowledgements

This work was supported by the Dept. Sci. Tech. (Govt. of India).

References

- Awasthi, N., Ray, J.S., Laskar, A.H., Kumar, A., Sudhakar, M., Bhutani, R., Sheth, H.C., Yadava, M.G. 2010. Major ash eruptions of Barren Island volcano (Andaman Sea) during the past 72 Kyr: Clues from a sediment core record. *Bulletin of Volcanology* 72: 1131–1136.
- Luhr, J.F., Haldar, D. 2006. Barren Island volcano (NE Indian Ocean): Island-arc high-alumina basalts produced by troctolite contamination. *Journal of Volcanology and Geothermal Research* 149: 177–212.
- Luhr, J.F., Simkin, T. 1993. *Paricutin: The Volcano Born in a Mexican Cornfield*. Geoscience Press, 441 p.
- Ollier, C.D. 1959. *Volcanoes (Developments in Geomorphology)*. Blackwell, Oxford, 320 p.
- Segerstrom, K. 1950. Erosion studies at Paricutin volcano, State of Michoacan, Mexico. *U. S. Geological Survey Bulletin* 956-A: 1–164.
- Sheth, H.C., Ray, J.S., Bhutani, R., Kumar, A., Smitha, R.S. 2009. Volcanology and eruptive styles of Barren Island: An active mafic stratovolcano in the Andaman Sea, NE Indian Ocean. *Bulletin of Volcanology* 71: 1021–1039.
- Sheth, H.C., Ray, J.S., Bhutani, R., Kumar, A., Awasthi, N. 2010. The latest (2008-09) eruption of Barren Island volcano, and some thoughts on its hazards, logistics and geotourism aspects. *Current Science* 98: 620–626.
- Sheth, H.C., Ray, J.S., Kumar, A., Bhutani, R., Awasthi, N. 2011. Toothpaste lava from the Barren Island volcano (Andaman Sea). *Journal of Volcanology and Geothermal Research* 202: 73-82.

Eruption of Alberca de los Espinos tuff cone causes transgression of Zacapu lake ca. 25,000 yr BP in Michoacán, México

Claus Siebe¹, Marie-Noëlle Guilbaud¹, Sergio Salinas¹ and Corentin Chédeville-Monzo²

¹ Depto. Vulcanología, Instituto de Geofísica, UNAM, Coyoacán, 04510 México D. F. – csiebe@geofisica.unam.mx

² Magmas et Volcans, Université Blaise Pascal, Clermont-Ferrand II, France

Keywords: phreato-magmatic, environmental change, Mexican Volcanic Belt

Alberca de los Espinos tuff cone is located at the NW margin of the Zacapu tectonic lacustrine basin in the north-central part of the present State of Michoacán. It is one of the ca. 1000 monogenetic Quaternary volcanoes that comprise the so-called Michoacán-Guanajuato Volcanic Field (Hasenaka and Carmichael, 1985) in the western-central part of the subduction-related Trans-Mexican Volcanic Belt (TMVB).



Fig. 1 –Aerial view of Alberca de los Espinos from the SE. Note large quarries exposing its deposits

The tuff cone is composed of phreato-magmatic products that include typical surge and fallout deposits and hence, indicate the availability of sufficient groundwater in a permeable soft-sediment substrate at the time of the eruption. The juvenile components of the deposits consist of dark grey andesite clasts ($\text{SiO}_2=57.6$ wt.%, phenocrysts of plagioclase and hornblende in a glassy matrix) that are partly vesiculated and show signs of rapid quenching (e.g. cauliflower-type surface textures). The non-juvenile components consist of older volcanic lithics and milled basin-fill deposits. The latter form most of the brownish indurated silty matrix of the abundant “wet” pyroclastic surge deposits observable at several large quarry walls at the outer slopes of the cone. At these quarries, many other features that are diagnostic for a phreato-magmatic eruption style (e.g. accretionary lapilli, cross-bedding, bomb impact-sags in ductile wet soft sediment, etc.) can be noticed.

The original morphology of the tuff cone is well preserved and indicates a relatively young age. The highest point of the crater rim (2100 masl) rises ca. 110 m above the ground of the lacustrine plains to the SE. The crater has an NE-SW oriented elliptical shape and a maximum diameter of 740 m. Its interior is occupied by a maar lake that has a maximum diameter of 350 m and reaches a maximum depth of 29 m below its present surface at 1980 masl. The edifice has an average basal diameter of 1200 m and surge deposits are preserved as far as 2 km from the present crater rim.

The relatively rare occurrence of monogenetic phreato-magmatic volcanoes (maars, tuff rings, tuff cones) within the TMVB (a few dozens versus ca. 3000 scoria cones) indicates that special conditions are needed for their formation. Namely, sufficient groundwater in a permeable near-surface substrate, needs to be encountered by a small batch of rising magma. This explains why many (but not all) of the phreato-magmatic volcanoes within the TMVB occur in the tectonic inter-montane lacustrine basins, that characterize the southern limit of the Mexican highland (e.g. Yuriria, Valley of Mexico, Serdán-Oriental, etc.). Hence, the occurrence of Alberca de los Espinos at the northern limit of such a tectonic lacustrine basin is not further surprising. What makes this volcano special is its exact location at the former outlet of the Zacapu basin. As a result of the eruption, the outlet became sealed and the water table of the lake in the basin rose several meters, before a topographic low near Villa Jiménez, located 2 km to the NE of Alberca de los Espinos, could serve as a new outlet reconnecting the basin with the drainage of the Lerma river to the north. Hence, the Zacapu lake deposit sequence should record a significant transgression after the timing of this short-lived monogenetic eruption.

Several of the large quarries at the outer slopes of the tuff cone expose clean contacts with the underlying paleosol. Two samples obtained from this paleosol at different quarries yielded radiocarbon dates of 26,085 \pm 545/-510 and 24,360 \pm 535/-500 yr. BP respectively. Hence, this eruption occurred around 25,000 yr. BP.

The above age is of importance because it not only dates the eruption, but indirectly also dates a

major lake transgression and in consequence an important environmental change which in this case was not controlled by climate (e.g. changes in temperature and precipitation), but by endogenous forces (those forces that also created the fault-controlled lacustrine basin surrounded by volcanoes in the first place).

The Zacapu basin was occupied by extensive marshlands before the end of the 19th century, when the owners of Hacienda Cantabria decided to build a canal at Villa Jiménez in order to drain the basin and gain new farmland (Noriega and Noriega, 1923). This engineering project put an end to the existence of an habitat that had hosted numerous aquatic and riparian plant and animal communities whose exploitation was attractive to nomadic early humans. Furthermore, this type of habitat seems to have promoted the development of agriculture (and the domestication of plants that supply staple foods, particularly *Zea mays*) in the Mexican highlands in general. In this context, the Zacapu basin does not represent an exception, as evidenced by the numerous pre-Hispanic archaeological sites discovered in this area in past decades (e.g. Arnould et al., 1994). In order to better understand the environmental factors that fostered the rise of early human civilization in this region, palaeo-climate studies focusing on the analysis of the lake sediments (and particularly on their microfossil contents) have been carried out (e.g. Metcalfe, 1992). Although particular attention has been paid to the Holocene record, some of these studies go back as far as 52,000 yr. BP (e.g. Tricart, 1992; Metcalfe and Harrison, 1984; Ortega et al., 2002). Interestingly enough, these studies (which include the analysis of lake sediment cores, up to 10 m in length) have identified a notorious discontinuity dated at 28,000-25,000 yr. BP. Interpretation by these authors in regard to the origin of this discontinuity varies (some interpret it to represent a regression or "hiatus", others mention a transgression of the lake) but all share a marked reluctance to come up with a clear-cut answer. As hinted above, we think to have found the answer to the question of the nature of this discontinuity by dating the eruption of the Alberca de los Espinos tuff cone at 25,000 yr. BP. Our study shows that palaeo-environmental studies of lake sequences need to consider not only climatic factors (which are admittedly important), but also tectonic and volcanic activity as potential variables controlling the level of the water table, which especially in the case of shallow lakes such as Zacapu, can have a considerable ecological impact. In this context, it is

worth mentioning that so far, we have been able to identify a total of 12 Late Pleistocene/Holocene (<25,000 yr. BP) monogenetic volcanoes within the catchment area (1480 km²) of the Zacapu basin which has a perimeter of 230 km. Judging by the young morphology of the numerous ENE-WSW oriented extensional fault escarpments, and the occurrence of coeval lake deposits at different altitudes (vertical displacements of tens of meters), this area is certainly still seismically active. Hence, study of the lake deposits should not only consider volcanic eruptions, but also the occurrence of sudden catastrophic differential vertical movements of the lake floor.

Acknowledgements

Research grants from CONACYT and UNAM-DGAPA defrayed the costs of this study.

References

- Arnould, C., Carot, P., Fauvet-Berthelot, M.-F. 1994. Introducción. In: Pétrequin, P. (Ed.): 8000 años de la Cuenca de Zacapu. Evolución de los paisajes y primeros desmontes. Collection Etudes Méso-américaines II-14: 9-28, CEMCA, México, D.F.
- Hasenaka, T., Carmichael, I.S.E. 1985. The cinder cones of Michoacán-Guanajuato, central Mexico: their age, volume and distribution, and magma discharge rate. *Journal of Volcanology and Geothermal Research* 25: 105-124.
- Metcalfe, S.E. 1992. Changing environments of the Zacapu basin, Central Mexico: A diatom-based history spanning the last 30,000 years. Research Paper No. 48, School of Geography, University of Oxford, UK.
- Metcalfe, S.E., Harrison, S.P. 1984. Cambio ambiental del Cuaternario Tardío en depósitos lacustres en la cuenca de Zacapu, Michoacán. *Reconstrucción preliminar*. Boletín del Instituto de Geografía 14: 127-151, UNAM, México.
- Noriega E., Noriega, A. 1923. La desecación de la ciénega de Zacapu y las leyes agrarias. Caso especial, único en el país. México.
- Ortega, B., Caballero, C., Lozano, S., Israde, I., Vilaclara, G. 2002. 52000 years of environmental history in Zacapu basin, Michoacán, Mexico: the magnetic record. *Earth and Planetary Science Letters* 202: 663-675.
- Tricart, J. 1992. La cuenca lacustre de Zacapu: Un acercamiento geomorfológico. In: Demant, D., Labat, J.-N., Michelet, D., Tricart, J., (Eds.), *El Proyecto Michoacán 1983-1987. Medio ambiente e introducción a los trabajos arqueológicos*. Collection Etudes Mésoaméricaines II-11: 113-197, CEMCA, México, D.F.

Soil Gas CO₂ Fluxes and Concentrations in the Auckland Volcanic Field, New Zealand: A Pilot Study

Elaine R. Smid¹, Agnès Mazot², Gill Jolly² and Jan Lindsay³

¹ Institute of Earth Science and Engineering, Private Bag 92019, Auckland 1142, New Zealand – e.smid@auckland.ac.nz

² GNS Science, Private Bag 2000, Taupo 3352, New Zealand

³ School of Environment, The University of Auckland, Private Bag 92019, Auckland 1142, New Zealand

Keywords: Auckland Volcanic Field, soil gas CO₂, volcanic gas monitoring.

The vent locations and timing of future volcanic eruptions in monogenetic fields are highly unpredictable. Soil gas CO₂ measurements may help resolve both of these unknowns, as anomalously high soil gas CO₂ fluxes and concentrations are typically one of the first precursors of volcanic activity, and soil gas CO₂ measurements have been used to detect unknown faults or fractures that may act as conduits for gases and magma to the surface (e.g., Baubron et al. 2002; Bruno et al. 2001; Connor et al. 1992; Fu et al. 2005; Giammanco et al. 1998). To date, very few studies have focused on soil gas CO₂ as a potential monitoring tool in monogenetic volcanic fields (Delgado-Granados and Villalpando-Cortes 2008; Delgado-Granados et al. 2011).

The Auckland Volcanic Field (AVF) is a dormant monogenetic basaltic field located in Auckland, New Zealand, on which there have been no previous studies of soil gas CO₂ fluxes or concentrations; atmospheric CO₂ is likewise not monitored, even though Auckland is New Zealand's most populated city and likely to sustain significant damage from an eruption. Given the young age of this field (~250,000 years) future eruptions are expected, with an estimated warning period as short as a few days (Sherburn et al. 2007). As part of the DEtermining VOLcanic Risk in Auckland (DEVORA) project, soil gas CO₂ fluxes and concentrations were measured in seven transects spanning various settings (e.g. urban, rural, areas of known or suspected faults, areas of no suspected faults) in the AVF over four days in November 2010 for a pilot study.

There were two main goals for this pilot study: (1) establish a baseline soil gas CO₂ flux and concentration for the AVF; and (2) attempt to detect subsurface structures such as faults that may act as a control on future vent locations.

Soil gas CO₂ fluxes were measured using a West Systems portable soil flux accumulation chamber. The accumulation chamber was a 200 mm diameter open-bottomed vessel, with a battery-powered fan affixed inside to ensure mixing. Flat surfaces were chosen for measurements and the chamber was held down in place by physical means to ensure minimal

atmospheric air entered the chamber during measurement. A pump, at a flow rate of 1,000 standard cubic centimeters per minute, introduced soil gas from the chamber to the LICOR 820 instrument (infrared spectrometer) via tubing with an inline Mg(ClO₄)₂ filter to absorb any moisture that may cause interference in the reading. Following the original method in Chiodini et al. (1998), after soil gas CO₂ gas passes through the chamber and the infrared sensor, it returns to the chamber where it accumulates with the subsequent emissions of soil gas CO₂. The flux is determined by calculating the increase of the CO₂ concentration with time (ppm-vol s⁻¹), to an accuracy of ±12.5% (Evans et al. 2001).

Soil gas CO₂ concentrations were measured at selected sites across Auckland by pumping the gas from the soil (25 - 40 cm deep) through a duralumin customized probe with several perforations above a pointed base. Tubing connected the probe to the LICOR instrument.

During this study, 72 measurements of CO₂ concentrations ranged from 393 parts per million (ppm) to 10,140 ppm; 443 fluxes varied from 0 to 108.7 g m⁻²d⁻¹. Using a graphical statistical approach, two populations of soil gas CO₂ fluxes were identified (Fig. 1).

Based on this pilot study, soil gas CO₂ concentration and flux baselines for the AVF are typical of those produced by biogenic sources and for New Zealand, with soil permeability as the main control. No volcanic component appears to be present at this time, although this cannot be confirmed categorically as no isotopic analyses were performed. No faults could be discerned using soil gas CO₂ fluxes or concentrations, although concentrations in fault areas are statistically different from those in no fault areas, which could relate to site-specific conditions rather than the presence of faults. It is also interesting to note that urban and rural areas are statistically different, perhaps reflecting a greater influx of atmospheric CO₂ into the soil in urban areas and illustrating the varied influence of site conditions.

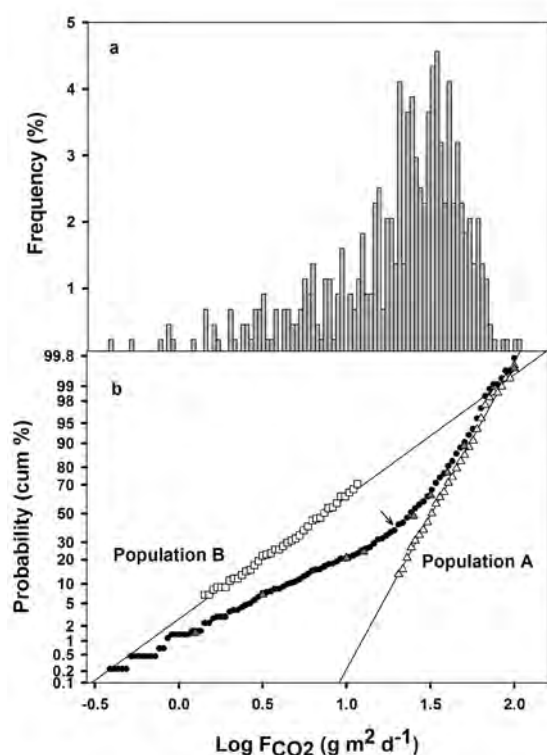


Fig. 1 – Soil gas CO₂ fluxes measured in November 2010 in the Auckland Volcanic Field, as described by a geographical statistical approach. Histogram (a) and probability plot (b) of CO₂ flux data (black circles). Populations A (open triangles up) and B (open squares) are shown as straight lines. The inflection point is indicated by an arrow and corresponds to 67% of population A and 33% of population B.

These results hint at interesting variations in soil gas CO₂ across Auckland; future work includes expanding the study area, examining seasonal differences, and identifying the sources of CO₂ in soil gas via $\delta^{13}\text{C}$ analysis.

Acknowledgements

The authors are grateful to Jo Hanley (Royal Society of New Zealand Primary Science Teaching Fellow) and Tracy Howe (University of Auckland) for field assistance. This work was carried out under the umbrella of the Determining Volcanic Risk in Auckland (DEVORA) project, which is financially supported by the Institute of Earth Science and Engineering, GNS Science, Ministry of Science and Innovation, the Earthquake Commission, The University of Auckland, Massey University, and the Auckland Council.

References

- Baubron, J.C., Rigo, A., Toutain, J.P. 2002. Soil gas profiles as a tool to characterise active tectonic areas: the Jaut Pass example (Pyrenees, France). *Earth and Planetary Science Letters* 196: 69-81.
- Bruno, N., Caltabiano, T., Giammanco, S., Romano, R. 2001. Degassing of SO₂ and CO₂ at Mount Etna (Sicily) as an indicator of pre-eruptive ascent and shallow emplacement of magma. *Journal of Volcanological and Geothermal Research* 110: 137–153.
- Chiodini, G., Cioni, R., Guidi, M., Raco, B., Marini, L. 1998. Soil CO₂ flux measurements in volcanic and geothermal areas. *Applied Geochemistry* 13(5): 543–552.
- Connor, C.B., Condit, C.D., Crumpler, L.S., Aubele, J.C. 1992. Evidence of Regional Structural Controls on Vent Distribution: Springerville Volcanic Field, Arizona. *Journal of Geophysical Research* 97(12): 12349-12359.
- Delgado-Granados, H., Villalpando-Cortes, R.E. 2008. Método para pronosticar la localización de un nuevo volcán al sur de la ciudad de México. *Tip Revista Especializada en Ciencias Químico-Biológicas* 11(1): 5-16.
- Delgado-Granados, H., Espinasa-Pereña, R., Rodríguez, S.R., Morales-Barrera, W.V., Jácome Paz, M.P., Álvarez Nieves, J.M. 2011. Use of soil gas CO₂ for the recognition of the most active zones in the Xalapa Monogenetic Volcanic Field. *Geophysical Research Abstracts* 13: EGU2011-12892.
- Evans, W.C., Sorey, M.L., Kennedy, B.M., Stonestrom, D.A., Rogie, J.D., Shuster, D.L. 2001. High CO₂ emissions through porous media: transport mechanisms and implications for flux measurement and fractionation. *Chemical Geology* 177: 15-29.
- Fu, C.-C., Yang, T.F., Walia, V., Chen, C.-H. 2005. Reconnaissance of soil gas composition over the buried fault and fracture zone in southern Taiwan. *Geochemical Journal* 39: 427 - 439.
- Giammanco, S., Gurrieri, M., Valenza, S. 1998. Anomalous soil CO₂ degassing in relation to faults and eruptive fissures on Mount Etna (Sicily, Italy). *Bulletin of Volcanology* 60: 252–259.
- Sherburn, S., Scott, B.J., Olsen, J., Miller, C.A. 2007. Monitoring seismic precursors to an eruption from the Auckland Volcanic Field, New Zealand. *New Zealand Journal of Geology and Geophysics* 50: 1-11.

Mantle Flow and the Origin of Tiny Igneous Provinces: an Example from the Late Cenozoic of Northern New Zealand

Ian E.M. Smith

School of Environment, The University of Auckland, Private Bag 92019, Auckland, New Zealand - ie.smith@auckland.ac.nz

Keywords: basalt, scoria cone, tuff ring, intraplate.

Northern New Zealand is well known for its succession of subduction-related volcanic episodes developed on the Pacific-Australian plate boundary during the late Cenozoic. The well-defined lower Miocene Northland Arc (Booden et al. 2011) is the precursor to the current magmatic expression of plate interactions in the New Zealand region, the well-known Taupo Volcanic Zone (TVZ).

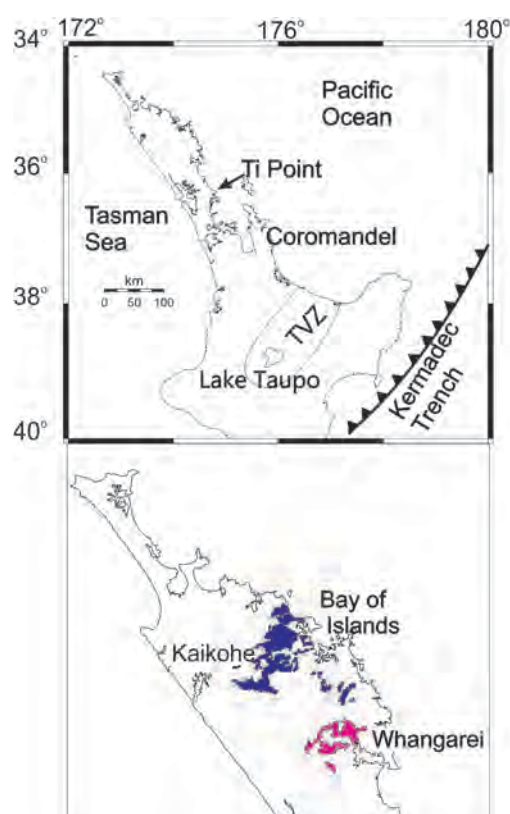


Fig. 1 - Top - the general features of northern New Zealand. Bottom - the distribution of intraplate basalt fields in Northland.

As convergent tectonics and associated andesitic magmatism migrated southward there developed a Late Miocene to Recent association of basalts with characteristic intra-plate chemistry forming discrete fields of volcanoes on very small spatial and short to medium (0.25 to 10.0×10^6 yr) but variable temporal scales. These are the Auckland province and the Northland province volcano fields. Differences between these volcano provinces are in longevity

and, in detail, their chemistry, indicating subtly differing conditions of magma generation and of mantle source regions. The Northland fields have characteristic trace element and isotopic signatures and the Auckland fields, share distinctive, trace element and isotopic signatures that are clearly different from those of the Northland Province

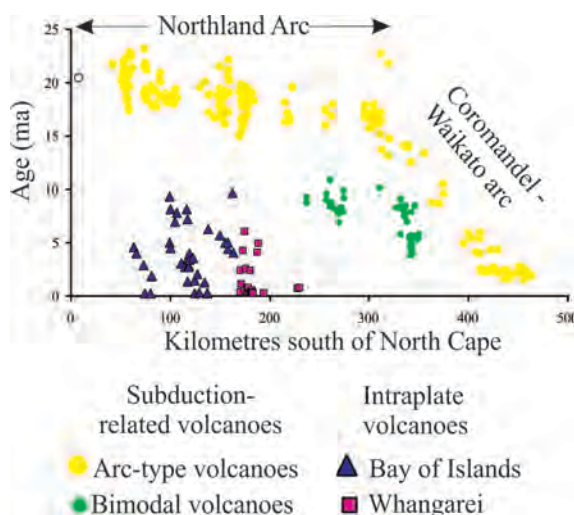


Fig. 2 - Plot of the ages of late Cenozoic volcanic rocks in northern New Zealand against distance southward from North Cape, the northern tip of the North Island. Ages are from Smith et al.(1993) and [8]Hayward et al. (2002). Distance south was calculated by projecting the sample site of dated rocks on to a line drawn between North Cape and Lake Taupo.

The Northland intraplate basalts outcrop over an area of 2500 km². Older rocks are mostly remnant lava flow sequences and younger rocks occur as small scoria cones together with associated lava flows. The predominant rock type is porphyritic basalt with typically 8-15 vol.% and up to 20 vol.% phenocrysts. Two sub groups are recognized, those with olivine as the dominant phenocryst and those in which plagioclase is dominant. Augite, although present as phenocrysts in most samples (3-5%) is never a major phase. The groundmass is plagioclase and augite with subordinate olivine and accessory magnetite. The two main fields in Northland are the Kaikohe/ Bay of Islands (K-BoI) field and the Whangarei Volcanic Field.

Fifty km to the south of the Whangarei Field are the Ti Point basalts, a part of the late Miocene

bimodal volcanism linked to the migrating arc and these have clear arc-type geochemical affinities.

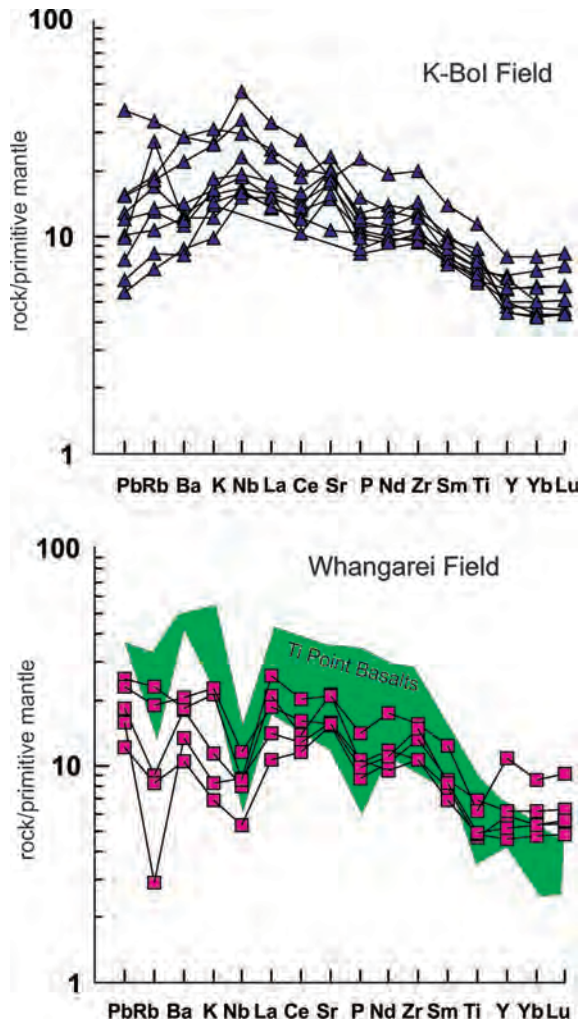


Fig. 3 - Mantle normalized trace element diagram for samples from the (a) the BKP field and (b) Whangarei field using primitive mantle values from Sun and McDonough [1989]. The K-Bol rocks have a smooth pattern with positive Nb anomalies while the Whangarei rocks have a similar pattern except for a negative Nb anomaly. Also shown for comparison is the pattern of trace elements from arc related basalts found at Ti Point.

The chemical compositions of basalts from the Kaikohe-Bay of Islands field are typical of intraplate basalts. The chemical compositions of the Whangarei field basalts are broadly similar but show negative Nb anomalies that indicate a subduction modified source (Fig.3). Ti-Point basalts have geochemical characteristics that clearly link them to the earlier episode of subduction. Using selected trace element ratios it is clear that the source area for both the K-BoI and Whangarei fields is within the spinel lherzolite facies of the upper mantle (Fig.4). The various chemical signatures and the spatial relationships can be reconciled if the mantle beneath Northland is made up of a modified component (Ti

Point mantle signature) and an unmodified component (K-BoI mantle signature).

There is a clear temporal and spatial relationship between the development of an arc-type geochemical signature and modification of the mantle wedge under New Zealand as shown by the Miocene arc associations; the preservation of this mantle in the arc-type signature of the Ti Point basalts which post date the subduction event and finally the disappearance of an arc-type signature in the intraplate basalts. A key feature of the intraplate basalts is that they show a decrease in age towards the south (Fig 2). Typically such a trend would be caused by a lithosphere plate moving over a static hotspot in the mantle. This is however not the case in Northland which has remained relatively stationary for the last 10 million years. It is suggested that this progression actually reflects an influx of new mantle material from the north west flowing towards the south east which totally replaced the supra-subduction modified mantle within a few million years beneath the Kaikohe-Bay of Islands field. The Whangarei field offers the southern limit of new material flowing south as here we see the mixing between new mantle material the (K - BOI signature) and the arc signature.

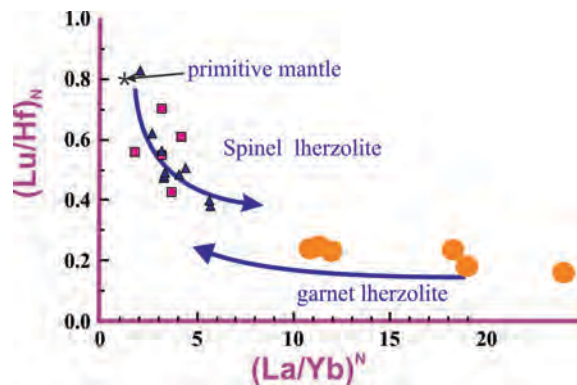


Fig. 4 - Plot of Ba/Ta versus La/Ta for Northland basalts. K-Bol lavas (filled squares) showing strong OIB signature and low LILE/HFSE and LREE/HFSE ratios compared to Ti Point mafic arc lavas (stippled field upper right corner). The Whangarei lavas (filled triangles) along the Ba/La=10 line lie between the Ti Point and BKP fields. Approximate fields for EM1, EM2 and HIMU type OIB are from Weaver 1991. Unfilled star is average OIB composition from Sun and McDonough (1989). Symbols as for Fig.3. For comparison samples from the Auckland Volcanic Field (orange dots) sourced in the garnet lherzolite stability field (McGee et al. 2011) are shown.

Upward flow of mantle from deep in the asthenosphere due to the displacement of supra-subduction modified mantle probably resulted in decompressional melting. Using the eruption times and distance from the northern most rocks a minimum mantle flow rate of 40mm/yr can be calculated.

There are four problems associated with the origin of intraplate magmatism in Northland:

1. The existence of the remnant volcanoes of the Northland Arc are evidence for a moderately long period of subduction beneath Northland during which time slab-wedge interaction produced a modified mantle source that supplied magmas to the volcanoes of the arc. In the northern intraplate volcanoes that followed only 5 ma afterward there is no trace of a supra subduction zone signature in the compositions of the erupted rocks. In the intraplate basalts of the Whangarei field which developed further to the south and a little later there is a clear indication of a supra subduction zone chemical signature. However, the Whangarei basalts are chemically and petrographically distinct from the Ti Point subduction related basalts that occur still further to the south.
2. Intraplate basaltic volcanism in Northland does not appear to be associated with active crustal extension or rifting although to the south the amagmatic Hauraki Rift is considered to be active.
3. There is no evidence for a thermal anomaly in the mantle eg uplift or the presence of high magnesium magmas
4. Although intraplate volcanism in Northland is on an extremely small scale it has persisted through the last 10ma indicating long-lived existence of the conditions required to produce magmas.

Similar volcanic sequences where arc-type associations are followed by younger non arc basaltic associations have been explained via slab window models. The formation of a slab window and its associated magmatism is a result of the collision and interaction of mid-ocean ridges with continental subduction zones. However, there is no evidence of a collision between a spreading system and the Miocene Arc in Northland. For this reason the intraplate basalts cannot be due to the opening of a slab window.

Extension in convergent margins has also been invoked to explain small outpourings of alkaline intraplate basalts occurring in a predominantly volcanic arc association. For extension of the lithosphere to result in decompression melting a β factor (β = original mechanical boundary layer thickness/post extension thickness) needs to exceed ~ 2.5 . In Northland there is no evidence for extension either during lower Miocene subduction or immediately prior to it. While minor amounts of subsequent extension can't be discounted it is unlikely that it could have achieved a β value as high as ~ 2.5 without leaving some evidence in the geological record. Limited extension can only generate melts if the potential temperature of the mantle was higher than normal.

In Northland as subduction and its associated volcanic arcs migrated southward in response to late Tertiary plate readjustments, mantle flowed in from the north to replace that beneath the northern part of the peninsula. This flow would also be enhanced by continued subduction and associated slab roll back in the Taupo Volcanic Zone. Beneath Whangarei subduction modified mantle mixed with incoming unmodified mantle and volcanism began a few million years later than in K-BoI field. To the south subduction modified mantle supplied basaltic magma to the bimodal complexes that developed as the arc migrated southward.

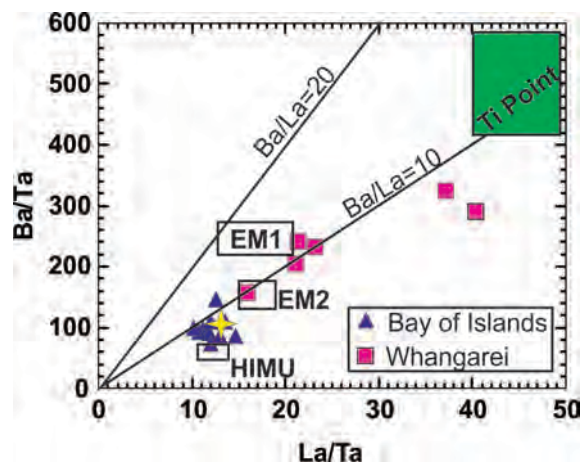


Fig.5. Chondrite normalized [12,14](Nakamura, 1974; Sun and McDonough 1989) La/Yb vs. Lu/Hf for Northland basalts. Also shown are trends of melt compositions produced by 1-15% partial melting of primitive mantle with the following mineralogy spinel lherzolite (40ol:40opx:10cpx:10sp) and garnet lherzolite (40ol:40opx:10cpx:10grn).

Models involving mantle plumes or slab-window opening, cannot readily explain these small intraplate basaltic fields in Northland. A possible explanation is edge driven convection where the boundary between thick and thin lithosphere focuses upwelling convection bringing hot material from under the thicker lithosphere to shallower levels. This hot mantle material then undergoes partial melting. Northland and other similar small basaltic systems where there is no associated rifting provide an example of a small scale end member for this model. In Northland the asymmetry and discontinuity in the thickness of the lithosphere is provided by the juxtaposition of Paleozoic and Mesozoic crust. As the mantle flowed southeast it would have crossed this junction and was then able to rise from below the thicker early Paleozoic basement/mantle boundary to the depth of the thinner late Mesozoic basement and therefore the shallower crust/mantle boundary. This would result in small amounts of adiabatic melting

References

- Booden, M.A., Smith, I.E.M., Black, P.M., Mauk, J.L. 2011. Geochemistry of the Early Miocene volcanic succession of Northland, New Zealand, and implications for the evolution of subduction in the southwest Pacific. *Journal of Volcanology and Geothermal Research* 199: 25–37.
- Hayward, B.W., Black, P.M., Smith, I.E.M., Ballance, P.F., Itaya, T., Doi, M., Takagi, M., Bergman, S., Adams, C.J., Herzer, R.H., Robertson, D.J. 2001. K-Ar ages of early Miocene arc-type volcanoes in northern New Zealand. *New Zealand Journal of Geology and Geophysics* 44: 285-310.
- McGee, L., Bier, C., Smith, I.E.M. Turner, S. in press. Dynamics of melting beneath a small-scale basaltic system: a U-Th–Ra study from Rangitoto volcano, Auckland volcanic field, New Zealand. *Contributions to Mineralogy and Petrology* DOI 10.1007/s00410-011-0611-x.
- Nakamura, N. 1974. Determination of REE Ba, Fe, Mg Na and k in carbonaceous and ordinary chondrites. *Geochemica et Cosmochimica acta* 38: 757-775.
- Smith, I.E.M., Okada, T., Itaya, T., Black, P. 1993. Age relationships and tectonic implications of late Cenozoic basaltic volcanism in Northland, New Zealand: *New Zealand Journal of Geology and Geophysics* 36: 385-393.
- Sun, S.S., McDonough, W.F. 1989. Chemical and isotope systematics of oceanic basalts: implications for mantle composition and processes. In: Saunders, A.D, Norry M.J. (eds) *Magmatism in the Ocean basins*. Geological Society Special Publication 42: 313-345.
- Weaver, B.L. 1991. The origin of oceanic basalt end-member compositions: trace element and isotopic constraints. *Earth and Planetary Science Letters* 104: 381-397.

Sedimentary and volcanotectonic evolution of a basaltic diatreme in a nonmarine backarc-margin basin (the Miocene Janggi Basin, SE Korea)

Moon Son¹, Jong Sun Kim¹, Soohwan Jung¹, Jin Seok Ki², Min-Cheol Kim¹ and Young Kwan Sohn²

¹ Department of Geological Sciences, Pusan National University, Pusan 609-735, Republic of Korea

² Department of Earth and Environmental Sciences, Gyeongsang National University, Jinju, 660-701, Republic of Korea – yksohn@gnu.ac.kr

Keywords: diatreme, vent migration, tectonic control.

Understanding the roles of external controls, such as paleohydrology and tectonics, is crucial for interpreting the evolution of a phreatomagmatic volcano and its subsurface structure called the diatreme. The Yangpo diatreme in a Miocene terrestrial half-graben basin of Korea provides an opportunity to assess the roles of synvolcanic tectonic activity in forming a maar-diatreme volcano. The diatreme fill consists of two offset-

stacked sequences with contrasting lithofacies characteristics: a lower sequence (early diatreme fill) of locally stratified or bedded basaltic lapilli tuff and tuff in the northeastern part and an upper sequence (later diatreme fill) of dacite clast-rich and disorganized tuff breccia in the southwestern part. The boundary between these sequences is abrupt, suggesting eruption of the volcano in two distinct phases.

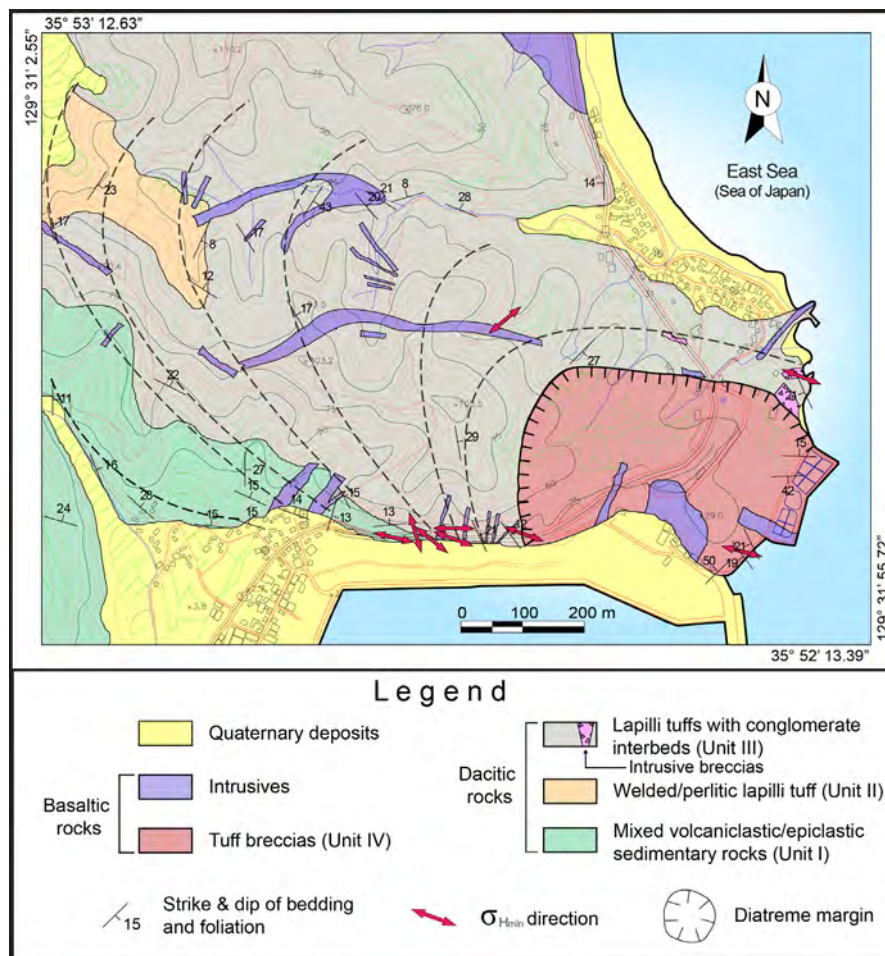


Fig. 1 - Geological map of the Yangpo diatreme in SE Korea, showing roughly concentric distribution of bedding traces and approximately radial alignment of mafic dikes with respect to the diatreme. The directions of horizontal minimum stresses are generally normal to the strikes of adjacent dikes, suggesting contemporaneous formation of faults and dikes.

The first phase of eruption was driven by hydroexplosions mainly within the basin fills. Some of the diatreme fill was deposited in a water-filled crater by subaqueous debris flows and suspension settling of fines. The second phase of eruption was driven by hydroexplosions at a fracture aquifer within the basement, because of sudden lowering of the explosion locus. The later diatreme fill therefore contains abundant basement-derived dacite clasts. The deposition was accomplished by *en masse* fallout of volcanic debris from dense collapsing columns. A number of faults and shear fractures were generated within and in the vicinity of the diatreme together with penecontemporaneous basaltic intrusions. Structural and geochemical analyses show that many of these structures are genetically related with the diatreme formation. The early diatreme fill was also tilted toward the southwest, suggesting southwestward shift of the

locus of hydroexplosion and diatreme excavation. The explosion locus of the Yangpori volcano is therefore interpreted to have migrated both vertically and laterally. The abrupt lithofacies boundary between the early and later diatreme fills suggests that the migration was caused by an abrupt tectonic activity near the basin margin. Most probably, the feeder dike was dislocated by the basin-margin fault activity, which instead created abundant fractures deep within the basement, rerouting the course of magma ascent and opening a new hydraulically active zone in the basement. Synvolcanic tectonic activity is therefore interpreted to have played a crucial role in forming the features of the Yangpori diatreme. The tectonic activity is also inferred to have influenced the morphology and internal facies architecture of the ejecta rimbeds significantly, although they are removed by erosion.

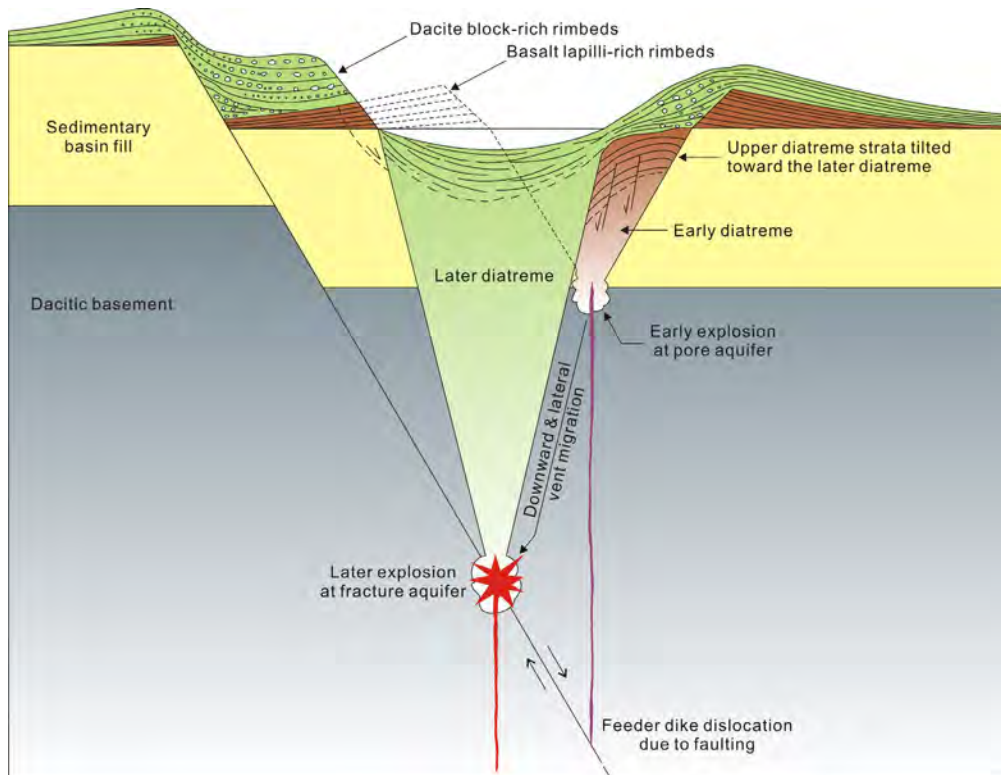


Fig. 2 - Schematic illustration of the geometry of the Yangpo diatreme consisting of two cross-cutting diatreme structures, which suggests tectonics-induced migration of the explosion locus. The ejecta ring around the crater is inferred to comprise multiple superposed rimbeds with contrasting geometry and lithofacies characteristics.

Evidence for sporadic Eocene to Pliocene effusive and explosive subaqueous volcanism in northern Chatham Island, SW-Pacific

Robert B. Stewart and Károly Németh

Volcanic Risk Solutions, Massey University, Palmerston North, New Zealand – R.B.Stewart@massey.ac.nz

Keywords: Surtseyan, hyaloclastite, hydromagmatic.

Erosional remnants of volcanic conduits and proximal pyroclastic successions form a typical eroded volcanic landscape in northern Chatham Island SW Pacific. They closely resemble buttes and plugs formed by exhumed pyroclast-filled volcanic conduits such as mafic diatremes; landforms typical of subaerial intraplate volcanic fields. In spite of this morphological similarity, here we present evidence that the preserved landforms are remnants of deeply eroded Surtseyan style volcanoes and associated subaqueous lava domes and *in situ* and reworked hyaloclastite successions that are commonly intercalated with carbonate-rich marine sedimentary layers. This work also highlights the difficulty of identifying independent geological evidence to establish the eruptive environment and hence the type of volcano on an old and eroded landscape.

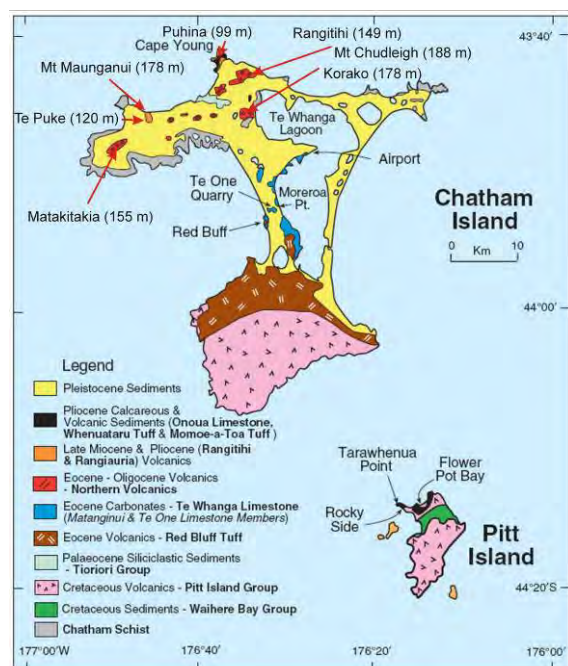


Fig. 1 – Schematic geological map of the Chatham Island. Red arrows point to studied locations. Geological data based on James, et al. (2011) and Campbell, et al. (1993).

The Chatham Islands are located on the eastern margin of the Zealandia micro-continent of the Pacific Plate ~700 km E of New Zealand and provide crucial evidence of the paleogeographic

history of Zealandia. The region was submerged in the Eocene, as shown by the eroded Surtseyan edifices of Red Bluff Tuff (Sorrentino et al 2011).



Fig. 2 – Korako hill is a typical Northern Volcanics butte (A) and composed of clast-supported angularly fragmented chilled lava indicating quench fragmentation and subaqueous emplacement (e.g. hyaloclastite).

Volcanic rocks in the northern part of Chatham are grouped into the poorly exposed but laterally extensive Northern Volcanics (Fig. 2) and the slightly younger unnamed volcanics that were inferred to have been erupted subaqueously. The youngest volcanism in Chatham, forming the Miocene–Pliocene Rangitihī Volcanics, provides evidence of the paleoenvironmental setting of the region at the time and helps constrain the timing of the emergence of the islands from the Pacific Ocean. Coastal sections in the Cape Young area expose Surtla and Surtseyan type volcanoes, cryptodomes and hyaloclastite piles (Fig. 3). At Maunganui Bluff a complex, elongated Surtseyan volcano developed over a pillow lava and hyaloclastite pile. The tuff cone emerged above sea level to form a scoriaceous

pyroclast pile in its crater. Local high points inland a few kms from the coastline are inferred to be volcanic remains of older Surtseyan volcanoes of the Northern Volcanics (Fig. 1). Conduit-filling and edifice-forming rocks overly a veneer of palagonitized, bedded reddish pyroclastic rocks (~few tens of m thick) which is inferred to be remnants of subaqueous pyroclastic mounds. Their present day elevation and the present elevations of the change in volcanic facies from subaqueous to emerged accumulation of pyroclasts in the coastal sections is curiously similar, suggesting that the present day 80 to 100 metres above sea level horizon represents the sea level in both Late Eocene-Early Oligocene and Miocene to Pliocene time.

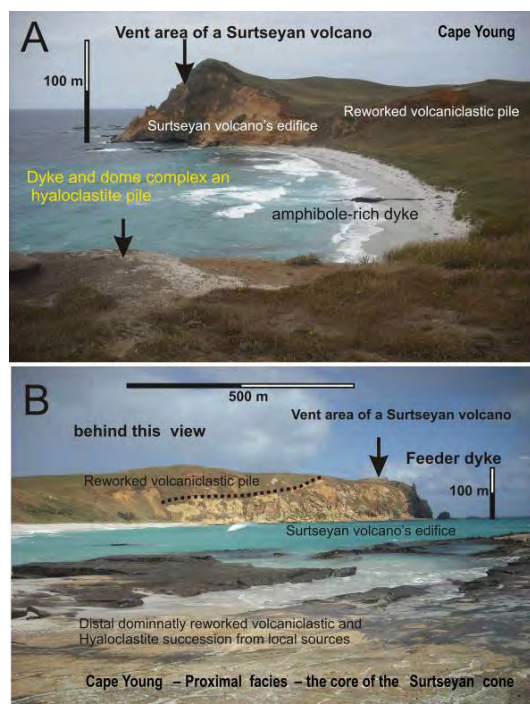


Fig. 3 –Cape Young (highest point Puhina) is inferred to be a half section of a Surtseyan volcano (A) and associated subaqueous lava dome and hyaloclastite complex invaded by multiple phases of mafic dykes (B).

Alternatively, the poorly dated Northern Volcanics may have erupted over a much longer time period making them indistinguishable from volcanics grouped in chronostratigraphically younger units. A significant morphological step in the landscape marks mound like features on which the 120 – 180 meters high conical buttes sit. These buttes are composed of sideromelane-dominated, massive lapilli tuffs and/or angular, chilled lava lapilli-dominated, class supported breccias, all indicating magma/water interaction-driven explosive (e.g. Surtla/Surtseyan) eruptions and/or autoclastic

fragmentation (e.g. hyaloclastite). Volcanic evidence suggests that Chatham must have been a shallow marine region dotted with small Surtseyan tuff cones since the Eocene and at least 100 m of uplift/sea-level drop is inferred in the past ~5 Ma.

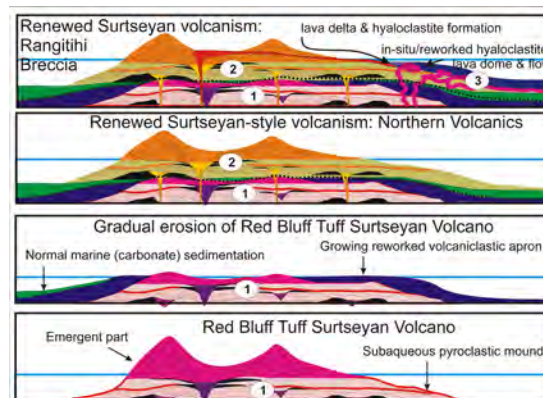


Fig. 4 – Simplified evolutionary model of the Northern Chatham based on the type sections of Cape Young: Initial stage represents the Red Bluff Tuff formation (1) period where subaqueous-to-emergent volcanism took place leaving behind a thick accumulation of Eocene volcanics. Erosion then partially eliminated the volcanic edifices and post-volcanic carbonate deposition occurred over the remnant volcanoclastic piles. Sporadically distributed rejuvenated multiple volcanic horizons of Surtseyan edifices and subaqueous pyroclastic mounds (e.g. Northern Volcanics) (2). Youngest stage of volcanism Rangitahi Volcanics) capping the older volcanic units (3).

Acknowledgements

Massey University Research Fund has provided financial support to conduct this research.

References

- Campbell, H.J., Andrews, P.B., Beu, A.G., Maxwell, P.A., Edwards, A.R., Laird, M.G., Hornibrook, N.D., Mildenhall, D.C., Watters, W.A., Buckeridge, J.S., Lee, D.E., Strong, C.P., Wilson, G.J., Hayward, B.W. 1993. Cretaceous-Cenozoic geology and biostratigraphy of the Chatham Islands, New Zealand. Institute of Geological & Nuclear Sciences Ltd, Lower Hutt, New Zealand, 269 pp.
- James, N.P., Jones, B., Nelson, C.S., Campbell, H.J., Titjen, J. 2011. Cenozoic temperate and sub-tropical carbonate sedimentation on an oceanic volcano - Chatham Islands, New Zealand. *Sedimentology* 58(4): 1007-1029.
- Sorrentino, L., Cas, R.A.F., Stilwell, J.D., 2011. Evolution and facies architecture of Paleogene Surtseyan volcanoes on Chatham Islands, New Zealand, Southwest Pacific Ocean. *Journal of Volcanology and Geothermal Research* 202(1-2): 1-21.

Maar-Diatreme Volcanism and its post-eruptive Subsidence

Peter Suhr¹, Volker Lorenz² and Kurt Goth¹

¹ *Sächsisches Landesamt für Umwelt, Landwirtschaft und Geologie, (LfULG). P.O. Box 540137, D-01311 Dresden, Germany – Peter.Suhr@smul.sachsen.de*

² *Physical Volcanological Laboratory, University Wuerzburg, Pleicherwall 1, D-97070 Wuerzburg, Germany*

Keywords: maar-diatreme volcano, maar crater sediments, post-eruptive subsidence.

Introduction: The phreatomagmatic model of the formation of maar-diatreme volcanoes has been discussed already by Lorenz and Kurszlaukis (2007) and White and Ross (2011). As long as maar-diatreme-forming phreatomagmatic explosions and eruptions continue the deeper the explosion chambers migrate towards depth jointly forming the root zone and the larger the overlying diatreme and maar crater get via collapse (Lorenz and Kurszlaukis 2007). Already from very early on during the volcano's activity and growth of the maar crater in size, a maar crater acts as a depot centre for both collapsing country rocks from the crater wall and for collapsing tephra that had accumulated on the surrounding country rocks forming the tephra ring. The tephra collapsing during growth of the crater forms lahars on the crater floor. From a certain size onwards, base surges deposit part of their load also on the crater floor and consequently get interbedded with the reworked tephra. Many small maar-diatremes may have been active during days to weeks only. However, large maar-diatreme volcanoes may have been active for years, perhaps up to ten years – as the scoria cone of Paricutin in Mexico almost did (Luhr and Simkin 1993), that represents the magmatic equivalent of a maar-diatreme volcano. Small tephra-filled diatremes may reach towards a depth of several hundred meters only. Large tephra-filled diatremes are assumed to reach depths of not more than 2-2.5 km (Lorenz and Kurszlaukis 2007). Thus at the end of its eruptive activity a diatreme represents a cone that has been filled during its rather short period of eruptive activity with several hundred to up to perhaps 2.5 km of tephra. At the end of the phreatomagmatic activity this cone of tephra should have been mostly unconsolidated.

Post-phreatomagmatic processes: Phreatomagmatic eruptions end because there is either a lack of groundwater or a lack of magma to continue the activity. When sufficient ground-water is lacking but magma is still available then it intrudes the root zone and diatreme. In case magma even reaches the crater floor it may form a scoria cone (as in c. 130 small maars in the West Eifel Volcanic Field) or a lave lake (as, e.g., in the High Eifel Volcanic Field and the Hegau Volcanic Field, SW-Germany).

When, in contrast, magma does not reach the crater floor, then groundwater enters the crater and fills the accessible void space of the unconsolidated diatreme tephra fill underneath. In addition, a crater lake forms as happened in many maars whenever the crater floor has intersected the local groundwater table. In case post-phreatomagmatic eruptions had occurred in the crater groundwater will also fill the accessible void space of the intra-crater scoria cone and solidified lava lake up to the groundwater table. Maar crater lakes represent local depot centres. They accumulate characteristic lacustrine and subaerial sediments, i.e. Corg-rich pelites, carbonates, subaerial and subaqueous fan-delta deposits and turbidites that initially consist predominantly of reworked tephra, to name only the most common maar crater deposits. The lacustrine sediments may be up to several hundred m thick in large maar craters (Suhr et al. 2006 and references therein) and may have been deposited during several hundred or more thousand years. Via peat deposits as occur in many maars purely subaerial sediment deposition follows.

Post-eruptive compaction/diagenesis and subsidence of the diatreme fill: During the period of post-eruptive erosion of the maar tephra ring and the filling of the maar crater lake with sediments, important processes are active in the diatreme fill underneath the last syn-eruptive crater floor. The unconsolidated permeable tephra and unconsolidated country rock collapse “breccias” inside the diatreme, deposited within weeks, months or years only, will get water-saturated rather fast. Simultaneously, compaction of the diatreme fill and hydrothermal as well as other diagenetic processes, i.e. low-temperature alteration and cementation, start. The amount of post-eruptive subsidence as a consequence of compaction was first studied in the Kleinsaubernitz maar-diatreme in eastern Saxony (Suhr et al. 2006 and references therein). Three Miocene lignite seams in near-shore sediments and a Holocene diatomite, all deposited and then subsided only above the Oligocene (27.3 Ma) Kleinsaubernitz maar-diatreme volcano. A subsidence curve was calculated from the ages and present depths of the respective 4 horizons (Suhr et al. 2006). According to the subsidence curve compaction of the

Kleinsaubernitz diatreme fill began in early post-eruptive time relatively fast. The subsidence continued and its rate steadily decreased over the 27.3 million years. In fact subsidence is still going on in and above the Kleinsaubernitz and the near-by Baruth maar-diatremes (Suhr et al. 2006).

Evaluation of the lake level variations of and sediment deposition in Ukinrek East Maar lake during its 27 post-eruptive years (1977-2004) led to an estimate of the amount of subsidence of the pre-sedimentation crater floor of 1977 of c. 15 m (on average 55.6 cm/year) (Pirring et al. 2007). Thus, the initial subsidence rate in the Ukinrek East Maar has been much higher than that evaluated from the Kleinsaubernitz subsidence curve (Suhr et al. 2006). However, it has to be realized that the diatreme of Ukinrek East Maar is much smaller in diameter (c. 208 m E-W) and an assumed depth (c. 700 m at a diatreme wall angle of c. 82°) than that of Kleinsaubernitz (c. 1700 m in diameter). Thus, the subsidence curve for Kleinsaubernitz, in all probability, can not be representative for its initial subsidence rate.

It is conceivable, however, that the rate of initial subsidence of a diatreme fill will be controlled predominantly by compaction of the unconsolidated fill, whereas alteration processes will join slightly later and change the subsidence rate, either enhance it or slow it down. Cementation will ultimately lead to an end to compaction and subsidence. Thus, the subsidence curve determined at the Oligocene Kleinsaubernitz maar-diatreme volcano from data in Miocene and Quaternary times probably will have followed a compaction influenced at those time intervals by different proportions of the various diagenetic processes than happened during the initial post-eruptive subsidence.

Subsidence effects on the crater fill: After phreatomagmatic eruptions have ended and were not followed by magmatic activities in the crater, mostly pelitic lake deposits will accumulate, that mostly have a small sedimentation rate. The beds are interbedded with turbidites sourced in the crater walls and also in a later delta fan. In this confined depot centre turbidites have the capacity to result repeatedly in an almost horizontal crater floor. The finely-bedded, unconsolidated and water-saturated sediments react to subsidence of the underlying diatreme fill by subsiding with the diatreme fill and compacting on their own - since the time of their

deposition. As the maar crater has been cut back outwards into the country rocks only those lake beds overlying the area inside the ring-fault of the diatreme can subside, as happened, e.g., at the Messel diatreme near Frankfurt. Thus, the diatreme ring-fault is propagated upwards into the lake beds. The lake beds occurring laterally outside the underlying ring-fault can only go through their own diagenesis. The decrease in diameter of the cone-shaped diatreme downwards results in deformation of the lake beds into a bowl-shaped structure and marginal ring-folds, as, e.g., the lake beds of the Eocene Messel maar-diatreme and of the Oligocene Baruth maar-diatreme show (Suhr et al. 2006).

On the floor of Marteles Maar on Gran Canaria the ring-fault surrounding the underlying diatreme and, because of compaction of the diatreme fill, assumed to have been propagated upward has resulted in an arcuate-shaped fissure that repeatedly opens up (Schmincke and Sumita 2010). The arcuate fissure clearly demonstrates that tensional stress during subsidence allows the opening of arcuate ring-shaped fissures on the ring-fault that could be used at depth by dykes during late intrusions into the diatreme.

References

- Lorenz, V., Kurszlaukis, S. 2007. Root zone processes in the phreatomagmatic pipe emplacement model and consequences for the evolution of maar-diatreme volcanoes. *Journal of Volcanology and Geothermal Research* 150: 4-32.
- Luhr, J.F., Simkin, T., eds. 1993. Parícutin. The volcano born in a Mexican cornfield. 427 pp., Geoscience Press, Phoenix, Arizona.
- Pirring, M., Büchel, G., Lorenz, V., Treutler, H.-C. 2008. Post-eruptive development of the Ukinrek East Maar since its eruption in 1977 A.D. in the periglacial area of south-west Alaska. *Sedimentology* 55: 305-334 DOI: 10.1111/j.1365 3091.2007.00900.x.
- Schmincke, H.-U., Sumita, M. 2010. Geological evolution of the Canary Islands. 196 pp., Görres Verlag; Koblenz, Neuwied, Germany.
- Suhr, P., Goth, K., Lorenz, V., Suhr, S. 2006. Long lasting subsidence and deformation in and above maar-diatreme volcanoes - a never ending story. *Zeitschrift der deutschen Gesellschaft der Geowissenschaften* 157: 491-511.
- White, J.D.L., Ross, P.-S. 2011. Maar-diatreme volcanoes: a review. *Journal of Volcanology and Geothermal Research* 201: 1-29.

Insights on behaviour of granular flows from field analysis and laboratory experiments

Roberto Sulpizio¹, Damiano Sarocchi², Roberto Bartali² and Luis Ángel Rodríguez-Sedano²

¹ CIRISIVU, c/o Dipartimento Geomineralogico, Bari, Italy – r.sulpizio@geomin.uniba.it

² Instituto de Geología, UASLP, San Luis Potosí, Mexico

Keywords: pyroclastic density current, pyroclastic flow, pyroclastic surge.

Gravity-driven flows in volcanic areas comprise some of the most complex and hazardous natural phenomena, and can occur either during explosive eruptions or during volcanic quiescence. Among volcanic gravity-driven flows the study of those characterised by high-particle concentration is exceedingly important, since they encompass some of the most destructive volcanic phenomena. In all these phenomena the same basic forces govern motion, but differing mixture compositions, initial and boundary conditions yield varied dynamics and deposits. Examples range from dry rock avalanches, in which pore fluid may play a negligible role, to liquid-saturated debris flows and gas-charged pyroclastic density currents, in which fluids may enhance bulk mobility. Field studies on real volcanic gravity-driven deposits remain an irreplaceable tool for obtaining crucial information about their

behaviour. This is because a volcanic gravity-driven deposit records the physical processes that occurred at time of deposition, and particle morphology and deposit texture can yield precious information about transportation regime. New insights on behaviour of granular flows come from combining field study on texture of block and ash flows, particle shapes and laboratory experiments carried out using a 3.5 m flume engineered at the Instituto de Geología. The flume is equipped with different sets of sensors and the spreading area is bordered with glassy walls in order to observe the deposit aggradation. The experimental runs are carried out using real volcanic particles combined to form synthetic grain size distributions. First results highlight some fundamental processes in particle transportation and deposit aggradation that are compared with real deposits.

Cetate Breccia, Roşia Montana, Romania – a Dacite Related Au-Ag Mineralized Maar-Diatreme Structure

Călin G. Tămaş¹ and Adrian Minuţ²

¹ University Babeş-Bolyai, Department of Geology, Cluj-Napoca, Romania – calingtamas@yahoo.fr

² Roşia Montana Gold Corporation (RMGC), 321, Piaţa Str., Roşia Montana, Alba County, Romania

Keywords: Au-Ag ores, phreatomagmatic diatreme, Roşia Montana.

Roşia Montana is a world class Au-Ag deposit (Manske et al., 2006) situated in the Apuseni Mts., Romania. The ore bodies are hosted by Neogene dacite and related vent breccia as well as Cretaceous rocks (flysch). Roşia Montana represents the north-western part of a NW–SE trending extensional basin (Roşia Montana–Bucium), which, together with Stănişia–Zlatna and Brad–Săcărâmb basins, host the majority of Neogene volcanic rocks and the related Au-Ag and Cu ore deposits located in the southern part of the Apuseni Mts.

The volcanic activity from Roşia Montana started with the emplacement of Cetate dacite (13.5 ± 1.1 Ma) and continued with the Rotunda andesite (9.3 ± 0.47 Ma) (Pécskay et al., 1995; Roşu et al., 1997). An important phreatomagmatic activity took place before, during and after the emplacement of Cetate dacite.

Roşia Montana is a low- to intermediate sulfidation deposit (Mârza et al., 1997; Leary et al., 2004; Tămaş et al., 2006). The ore bodies are represented by veins, breccias, impregnations, stockworks, and paleoplacers. Several genetic types of mineralized breccias have been identified (Tămaş, 2002; Minuţ et al., 2004; Tămaş, 2007): phreatomagmatic (Cetate Breccia, Black Breccia, Corhuri Breccia, Găuri Breccia, Piatra Corbului Breccia, Căntăleşte Breccia etc.), phreatic (many breccia bodies all around the deposit) and tectonic (Zeus Breccia from Cetate massif).

Roşia Montana is a breccia pipe hosted epithermal Au-Ag deposit (Tămaş, 2002). Cetate breccia, a phreatomagmatic breccia reworked by several phreatic brecciation events represents the most important ore body. This breccia structure was mined at surface and in the underground since Roman times.

Glamm Formation (Mârza et al., 1990, Tămaş, 2002), or Black Breccia (Leary et al., 2004) is a matrix dominated breccia body closely related to Cetate breccia. This breccia is regarded by Leary et al. (2004) as an independent structure, postdating the Cetate Breccia, while Tămaş (2002) considered the Black Breccia as a particular facies of the Cetate Breccia, *i.e.* the fluidization channel of the Cetate phreatomagmatic breccia body (Fig. 1). The late mineral timing of brecciation for Black Breccia in

respect with Au-Ag mineralization is proved by the presence of ore fragments and an undisturbed vein swarm of Mn-bearing gangue minerals hosted in its central-western part. The close spatial relationship among rock fragments with different origin and their position within the breccia body (e.g. metamorphic fragments from depth and wood fragments from the surface) indicates the setup of fluidization (*sensu* Lorenz, 1975) during the phreatomagmatic evolution of Black Breccia.

As concerns the relationships between the Black Breccia and the Cetate Breccia, there is no sharp or irregular contact between them, but a gradual transition marked by color change, matrix grain size, as well as rock fragments (frequency, size, shape, composition) and open spaces (frequency, size).

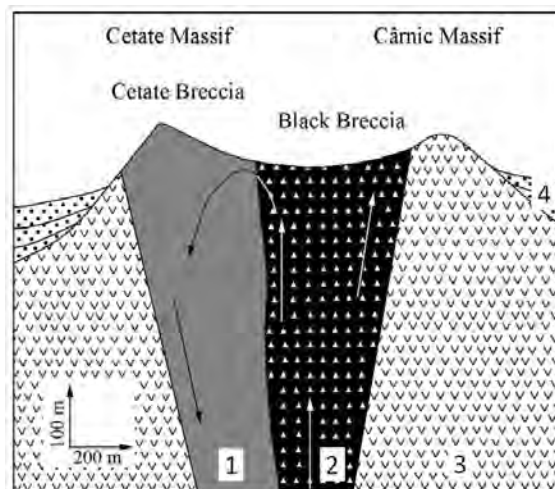


Fig. 1 - Simplified model of the Cetate phreatomagmatic breccia pipe genesis with non-axial position of the fluidization channel (Black Breccia), respectively the set up of a fluidization cell (from Tămaş, 2002). Legend: 1 – Cetate Breccia (*sensu stricto*, Leary et al., 2004); 2 – Black Breccia; 3 – Cetate dacite; 4 – vent breccia; arrows – transport direction within Cetate Breccia (*sensu lato*, Tămaş, 2002).

Within the Cetate Breccia body and the dacite host rock several genetic types of mineralization and corresponding mineral assemblages were identified (Tămaş, 2002 and 2007; Ciobanu et al., 2004). The mineralogy of the ore hosted by the Cetate Breccia is dominated by pyrite, electrum, chalcopyrite,

galena, sphalerite, tetrahedrite, acanthite, quartz, K-feldspar (adularia), and minor tellurides.

The mineralization styles identified within Cetate and Black breccias as well as within dacite host rock are listed below:

- quartz-adularia stockwork veining (dacite host rock), with pyrite-electrum and sphalerite-electrum associations and mineral assemblage consisting of quartz, pyrite, sphalerite, marcasite, chalcopyrite, galena, electrum, achantite, Ag bearing tetrahedrite-tennantite;
- milky quartz veins with common sulphides (Cetate Breccia), with quartz, pyrite, sphalerite, galena, chalcopyrite, tetrahedrite, tennantite;
- fissures and open spaces filled with amethyst (Cetate Breccia), with pyrite-electrum and quartz amethyst-electrum association and a mineral assemblage composed of quartz amethyst, pyrite, electrum;
- clast-supported breccias (Cetate Breccia), with galena-electrum association and the following mineral assemblage: calcite, pyrite, galena, sphalerite, electrum;
- phreatic breccias (Cetate Breccia), with sphalerite-electrum association and a mineral assemblage represented by carbonates, sphalerite, galena, pyrite, electrum;
- veins with Mn-gangue minerals (Black Breccia), with galena-chalcopyrite-electrum, hessite-electrum-sphalerite, and quartz-electrum associations and a mineral assemblage consisting of quartz, rhodochrosite, rhodonite, sphalerite, galena, chalcopyrite, hessite, cervelleite, petzite, electrum.

Acknowledgements

Thanks are addressed to Roşia Montana Gold Corporation for continuous field support and financial assistance.

References

- Ciobanu, C.L., Cook, N.J., Tămaş, C., Leary, S., Manske, S., O'Connor, G., Minuţ, A. 2004. Telluride-gold-base metal associations at Roşia Montană: the role of hessite as gold carrier. In: Cook, N.J., Ciobanu, C.L. (eds): Gold-silver-telluride deposits of the Golden Quadrilateral, South Apuseni Mts., Romania: guidebook of the International Field Workshop of IGCP project 486, Alba Iulia, August-September 2004. IAGOD Guidebook Series 12: 187–202.
- Leary, S., O'Connor, G., Minuţ, A., Tămaş, C., Manske, S., Howie, K. 2004. The Roşia Montană deposit, In Cook, N. J., Ciobanu, C.L. (eds.): Gold-silver-telluride deposits of the Golden Quadrilateral, South Apuseni Mts., Romania: guidebook of the International Field Workshop of IGCP project 486, Alba Iulia, Romania, 31st August - 7th September 2004. IAGOD Guidebook Series 12: 89–98.
- Lorenz, V. 1975. Formation of phreatomagmatic maar-diatreme volcanoes and its relevance to kimberlite diatremes. *Physics and Chemistry of the Earth* 9: 17–27.
- Manske, S.L., Hedenquist, J.W., O'Connor, G., Tămaş, C., Cauuet, B., Leary, S., Minuţ, A. 2006. Roşia Montană, Romania: Europe's largest gold deposit. *Society of Economic Geologists Newsletter* 64 (1): 9–15.
- Mârza, I., Ghergari, L., Nicolescu, Şt., Avram, R. 1990. Petrographical and mineralogical study of the Roşia Montană gold-silver ore deposit (Cetate Massif), Alba County. Unpublished Report, E.M. Roşia Montană Archives, 42 p (in Romanian).
- Mârza, I., Tămaş, C., Ghergari, L. 1997. Low sulfidation epithermal gold deposits from Roşia Montană, Metaliferi Mountains, Romania. *Studii şi Cercetări de Geologie* 42: 3–12.
- Minuţ, A., Leary, S., Szentesy, C., O'Connor, G. 2004. A new style of mineralization identified at Roşia Montană. *Romanian Journal of Mineral Deposits*, 81, Special Issue ("Fourth National Symposium of Economic Geology – Gold in Metaliferi Mountains", 3–5 September 2004, Alba Iulia, Romania): 147–148.
- Pécskay, Z., Edelstein, O., Seghedi, I., Szakács, A., Kovacs, M., Crihan, M., Bernard, A. 1995. K–Ar datings of Neogene–Quaternary calc-alkaline volcanic rocks in Romania. *Acta Vulcanologica* 7: 53–61.
- Roşu, E., Pécskay, Z., Stefan, A., Popescu, G., Panaiotu, C., Panaiotu, C.E. 1997. The evolution of the Neogene volcanism in the Apuseni Mountains (Romania): constraints from new K–Ar data. *Geologica Carpathica* 48: 353–359.
- Tămaş, C.G. 2002. Breccia pipe structures associated to some hydrothermal ore deposits from Romania. Structuri de "breccia pipe" asociate unor zăcămintele hidrotermale din România. Ph.D. thesis, Babeş-Bolyai Univ., Cluj-Napoca, Romania, 336 p. (in Romanian).
- Tămaş, C.G. 2007. Endogene breccia structures (breccia pipe – breccia dyke) and the petrometallogeny of Roşia Montană ore deposit (Metaliferous Mountains, Romania). Cluj-Napoca: Casa Cărţii de Ştiinţă, 230 p. (in Romanian).
- Tămaş, C.G., Bailly, L., Ghergari, L., O'Connor, G., Minuţ, A. 2006. New occurrence of tellurides and argyrodite at Roşia Montană, Apuseni Mountains, Romania and their metallogenetic significance. *Canadian Mineralogist* 44/2: 689–705.

Understanding the dynamics of complex magma-water interaction of a system with alternating magmatic and phreatomagmatic eruption styles, Mt. Gambier, Australia

Jozua van Otterloo and Ray Cas

MONVOLC, School of Geosciences, Monash University, Clayton, VIC 3800, Australia – jozua.vanotterloo@monash.edu

Keywords: alternating eruption styles, magma-water interaction, aquifer dynamics

The relationship between the dynamics of the magmatic and the hydrological systems during magma-water interaction are still poorly understood. Ratios of magma:water mass interaction of 3:1 (pure water) and less (“dirty” water or slush) have been determined experimentally and mathematically (Wohletz, 1983). The model of magmatic fuel-coolant interaction (MFCI) has been adopted to explain hydrovolcanic processes. However, how the water and the magma reach each other and how the occurrence or prevention of phreatomagmatic activity depends on the dynamics of both the magmatic and the hydrological systems, is still an unknown quantitatively.

The monogenetic Mount Gambier Volcanic Complex (5 ka) is located in the western part of the intraplate basaltic Newer Volcanics Province of south-eastern Australia (4.6 Ma-Recent). This volcanic complex overlies thick carbonate and siliciclastic deposits of the Otway Basin, which was formed during the break-up between Australia and Antarctica 90 Ma. It has a complex structure of multiple craters of maars and explosively excavated cones, which are aligned WNW-ESE parallel to the major Tartwaup Fault System.



Fig. 1 – View over the Blue Lake of Mt. Gambier, the eastern most maar of this volcanic complex. The rim consists of the Gambier limestone at the base overlain by massive basalt, scoriaceous tuff and lapilli and ash deposits. The lake itself is fed from the two aquifers.

The stratigraphy of Mount Gambier shows deposits of multiple alternating phreatomagmatic and magmatic eruption styles. Multiple eruption points (>12) have been identified using detailed mapping and sedimentary and stratigraphic relationships. The eruption points appear to have been active in a random manner (i.e. no migration of eruption points from one side to the other of the complex) and over a very brief period of time (i.e. days to months, possibly years).

The different magmatic facies found are massive coherent basalt associated with effusive activity, spatter and fluidal shaped bombs from Hawaiian-style fire-fountaining, and scoria and scoria with coarse ash from Strombolian activity. Phreatomagmatic facies are cross-bedded ash-rich deposits associated with base surges and massive block, ash and lapilli deposits interpreted as pyroclastic flow deposits. Transitional magmatic-phreatomagmatic facies occur as bedded scoriaceous tuff; these have been classified as violent Strombolian.

These deposits were analyzed in great detail using petrographic studies, electron microprobe analysis (EMPA), back-scattered SEM imaging and Fourier Transform IR spectroscopy (FTIR) to constrain the magmatic system and its variables. A detailed magmatic model can be built from this including the pre-eruptive ascent rates, temperatures, volatile contents and viscosities, syn-eruptive degassing, quenching, fragmentation and crystallization, and post-eruptive deposition. However, based on stratigraphic evidence these variables do neither change significantly over time during the eruption, nor does a great variation exist of these parameters between the different magmatic and phreatomagmatic deposits. This indicates that external factors mainly controlled the volcanic system.

The phreatomagmatic deposits, however, are characterized by a large fraction of accessory lithics of limestone, sandstone and to a lesser extent clay. These lithics correspond to the two main lithostratigraphic units of the Gambier Limestone (carbonates) and the Dilwyn Formation (sandstone and clay). These two units also hold the two main

aquifers: the confined Tertiary Sandstone Aquifer and the unconfined Tertiary Limestone Aquifer. Hence these lithics show the evidence that both aquifers interacted with the rising magma at some stage during the eruption.

Within the deposits of single eruption points a deepening trend can be found based on the ratio limestone:sandstone which decreases from bottom to top in the stratigraphy. Knowing that the limestone is shallower than the sandstone, it can be determined that first mainly the unconfined limestone aquifer interacted with the magma followed by the confined sandstone aquifer. This happened repeatedly at different eruption points in the volcanic complex.



Fig. 2 – The remains of the scoria cone which was excavated during the later stage phreatomagmatic activity. The section shows the stratigraphy and all the different facies in a spectacular way.

Also these accessory lithics can be used to determine the efficiency of fragmentation of the country rock during the explosions, as well as giving insights in the aquifer characteristics at the depths of the deepening eruption foci. These parameters can then be used, along with the magmatic variables, as input data for a numerical model. This model then will provide new insights how the characteristics of the rising magma, mainly ascent rate, temperature and viscosity, relate to the permeability and recharge rate of the interacting aquifers. When the recharge rate is high enough, the aquifer will not be depleted and phreatomagmatic activity will continue. However if the recharge rate is low and the magma rise rate is high, drying of the aquifer might prevent phreatomagmatic activity to occur. In the latter case the eruption style will be magmatically controlled.

Such modeling provides new insights; however, it is not the Holy Grail. Limitations to this kind of modeling exist in the actual understanding of the mixing of magma and water and how the surface area of magma-water contact relates to the intensity of phreatomagmatic activity. This should be resolved using different models, both numerical and analogue.

References

- Wohletz, K.H. 1983. Mechanisms of hydrovolcanic pyroclast formation: grain-size, scanning electron microscopy, and experimental studies. *Journal of Volcanology and Geothermal Research* 17: 31-63.

Cinder cone fields associated with warm-slab subduction zones: Magma generation and shallow volcanic processes in the Cascades and Central Mexico as revealed by melt inclusions and experimental phase equilibria

Paul Wallace¹, Dan Ruscitto^{1,2}, Stephanie Weaver¹, Emily Johnson¹, Rachel Weber¹, Dana Johnston¹ and Katharine Cashman¹

¹ Dept. of Geological Sciences, University of Oregon, Eugene, OR 97403, USA – pwallace@uoregon.edu

² Earth and Environmental Sciences, Rensselaer Polytechnic Institute, Troy NY 12180, USA

Keywords: cinder cone, mantle melting, volatiles.

Mafic cinder cones are common in both the Cascades and the Trans-Mexican Volcanic Belt (TMVB). They are spatially associated, to varying degrees, with intermediate-sized, steep-sided shield volcanoes and larger stratovolcanoes. In both of these continental margin arcs, the abundance of cinder cones appears to be caused by extensional stress in the crust. Within each arc, regions of greater extension contain more abundant cinder cones.

Both the Cascades and TMVB are associated with subduction of relatively young oceanic lithosphere (6-9 Ma and 11-18 Ma, respectively). The Cascades, in particular, is nearly a global endmember in terms of the young subducted plate age. Recent geodynamic modeling suggests that subduction of such young oceanic crust results in relatively shallow dehydration of the plate beneath the forearc rather than the arc because the plate is already relatively hot when it enters the trench. A predicted consequence of this is that the magmas in the arc are expected to be relatively poor in H₂O compared to magmas produced in subduction zones where the subducted plate is much older. An assessment of what controls the H₂O contents of mafic magmas in different arcs is thus useful because the H₂O content of magmas affects the depths at which they stall and crystallize as well as eruption explosivity and tephra production.

Our studies of melt inclusions from basalt and basaltic andesite tephra from a number of cinder cones in the Cascades and TMVB show, surprisingly, that H₂O contents are largely within the range of values found in arcs worldwide, many of which have much older subducted plate ages. A compilation of data for 114 primitive arc magma compositions from melt inclusion and whole rock analyses from 16 arcs shows a global average primitive magma H₂O content of 3.3 ± 1.2 wt.% (1 s.d.) for magmas erupted within 50 km of the volcanic front (Ruscitto et al., in review). Mafic magmas in the Cascades have H₂O contents from

1.3-4.0 wt.% (Ruscitto et al., 2010), lower on average than the other arcs, but with considerable overlap, consistent with the expected effects of the young subducted plate age. Mafic magmas in the central TMVB have higher H₂O contents (mostly 3.0-5.5 wt.%), comparable to the global average (Johnson et al., 2009). Lower values in the TMVB are found in transitional to alkalic basalts (1.0-1.5 wt.%), which become increasingly common farther behind the volcanic front (Cervantes et al., 2003; Johnson et al., 2009). Data from the Cascades and TMVB thus show that fluxing of a hydrous component from the subducted plate is occurring beneath the zone of magma generation in the mantle, despite predictions based on the young subducted plate age.

A recently proposed slab surface geothermometer makes it possible to use the H₂O/Ce ratios of arc magmas to estimate slab temperatures beneath the arc (Plank et al., 2009). The thermometer is based on experimental data showing that the trace element concentrations of fluids and hydrous melts released from the slab increase strongly with slab temperature whereas the H₂O contents of the hydrous phase decrease. Application of this method to the global dataset for arc magmas shows a strong correlation of H₂O/Ce temperatures to those predicted by geodynamic models (Cooper et al., in review; Ruscitto et al., in review). In the case of the Cascades and TMVB, this correspondence provides strong evidence that mafic magmas erupted from cinder cones have an origin in the convecting asthenospheric mantle and that the transport of hydrous components from the slab to the mantle wedge is largely vertical rather than being deflected by mantle wedge corner flow.

Experimental phase equilibria for primitive mafic magmas from the TMVB with H₂O contents constrained by our melt inclusion data provide information on depths of melting within the mantle wedge (Weaver et al., 2011; Weber et al., in press). An important result from these studies is that

primitive melts record final equilibration with the mantle at pressures just below the base of the crust at temperatures that are above those predicted by steady-state geodynamic models. A likely explanation for this is that melts extracted from the “hot nose” of the mantle wedge ascend upward, advecting heat and raising mantle isotherms, such that the uppermost mantle is unusually hot beneath the arc. Our experimental studies further show that melts reequilibrate with the shallow mantle during this process. The reequilibration creates a spectrum of primitive melts from basalt to basaltic andesite to even andesite in composition depending on the proportions of lherzolite (which produces basaltic melts) and refractory harzburgite (which produces more SiO₂-rich melts) in the uppermost mantle.

Melt inclusions in olivine phenocrysts in mafic magmas from cinder cones in the Cascades and TMVB record trapping and crystallization pressures in the upper to middle crust (≤ 4 kbar) (Johnson et al., 2010; Ruscitto et al., 2010). The values are similar in primitive compositions, which crystallize olivine with Fo \geq 88, and slightly evolved compositions, with Fo₈₂₋₈₅ olivine, despite the fact that the former must have transited the lower crust with minimal cooling and crystallization, whereas the latter must have stalled in the lower crust and undergone differentiation. Relations between major element compositions and dissolved H₂O in the melt inclusions suggest that upper to middle crustal crystallization is driven by degassing of H₂O.

In some of the longer lived cinder cone eruptions in Mexico (e.g., Jorullo, Paricutin), melt inclusions from later stages of the eruption record very low trapping pressures and extensive degassing (Johnson et al., 2008). This suggests that a shallow storage reservoir or enlarged portion of the feeding dike formed during the course of the eruption, leading to longer magma residence times later in the eruption. We do not find any evidence of this evolutionary pattern in the Cascade cinder cones despite many other similarities. Most of the cinder cones we have studied produced violent Strombolian eruptions, leading to widespread tephra deposition. The more H₂O-poor types (alkali basalt in Mexico, low-K tholeiite in the Cascades) were usually less explosive. These patterns suggest a major role for magmatic volatiles in driving the explosive eruptions. Evidence for phreatomagmatic eruptions is found mainly in areas where a role for shallow groundwater is likely. One maar in the Oregon Cascades (Blue Lake) has melt inclusion compositions and volatile contents that are similar to many of the cinder cones, attesting to similar depths

of shallow crystallization and degassing before eruption. Maars in the northernmost central TMVB erupted alkali basalts, some of which are megacryst bearing. The olivine megacrysts contain melt inclusions with low H₂O but high CO₂ extending up to 6000 ppm, suggesting middle to lower crustal crystallization pressures.

References

- Cervantes, P., Wallace, P. 2003. The role of water in subduction zone magmatism: New insights from melt inclusions in high-Mg basalts from central Mexico. *Geology* 31: 235-238.
- Cooper, L.B., Ruscitto, D., Plank, T., Wallace, P.J., Syracuse, E., Manning, C. in review. Global variations in H₂O/Ce, I: Slab surface temperatures beneath volcanic arcs. *Geochemistry, Geophysics, Geosystems*.
- Johnson, E., Wallace, P., Cashman, K., Delgado Granados, H., Kent, A.J.R. 2008. Magmatic volatile contents and degassing-induced crystallization at Jorullo Volcano, Mexico: Implications for the plumbing systems of monogenetic volcanoes. *Earth and Planetary Science Letters* 269: 477-486.
- Johnson, E.R., Wallace, P.J., Delgado Granados, H., Manea, V.C., Kent, A.J.R., Bindeman, I. 2009. The origin of H₂O-rich subduction components beneath the Michoacán-Guanajuato Volcanic Field, Mexico: insights from magmatic volatile contents, oxygen isotopes, and 2-D thermal models for the subducted slab and mantle wedge. *Journal of Petrology* 50: 1729-1764.
- Johnson, E.R., Wallace, P.J., Cashman, K.V., Delgado Granados, H. 2010. Degassing of volatiles (H₂O, CO₂, S, Cl) during ascent, crystallization, and eruption of basaltic magmas at mafic monogenetic volcanoes in central Mexico. *Journal of Volcanology and Geothermal Research* 197: 225-238.
- Plank, T., Cooper, L.B., Manning, C.E. 2009. Emerging geothermometers for estimating slab surface temperatures. *Nature Geoscience*. DOI: 10.1038/NGEO614.
- Ruscitto, D.M., Johnson, E., Wallace, P.J., Kent, A.J.R., Bindeman, I.N. 2010. Volatile contents of mafic magmas from cinder cones in the Central Oregon High Cascades: Implications for magma formation and mantle conditions in a hot arc. *Earth and Planetary Science Letters* 298: 153-161.
- Ruscitto, D., Wallace, P.J., Cooper, L.B., Plank, T. in review. Global variations in H₂O/Ce, II: Relationships to arc magma geochemistry and volatile fluxes. *Geochemistry, Geophysics, Geosystems*.
- Weber, R.M., Wallace, P.J., Johnston, A.D. 2011. Experimental insights into the formation of high-Mg basaltic andesites in the Trans-Mexican Volcanic Belt. *Contributions to Mineralogy and Petrology*, in press.

The impact of drainage basin dynamics on volcanic activity style: a detailed Ar-Ar dating of a dry-wet transition

Yishai Weinstein¹, Ram Weinberger² and Andrew Calvert³

¹ Department of Geography and Environment, Bar-Ilan University, Ramat-Gan, 52900 Israel – weinsty@biu.ac.il

² The Geological Survey of Israel, 30 Malkei Israel st., Jerusalem, Israel

³ Volcano Science Center, U.S. Geological Survey, 345 Middlefield Road, Menlo Park, CA 94025, USA

Keywords: phreatomagmatic eruption, tuff ring, lava flow, Ar-Ar chronology

We present a high resolution Ar-Ar age determination of a change in a northern Golan drainage basin and of the consequential shift from strombolian to phreatomagmatic activity in a nearby eruption site. The volcanic landscape of the northern Golan is dominated by scoria cones and lava flows, while phreatomagmatic (hydrovolcanic) deposits are rare. This is probably because the regional water table is usually very deep in this area (200-300 m below surface). The tuff ring of Mt. Avital is an exception to this rule, indicative of a dry-wet transition and of the interaction of shallow/surface water and magma. The nearby poorly-drained Quneitra Valley, with its depocenter just 20 m lower than the tuff ring center and the evidence for the existence of a Late Pleistocene lake in this valley suggest that this could be the source of surface water and the cause of the shift to phreatomagmatic eruption style. It was previously suggested that the lake was created as a result of the damming of a local creek by a lava flow originated a few km to the north of Mt. Avital. However, K-Ar ages implied no synchronicity between this flow and the phreatomagmatic shift.

We present here a set of Ar-Ar ages taken on holocrystalline samples representing different volcanic phases in the history of Mt. Avital as well as that of the damming flow. It was found that the history of Mt. Avital includes two main periods of volcanic activity, at ca. 700 and 110±10 ka. It was further found that most of the 2nd stage activity was continuous (within the Ar-Ar error), including the change to phreatomagmatic explosions, which occurred at 111±4 ka. More interestingly, the damming flow was found to be 115.6±3.1 ka, which suggests that the volcanic activity immediately reacted to the change in local drainage basin. Finally, shortly afterwards (100±4 ka), volcanic activity restored to a dry, lava flow eruption, probably due to the establishment of the tuff ring levees and to the probable decline in lake water level.

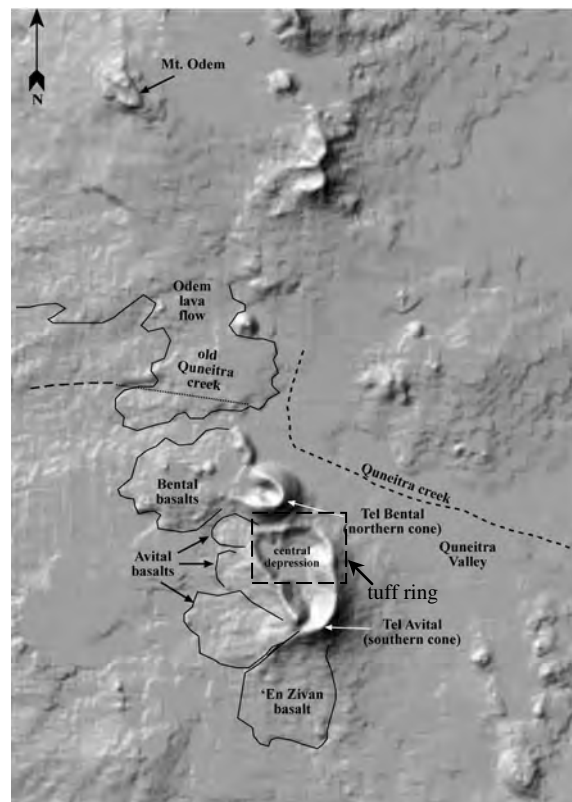


Fig. 1 - A DTM (Digitized Terrain Model) image of the northern Golan, showing the tuff ring of Mt. Avital and the damming Odem lava flow that dammed the old Quneitra creek.

References

- Mor, D. 1973. The volcanism of the central Golan Heights. M.S. thesis, The Hebrew University of Jerusalem, 179 pp. (in Hebrew).
- Weinstein, Y. 2007. A transition from strombolian to phreatomagmatic activity induced by a lava flow damming water in a valley. *Journal of Volcanology and Geothermal Research* 159: 267-284.
- Weinstein, Y., Weinberger, R. 2006. The geology and volcanological history of Mount Avital. *Israel Journal of Earth Sciences* 55: 237-255.

Fragments within fragments: are composite pyroclasts hints of weakness or sustained violence?

James D.L. White

Department of Geology, University of Otago, P.O. Box 56, Dunedin, New Zealand – james.white@otago.ac.nz

Keywords: pyroclast recycling, magma mingling, maar, diatreme, phreatomagmatism

Bombs and lapilli containing or consisting of smaller fragments are composite clasts, and are produced in many mafic eruptions. They have been attributed to accretion of highly fluid pyroclasts in gas suspensions of either conduits (Stoppa and Principe, 1998) or plumes (Carracedo-Sanchez et al., 2009), to hot-state recycling of pyroclasts in conduits characterized by episodic phreatomagmatic fragmentation (White, 1991; Ross and White, 2006), and to formation by depositional amalgamation as they roll down the flanks of pyroclastic cones (Heiken, 1978). It is important to distinguish composite clasts formed within sustained eruption columns from those formed by episodic explosions or depositional amalgamation because the hazard and depositional footprint of the former is much larger.

Bombs of nephelinitic composition inferred to form in gas-rich systems are believed to grow by particle collisions under thermal conditions that allow surface-tension reshaping. The picture is of a highly energetic process sustained to allow assembly of bombs while immersed in a gas jet. The jet is also considered to elutriate, rather than accrete, fine ash, because pyroclasts within the bombs are commonly lapilli rather than ash, and pore space remains open between the fragments assembled in the bombs. Suspension of a 20 cm bomb in gas-rich particle-poor conduit flow or in gas-thrust regions of plumes requires sustained velocities approximating 200 m/s, velocities associated with "violent Strombolian" eruptions that blanket many tens of square kilometres with decimetres-thick deposits.

Basaltic to nephelinitic bombs formed by discrete explosions in conduits characteristically contain wallrock fragments. The explosions fragment fluid magma and wallrock, but are ineffective in clearing the material from the conduit or vent. Although developed for bombs of inferred phreatomagmatic eruptions, this general mechanism simply requires discrete explosions, not necessarily water-drive ones, and the picture is of a process associated with only limited particle dispersal. Fine fragmentation takes place in some phreatomagmatic explosions, and this fact is sometimes improperly inverted to infer that deposits lacking fine particles



Fig. 1 – Composite, domainal, lapillus of nephelinitic composition containing sandstone and siltstone fragments. From West Standing Rocks diatreme, Hopi Buttes, Arizona.

cannot involve magma-water explosions, even though it is well known that littoral magma-water explosions produce coarse spatter deposits. Such littoral deposits result from relatively weak explosions, of a sort that may be driven by intense but small fuel-coolant interactions that tear apart enclosing magma, or perhaps by less-violent fragmentation with simple vaporization of entrapped water driving the disruption.

Composite fragments from maar-diatreme environments of nephelinitic to basaltic tholeiitic compositions are typically country-rock rich and display a variety of textures, surface features, and styles of assembly. Bombs at Rotomahana incorporated many fragments that show minimal thermal alteration and must have been assembled and cooled over short timescales. Associated with fragmentation zones in Hopi Buttes maar-diatremes, are composite bombs and a variety of clastogenic

lithic-rich coherent rocks, whereas in the Karoo province such composite clasts accompany lithic-rich lava flows.



Fig. 2 – Composite, domainal clast of basalt containing unmelted rhyolite fragments. Rotomahana maar deposits, New Zealand. (See Rosseel et al., 2006)

Composite fragments in the Antarctic Ferrar province are present in pyroclastic flow deposits of substantial extent, but also with locally dispersed layers; plume-fed fall deposits are not significant.



Fig. 3 – Composite, domainal clast of basalt (pale) with swirls of mingled clastic material. Coombs Hills, Antarctica. (See McClintock and White, 2006).

The most consistent feature of reported occurrences of composite clasts is their occurrence in mafic-intermediate to ultramafic cones or maar/diatremes, and not associated with

substantially dispersed fall deposits. The range of magma types and volcanic environments with which composite bombs occur argues against an origin dependent on unusually fluid magmas or extreme eruption conditions. Weak dispersal of fragments formed in discrete explosions allows fallback and amalgamation or re-incorporation into magma of first-generation fragments, re-ejected by subsequent explosions as lapilli or bombs. Where fragmentation also produces wallrock fragments, these are incorporated into the composite fragments.

Acknowledgements

This research was supported by GNS funding, University of Otago research grants, and Antarctica New Zealand.

References

- Carracedo Sánchez, M., Sarrionandia, F., Arostegui, J., Larrondo, E., Ibarguchi, J.I.G. 2009. Development of spheroidal composite bombs by welding of juvenile spinning and isotropic droplets inside a mafic eruption column. *Journal of Volcanology and Geothermal Research* 186(3-4): 265-279.
- Heiken, G. 1978. Characteristics of tephra from Cinder Cone, Lassen National Volcanic Park, California. *Bulletin Volcanologique* 41: 119-130.
- McClintock, M.K., White, J.D.L. 2006. Large phreatomagmatic vent complex at Coombs Hills, Antarctica: Wet, explosive initiation of flood basalt volcanism in the Ferrar-Karoo LIP. *Bulletin of Volcanology* 68: 215-239.
- Ross, P.-S., White, J.D.L. 2006. Debris jets in continental phreatomagmatic volcanoes: A field study of their subterranean deposits in the Coombs Hills vent complex, Antarctica. *Journal of Volcanology and Geothermal Research* 149: 62-84.
- Rosseel, J.B., White, J.D.L., Houghton, B.F. 2006. Complex bombs of phreatomagmatic eruptions: Role of agglomeration and welding in vents of the 1886 Rotomahana eruption, Tarawera, New Zealand. *Journal of Geophysical Research* 111: B12205
- Stoppa, F., Principe, C. 1998. Eruption Style and Petrology Of a New Carbonatitic Suite From the Mt. Vulture (Southern Italy) - the Monticchio Lakes Formation. *Journal of Volcanology and Geothermal Research* 80: 137, 139-153.
- White, J.D.L. 1991. Maar-diatreme phreatomagmatism at Hopi Buttes, Navajo Nation (Arizona), USA. *Bulletin of Volcanology* 53: 239-258.

Pollen analysis of a Late Glacial and Holocene sediment core from Moon Lake, Northeast China

Jing Wu, Qiang Liu, Luo Wang and Guoqiang Chu

Key Laboratory of Cenozoic Geology and Environment, Institute of Geology and Geophysics, Chinese Academy of Sciences, Beijing, China – wujing@mail.iggcas.ac.cn

Keywords: Aershan-Chaihe Volcanic Field, pollen, Late Glacial.

The palaeoclimate research of maar- and crater lakes of the Aershan-Chaihe Volcanic Field (Inner Mongolia, NE China) started several years ago. Two coring were obtained from a crater lake named Moon Lake (Fig.1, 47°30'25"N, 120°52'05"E) for pollen analysis. A sediment profile of 8.86m length was built by overlapping based on coring.

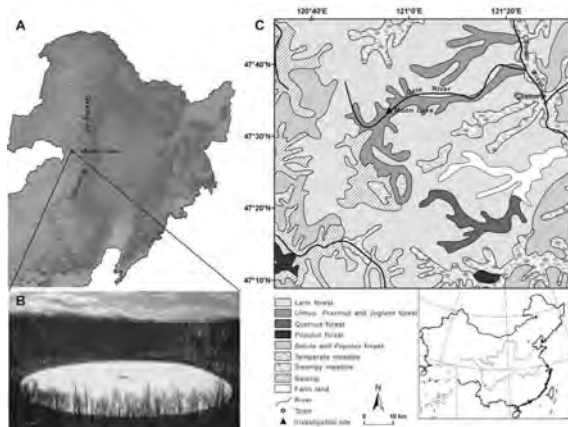


Fig. 1 – (A) Map showing the location of Moon Lake in the Northeast China. (B) Photo of Moon Lake in winter and the forest surrounding it. (C) Figure of the vegetation in study area modified after Zhang (2007).

A depth-age curve in cal. a BP is constructed for the whole sequence based on the 21 AMS ^{14}C dates obtained from Poznan radiocarbon Laboratory, which reveals that the sediment accumulation rate is relatively uniform. The upper end of section under investigation indicated by pollen spectra are at 0.8 cal ka B.P., with the lower end at 20.9 cal ka B.P..

One hundred and twenty-eight pollen taxa were identified from 419 subsamples of Moon Lake. Eleven pollen assemblage zones were recognized based on the characteristic of coniferous, deciduous broad-leaved and herbs percentage and pollen concentration.

The domination of herbs pollen, and the trade-offs of *Artemisia* and Cyperaceae percentages reveal herbs dominate the vegetation composed of *Artemisia*, Cyperaceae and Gramineae with Chenopodiaceae and *Thalictrum*. The extremely low arboreal pollen also infers the vegetation of study

area is steppe under very cold and dry climate from 20.9 to 16.7 cal. ka B.P..

The component of herbs pollen is still dominant, the percentages of *Artemisia* and *Betula* increase synchronously. The expansion of arbor identifies the transition from steppe to forest with tendency to warm and humid climate from 16.7 to 14.0 cal. ka B.P..

The component of arbor pollen increase substantially, but still slightly lower than arbor, *Artemisia* and *Betula* rise and fall with each other. It indicates the up growth of current vegetation community which is dominant by *Larix*, patches of *Betula* mosaic, with herbaceous layer composite of *Artemisia*, Chenopodiaceae and Gramineae from 14.0 to 0.8 cal. ka B.P., implying the warm climate with a very humid beginning and convert to drought.

There is a series of rapid climate change of global events in the Late-glacial, the transition of Last Glacial to Holocene, including Oldest Dryas, Bølling, Older Dryas, Allerød, Younger Dryas equivalents and so on. The characteristic of pollen spectra infer a few of cold and warm climate change events, which the reduction of broadleaf pollen and increasing of herbaceous pollen indicate cold climate, and vice versa when the climate is warm.

The pollen records of Moon Lake display that the cold event from 14.4 to 14.0 cal. ka B.P. may correspond with Oldest Dryas; the warm event from 14.0 to 13.4 cal. ka B.P. corresponded with Bølling; the cold event from 13.4 to 13.2 cal. ka B.P. corresponded with Older Dryas; the warm event from 13.2 to 12.8 cal. ka B.P. corresponded with Allerød; the cold event from 12.8 to 11.8 cal. ka B.P. corresponded with Younger Dryas (Fig. 2). The duration of Oldest Dryas lasts 400a, the Older Dryas only 200a. Generally, the ends of cold events come earlier, the duration is relative short; the beginnings of warm events come later, the duration is relative long.

The stalagmite record of Hulu Cave, located in Nanjing, Southeast China, shows that the rapid transition from Last glacial to Bølling-Allerød occurred in 180a before and after of 14.6 cal. ka B.P.; Bølling-Allerød starts at 14.5 cal. ka B.P., ends at 12.8 cal. ka B.P., which lasted about 1,700a (Wang

et al., 2001). The $\delta^{18}\text{O}$ records of Dongge cave, located in Southwest China, became lighter since 16.0 cal. ka BP implying the gradually increase of the East Asian summer monsoon; the dramatic changes to lighter trends since 14.7 cal ka B.P. marks the beginning of Bølling-Allerød in Greenland, the duration lasts about 1,700a (Dykoski et al., 2005). In this study, the rapid transition of last glacial to Bølling-Allerød begin in 14.3 cal. ka B.P., end in 13.9 cal. ka B.P., which last about 350a. Compared to other studies, the transition begin relatively late and last longer, which maybe cause by the higher latitudes of the study area, or the delay in response of continental boreal vegetation to climate. Bølling-Allerød begin at 13.9 cal. ka B.P. and end at 12.8 cal. ka BP, lasted about 1,100a.

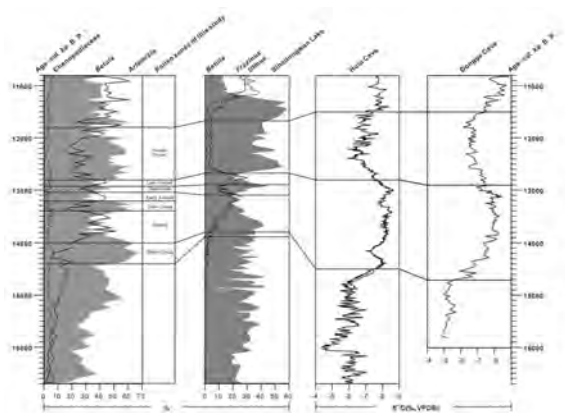


Fig. 2 –Comparison of the Moon Lake pollen record with the palynological record from Sihailongwan (Northeast China; Stebich et al., 2009), Hulu Cave (Southeast China; Wang et al., 2001) and Dongge Cave (Southwest China, Dykoski et al., 2005).

Younger Dryas is the last cold event in the transition from Last glacial to Holocene, which is the most understanding climate event so far. The generally accepted view on the duration of Younger Dryas is 12.9-1.5 cal. ka B.P. lasting about 1,300a, and terminate abruptly (Bond et al., 1997). The stalagmite of Hulu Cave record the beginning of Younger Dryas at 12.8 cal. ka B.P., and the terminate at 11.5 cal. ka B.P. (Wang et al., 2001), that of Dongge hole at 13.0 cal. ka B.P. and 11.5 cal. ka B.P. respectively (Dykoski et al., 2005). In this study the start time of Younger Dryas is 12.8 cal. ka B.P. in the middle part of Daxing'an Mountain Range surrounding Moon Lake, consistent with the

results of Hulu Cave and Dongge Cave, but earlier than that of Sihailongwan Maar Lake which is in the same vegetation belt (Stebich et al., 2009). Younger Dryas in this study has an abrupt termination at 11.8 cal. ka B.P., the end of time earlier, the process rapidly, the duration only 1,000a, consistent with the Younger Dryas duration of 1,000-1,300a resulted from the pollen record of Sihailongwan Maar Lake.

It is obvious that these rapid climate changes recorded by pollen data of Moon Lake have good correspondence with high-resolution records of other regions influenced by East Asian monsoon. All these events are good at synchronization considered the errors of dating, which displays that the climate in the middle part of Daxing'an Mountain Range is closely related with the East Asian Monsoon. The cold events recorded by Moon Lake take place when the East Asian summer monsoon is weak, while the warm events happen when it is strong, thus Moon Lake pollen record reflects sensitively to the strength changes of the East Asian Monsoon.

Acknowledgements

This research was supported by the National Natural Science Foundation of China (40872206) and National Basic Research Program of China (973 Program) (No: 2010CB950201).

References

- Bond, G., Shower, W., Cheseby, M., Lotti, R., Almasi, P., Cullen, H., Hajdas, I., Bonani, G. 1997. A pervasive millennial-scale cycle in North Atlantic Holocene and glacial climates. *Science* 278: 1257-1266.
- Dykoski, C.A., Edwards, R.L., Cheng, H., Yuan, D., Cai, Y., Zhang, M., Lin, Y., Qing, J., An, Z., Revenaugh, J. 2005. A high-resolution, absolute-dated Holocene and deglacial Asian monsoon record from Dongge Cave, China. *Earth and Planetary Science Letters* 233: 71-86.
- Stebich, M., Mingram, J., Han, J., Liu, J. 2009. Late Pleistocene spread of (cool-) temperate forests in Northeast China and climate changes synchronous with the North Atlantic region. *Global and Planetary Change* 65: 56-70.
- Wang, Y.J., Cheng, H., Edwards, R.L., An, Z.S., Wu, J.Y., Shen, C.C., Dorale, J.A. 2001. A high-resolution absolute-dated Late Pleistocene Monsoon record from Hulu cave, China. *Science* 294(14): 2345-2348.
- Zhang X.S., 2007. *The Vegetation Map of the People's Republic of China*. Geography Press: Beijing. (in Chinese.)

History of ash fall events trapped in maar lake sediments

Aleksandra Zawalna-Geer¹, Phil Shane¹, Siwan Davies² and Paul Augustinus¹

¹ School of Environment, The University of Auckland, Private Bag 92019, Auckland, New Zealand - a.geer@auckland.ac.nz

² School of the Environment and Society, Swansea University, Singleton Park, Swansea, SA28PP, UK

Keywords: maar lakes, cryptotephra, reworking

Post-eruptive maar lakes can be excellent repositories for volcanic ash embedded in lacustrine sediment. Maars are the second most common terrestrial volcanoes after scoria cones (Wohletz and Heiken, 1992), formed as a result of phreatomagmatic explosions originating from the contact of the magma or its heat with subsurface or surface water (Schmincke, 1977; Lorenz, 1986). Phreatomagmatic activity forming explosion craters has been recognised at ~35 volcanoes in the Auckland Volcanic Field (AVF), of which many evolved to magmatic activity producing scoria cones (Kermode, 1992; Allen and Smith, 1994). Many post-eruptive maar depressions have been filled up with lacustrine sediments of peats and lakes. However, limited accessibility for drilling equipment or obliteration and erosion resulted from urban expansion has allowed only several of them to be drilled (Pukaki Lagoon, Hopua, Panmure Basin, Orakei Basin, Onepoto and Pupuke Lake) (fig. 1).

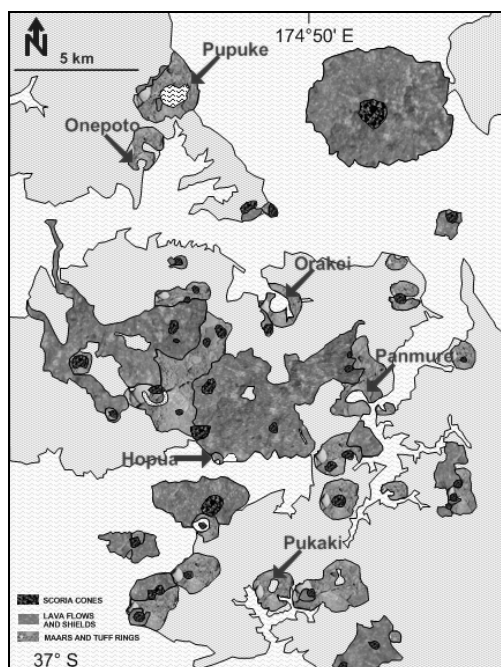


Fig. 1 – Map of the Auckland Volcanic Field, showing maars that have been drilled for tephra studies

Previous studies on tephrochronology of the maar lakes allowed the recognition of ash falls from

distal and local volcanic sources. 24 rhyolitic tephra layers from the Taupo Volcanic Zone and Mayor Island, 58 andesitic ash beds from Egmont and Tongariro Volcanic Centres and 24 basaltic layers were identified and contributed to establish a frequency of ash falls over 80 ka averaging 1 event per 700 yrs (Molloy et al., 2009).

In new studies two cores were obtained from Pupuke and Pukaki maars (fig. 2). The Pukaki core was examined only for visible tephra layers. Despite the fact, that the maar was drilled previously, 29 new tephra layers were identified allowing the re-calculation of ash fall recurrence to 1 per 400 yrs over the last 80 ka.

Some past eruptions are, however, not evident as visible tephra layers in the cores e.g. the eruption of Ruapehu in 1995 that caused the temporary closure of Auckland airport. Crypto-tephra studies may reveal ash falls from past eruptions such as this. The Pupuke core, representing almost the whole Holocene was investigated for discrete crypto-tephra. The core was subsampled at 1cm intervals producing a total of 488 samples. Glass shards were extracted from the sediment, and their concentrations determined microscopically. Shards were then analyzed by electron microprobe to determine volcanic sources and individual eruptive events.

The crypto-tephra record in Pupuke core reveals new ash sequences previously unknown in the Auckland area, from Taupo, Egmont and Tongariro Volcanic Centers and thus our study permits the re-evaluation of the recurrence of ash fall from both local and distal volcanoes in the last 10 ka. The new results indicate that the Auckland region has been affected by ash fall on average every 400 years in the Holocene. Taupo Volcanic Centre is the main contributor to ash falls over the past 10 kyrs. Re-drilling maars within the Auckland Volcanic Field may be valuable for finding new macro-tephra beds in addition to crypto-tephra studies.

Crypto-tephra studies also highlight extensive upward reworking of the glass shards over time periods of 10^2 - 10^3 yrs in a lake with a closed and limited catchment. For some sediment records, cryptotephra could be mostly artifacts of reworking rather than the signal of new ash fall events.



Fig. 2 – Lake Pupuke with the Rangitoto scoria cone and lava flows in the background

Acknowledgements

Many thanks to the DEVORA Project for partly funding this project and to the technicians at the University of Auckland, specifically to Ritchie Sims, who assisted with Electron Microprobe analyses.

References

- Allen, S.R., Smith, I.E.M. 1994. Eruption styles and volcanic hazard in the Auckland volcanic field, New Zealand. *Geoscience Reports - Shizuoka University* 20: 8-14.
- Kermode, L.O. 1992. Geology of the Auckland urban area. Scale 1:50000. Institute of Geological and Nuclear Sciences geological map 2, 1 sheet and 63p. Lower Hutt, New Zealand, Institute of Geological and Nuclear Sciences Ltd.
- Lorenz, V. 1986. On the growth of maars and diatremes and its relevance to the formation of tuff rings. *Bulletin of Volcanology* 48(5): 265-274.
- Molloy, C., Shane, P., Augustinus, P. 2009. Eruption recurrence rates in a basaltic volcanic field based on tephra layers in maar sediments: Implications for hazards in the Auckland volcanic field. *Geological Society of America Bulletin* 121(11-12): 1666-1677.
- Schmincke, H.-U. 1977. Phreatomagische Phasen in quartären Vulkanen des Osterfelds. *Geol. Jahrbuch A-39*: 3-45.
- Wohletz, K., Heiken, G. 1992. Volcanology and geothermal energy.

Eruptibility of Gas-driven Eruptions

Youxue Zhang

Department of Earth and Environmental Sciences, the University of Michigan, Ann Arbor, MI 48109-1005, USA – youxue@umich.edu

Keywords: Explosive eruptions, eruptible fraction, overcoming gravity, MORB.

Magmas erupt due to either gas exsolution that leads to volume expansion forcing an expanded magma to go up (magma can also go sideways, in which case it is not an eruption), or buoyancy because a magma is less dense than the average overlying rock column, or a combination of both. Buoyancy-driven volcanic eruptions are nonexplosive while gas-driven eruptions can be explosive. In order to understand the dynamics of eruptions, it is important to know the factors that contribute the most to an eruption for a given gas-liquid system. Here I investigate the eruptibility of gas-driven eruptions as an end-member process without the help of buoyancy.

The key in whether a gas-containing melt can erupt is whether energy harvested from gas exsolution without the help of buoyancy will be enough. That is, the energy provided by gas-separation and volume expansion is enough to overcome the gravitational energy to lift the melt to the surface.

Consider a thin disk-shaped magma chamber so that the whole chamber can be characterized by a single pressure (i.e., pressure increase with depth inside the chamber is small and can be ignored). Assume mechanical equilibrium between the gas and liquid phases and ignore surface effects so that the pressure in the liquid is the same as that in the gas phase. The conduit is assumed to be completely open (no additional work is needed to open the conduit). If chemical equilibrium between the gas and liquid phases is maintained during eruption (this assumption means the maximum amount of energy can be obtained from the exsolution process), for ideal gas and constant solubility coefficient, the maximum exit velocity (u_{exit}) can be related to other parameters as follows (Wilson 1980; Wilson et al., 1980; Zhang, 1996; 2000, 2004, 2006):

$$\frac{1}{2}u_{\text{exit}}^2 = \frac{1}{\rho_{\text{melt}}}[(1-\lambda)(P_{\text{ch}} - P_{\text{exit}}) + \lambda P_{\text{sat}} \ln \frac{P_{\text{ch}}}{P_{\text{exit}}}] - gz$$

where ρ_{melt} is melt density, λ is the Ostwald solubility (assumed to be independent of pressure), P_{ch} , P_{sat} , and P_{exit} are pressures in the magma

chamber, at saturation, and at the exit (surface), g is acceleration due to Earth's gravity, and z is the depth of the magma chamber. In the above equation, the first term on the right-hand-side is maximum energy available from gas exsolution from an initial pressure of P_{ch} to the final pressure of P_{exit} , and the second term (gz) is the gravitational energy needed to lift a unit mass of magma to the surface.

It is assumed that the initial pressure in the chamber exceeds or equal to the saturation pressure (otherwise, the eruption cannot be purely gas-powered). If feeding of magmas into the chamber is ignored, eruption leads to a decrease of the mass in the magma chamber. Considering the end-member process in which buoyancy does not play any role (the lithosphere does not relax viscously) and ignoring the elastic effect on the magma chamber volume, the volume of the magma chamber is roughly constant. (If a piece of roof rock falls into the chamber, it would not significantly affect the effective chamber volume occupied by the magma because the volume occupied by the rock before falling is now occupied by the magma.) Hence the chamber pressure decreases as eruption goes on. when the chamber pressure becomes low enough, the available energy would not be able to lift magma to the surface. The chamber pressure at which this occurs will be referred to as the critical chamber pressure, below which there would be no eruption. Hence, the fraction of eruptible mass can also be estimated.

Calculations show that when λ value is large, it is easy to drive explosive eruptions. Using relevant parameters for subaerial H₂O-driven volcanic eruptions, subaerial CO₂-driven lake eruptions (Kling et al., 1988), and experimental CO₂-driven eruptions (Mader et al., 1994; Zhang et al., 1997), because of the large λ values, these systems can erupt violently. However, when λ value is smaller than 0.01, such as CO₂ in basaltic melt (Dixon et al., 1995a,b), only a very small fraction of magma can be erupted.

As pointed out by Kieffer (1995), the exit pressure plays a critical role in controlling the exit velocity. It can be shown that it also partially controls the eruptibility. A case of interest is mid-ocean ridge eruptions. Another case of interest is for

eruptions on Venus (9 MPa surface pressure). For mid-ocean ridges, the exit pressure is about 25 MPa. The gas pressure is provided by carbon dioxide. Assume $P_{\text{ch}} = P_{\text{sat}} = 200$ MPa (about 1000 ppm CO_2), the eruptible mass fraction is about 0.005%. Incorporating the nonideality of CO_2 and pressure dependence of λ does not change the results significantly. That means, essentially, CO_2 -saturated basaltic melt is not enough to drive an explosive eruption.

In summary, the eruptibility is largely determined by the solubility coefficient (solubility per unit pressure) of the gas in the liquid and the exit pressure. For H_2O -saturated magmas, energy available from gas exsolution is so large that buoyancy is not necessary and the eruptibility is probably limited by the collapse of the magma chamber that blocks the conduit. However, for submarine eruptions of CO_2 -saturated basaltic magmas, only a minuscule fraction of the total magma mass is eruptible through the rigid lithosphere using power by gas exsolution from the liquid, and 0.024% eruptible for subaerial eruptions. The additional H_2O content in mid-ocean ridge basalt (MORB) is not enough for MORB magma to erupt violently on the ocean floor. Hence it is almost impossible for CO_2 -dominated magmas to erupt violently. The massive eruption of MORB magma is largely driven by buoyancy, instead of gas exsolution.

References

- Dixon, J.E., Stolper, E.M., Holloway, J.R. 1995a. An experimental study of water and carbon dioxide solubilities in mid-ocean ridge basaltic liquids. Part I: calibration and solubility models. *Journal of Petrology* 36: 1607-1631.
- Dixon, J.E., Stolper, E.M. 1995b. An experimental study of water and carbon dioxide solubilities in mid-ocean ridge basaltic liquids. Part II: Applications to degassing. *Journal of Petrology* 36: 1633-1646.
- Kieffer, S.W. 1995. Numerical models of caldera-scale volcanic eruptions on Earth, Venus, and Mars. *Science* 269: 1385-1391.
- Kling, G.W., Clark, M.A., Compton, H.R., Devine, J.D., Evans, W.C., Humphrey, A.M., Koenigsberg, E.J., Lockwood, J.P., Tuttle, M.L., Wagner, G.N. 1987. The 1986 Lake Nyos gas disaster in Cameroon, West Africa. *Science* 236: 169-175.
- Mader, H.M., Zhang, Y., Phillips, J.C., Sparks, R.S.J., Sturtevant, B., Stolper, E.M. 1994. Experimental simulations of explosive degassing of magma. *Nature* 372: 85-88.
- Wilson, L. 1980. Relationships between pressure, volatile content and ejecta velocity in three types of volcanic explosions. *Journal of Volcanology Geothermal Research* 8: 297-313.
- Wilson, L., Sparks, R.S.J., Walker, G.P.L. 1980. Explosive volcanic eruptions—IV. The control of magma properties and conduit geometry on eruption column behavior. *Geophysical Journal of the Royal Astronomical Society* 63: 117-148.
- Zhang, Y. 1996. Dynamics of CO_2 -driven lake eruptions. *Nature* 379: 57-59.
- Zhang, Y. 2000. Energetics of gas-driven limnic and volcanic eruptions. *Journal of Volcanology Geothermal Research* 97: 215-231.
- Zhang, Y. 2004. Dynamics of explosive volcanic and lake eruptions. *Environment, Natural Hazards and Global Tectonics of the Earth* (in Chinese). Higher Education Press, Beijing.
- Zhang, Y., Kling, G.W. 2006. Dynamics of lake eruptions and possible ocean eruptions. *Annual Review of Earth and Planetary Science* 34: 293-324.
- Zhang, Y., Sturtevant, B., Stolper, E.M. 1997. Dynamics of gas-driven eruptions: experimental simulations using CO_2 - H_2O -polymer system. *Journal of Geophysical Research* 102: 3077-3096.

Sedimentological responses to hydrological variability for the last 50 ka as recorded in the maar lake Laguna Potrok Aike (Pali Aike Volcanic Field, Argentina)

Bernd Zolitschka¹, A. Catalina Gebhardt², Christian Ohlendorf¹, Jan-Pieter Buylaert³, Pierre Kliem¹, Christoph Mayr^{4,5}, Stefan Wastegård⁶, and the PASADO Science Team⁷

¹ Institute of Geography (Geopolar), University of Bremen, Germany – zoli@uni-bremen.de

² Alfred Wegener Institute of Polar and Marine Research, Bremerhaven, Germany

³ Nordic Laboratory for Luminescence Dating, Aarhus University, Denmark

⁴ Dept. of Earth and Environmental Sciences, University of Munich, Germany

⁵ Institute of Geography, University of Erlangen-Nürnberg, Germany

⁶ Department of Physical Geography and Quaternary Geology, Stockholm University, Sweden

⁷ PASADO Science Team as cited at: http://www.icdp-online.org/front_content.php?idcat=1494



Keywords: lacustrine sediments, hydrological variability, ICDP-project PASADO

Semiarid conditions are prevailing at Laguna Potrok Aike (52°S, 70°W; 116 m asl; diameter: 3.5 km, water-depth: 100 m), a currently terminal maar lake in the steppe of southern Patagonia (Fig. 1). Here depositional processes are strongly controlled by the inflow-to-evaporation ratio, a direct function of climatic variables. In this climatic zone it is expected that the lake underwent distinct hydrological changes from open to terminal lake conditions, especially at glacial/interglacial temporal scales. The variability could have ranged from a freshwater lake with an outflow in which solutes were diluted to a saline lake where dissolved loads tended to build up over time, increased salinity as well as pH and caused the formation of chemical precipitates. Such distinct changes are reflected in the chemical composition of sediments. Additionally, terminal lakes are characterized by rapid water-depth and shoreline fluctuations accompanied by variations in lake area and water volume. These in turn are the trigger for processes of sediment re-deposition and, sometimes, even desiccation of lakes.

Four seismic surveys (Anselmetti et al., 2009; Gebhardt et al., 2011) and a stratigraphic record based on 51 AMS ¹⁴C dates obtained in the framework of ICDP expedition 5022 “Potrok Aike Maar Lake Sediment Archive Drilling Project” (PASADO: Zolitschka et al., 2009) provide a database to compare the 106 m composite profile from the lake centre (site 2; Fig. 1) with piston cores from the littoral and outcrops in the catchment. Based on event correlation using distinct volcanic ash layers with unique geochemical composition and additional optically stimulated luminescence (OSL) dates on feldspars, sediment records are firmly linked. Moreover, this approach allows to match the sediment record with water levels during the past ca. 50 kyrs providing evidence for lake level variations up to 200 m. Seismic reflection data even points to

very low lake levels before ca. 55 kcal BP (Gebhardt et al., in press). This is supported by dune-like structures in the eastern lake basin unconformably overlain by a series of paleo-shorelines as interpreted from seismic records. This suggests a rapidly rising lake level preceded by desiccation. Flooding of the lake basin ended with freshwater lake conditions established a couple of millennia later which continued until the early Late Glacial (Fig. 2).

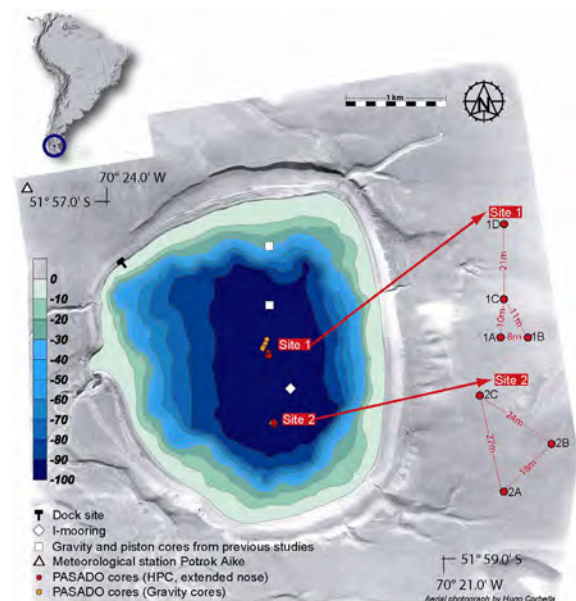


Fig. 1 – Bathymetric map of Laguna Potrok Aike with indicated ICDP drilling positions (site 1 and site 2). The geographical location in South America is shown in the upper left insert.

At the end of the Pleistocene sediment-facies are characterized by depositional systems with three transitions between clastic-dominated (high inflow lake conditions, perhaps with an outflow) and carbonate-rich (end lake conditions) (Fig. 2). During the late Pleistocene (13.5-11.5 kcal BP) carbonate is precipitated biologically by *Phacotus*, whereas at the

transition from the Late Glacial to the early to mid Holocene (11.5-9.3 kcal BP) clastic sediments regain dominance. Since 9.3 kcal BP intense carbonate precipitation (up to 35% calcite) is recorded that continues until today with one marked interruption for the neoglacial "Little Ice Age" (Haberzettl et al., 2007).

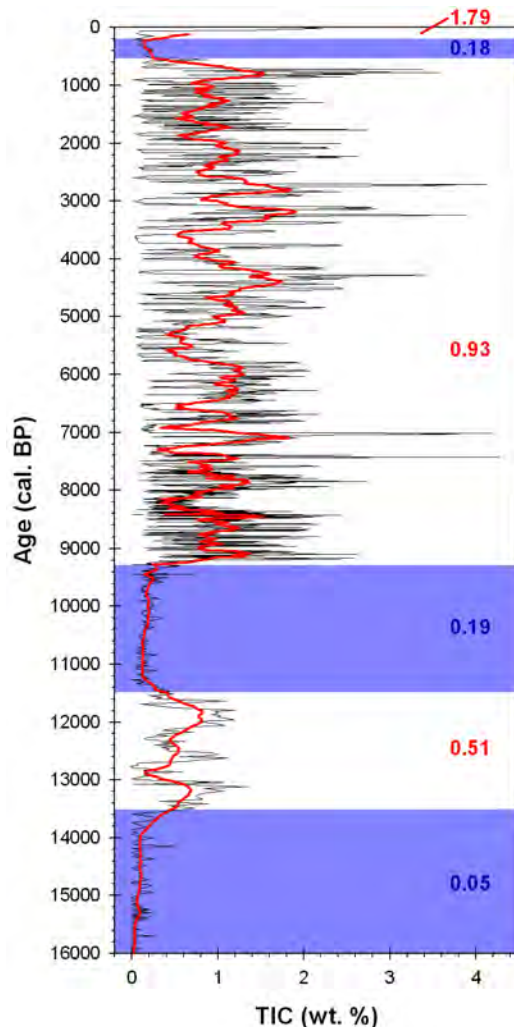


Fig. 2 – Total inorganic carbon (TIC) versus time (PASADO age model V.3) as a proxy for increased salinity of the lake water causing precipitation of carbonates linked to lake level low stands. Periods when the threshold for formation of carbonates was not passed (i.e. higher lake levels) are marked in blue. TIC data are plotted as black line with their 21-point running mean in red (data from Haberzettl et al., 2007). Individual values given relate to mean TIC values for respective periods. The mean TIC value is 0.04% for the time before 16 kcal. BP (not shown, from Recasens et al., in press).

Such geochemical changes are related to hydrological variability which is probably caused by (1) changes in runoff due to permafrost sealing of the ground during the Pleistocene, (2) changes in intensity and position of the Southern Hemispheric Westerlies linked to variations in precipitation and

wind-induced evaporation and (3) the glacial to Holocene temperature increase (Toggweiler, 2009).

Acknowledgements

This study is supported by the International Continental Scientific Drilling Program (ICDP) in the framework of the "Potrok Aike Maar Lake Sediment Archive Drilling Project" (PASADO). Funding for drilling was provided by the ICDP, the German Science Foundation (DFG grants ZO-102/11-1,2), the Swiss National Funds (SNF), the Natural Sciences and Engineering Research Council of Canada (NSERC), the Swedish Vetenskapsradet (VR) and the University of Bremen.

For their invaluable help in field logistics we thank the staff of INTA Santa Cruz, the Moreteau family and the DOSECC drilling crew.

References

- Anselmetti, F.S., Ariztegui, D., De Batist, M., Gebhardt, A.C., Haberzettl, T., Niessen, F., Ohlendorf, C., Zolitschka, B. 2009. Environmental history of southern Patagonia unravelled by the seismic stratigraphy of Laguna Potrok Aike. *Sedimentology* 56: 873-892.
- Gebhardt, A.C., De Batist, M., Niessen, F., Anselmetti, F.S., Ariztegui, D., Haberzettl, T., Kopsch, C., Ohlendorf, C., Zolitschka, B. 2011. Deciphering lake and maar geometries from seismic refraction and reflection surveys in Laguna Potrok Aike (southern Patagonia, Argentina). *Journal of Volcanology and Geothermal Research* 201: 357-363.
- Gebhardt, A.C., Ohlendorf, C., Niessen, F., De Batist, M., Anselmetti, F.S., Ariztegui, D., Kliem, P., Wastegård, S., Zolitschka, B. in press. Seismic evidence of up to 200 m lake-level change in Southern Patagonia since MIS4. *Sedimentology*, DOI: 10.1111/j.1365-3091.2011.01296.x.
- Haberzettl, T., Corbella, H., Fey, M., Janssen, S., Lücke, A., Mayr, C., Ohlendorf, C., Schäbitz, F., Schleser, G.-H., Wessel, E., Wille, M., Wulf, S., Zolitschka, B. 2007. A continuous 16,000 year sediment record from Laguna Potrok Aike, southern Patagonia (Argentina): *Sedimentology, chronology, geochemistry. The Holocene* 17: 297-310.
- Recasens, C., Ariztegui, D., Gebhardt, C., Gogorza, C., Haberzettl, T., Hahn, A., Kliem, P., Lisé-Pronovost, A., Lücke, A., Maidana, N.I., Mayr, C., Ohlendorf, C., Schäbitz, F., St-Onge, G., Wille, M., Zolitschka, B. and the PASADO Science Team, in press. New insights into paleoenvironmental changes in Laguna Potrok Aike, Southern Patagonia, since the Late Pleistocene: the PASADO multiproxy record. *The Holocene*.
- Toggweiler, J.R. 2009. Shifting Westerlies. *Science* 323: 1434-1435.
- Zolitschka, B., Anselmetti, F., Ariztegui, D., Corbella, H., Francus, P., Ohlendorf, C., Schäbitz, F. and the PASADO Scientific Drilling Team, 2009. The Laguna Potrok Aike Scientific Drilling Project PASADO (ICDP Expedition 5022). *Scientific Drilling* 8: 29-33.

Eruptive and depositional characteristics of the Loolmurwak and Eledoi maar volcanoes, Lake Natron – Engaruka monogenetic volcanic field, northern Tanzania

Jaap F. Berghuijs, Hannes B. Mattsson and **Sonja A. Bosshard**

Institute of Geochemistry and Petrology, Swiss Federal Institute of Technology (ETH Zürich), Zürich, Switzerland – sonja.bosshard@erdw.ethz.ch

Keywords: maar volcanism, depositional characteristics, fragmentation mode.

The Eledoi and Loolmurwak maars form two of the largest craters in the Lake Natron - Engaruka monogenetic volcanic field (LNE-MVF; northern Tanzania), an area consisting of approximately 200 cones scattered between four large central volcanoes. We here describe depositional characteristics of the two maars as observed in the field and present preliminary findings on the petrography (from traditional optical microscopy in combination with Scanning Electron Microscopy), which provides insights into the eruption dynamics of these two maar-forming eruptions.

Typically, maar-diatreme volcanoes are considered to be produced by phreatomagmatic eruptions in which rising magma interacts with external water (Lorenz, 1973; White and Ross, 2011). The emplacement mechanisms in maar-forming eruptions have been compared to those of kimberlites (Lorenz, 1975). Recent work has questioned the necessity of external water to produce all observed kimberlite deposits (Sparks et al., 2006).

The Loolmurwak and Eledoi maars are located on the Kerimasi block, which is elevated by more than 200 m with respect to the surrounding Lake Natron and Engaruka basins (Mattsson and Tripoli, 2011). Also, the LNE-MVF is characterized by an arid climate in which evaporation exceeds precipitation on an annual basis. Thus the sufficient accumulation of external water, required to drive phreatomagmatic fragmentation, is not obvious in this area. Instead, a fundamentally different mechanism may be responsible for these two maar-forming eruptions.

Preliminary field studies indicate that the ejecta rings both Eledoi and Loolmurwak display various characteristics common to many maar deposits, such as an abundance of lithic material and the occurrence of coarse-grained lenses within a finer matrix. However, as noted by Mattsson and Tripoli (2011), neither of the two craters provides clear evidence of wet eruption or deposition. Indicative features such as accretionary lapilli, vesiculated tuffs or plastering against objects were not observed. Rather, several observations point towards a dry

mode of deposition, including a presumably wind-induced asymmetry of the crater rim (Eledoi; towards 338° [i.e., NW]) and the dominance of subspherical armored lapilli. These also occur on a larger (i.e., > 6.4 cm) and a smaller (< 2 cm) scale, in case of which they are here referred to as 'cored melt blobs' and 'cored melt droplets', respectively. Irrespective their size, these cores consist of olivine, pyroxene or phlogopite phenocrysts (Loolmurwak, Fig. 1). Many of the armored lapilli show slight flattening parallel to the bedding plane, indicating that they were emplaced as molten droplets.

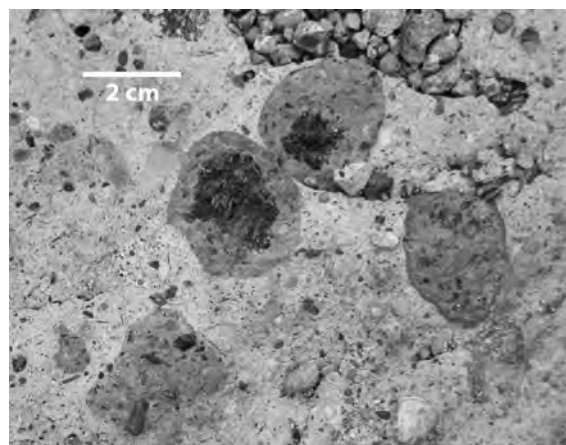


Fig. 1 – Subspherical armored lapilli within an ash-sized matrix (Loolmurwak). Lapilli cores predominantly consist of olivine, pyroxene and phlogopite.

The abundance of olivine, pyroxene or phlogopite megacrysts (up to 11 cm in diameter) in the Loolmurwak deposits indicates that this magma originally had a high volatile content. Present in both maars but especially common in the Eledoi deposits are mantle xenoliths (predominantly dunites and wehrlites) that are frequently cut by several generations of metasomatic veins (containing amphibole, phlogopite, clinopyroxene and spinel). Based on Stoke's law and the maximum size of mantle xenoliths, a minimum average magma ascent rate of 0.85 ms^{-1} can be calculated for the Eledoi eruption. This ascent rate is similar to that associated

with the adjacent scoria cone of Pello Hill (Matsson et al., 2011b) as well as those of kimberlitic magmas (Sparks et al., 2006).

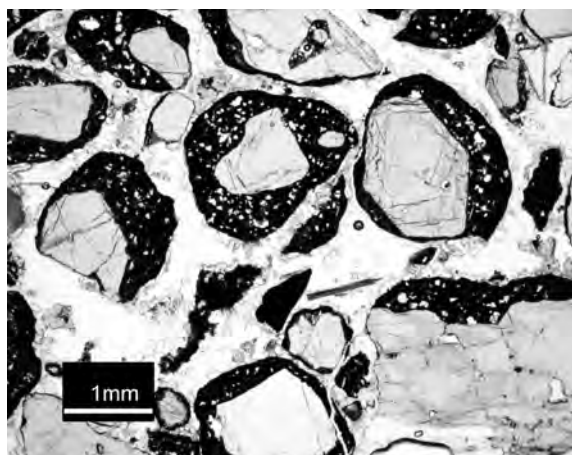


Fig. 2 – Photomicrograph of cored melt droplets within the Loolmurwak deposits. Droplet cores in this picture predominantly consist of clinopyroxene but also some olivine (e.g., bottom center of picture).

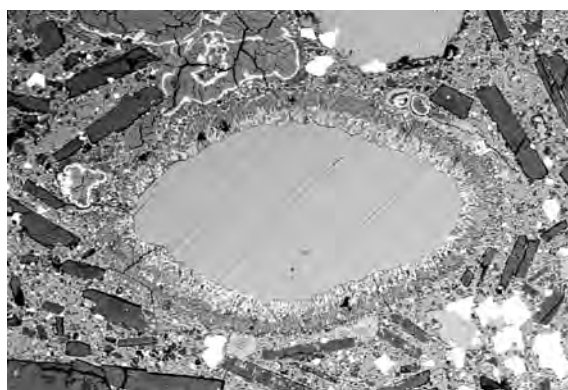


Fig. 3 – Backscattered SEM image showing a reaction rim around a phlogopite crystal. Dark, lath-shaped melilite crystals stand out from a finer matrix. Width of image is 540 μ m.

Preliminary petrographic results (using both optical microscopy and Scanning Electron Microscopy) show that, just as observed on a slightly larger scale in the field (i.e., armored lapilli or cored melt blobs), olivine, pyroxene and phlogopite crystals encased in a fine crystalline matrix commonly occur on a (sub)mm-scale (Fig.

2). The matrix of these melt droplets consists of the same three phases as well as melilite and opaque minerals. Phlogopite edges are commonly degraded (Fig. 3), which suggests that this phase was no longer stable at shallow depth and may have released additional volatiles that enhanced the explosivity of the eruption.

The rapid ascent rate of the involved magmas from upper-mantle depths and the exsolution of abundant volatiles, together with depositional characteristics that indicate ‘dry’ magmatic fragmentation and deposition, indicate that the emplacement mechanism of the Eledoi and Loolmurwak maar craters is very similar to that typical for many kimberlites (i.e., Sparks et al., 2006). Consequently, a more detailed study of pyroclast textures, mineralogy and chemistry of the Eledoi and Loolmurwak deposits can provide valuable new insights into maar emplacement processes.

References

- Lorenz, V. 1973. On the formation of maars. *Bulletin of Volcanology* 37: 183–204.
- Lorenz, V. 1975. Formation of Phreatomagmatic Maar-Diatreme Volcanoes and its Relevance to Kimberlite Diatremes. *Physics and Chemistry of the Earth* 9: 17–29.
- Mattsson, H.B., Tripoli, B.A. 2011a. Depositional characteristics and volcanic landforms in the Lake Natron–Engaruka monogenetic field, northern Tanzania. *Journal of Volcanology and Geothermal Research* 203: 23–34.
- Mattsson, H.B., Bosshard, S.A., Berghuijs, J.F. 2011b. Rapid magma ascent and short eruption durations in the Lake Natron - Engaruka monogenetic volcanic field (northern Tanzania): Evidence from the Pello Hill scoria cone. IAS Fourth International Maar Conference.
- Sparks, R.S.J., Baker, L., Brown, R.J., Field, M., Schumacher, J., Stripp, G., Walters, A. 2006. Dynamical constraints on kimberlite volcanism. *Journal of Volcanology and Geothermal Research* 155: 18–48.
- White J.D.L., Ross, P.-S. 2011. Maar-diatreme volcanoes: A review. *Journal of Volcanology and Geothermal Research* 201: 1–29.

Developing probabilistic eruption scenarios for distributed volcanism in the Auckland Volcanic Field, New Zealand

Shane Cronin¹, Karoly Nemeth¹, Mark Bebbington^{1,2}, Ian Smith³, Jan Lindsay³ and Gill Jolly⁴

¹ *Volcanic Risk Solutions, Massey University, Palmerston North, New Zealand – s.j.cronin@massey.ac.nz*

² *IFS-Statistics, Massey University, Palmerston North, New Zealand*

³ *School of Environment, University of Auckland, Auckland, New Zealand*

⁴ *GNS Science, Wairakei Research Centre, Taupo, New Zealand*

Keywords: hazard

The prospect of planning for a future eruption is a complex task for emergency managers of the City of Auckland (pop. >1.4 million); not only must the likelihood of eruption timing be determined, but also estimations of the potential location, style and size of the next eruption. Beneath Auckland lies a monogenetic volcanic field, in which almost all past eruptions have occurred in different locations, from a few hundred metres up to >10 km apart, within an overall ellipsoidal 360 km² area (Searle, 1962; Allen and Smith, 1994). Using the known eruptive history of this volcanic field, independent spatial and temporal probabilistic forecasts were developed for future eruptions (Bebbington and Cronin, 2011). This leads on to the need for evaluations of potential eruption magnitude, and hazard potential. The hazard of eruptions in these types of geological settings is strongly correlated with the potential explosivity of eruptions (Houghton et al., 1999; Edbrooke et al., 2003), which, in turn, primarily depends on whether or not a magma-water interaction occurs, ideally under favourable conditions involving abundant (but not too much) water, with the specific dynamics depending on a diverse range in properties of the substrate sediments (Lorenz, 2007; Nemeth et al., in review).

To develop scenarios of the potential styles of eruption, their magnitudes and associated probabilities for Auckland, analysis of past erupted magma volumes, compositions, edifice types, volcanic processes and deposit distribution is needed. Around ~50 past eruptions are known from this field, and hence only a few examples of each of various volcanic styles and magnitude are known. The overriding feature of this field, however, appears to be the ubiquity of phreatomagmatism, with over two thirds of eruption events experiencing major explosive phreatomagmatic phases, and most of the others probably having at least eruption onsets being dominated by explosive magma-water interactions. This is driven by the relatively soft substrate rock underlying much of Auckland, with a combination of Recent unstructured estuarine and alluvial muds and Tertiary-aged weakly

consolidated, layered marine muds and sands, many of which host locally confined aquifers.

Based on the known past eruptions, a general classification of event-types can be made that can be used to develop realistic eruption scenarios in an increasing order of potential hazard to human life and economic activity. In general, large-volume eruptions may impact greater areas and thus lead to longer term disruption; however, it is the eruption onset style, along with the time available for warning and evacuation, that will determine the potential for loss of life.

The type of eruption that may eventuate will most critically depend on where it occurs, with its manifestation controlled not only by internal factors (magma flux, composition, gas content and volume), but also external geo-hydrological factors (sediment strength and saturation, water cover) and other environmental conditions (wind, rain etc). Where the magma flux and volume are low, such as is commonly the case in the Auckland Volcanic Field, external forces often dominate.

We attempt here to probabilistically integrate all known parameters to forecast the likely range of hazard scenarios of the Auckland Volcanic field. Considering threat to human life, the most hazardous eruptions are those caused by the interaction of magma rising at intermediate rates with thick, water-saturated soft-sediments or in water depths of >20 m. Since the principal hazards are controlled primarily by external factors in this case, we can forecast the potential initial eruptive style by mapping and classifying substrate strength and saturation conditions and water depths in offshore/lake areas. Hazard factors of consequent eruption progression, relevant for ongoing response and recovery management, include: production of ashfall, the eruption duration and the area covered by lava flows. These are probably also the most significant economic risk indicators, when factored with the socio-economic activity of the specific impacted site.

By classifying eruptions based on a mixture of internal (magmatic) and external parameters, we can apply AVF spatio-temporal probabilities from

Bebbington and Cronin (2011) and propagate these through an event-tree approach to constrain a series of onset and consequential eruption scenarios. This process allows us to apply hard-won volcanological information into annual forecasts of likely impacts, by integrating the scenario results within spatio-temporal economic growth models also developed for this city, such as those by McDonald and Patterson (2008).

References

- Allen, S.R., Smith, I.E.M. 1994. Eruption styles and volcanic hazard in the Auckland Volcanic Field, New Zealand. *Geoscience Reports of Shizuoka University* 20: 5-14.
- Bebbington, M.S., Cronin S.J. 2011. Spatio-temporal hazard estimation in the Auckland Volcanic Field, New Zealand, with a new event-order model. *Bulletin of Volcanology* 73: 55–72.
- Edbrooke, S.W., Mazengarb, C., Stephenson, W. 2003. Geology and geological hazards of the Auckland urban area, New Zealand. *Quaternary International* 103: 3-21.
- Houghton, B.F., Wilson, C.J.N., Smith, I.E.M. 1999. Shallow-seated controls on styles of explosive basaltic volcanism: a case study from New Zealand. *Journal of Volcanology and Geothermal Research* 91: 97-120.
- Lorenz, V. 2007. Syn- and post-eruptive hazards of maar-diatreme volcanoes. *Journal of Volcanology and Geothermal Research* 159: 285-312.
- McDonald, G.W., Patterson, M.G. 2008. Auckland Region Dynamic Ecological-Economic Model: Technical Report. NZCEE Research Monograph Series – No. 13. Palmerston North: NZCEE. ISBN 978-0-9582782-2-5.
- Searle, E.J. 1962. The volcanoes of Auckland City. *NZ Journal of Geology and Geophysics* 5: 193-227.

Up to 200 m lake-level change since MIS4 recorded in maar lake Laguna Potrok Aike, Southern Patagonia

A. Catalina Gebhardt¹, Christian Ohlendorf², Frank Niessen¹, Marc De Batist³, Flavio S. Anselmetti⁴, Daniel Ariztegui⁵, Pierre Kliem², Stefan Wastegård⁶ and **Bernd Zolitschka**²

¹ Alfred Wegener Institute of Polar and Marine Research, Bremerhaven, Germany

² Institute of Geography (Geopolar), University of Bremen, Germany – zoli@uni-bremen.de

³ Renard Centre of Marine Geology, University of Gent, Belgium

⁴ Swiss Federal Institute of Aquatic Science and Technology, Dübendorf, Switzerland

⁵ Section of Earth Sciences, University of Geneva, Switzerland

⁶ Department of Physical Geography and Quaternary Geology, Stockholm University, Sweden



Keywords: ICDP, PASADO, lake-level change, seismic stratigraphy

Laguna Potrok Aike is a terminal maar lake situated just north of the Strait of Magellan in the Patagonian steppe (Fig. 1). The lake is located in an area influenced by the strong Southern Hemisphere Westerlies (SHW) and lies in the rain shadow of the Andes with a modern annual precipitation of less than 300 mm. The SHW are subject to latitudinal shifts of up to 5° between glacial and interglacial times (e.g. Lamy et al., 2001), which results in distinct changes in available moisture. Recent studies on piston cores and on high-resolution seismic data have shown that Laguna Potrok Aike is highly sensitive to moisture changes (e.g. Haberzettl et al., 2008; Anselmetti et al., 2009). The lake sediments thus serve as a unique terrestrial archive of southern South American climate history and were recently drilled in the context of the International Continental Scientific Drilling Program (ICDP) co-sponsored project “Potrok Aike Maar Lake Sediment Archive Drilling Project” (PASADO). Seven cores were recovered from two sites in the lake penetrating the uppermost ~100 m of the lacustrine sediments. The record drilled within PASADO reaches back to ~51 ka cal. BP and contains roughly 50% of redeposited material, intercalated with the same amount of pelagic lake sediments.

Seismic surveys were carried out between 2003 and 2005 in order to get a deeper knowledge on the lake sediments and the deeper basin geometries. A raytracing model of the Laguna Potrok Aike basin was calculated based on refraction data while sparker data were additionally used to identify the crater-wall discordance and thus the upper outer shape of the maar structure (Fig. 2). The combined data sets show a rather steep funnel-shaped structure embedded in the surrounding Santa Cruz Formation that resembles other well-known maar structures. The infill consists of up to 370 m lacustrine

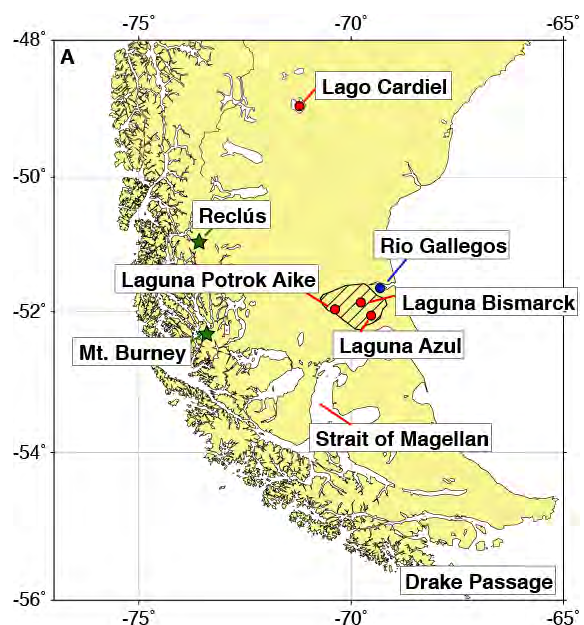


Fig. 1 – Geographical location of Laguna Potrok Aike.

sediments underlain by probably volcanoclastic sediments of unknown thickness. The lacustrine sediments show a subdivision into two sub-units: (a) the upper with seismic velocities between 1500 and 1800 m s⁻¹, interpreted as unconsolidated muds, and (b) the lower with higher seismic velocities of up to 2350 m s⁻¹, interpreted as lacustrine sediments intercalated with mass transport deposits of different lithology and/or coarser-grained sediments. The postulated volcanoclastic layer has acoustic velocities of >2400 m s⁻¹.

Seismic reflection profiles revealed a highly dynamic paleoclimate history. Dunes were identified in the eastern part of the lake (Fig. 3) at ca. 30 to 80 m below lake floor overlying older lacustrine strata and suggest that the region experienced dry conditions probably combined with strong westerly

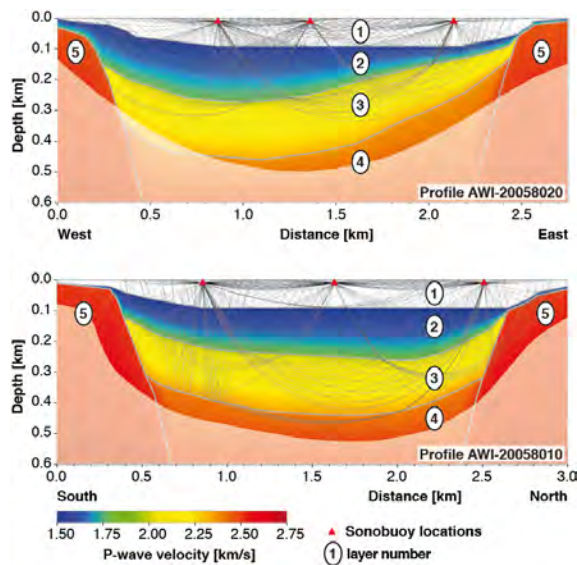


Fig. 2 – Five-layer seismic velocity model of the Laguna Potrok Aike maar (Gebhardt et al., 2011).

winds. As a nearby example, the recent Laguna Bismarck serves as a modern analogue to the ancient dry Laguna Potrok Aike with coarse-grained sediments accumulated down and upslope on the wind-sheltered side inside the crater and fine-grained material blown over the crater rim towards east-north-east, building up a fan-shaped depositional area. The dry phase quite likely can be linked to a major dust event recorded in the Antarctic ice cores during MIS4. The dunes are overlain by a series of paleo-shorelines (Fig. 3) indicating a stepwise water level evolution of a new lake established after this dry period, and thus a change towards wetter conditions. After the initial, rapid and stepwise lake-level rise, the basin became deeper and wider, and sediments deposited on the lake shoulder at approximately 33 m below present day lake level. This points towards a long period of a lake-level highstand between roughly 53.5 ka cal. BP and 30 ka cal. BP with a maximum lake level some 200 m higher than the desiccation horizon. This highstand was then followed by a regressional phase of uncertain age although it must have happened sometime between approximately 30 ka cal. BP and 6750 yrs cal. BP. Drier conditions during the Mid-Holocene are witnessed by a dropping lake level, resulting in a basin-wide erosional unconformity on the lake shoulder. A second stepwise transgression between ~5.8 to 5.4 ka cal. BP and ~4.7 to 4 ka cal. BP with paleo-shorelines deposited on the lake shoulder unconformity indicates again a change towards wetter conditions (Anselmetti et al., 2009).

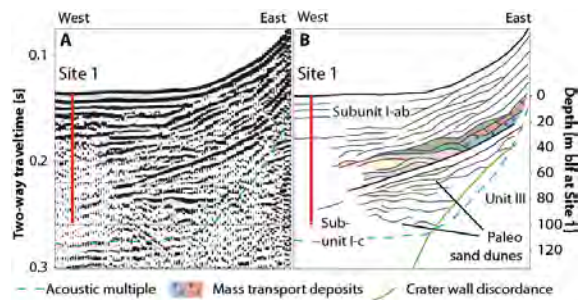


Fig. 3 – Seismic data showing stacked sand dunes overlain by paleo-shorelines (Gebhardt et al., in press).

Acknowledgements

We thank all expedition members in 2004 and 2005 for their excellent cooperation and support during fieldwork at the lake. Financial support by the Deutsche Forschungsgemeinschaft (DFG grants GE-1924/2-1 and ZO-102/5-1, 2, 3) is gratefully acknowledged.

References

- Anselmetti, F.S., Ariztegui, D., De Batist, M., Gebhardt, A.C., Haberzettl, T., Niessen, F., Ohlendorf, C., Zolitschka, B. 2009. Environmental history of southern Patagonia unravelled by the seismic stratigraphy of Laguna Potrok Aike. *Sedimentology* 56: 873-892.
- Gebhardt, A.C., De Batist, M., Niessen, F., Anselmetti, F.S., Ariztegui, D., Haberzettl, T., Kopsch, C., Ohlendorf, C., Zolitschka, B. 2011. Deciphering lake and maar geometries from seismic refraction and reflection surveys in Laguna Potrok Aike (southern Patagonia, Argentina). *Journal of Volcanology and Geothermal Research* 201: 357-363.
- Gebhardt, A.C., Ohlendorf, C., Niessen, F., De Batist, M., Anselmetti, F.S., Ariztegui, D., Kliem, P., Wastegård, S., Zolitschka, B. in press. Seismic evidence of up to 200 m lake-level change in Southern Patagonia since MIS4. *Sedimentology*, DOI: 10.1111/j.1365-3091.2011.01296.x.
- Haberzettl, T., Kück, B., Wulf, S., Anselmetti, F.S., Ariztegui, D., Corbella, H., Fey, M., Janssen, S., Lücke, A., Mayr, C., Ohlendorf, C., Schäbitz, F., Schlerer, G.H., Wille, M., Zolitschka, B. 2008. Hydrological variability in southeastern Patagonia and explosive volcanic activity in the southern Andean Cordillera during Oxygen Isotope Stage 3 and the Holocene inferred from lake sediments of Laguna Potrok Aike, Argentina. *Palaeogeography Palaeoclimatology Palaeoecology* 259: 213-229.
- Lamy, F., Hebbeln, D., Röhl, U., Wefer, G. 2001. Holocene rainfall variability in southern Chile: a marine record of latitudinal shifts of the Southern Westerlies. *Earth and Planetary Science Letters* 185: 369-382.

Volcano park, geoparks and outreach activities on volcanoes in Hungary

Szabolcs Harangi and Réka Lukács

Volcanology Group, Department of Petrology and Geochemistry, Eötvös University, Budapest, Hungary – szabolcs.harangi@geology.elte.hu

Keywords: volcano park, geopark, outreach.

Is there a sense to establish a volcano park and perform outreach activities on volcanoes in a country, where no active volcanoes exist? The answer is clearly, yes! The Carpathian-Pannonian region consists of a wide range of volcanic formations from basaltic to rhyolitic volcanic products and offers a unique opportunity to investigate them in detail and of course to use them to develop geotourism. In 2010, the Novohrad-Nógrád Geopark became the official member of the Geopark community and this year (2012) the Kemenes Volcano Park will be open. This will be the first thematic volcano park in central Europe and as far as we know the third one in Europe. The initial plan goes back to the early 1990's, when the volcanological studies of the Ság hill revealed the complex history of the 5.5 Ma basaltic volcano. It is situated at the western part of the Pannonian basin (Hungary) and belong to the extensive alkaline basaltic volcanism of this region occurred between 11 Ma and 0.1 Ma. The remarkable volcanological features of the Ság hill as well as of the nearby extinct volcanoes provide a strong background for the volcano park. A detailed realization plan has been worked out in 2003 and this was the basis of the proposal of the Council of Celldömölk, the town next to the Ság hill. The plan involves a Volcano House at the foot of the Ság hill, where the visitors could get a general picture about the volcanic processes and the 20 Ma long history of volcanic activity in the Carpathian-Pannonian region. There is going to be an opportunity to take a journey into the interior of the Earth and to have a short visit in a magma chamber. The volcano-horror room will show the destructive force of the volcanoes and gives place for a memorial of the destroyed settlements from Pompeii to Plymouth. An important part of the volcano park will be the construction of the Volcano path, which leads to the Ság hill and shows the main volcanological features. An open-air volcano-playground and rock exhibition could provide further opportunities to science education. The Kemenes Volcano Park as a tourist attraction could initiate the recovery of economy in this otherwise poor region.

The proposal for the Novohrad-Nógrád Geopark was also deeply based on the exceptional beauty of the past volcanoes. Devastating pumiceous ash-flows, submarine and subaerial lava flows, one of Europe's largest coherent lava plateau, exposed subvolcanic bodies and volcanic vents, maars, diatremes, "petrified" gas bubbles, lava spatters, platy and columnar jointed basalts and andesites including a unique "andesite-slide", garnet in the volcanic rocks and fragments from the upper mantle! The area of the Novohrad-Nógrád Geopark presents various volcanological phenomena, strongly associating with cultural and historical heritages: it is indeed a paradise for volcanologists, but also for visitors, who are looking for the exceptional relationships of nature and culture. Here, remnants of a 20 million year long volcanic activity can be found on a relatively small area: basalts, andesites, rhyolites formed both by effusive and explosive volcanic eruptions. Due to the strong erosion, the deep structure of the volcanoes is now nicely exposed. The Geopark is - without doubt - an excellent place to have a unique insight into the nature of one of the Earth's most important processes.

In the future, another proposal for a geopark could be approved; this is the Bakony-Balaton geopark, where the volcanological features play also a significant role. In this area, remnants of basaltic volcanism from 7.9 to 2.6 left a unique erosional landform, where maars, diatremes, scoria cones and shield volcanoes are waiting for the visitors.

The long history of volcanism in the Carpathian-Pannonian basin as well as the increasing attention towards volcanic eruptions encouraged us to strengthen our outreach activities. The Volcanology Group of the Eötvös University Budapest performs Volcano shows in various events such as during the Researchers' nights and Science days. The Tűzhányó blog ("Volcano blog"; <http://tuzhanyo.blogspot.com>) provides daily information about volcanic activities and give background explanations deliberately in Hungarian language. It is quite popular now and often referred by various news portals.

Fossil microorganisms, plants and animals from the Early Miocene Foulden Maar, Otago, New Zealand

Uwe Kaulfuss¹, Daphne Lee¹, Jennifer Bannister², John Conran³, Jon Lindqvist¹, Dallas Mildenhall⁴ and Elizabeth Kennedy⁴

¹ Department of Geology, University of Otago, PO Box 56, Dunedin, New Zealand – kauuw275@student.otago.ac.nz

² Department of Botany, University of Otago, Dunedin, New Zealand

³ ACEBB, School of Earth & Environmental Sciences, Benham Bldg DX 650 312, University of Adelaide, Australia

⁴ GNS Science, PO Box 30368, Lower Hutt, New Zealand

Keywords: maar lake ecosystem, Miocene, fossil biota.

Laminated diatomite infilling the crater of Foulden Maar provides crucial information on the terrestrial and freshwater biota of earliest Miocene New Zealand (~23 Ma) and the local ecosystem in and around the former maar lake. Palynological samples and plant macrofossils retrieved from surface exposures and a 180 m drill core of the maar sediments provide information about the local/regional floral history over a period of approx. 130,000 years, that probably spans the Oligocene–Miocene boundary (see Fox et al. 2012, this volume).

Pale and dark laminae couplets in the Foulden Maar diatomite average 0.5 mm thick and record mainly biogenic fallout from the water column and minor input from the lake fringe. Sedimentation in the low-energy lake setting was predominantly controlled by seasonal variations in sunlight, temperature, precipitation and nutrient influx.

Summer bioproduction in the small (~1500 m diameter) but deep (~200 m) maar lake was dominated by *Encyonema jordanii* and other pennate diatoms, whereas terrestrial organic detritus, siliceous sponge spicules, chrysophycean stomatocysts and centric diatoms were deposited in colder, presumably wet and windy seasons (Lindqvist & Lee 2009). The remarkably uniform composition of the 120 m laminated diatomite indicates long-lasting and very stable limnological conditions in a deep, thermally and chemically stratified lake, interrupted only by turbidity currents and occasional debris flows that originated in littoral and sub-aerial zones.

At least two species of fish were the dominant predators within the lake. The most common, *Galaxias effusus* Lee, McDowall & Lindqvist provides the earliest record globally of the Southern Hemisphere whitebait family Galaxiidae. Specimens range from large-eyed juvenile *inanga* to 140 mm long adults (Fig. 1a), preserved as intact skeletons or soft tissue compressions on bedding planes (Lee et al. 2007). A recently discovered eel provides the first record of fossil *Anguilla* from the Southern Hemisphere.

The well-preserved flora from Foulden Maar indicates that a diverse rainforest community dominated by Lauraceae surrounded the lake. Macrofossils include numerous seeds, fruits, flowers, bark and wood as well as leaves, typically with cuticle preserved (Fig. 1b). Of special importance are flowers with *in situ* pollen that allow the floral assignment of isolated pollen from other Cenozoic sites in New Zealand (Bannister et al. 2005).

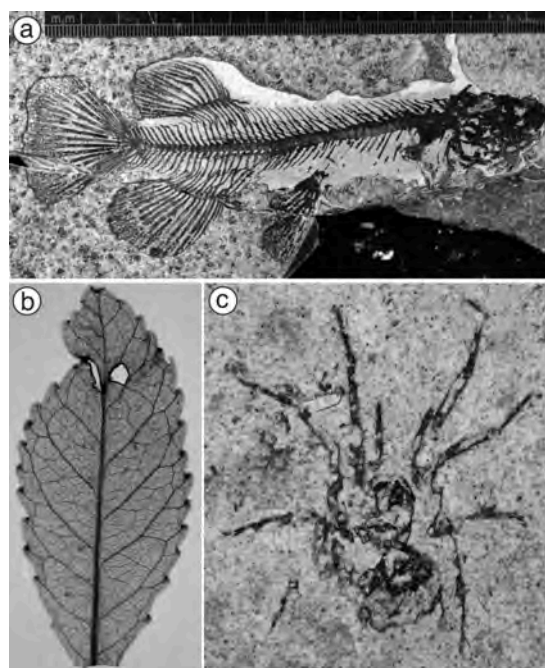


Fig. 1 – Fossils from Foulden Maar; a) *Galaxias effusus*; b) *Weinmannia* leaf with cuticle; c) an undescribed spider.

Angiosperms discovered to date include numerous Lauraceae and species of *Dysoxylum*, *Elaeocarpus*, *Fuchsia*, *Gymnostoma*, *Hedycarya*, *Laurelia*, *Mallotus–Macaranga*, *Myrsine*, *Nothofagus*, *Weinmannia* and diverse Araliaceae, Euphorbiaceae–Picrodendraceae, Loranthaceae, Menispermaceae, Rutaceae, Winteraceae, and others. Monocot genera include *Astelia*, *Cordylina*,

Luzuriaga, *Phormium*, *Ripogonum*, *Typha*, in addition to *Dendrobium* and *Earina*; the oldest known orchid macrofossils (Conran et al. 2009). Most of these genera and families are still represented in modern New Zealand ecosystems. The gymnosperm flora from Foulden Maar includes leaves, pollen or cones of *Araucaria*, *Agathis*, *Dacrycarpus*, *Dacrydium*, *Phyllocladus*, *Podocarpus*, *Prumnopitys* and *Wollemia*, all represented by species that are now extinct in New Zealand. Altogether, the palaeoforest at Foulden Maar was a warm temperate to subtropical notophyll vine forest that incorporated elements that are found in present day New Zealand, Australia, South America and New Caledonia.

Information about the vegetative (re)colonization of the freshly deposited tephra rim surrounding the maar can be obtained from palynological drill core samples, which cover early post-eruptive sub-aerial/shallow lacustrine to late post-eruptive fully lacustrine sedimentation stages at Foulden Maar. Preliminary analyses have shown a dominance of ferns and allies in the lowermost parts of the drilling core (mono- and trilete spores, *Dictyophyllidites arcuatus*, *Gleicheniidites circinidites*, etc.). Accompanying charcoal is probably derived from forest fires triggered by volcanic activity at Foulden Maar, or nearby volcanoes. Pioneer species successively disappear up-core and are replaced by pollen indicative of a rainforest, including canopy trees, understorey shrubs, mistletoes, epiphytes, ferns and vines, as well as forest margin pioneers, but few aquatic macrophytes. Local palynology is superimposed by regional vegetation signals, and work is currently underway to distinguish local versus regional influx into the maar lake.

The rainforest surrounding the maar lake provided a suitable habitat for insects and spiders. Among 115 arthropods collected to date are representatives of ~15 insect families, most of which are recorded as fossils for the first time from New Zealand. Confirmed orders include the Isoptera (termites), Hymenoptera (e.g. ants and wasps), Coleoptera (beetles), Hemiptera (true bugs), Diptera (true flies) and Blattodea (cockroaches). Other arthropods are represented by spiders (Fig. 1c). Most of these taxa belong to forest floor dwellers and flying insects. In contrast, aquatic taxa (e.g. water beetles and aquatic larvae) are present, but comparatively rare.

Modern representatives of some of these insect families or genera are still distributed in northern parts of New Zealand (e.g. the termite *Stolotermes*) while others are now extinct here and restricted to warm-temperate to tropical climates in Australia and/or other Pacific regions (e.g. the formicine ant *Myrmecorhynchus*). Advanced levels of insect-plant interaction in the paleoecosystem at Foulden Maar are evident on many leaves and include various types of feeding damage, mines, galls, and domatia structures as well as borings in wood fragments, and reproductive materials which indicate insect pollination.

Together, the fossils from Foulden Maar provide a unique window into a mid-latitude southern New Zealand terrestrial ecosystem at the Oligocene-Miocene boundary.

Acknowledgements

We thank the Gibson family and Featherston Resources for kindly allowing us access to the site, and the Marsden Fund and the Division of Science, University of Otago, for financial support.

References

- Bannister, J.M., Lee, D.E., Raine, J.I. 2005. Morphology and palaeoenvironmental context of *Fouldenia staminosa*, a fossil flower with associated pollen from the Early Miocene of Otago, New Zealand. *New Zealand Journal of Botany* 43: 515–525.
- Conran, J.G., Bannister, J.M., Lee, D.E. 2009. Earliest orchid macrofossils: Early Miocene *Dendrobium* and *Earina* (Orchidaceae: Epidendroideae) from New Zealand. *American Journal of Botany* 96(2): 466–474.
- Fox, B., Haworth, M., Wilson, G., Lee, D., Wartho, J.-A., Bannister, J., Jones, D., Kaulfuss, U., Lindqvist, J. 2012. Greenhouse gases and deglaciation at the Oligocene/Miocene boundary: palaeoclimate evidence from a New Zealand maar lake. IAS 4IMC Conference, abstract volume.
- Lee, D.E., McDowall, R.M., Lindqvist, J.K. 2007. *Galaxias* fossils from Miocene lake deposits, Otago, New Zealand: the earliest records of the Southern Hemisphere family Galaxiidae (Teleostei). *Journal of the Royal Society of New Zealand* 37(3): 109–130.
- Lindqvist, J.K., Lee, D.E. 2009. High-frequency paleoclimate signals from Foulden Maar, Waipiata Volcanic Field, southern New Zealand: An Early Miocene varved lacustrine diatomite deposit. *Sedimentary Geology* 222: 98–110.

Spatial distribution of monogenetic volcanoes on volcanic islands

Gábor Kereszturi¹, Károly Németh¹, Shane J. Cronin¹ and Mark Bebbington^{1,2}

¹ *Volcanic Risk Solutions, Massey University, Palmerston North, New Zealand – kereszturi_g@yahoo.com*

² *Institute of Fundamental Sciences–Statistics, Massey University, Palmerston North, New Zealand*

Keywords: nearest neighbour statistics, scoria cone, volcanic rift.

The plate tectonic model explains the origin of a large proportion of volcanoes along plate boundaries, but not those within the plates, such as many volcanic islands. The origin of the magma supply beneath these volcanoes can be either related to deep sourced plumes from the core-mantle boundary (DePaolo and Manga, 2003), a consequence of plate motion (Foulger and Natland, 2003) or incipient crustal extension (Cronin and Neall, 2001). Over the largest mantle convection zones or plumes, extensive volcanism commonly forms archetypical volcanic islands such as the Hawaiian or the Canary Island chains (Fig. 1). Intraplate mantle-convection related volcanic islands show a systematic geomorphic evolution from an initial submarine stage through to an island form and following erosion and subsidence final atoll and guyot stages. This evolution generally requires a few million years for the formation of the largest (<10 km high) volcanic edifices on Earth (Clague and Dalrymple, 1989; Walker, 1990). Besides the continuous constructive phases, large-scale dramatic changes such as caldera-forming eruptions or tsunami-forming landslides may also control the morphology and architecture of a volcanic island. The triggering mechanisms and consequences of these processes have been widely described in detail for classical volcanic archipelagos such as the Hawaiian Islands (Clague and Dalrymple 1989, Carracedo, 1999).

Parallel to the evolution of the entire large volcanic system, significantly smaller, but still diverse and long-lasting, monogenetic fields appear on the flanks of the polygenetic volcanoes, or are present before, during and following the growth of a volcano, e.g., Jeju Island in South Korea (Sohn et al., 2008). Monogenetic volcanoes, expressed as maars, tuff rings, scoria and spatter cones, along with lava flows are formed by rapidly ascending, small-volumes of magma. The location of these monogenetic eruption centres may range from the coastal region up to the peaks of volcanic islands. On some islands, they are concentrated along extensional rifts, related to the overall sense of crustal extension in the area or even rather more diffusely spread across the island.

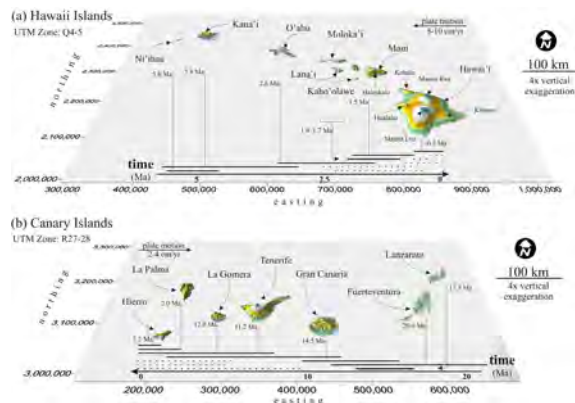


Fig. 1 – Overview map of the two typical volcanic chains, Hawaii Islands (A) and the Canary Islands (B).

Response of volcanic islands to plate motion has also been widely investigated (Clague and Dalrymple, 1989; Walker, 1990), but the link between the development of polygenetic systems producing large-volume eruptions and small-monogenetic volcanoes remains poorly understood. The fact that monogenetic volcanoes within a rift zone erupt frequently, and that the location of the next eruptive centre can only be characterised poorly compared to the well-localized central vent(s) of polygenetic volcanoes, mean that separate hazard models are needed to understand the threat to heavily populated volcanic islands. In this study, point-pattern analysis was carried out in order to understand the evolution, major controls and volcanic hazards represented by monogenetic volcanoes on typical volcanic islands such as Hawaii, Canary and Samoa Islands as well as atypical volcanic islands such as Jeju in South Korea and Taveuni in Fiji (Fig. 2).

Vent locations were digitalized directly from remotely sensed ASTER GDEMs, sourced from METI and NASA. In order to increase the accuracy of these locations, geo-referenced geological-, topographical maps, satellite and orthophotos were used. Every digitalized point defines either the centre of a monogenetic volcano crater, or a centre of a preserved mound built up by pyroclastics. Some limitation may derive from the fact that a vent does not always mean a single magma ascent, i.e. volcanic event, due to vent migration or dispersion of dykes feeding multiple vents. However, the poor

temporal constraints on such volcanic islands make it hard to discriminate vents and multiple vents from each other. A further limitation is that these rift zones do not end at the present coastal line of the island, but continue beneath sea level. Our measurements, however, are based on enough input point to evaluate the spatial distribution within a certain proportion of the volcanic rift zone.

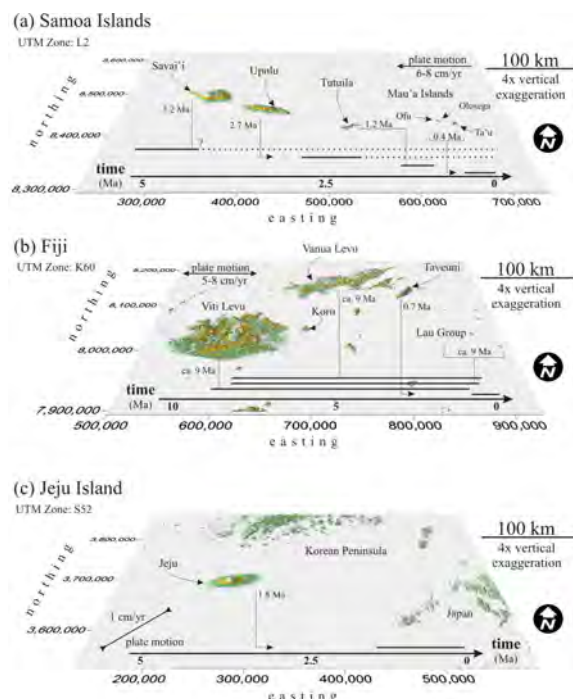


Fig. 2 – Overview map of the three analyzed atypical volcanic islands, Samoa Islands (A), Taveuni in Fiji (B) and Jeju (C).

Nearest neighbour analysis describes the spatial distribution of point-like features such as monogenetic volcanoes or rootless cones. To calculate nearest neighbour statistics for the eight volcanic islands, the sample-size-dependent method was used (Baloga et al., 2007).

The point patterns of monogenetic volcanic vents located on these volcanic islands and volcanoes range from having extremely clustered patterns (e.g. $Z_R = -9.4$ for Mauna Loa) to the ‘true’ random patterns (e.g. $Z_R = 0$ for Gran Canaria). The average spacing between nearest centres (r_a) varies from 554 ± 30 m in Hualalai to $1,431 \pm 171$ m in Oahu, both in Hawaii. Based on the observed distribution characteristics, the patterns of monogenetic volcanism on volcanic island can be subdivided into three groups: (1) strongly clustered, (2) declining clustering, and (3) true random patterns.

In summary, the observed changes in pattern show correlation with the evolution stage and thus the age of the island. Generally, the patterns of volcanism have been characterized by decreasing significance in clustering during the evolution of the volcanic island toward statistically random patterns. In addition monogenetic volcanoes along rift zones in Hawaiian-type volcanic islands appear close to well-defined rift zones on the flanks of the larger polygenetic volcanoes. In contrast, on the Canarian-type volcanic island, monogenetic eruptions are prone to occur relatively far from the geometrical centre of the rifts, resulting in less visible and predictable patterns of volcanism. These changes can be used to inform specific eruption forecasting models for different evolution phases for the often densely populated volcanic islands.

Acknowledgements

This study was supported by the NZ FRST-IIOF Grant “Facing the challenge of Auckland’s Volcanism” (MAUX0808).

References

- Baloga, S.M., Glaze, L.S., Bruno, B.C. 2007. Nearest-neighbor analysis of small features on Mars: applications to tumuli and rootless cones. *Journal of Geophysical Research* 112: E03002 DOI:10.1029/2005JE002652.
- Carracedo, J.C. 1999. Growth, structure, instability and collapse of Canarian volcanoes and comparisons with Hawaiian volcanoes. *Journal of Volcanology and Geothermal Research* 94: 1-19.
- Clague, D.A., Dalrymple, G.B. 1989. The Hawaiian-Emperor volcanic chain. Tectonics, geochronology, and origin of the Hawaiian-Emperor Volcanic Chain. In: Winterer, E.L., Hussong, D.M., Decker, R.W., (eds), *The geology of North America*. Geological Society of America, Boulder, Colorado, pp. 188-217.
- Cronin, S.J., Neall, V.E. 2001. Holocene volcanic geology, volcanic hazard and risk on Taveuni, Fiji. *New Zealand Journal of Geology and Geophysics* 44: 417-437.
- DePaolo, D.J., Manga, M. 2003. Deep origin of hotspots – the mantle plume model. *Science* 300: 920-921.
- Foulger, G.R., Natland, J.H., 2003. Is “hotspot” volcanism a consequence of plate tectonics? *Science* 300: 921-922.
- Sohn, Y.K., Park, K.H., Yoon, S.-H. 2008. Primary versus secondary and subaerial versus submarine hydrovolcanic deposits in the subsurface of Jeju Island, Korea. *Sedimentology* 55(4): 899-924.
- Walker, G.P.L. 1990. Geology and volcanology of the Hawaiian Islands. *Pacific Science* 44(4): 315-347.

Lava flows and related hazards at the Auckland Volcanic Field (New Zealand)

Gábor Kereszturi¹, Jonathan Procter¹, Károly Németh¹, Mark Bebbington^{1,2} Shane J. Cronin¹ and Jan Lindsay³

¹ Volcanic Risk Solutions, Massey University, Palmerston North, New Zealand – kereszturi_g@yahoo.com

² Institute of Fundamental Sciences–Statistics, Massey University, Palmerston North, New Zealand

³ School of Environment, The University of Auckland, Auckland, New Zealand

Keywords: scoria cone, LiDAR DEM, morphometry

The Auckland Volcanic Field (AVF, Fig. 1), New Zealand consists of ca. 50 monogenetic volcanoes such as maars, tuff rings and scoria cones that have erupted over the last 250 ka (Bebbington and Cronin, 2011). The entire field (~360 km²) is located within the area of Auckland City which has a total population of about 1.4 million. The location of the field means that future volcanic event(s) are most likely going to be within the city area or the outskirts of the city giving little chance for the city to prepare. Previous studies have mostly focused on determining the location, nature and the possible effects of the future eruptions on the city. However, detailed measurement of the lava flow hazard and possible pathways of future flows have not been studied despite being considered as a hazardous event posing great risk to people and infrastructure (Magill and Blong, 2005). To spatially classify and better determine this hazard we intend to calculate the average morphometric characteristic of past lava flows in order to determine future lava flow affected areas. We have delineated the possible pathways for future lava flows using GIS-based characterization of the present topography and developed a new hazard-based classification of the city.

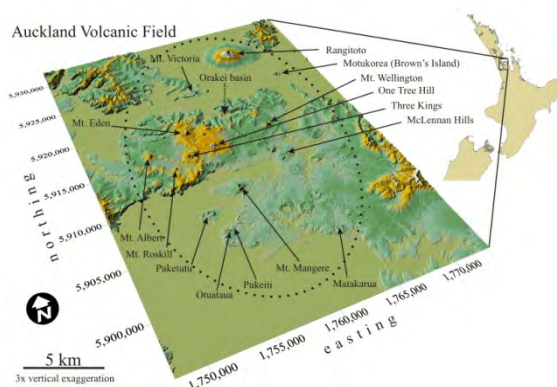


Fig. 1 – Overview map of the Auckland Volcanic Field with the location of measured lava flows.

In the present study, elevation data which have been detected by **Light Detection and Ranging** (LiDAR) in 2008 were used to generate the DEM of

the entire volcanic field. The DEM was interpolated by the **Triangulated Irregular Network** (TIN) method and converted into a grid-based DEM with 2x2 m grid cell size. This DEM was resampled into 10 m and 20 m grid size by a nearest neighbour method and smoothed by a low, average 3x3 (60x60 m) filter. The limits of lava flows were determined on the basis of previously published geological maps (Kermode, 1992), aerial photographs and field observation. The morphometrical parameters include maximum length and thickness (L_{max} and T_{max}) and mean length and thickness (L_{mean} and T_{mean}) of lava flows, as well as area (A_{lava}) and volume (V_{lava}). The volumes were calculated between the present LiDAR DEM and either a surface of equal base heights for those cones that were located on flat areas or interpolated paleo-surface based on drill core descriptions. The other important factor to be determined was the theoretical drainage systems which were extracted from the resampled, 20 m LiDAR DEM by using the **TOpographic PArameterIZatiOn** (TOPAZ) application developed by Garbrecht and Martz (1995). This allowed for the identification of catchments, basins and flow paths.

The derived drainage network and the present topography was classified as (1) depressions (topographic depressions which are most likely to be filled by lava flows), (2) low-lying areas (currently located and characterized by low elevation differences, in other words, they can be buried easily by the average lava flow), (3) ‘buffer’ areas and (4) ridges. To delineate these areas, we used the theoretical drainage system as a basis with the assumption of that future lava flow will follow the topography therefore the drainage system. The constant values used to determine “filling” of areas were the previously calculated average (T_{ave}) and maximum (T_{max}) lava flow thicknesses for AVF with and without lava flow thicknesses from Rangitoto volcano. This leads to two slightly different scenarios (Scenario 1 and 2) in our simulation because there are differences between the maximum and average values of lava flow thicknesses, e.g. average (T_{ave}) lava flow thickness is 14.8 m and 12.7 m with and without Rangitoto volcanoes,

respectively. Those areas that are underlying the level of T_{ave} are defined as Zone 2, i.e. low-lying areas. Using the same technique, but with the T_{max} values (48.2 and 38.7 m) the upper boundary between the ‘buffer’ zone and upper parts like ridges can be delimited. An additional, coastal buffer zone (400 m wide) was added because these areas can commonly be affected by a local-scaled, phreatic explosion due to lava-sea water interactions (Mattox and Mangan 1997).

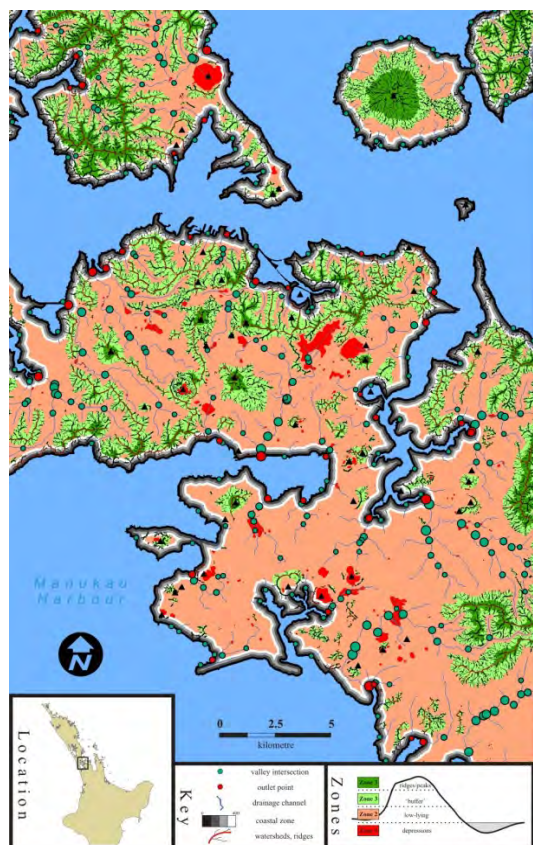


Fig. 2 – Classification of topography against lava flows. Zones: red – depressions, pink – low-lying area, light green – buffer zone, dark green - ridges

The morphometric parameters of fifteen studied lava flows provide the following values: average maximum lengths of 2.5 km; average and maximum thicknesses of 14.7 m and 48.7 m, respectively. The average area occupied by individual lava flows is 5.1 km², while the average volume is 0.12 km³. The largest depressions display shallow depth, with an average of 1.8 m cover over an area of 9 km² (ca. 1.1% of the total area). The volume capacity of these depressions that can be filled by future lava flows is around 0.062 km³. The low-lying zone in the cases of the two scenarios is ~300 km² and ~319 km², respectively. Consequently, an overwhelming proportion of the AVF is classified as area that can

be covered easily by an average AVF lava flow (Fig. 2). The ‘buffer’ zone is located between low-lying and ridge zones. The total area of this zone is around 121 km² and 118 km² for the two scenarios. This area is about 15% of the total study area. The existence of this buffer zone is mostly due to the abundance of sandstone ridges made up by Waitemata Group sediments. The largest differences in area can be found in the case of the most elevated parts, i.e. ridges. The ‘Scenario 1’ predicts 35 km² (ca. 4.4%) area that is located significantly higher than the surrounding topography. In other words, these areas are relatively safe unless a future eruption takes place on these ridges. A slightly lower amount of safe area approximately 19 km² (ca. 2.4%) is associated with ‘Scenario 2’.

To conclude, the AVF comprises two distinct parts (Fig. 2), the relatively flat southern areas and the hilly northern and central area. In the case of future activity, the southern areas have a lack of topographical boundaries that control the spreading of lava flows. In contrast, in the northern part natural topographical boundaries (i.e. watersheds) may act as obstacles for lava flows directing future flows.

Acknowledgements

GK would like to thank to the PhD Research Fellowship offered by the Institute of Natural Resources at Massey University (New Zealand). The authors would like to thank the LiDAR dataset for the Auckland City Council.

References

- Bebbington, M.S., Cronin, S.J. 2011. Spatio-temporal hazard estimation in the Auckland Volcanic Field, New Zealand, with a new event-order model. *Bulletin of Volcanology* 73(1): 55-72.
- Garbrecht, J., Martz, L.W. 1995. TOPAZ: An automated digital landscape analysis tool for topographic evaluation, drainage identification, watershed segmentation and subcatchment parameterisation: TOPAZ User Manual. U.S. Department of Agriculture, El Reno, Oklahoma.
- Kermode, L. 1992. Geology of the Auckland urban area. Scale 1 : 50,000. Institute of Geological and Nuclear Sciences geological maps 2. Institute of Geological and Nuclear Sciences, Lower Hutt, New Zealand, 1-63 pp.
- Magill, C., Blong, R. 2005. Volcanic risk ranking for Auckland, New Zealand. II: Hazard consequences and risk calculation *Bulletin of Volcanology* 67(4): 340-349.
- Mattox, T.N., Mangan, M.T. 1997. Littoral hydrovolcanic explosions: a case study of lava-seawater interaction at Kilauea volcano. *Journal of Volcanology and Geothermal Research* 75(1-2): 1-17.

Holocene explosive eruptions of Ulleung Island, a potentially active volcano and a source of marine tephra in the East Sea

Gi Bom Kim¹ and Young Kwan Sohn²

¹ School of Earth and Environmental Sciences, Seoul National University, Seoul, Republic of Korea – corona@snu.ac.kr

² Department of Earth and Environmental Sciences, Gyeongsang National University, Jinju, Republic of Korea

Keywords: fallout, pyroclastic density current, trachyte, Holocene eruption.

The Ulleung Basin is one of three deep basins of the East Sea that has originated from multi-axial backarc extension since the Early Oligocene. Volcanic activity was vigorous in the basin associated either with continental rifting and backarc opening during the Late Oligocene to Early Miocene or with post-rift magmatism during the Late Middle Miocene involving residual magma sources. Afterwards, volcanic activity of controversial origin occurred in the northern part of the basin, resulting in several seamounts and Pliocene to Quaternary volcanic islands (Fig. 1). Ulleung Island is one of these volcanoes that has been active until the recent geological past. Studies of marine sediment cores from the Ulleung Basin suggest that the volcano was the source of many Late Pleistocene tephra layers and at least one Holocene tephra layer. In order to get a more complete picture of the recent eruptions of Ulleung Island, we measured in detail the characteristics of the trachytic to phonolitic

pumiceous deposits within the Nari Caldera of the island, named the Nari Formation.

We found that the formation can be divided into seven eruptive/depositional units that are bounded by erosion surfaces and locally intercalated with reworked volcanoclastic sediments and paleosol layers. Unit 1 consists of crudely and undulatory-stratified lapilli tuff with lenses of microvesicular pumice fragments. It is interpreted to have formed by a series of pyroclastic density currents possibly together with resedimentation processes. Unit 2 consists of massive to crudely stratified and framework-supported pumice lapilli with scattered lithic blocks. It is interpreted to have formed by rapid fallout of volcanic debris from dense collapsing columns, probably involving downslope transport over short distances. Unit 3 consists of a succession of massive, inverse-to-normally graded, and crudely to thinly stratified lithic-rich lapilli tuffs that are interpreted to have been emplaced by

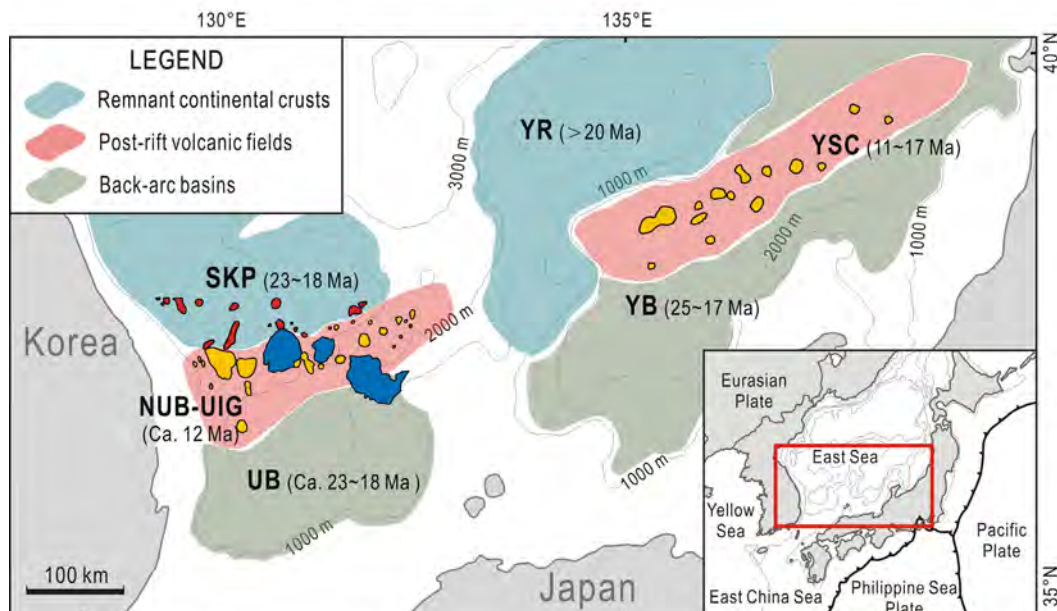


Fig. 1 - Maps showing the types of acoustic basement and spatio-temporal variation of volcanic activities in the southern East Sea. UB: Ulleung Basin, YB: Yamato Basin, SKP: South Korea Plateau, NUB: northern Ulleung Basin, UIG: Ulleung Interplain Gap, YR: Yamato Rise, YSC: Yamato Seamount Chain.

pyroclastic density currents. Unit 4 is a 30-40 cm-thick, medium-to-fine ash layer containing abundant accretionary lapilli, suggesting fallout from a moisture-rich ash plume. Unit 5 consists of plane-parallel to undulatory-bedded pumiceous lapilli tuff with upslope-migrating megaripple bedforms. The unit suggests deposition from dilute pyroclastic density currents that moved upslope on the inner caldera wall. Unit 6 is a succession of plane-parallel-stratified pumice lapilli, which are light gray at the base, orange in the middle, and black at the top. The unit suggests fallout of pumice lapilli from a sustained eruption column that was fed from a stratified magma chamber. Unit 7 is a succession of pumiceous deposits on the floor of the Nari Caldera, consisting of parallel-stratified deposits in the lower part and low-angle inclined-stratified and scour-fill-bedded deposits in the upper part. The unit suggests post-eruptive reworking of the underlying units by surface runoffs and deposition in a caldera lake that was promptly overfilled.

To summarize, six of the units of the Nari Formation comprise primary volcanoclastic deposits that were emplaced mainly by pyroclastic density currents (Units 1, 3, and 5) or fallouts (Units 2, 4 and 6) involving either magmatic (Units 2 and 6) or phreatomagmatic eruptions (Units 1, 3, 4 and 5). ^{14}C age data from published literatures suggest that only the lowest unit 1 is pre-Holocene and the rest resulted from Holocene eruptions. The eruption frequency of the volcano is thus estimated to have been high during the Holocene, and the potential for future eruption and related hazards needs to be reappraised. In the meantime, the tephra layers from Ulleung Island can be used as high-resolution marker horizons within the marine sediment of the East Sea, if the timing of each eruption and the textural/geochemical characteristics of tephra are constrained by future studies.

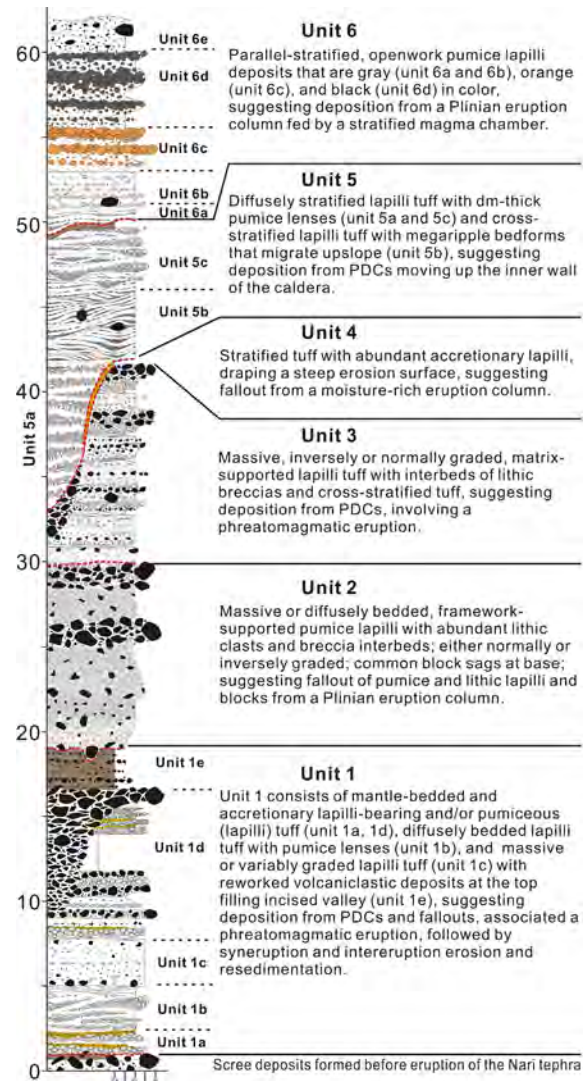


Fig. 2 - Columnar log of the Nari Formation with brief descriptions and interpretations of six eruptive units.

Geomorphology and paleogeography of lava-capped buttes in Tapolca Basin (Hungary) as reflected by 3D elevation models

Szabolcs Kósik¹, Tamás Nagy², Melinda Kaproncai¹, Dávid Karátson¹ and Károly Németh³

¹ Department of Physical Geography, Eötvös Loránd University, 1117, Pázmány Péter strny. 1/C, Budapest, Hungary

² Geographical and Geophysical Research Institute of the Hungarian Academy of Sciences, Sopron, Hungary

³ Volcanic Risk Solutions, Massey University, Palmerston North, New Zealand - k.nemeth@massey.ac.nz

Keywords: basaltic volcanism, lava lake, maar, tuff ring, phreatomagmatism, Pannonian Basin, Hungary,

The Tapolca Basin is located in the western part of the Pannonian Basin, Hungary. It is located in the central part of the Bakony-Balaton Highland Volcanic Field (BBHVF), which is a Late Miocene/Pleistocene alkaline basaltic intraplate monogenetic volcanic field (Szabó et al 1992, Martin et al. 2003).

The volcanic eruptions dominantly started with an explosive phreatomagmatic eruptive phase in the low-lying basin areas filled with water-saturated Late Miocene to Pliocene siliciclastic sediments. Phreatomagmatism is inferred to have been fuelled by explosive interactions between rising mafic magma and various type of ground water either from the uppermost porous media aquifers or from fractured hard rocks in the basement. In elevated areas due to the lack of ground water magmatic gas-driven explosive eruptions and lava effusions produced valley filling lava flows and lava fields such as the Agár-tető and Kab-hegy (Németh and Martin 1999).

We examined four volcanoes (Badacsony, Csobánc, Haláp and Szent György-hegy) located on thick siliciclastic sediment-filled grabens acted as an active fluvio-lacustrine environment. The initial phases of the eruptions of these volcanoes were phreatomagmatic as a consequence of the interaction of rapidly rising hot magma and water-saturated fine-grained siliciclastic sediments. This eruptions formed initial maars surrounded by tephra rims. Subsequently, the decreasing water to magma ratio gradually suppressed the potential kinetic energy release driven from the magma and the water interaction allowing the eruptions to transform to purely magmatic volatile-driven explosions and effusions of lava. The lava ponded between the tephra rims and formed crater-filling lava lakes.

Post-volcanic erosion of the tephra rims of lava filled maars was enhanced by regional uplift, rapidly changing climatic conditions, aeolian and fluvial processes (Németh et al. 2003).

Today, due to their contrasting erodibility, the crater-filling columnar jointed basalts, the primary pyroclastic successions and post-volcanic deposits

bear characteristically different present-day slope angle values (Fig 1.).



Fig. 1 – The lava capped Badacsony Hill as viewed from Lake Balaton (from the SW).

In our study, we used Digital Elevation Model (DEM) and DEM derivatives (e.g., slope maps) to quantify the geomorphology of the casket-shaped buttes. The morphological data source was a 2 m contour-line resolution topographic map, from what an optimally predicted 10x10 m grid was generated. Based on the DEM, we derived slope profiles along 8 main azimuth directions (Fig. 2 and Fig. 3).

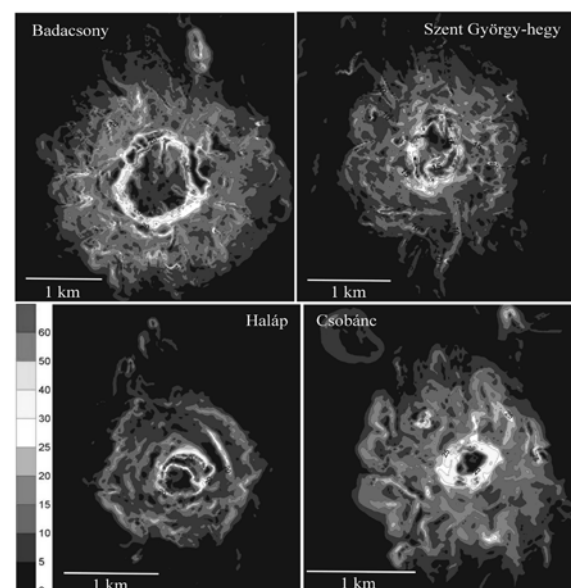


Fig. 2 – Slope maps showing the shape and size of the buttes, helps to define the morphology of the original craters characteristics: after Kaproncai (2010).

We modelled all the collected elevation profiles as a continuous, piecewise linear function with a certain number of breaks, i.e. changes in slope. Our objective was to estimate the number and location of the breaks. Solving this problem requires detecting changes in coefficients, or so-called structural breaks in a linear regression model. We used the methods proposed by Bai and Perron (2003) using the **strucchange** (Zeileis et al. 2002) package of the **R** system for statistical language and the recommended computation of Zeileis et al. (2003) in order to carry out our calculations.

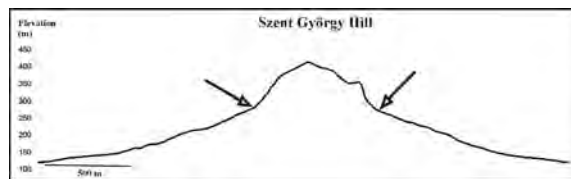


Fig. 3 – E-W oriented slope profile of the Szent György-hegy. Arrows point to characteristics slope breaks that are inferred to indicate the boundary of original crater infill.

Slope profiles were used to identify morphological breakpoints that we assumed to be identical with the position of the contact between the lava and the country rocks and eventually inferred to mark the position of the crater/conduit wall on the eroded landscape (Fig. 3). Using this method we were able to provide a purely morphology-based model to reconstruct the former shape and size of the magmatic infills. Interestingly, our calculated present day slope breakpoint elevations mismatch the present day elevation of the geological contacts between volcanic and pre-volcanic rock units mapped earlier (e.g. Csillag 2003). The deviation between the mapping data and the calculated slope breakpoint elevations is inferred to influence the estimated as well as the estimated volume of material that may have occupied the volcanic craters. Here we provide a new dataset with recalculated crater dimensions and associated magmatic volume estimates. Following this new method, two types of theoretical crater geometry were identified: craters with steep and with low-angle inner walls. It is inferred that the Badacsony and Szent György-hegy

had a steeper crater profile in comparison to the Haláp and Csobánc.

This method provides new view on crater dimension reconstruction of old small monogenetic volcanoes based on pure geomorphological analyses of the preserved landforms. However, it cannot be used as a stand alone tool for generating volcanic architecture reconstructions and the results need to be aligned to and justified with direct geological observations.

References

- Bai, J., Perron, P. 2003. Computation and analysis of multiple structural change models, *Journal of Applied Econometrics*, John Wiley & Sons, Ltd., vol. 18(1): 1-22.
- Csillag, G. 2003. *Földtani természetvédelmi értékelés a Káli-medence példáján*. PhD értekezés, PTE, Földrajzi Intézet, Pécs 139 p
- Kaproncai, M. 2010. *A Tapolcai-medence tanúhegyeinek vizsgálata térinformatikai módszerek segítségével*, Szakdolgozat, ELTE TTK FFI, Természetföldrajzi Tanszék, Budapest.
- Martin, U., Németh, K., Auer, A., Breikreuz, C. 2003. Mio-Pliocene phreatomagmatic volcanism in a fluvio-lacustrine basin in Western Hungary. *Geolines* 15: 75-81.
- Németh, K., Martin, U. 1999. Large hydrovolcanic field in the Pannonian Basin: general characteristics of the Bakony- Balaton Highland Volcanic Field, Hungary. *Acta Vulcanologica* 11: 271-282.
- Németh, K., Martin, U., Csillag, G. 2003. Calculation of erosion rates based on remnants of monogenetic alkaline basaltic volcanoes in the Bakony-Balaton Highland Volcanic Field (Western Hungary) of Mio/Pliocene age. *Geolines* 15: 93-97.
- Szabó, Cs., Harangi, Sz., Csontos, L. 1992. Review of Neogene and Quaternary volcanism of the Carpathian-Pannonian Region. *Tectonophysics* 208: 243-256.
- Zeileis, A., Kleiber, C., Krämer, W., Hornik, K. 2003. Testing and dating of structural changes in practice. *Computational Statistics and Data Analysis* 44(1-2): 109-123.
- Zeileis, A., Leisch, F., Hornik, K., Kleiber, C. 2002. *Strucchange: An R package for testing for structural change in linear regression models*. *Journal of Statistical Software* 7(2).

Tuff cones and maars along the Liquiñe-Ofqui Fault Zone (Southern Andes, Chile): tectonic control of magma-water interactions?

Luis E. Lara

Sernageomin, Avda Sta María N° 0104, Santiago, Chile - lelara@sernageomin.cl

Keywords: phreatomagmatic, Surtseyan, sideromelane.

Quaternary monogenetic volcanism occurred repeatedly along the Liquiñe-Ofqui Fault Zone (LOFZ) in Southern Andes. Holocene and even historical maars and tuff cones are also spatially related to this structural system. Two case-studies located atop of the LOFZ are analyzed in order to understand first-order constrains for magma-water interactions. Riñinahue maar was formed in 1907 AD after two months of phreatomagmatic activity that culminated in a strong Strombolian phase. Carrán maar erupted in 1955 AD after a year of crustal seismicity followed by three months of intermittent explosions. Different magma-water

ratios have been inferred from physical properties of the layers and pyroclastic fragments being higher in Carrán. On the other hand, Riñinahue vent would be fed by a S_{hmax} NE-trending dyke following the regional extension but Carrán maar seems to be rooted in a misoriented fault. Thus, being both similar in water budget, magma composition and eruptive flux, contrasting eruptive behavior could be explained by distinct differential stress regimes. LOFZ exert a control on monogenetic volcanism but also modifies the way of magma-water interactions along the local fault-fracture network.

Eruptive styles of rhyolite volcanoes in the sedimentary basin setting: the case of the Jastrabá Formation in Central Slovakia

Jaroslav Lexa and Katarína Pošteková

Geological Institute of SAS, Dúbravská cesta 9, 840 05 Bratislava, Slovakia – geoljalx@savba.sk

Keywords: phreatomagmatic, Peléean, extrusive.

It is generally recognized that aquifers in the sedimentary basin infill stimulate phreatomagmatic eruption styles of alkali basalt volcanoes in monogenetic volcanic fields. We have observed a similar phenomena in the case of rhyolite volcanoes situated in the Žiar intravolcanic basin of the Miocene Central Slovakia Volcanic Field – their main extrusive phase was preceded by phreatomagmatic explosive activity.

Rhyolites of the Jastrabá Formation represent, along with almost coeval high-alumina basalts, the youngest volcanic products of the mostly andesitic volcanic field (Konečný et al., 1995) associated with the back-arc extension of the Carpathian arc. Rhyolites are associated with a system of N-S to NE-SW trending faults, including marginal faults of the Žiar basin. They extend over a 50 x 20 km area. Only dikes and extrusive dome roots appear in uplifted areas of horst, usually in association with epithermal hydrothermal systems. In less eroded parts of the formation outside of the Žiar basin dykes, extrusive domes and dome-flows associate with sporadic remnants of tuffs and epiclastic breccias. Within the Žiar basin, the formation has thicknesses of up to 300 m, represented by a dome/flow complex with associated pyroclastic and epiclastic volcanic rocks. The complex rests on volcanic/sedimentary fill of the basin showing thicknesses of 2000 – 2500 m (Lexa et al., 1998). The uppermost 600 – 800 m of the fill is represented by lacustrine and fluvial sedimentary rocks including gravel and sand horizons – aquifers that stimulated phreatomagmatic explosive activity of rising rhyolite magma.

Phreatomagmatic tuff/agglomerates and tuffs dominate in the lower part of the formation. They are coarse to fine, composed in highly variable proportion of angular perlite and rhyolite fragments, vesicular glassy rhyolite, pumice, and coarse to fine ash with admixture of andesite/quartzite pebbles and sand grains and siltstones fragments (Fig. 1). Thicker units of unsorted tuff/agglomerates and coarse tuffs alternate with horizons of well stratified and sorted fine tuffs. Very fine dusty tuffs contain often accretionary lapilli (Fig. 1). Textures imply flow, surge and fall type deposits, variably of proximal, medial or distal facies.

Succession of phreatomagmatic tuffs includes horizons of tuffs enriched in pumice, pumice tuffs and rare unwelded pumice flow deposits.

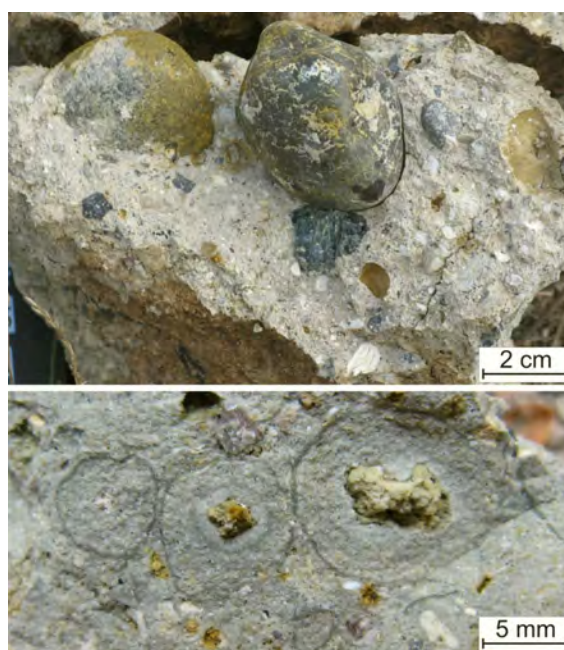


Fig. 1 – Phreatomagmatic tuffs in the lower part of the Jastrabá Fm.: up – unsorted pyroclastic flow tuffs including pebbles and siltstone fragments; down – fine fall tuffs with accretionary lapilli.

Proximal facies pyroclastic surge deposits, identified first by Bezák and Lexa (1982), form remnants of “tuff” rings. Angular fragments and blocks of dense/vesiculated glassy rhyolite (perlite), including chilled phreatomagmatic bombs (Fig. 2), dominate over fragments of felsitic/spherulitic rhyolites and pebbles of andesite and quartzite (Fig. 2). Bedding is quite irregular with thicker beds of unsorted coarser material prevailing over stratified sorted tuff horizons (Fig. 2). Textures imply pyroclastic surge deposits alternating with subordinate pyroclastic flow and fall type deposits. Characteristically there are numerous bomb sags, created also by large pebbles. Above there are well sorted and stratified fall-type tuffs and lapilli tuffs composed dominantly of angular pumiceous glassy rhyolite fragments.

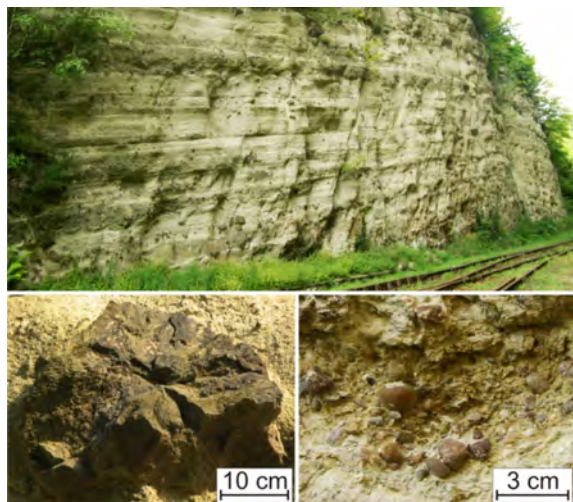


Fig. 2. Rhyolite tuff ring: up – stratified tuffs and agglomerates with abundant bomb sags; down, left – glassy rhyolite phreatomagmatic bomb; down, right – bomb sag filled with lapilli tuff with pebbles.

Extrusive domes show a great variability of forms from upheaved plugs through peleean domes and low lava domes to couleés and lava flows. While massive felsitic or felsospherulitic rhyolite forms their internal parts, closer to margins spherulitic rhyolites show banded texture and vesiculation arranged into the fan-like pattern. At margins, extrusive domes are glassy, passing into perlitic extrusive breccias.

In surroundings of less eroded extrusive domes there are accumulations of coarse, poorly stratified perlitic breccias. Next to these breccias aprons of block-and-ash pyroclastic flow deposits (Fig. 3) and debris flow deposits occur, including horizons of fall-type tuffs with sporadic bomb sags.



Fig. 3 - Block and ash pyroclastic flow deposits covered at the top by stratified co-ignimbrite surge and fall tuffs.

Jastrabá Fm. also includes numerous cryptodomes. They were emplaced into succession of rhyolite tuffs, mostly showing the loaf-like form. Their internal part is formed of massive and/or vesicular felsospherulitic rhyolite. Banded textures and oriented vesicles point to a combination of vertical and onion-like patterns. At margins there are felsitic or perlitic breccias showing textures characteristic of hydraulic fracturing.

Lithology described above allows for recognition of eruption types. Lithology of tuff/agglomerates and tuffs in the lower part of the formation points to high-energy phreatomagmatic eruptions caused by interaction of rising lava with ground water in gravel and sand horizons of the Žiar basin. Increased proportion of pumice and rare pumice tuff horizons higher up imply a transition from the dominant Vulcanian type to the subordinate phreato-plinian or even sub-plinian types of eruptions.

Early phreatomagmatic stage represented by remnants of “tuff” rings has been recognized also in the evolution of several volcanic centers higher up in the succession of the formation. Violent eruptions characterized by prevailing surge deposits and ballistic blocks gave the way, eventually, to the less violent Vulcanian type of eruptions that created overlying fall tuffs as water in the aquifer was exhausted and rising lava moved closer to the surface.

Extrusion of lava and or emplacement of cryptodomes represented a final stage of the eruptive cycle. Variability of forms reflected lava viscosity, volume and rate of extrusion. The fan-like structure of superficial extrusive domes points to their lateral spreading. The onion-like pattern of cryptodomes favors ballooning as major process of their growth.

The growth of superficial extrusive domes was accompanied by gravity driven non-explosive avalanching, including the Merapi type glowing avalanches, giving rise to coarse to blocky perlitic breccia accumulations in their proximal zone. Less frequently there were the Peleean type eruptions giving rise to block and ash pyroclastic flows and the Vulcanian type eruptions giving rise to fall type tuffs interbedded with pyroclastic flow and debris flow deposits in the medial zone. No interaction with ground water took place at this stage.

Acknowledgements

Authors acknowledge support of VEGA grants 2/0171/08 and 2/0162/11 and grant 1506 of the Ministry of Environment SR.

References

- Bezák, V. a Lexa, J., 1982. Genetic types of rhyolite volcanoclastic rocks in surroundings of Žiar nad Hronom. *Geol. práce, Bratislava, Správy* 79: 83-112.
- Konečný, V., Lexa, J., Hojstřičová, V. 1995. The Central Slovakia Neogene volcanic field: a review. In: Downes, H. and Vaselli, O. editors: *Neogene and related magmatism in the Carpatho-Pannonian region. Acta Volcanologica*, 7: 63-78.
- Lexa, J., Halouzka, R., Havrila, M., Hanzel, V., Kubeš, P., Liščák, P., Hojstřičová, V., 1998. Explanatory notes to the geological map of the Kremnické vrchy mountain range (in Slovak with English summary). D. Štúr Institute of Geology, Bratislava: 1-308.

Eckfeld Maar: Window into an Eocene Terrestrial Habitat in Central Europe

Herbert Lutz¹, Uwe Kaulfuss², Torsten Wappler³, Werner Löhnertz⁴, Volker Wilde⁵, Dieter F. Mertz⁶, Jens Mingram⁷, Jens L. Franzen⁸, Herbert Frankenhäuser¹ and Martin Koziol⁹

¹ Mainz Natural History Museum/State Collection for Natural History of Rhineland-Palatinate, Mainz, Germany – Dr.Herbert.Lutz@stadt.mainz.de

² Department of Geology, University of Otago, Dunedin, New Zealand

³ Section Palaeontology, Steinmann Institute, University of Bonn, Bonn, Germany

⁴ Hermann-Josef-Kolleg Steinfeld, Kall-Steinfeld, Germany

⁵ Section Palaeobotany, Senckenberg Research Institute and Natural History Museum, Frankfurt am Main, Germany

⁶ Institute for Geosciences, Johannes Gutenberg University Mainz, Mainz, Germany

⁷ Section Climate Dynamics and Landscape Evolution, Helmholtz Centre Potsdam GFZ German Research Centre for Geosciences, Potsdam, Germany

⁸ Section Messelresearch, Senckenberg Research Institute and Natural History Museum, Frankfurt am Main, Germany, and Naturhistorisches Museum Basel, Switzerland

⁹ Maarmuseum Manderscheid/State Collection for Natural History of Rhineland-Palatinate, Manderscheid, Germany

Keywords: maar lake, Eocene, central Europe.

After 25 years of continuous fieldwork – including detailed geological mapping, geophysics, drillings, and intensive excavation activities – and interdisciplinary research we present a short account of the present state of knowledge on the Eckfeld Maar, the oldest among more than 400 eruption sites in the so-called Tertiary Hoheifel Volcanic Field. In between, more than 250 papers and books have been published, which are dealing with or referring to results of our work. Our poster presents only a few of the more important results concerning e.g. the lithofacies, the local and regional morphological development since Eocene times, or the highly diverse and excellently preserved fossils.

The Eckfeld Maar is a unique completion to other Middle Eocene lagerstaetten which allows another detailed insight into the continental Eocene greenhouse ecosystem in central Europe. The fossil record includes taxa that lived in the meromictic lake as well as those living in the dense forest surrounding the crater. There are biomarkers and lithified bacteria, algae, a great diversity of tracheophytes, numerous arthropods, few molluscs and a wide range of vertebrates.

Biochronologically the biota of the Eckfeld Maar represent the late Geiseltalium of the European Land Mammal Ages (ELMA) which corresponds to the middle part of the Lutetian of the global geochronological time scale. The mammals clearly indicate reference level Mammal Paleogene (MP) 13. The Eckfeld Maar was the first European site yielding fossil mammals which could be dated radiometrically by using ⁴⁰Ar/³⁹Ar thus providing the first calibration mark for the continental Paleogene of Europe. Eckfeld erupted approximately 44 million years ago. On the other hand, Messel is representing MP 11 and meanwhile provided a radiometric age of approximately 47 Million years.

Correlating geochemical and sedimentological information with field data about the vertical distribution of fossils provided insight into the development of the lake over the time period which is represented by 3 m of sediments exposed by the excavation site corresponding with a time span of approximately 6000 years. Numerous individual data suggest that the lake's water level changed considerably over this time span. At times of lower water levels the basin was isolated. In between a higher water level led to connection with the regional drainage system at least by an outlet. These changes most probably reflect changes of the climate, especially with respect to humidity and precipitation. This dynamic model for a rather early stage of the maar lake of Eckfeld also aids in understanding taphonomic processes in meromictic (maar) lakes in general.

At the time of Eckfeld mean ocean bottom temperatures had already decreased by c. 2-3°C compared to the time of Messel (comp. Zachos et al. 2001). Together, both lagerstaetten do not only allow for a calibration of the terrestrial biochronological time scale in Europe. There is also the possibility for deciphering the rate of changes in biodiversity, coevolutionary processes and even whole ecosystems in this part of Europe. Furthermore, Eckfeld proved to be of outstanding importance for the reconstruction of geological and geodynamical processes within the Eifel in general.

References

- Zachos, J., Pagani, M., Sloan, L., Thomas, E., Billups, K. 2001. Trends, Rhythms, and Aberrations in Global Climate 65 Ma to Present. *Science* 292: 686-693.

The following two papers provide comprehensive bibliographies of papers we are here referring to.

Frankenhäuser, H., Franzen, J.L., Kaulfuß, U., Koziol, M., Löhnertz, W., Lutz, H., Mertz, D.F., Mingram, J., Wappler, T., Wilde, V. (2009): Das Eckfelder Maar in der Vulkaneifel – Fenster in einen küstenfernen Lebensraum vor 44 Millionen Jahren. *Mainzer Naturwissenschaftliches Archiv* 47 (Festschrift): 263-324.

Lutz, H., Kaulfuß, U., Wappler, T., Löhnertz, W., Wilde, V., Mertz, D., Mingram, J., Franzen, J., Frankenhäuser, H., Koziol, M. (2010): Eckfeld Maar: Window into an Eocene Terrestrial Habitat in Central Europe. *Acta Geologica Sinica (English Edition)* 84 (4): 984-1009.

A regularly updated complete list of publications since 1987 can be found in the internet under the address <http://www.eckfelder-maar.de>.



Fig. 1: Today the Eckfeld Maar is hardly recognizable owing to intensive erosion during the Rhenish Uplift and the dense forest which is covering large parts of the Eifel. The inset photo gives an idea of how our excavation site looks like.

Rapid magma ascent and short eruption durations in the Lake Natron - Engaruka monogenetic volcanic field (northern Tanzania): Evidence from the Pello Hill scoria cone

Hannes B. Mattsson, **Sonja A. Bosshard** and Jaap F. Berghuijs

Institute of Geochemistry and Petrology, Swiss Federal Institute of Technology (ETH Zürich), Zürich, Switzerland – sonja.bosshard@erdw.ethz.ch

Keywords: scoria cone, ascent rate, eruption duration.

Many volcanic landforms in the Lake Natron - Engaruka monogenetic field (LNE-MVF; northern Tanzania) are characterized by strong depositional asymmetries (Dawson and Powell, 1969; Mattsson and Tripoli, 2011). One of the most prominent asymmetric cones in the area is the Pello Hill scoria cone (Fig. 1). Here we reconstruct the dynamics of this eruption and evaluate the underlying reason for the observed depositional asymmetry.



Fig. 1 – View of the asymmetric Pello Hill scoria cone.

The height of the Pello Hill crater rim varies between 14 and 111 m above the surrounding rift-plain, with maximum deposition towards NE (i.e., 327°). The cone is thus rather small and has a total volume of $16.3 \times 10^6 \text{ m}^3$ (DRE). During fieldwork in 2011 we mapped and sampled deposits from the crater facies as well as in the direction of elongation. Overall the material is highly scoriaceous and dominated by fluidal-shaped pyroclast rich in vesicles. The finer grain-sizes (<0.5 mm) are dominated by cusped-shaped shards and remnants of broken bubble walls, indicating that the fragmentation process in this eruption was driven by exsolution of volatiles (i.e., magmatic fragmentation).

The erupted magma is nephelinitic in composition, similar to many other scoria cones in the area, but with $\text{K}_2\text{O} > \text{Na}_2\text{O}$ (Dawson and Smith, 1988). Pello Hill is famous for its abundance in metasomatized upper-mantle xenoliths (Dawson and Smith, 1988), which constitute up to 30 vol.% in some layers. These mantle xenoliths range in size from 42 cm in diameter down to mm-scale, and

often contain several metasomatic veins that display cross-cutting relations (Fig. 2).



Fig. 2 – Mantle xenoliths (i.e., dunites and wehrlites), cut by metasomatic veins are abundant in the scoria deposits of Pello Hill.

Based on the maximum size of the mantle xenoliths that are embedded in the deposit we can calculate an averaged ascent rate of the Pello Hill magma (following Sparks et al., 2006; assuming a density difference between xenolith and magma of 510 kg m^{-3}). These calculations yield an ascent rate of 0.95 ms^{-1} , which is nearly identical to that previously calculated for kimberlitic magmas (Sparks et al., 2006). It is important to remember that this is the minimum ascent rate required to keep mantle debris entrained in the rising magma during transport to the surface. From geophysical investigations we know that the thickness of the lithosphere in this region is approximately 90 km (Ebinger et al., 1997). Thus, assuming that the xenoliths were picked up at this depth, the Pello Hill magma must have reached the surface within 25 hours from leaving the source.

We can further expand our calculations by assuming that the conduit at the time of eruption had an approximate cross-sectional area of $50\text{-}100 \text{ m}^2$. This value which seems realistic for the Pello Hill eruption as there is no evidence for any long eruptive fissure being present to the sides of the scoria cone.

By combining the minimum average ascent rate, with the assumed conduit areas, we estimate that the magma supply rate must have been in the order of 47.5 to 95 m³s⁻¹. By dividing the total volume of the Pello Hill scoria cone (as DRE) with the eruption rate we can calculate the eruption duration. This exercise yields an eruption duration ranging between 11 and 71 hours. Even a conduit diameter as small as 5 m, would still yield a total eruption duration of less than 6 days. Therefore it is likely that most individual eruptions that carry mantle-xenoliths within the LNE-MVF are short-lived but also rather strong, as indicated by their relatively high magma supply rates.

The reason for the strong depositional asymmetry in many of the landforms within the LNE-MVF has been suggested to be either the result of: (i) cross-winds at the time of eruption, or (ii) an inclined vent (Dawson and Powell, 1969; Mattsson and Tripoli, 2011). However, hitherto no clear evidence for (or against) either of these scenarios has been presented. Theoretically, a scenario involving an inclined vent should deposit both ballistic ejecta and fall-out from a plume to one side of the vent. If the depositional asymmetry is due to cross-winds, on the other hand, only the fall-out from the plume itself is likely to be affected (i.e., the cross-winds are not strong enough to deflect the ballistic ejecta). On closer inspection, there are significant differences in the abundance of mantle xenoliths around the Pello Hill vent. In general, the three lower sides of the crater (14-20-38 m high) contain up to 30 vol.% of mantle xenoliths. This is in sharp contrast to the deposits where maximum accumulation occurred, which only has a few vol. % of mantle xenoliths. We thus conclude that the depositional asymmetry, in the case of Pello Hill, must have been caused by strong cross winds and not an inclined vent (Fig. 3). These plumes must have been dry at the time of eruption (i.e., no moisture present), otherwise smaller particles would adhere to the outer surface of the larger due to a combination of electrostatic and capillary forces. This would make efficient segregation of grain-sizes, as seen in the deposits, impossible.

We conclude that eruptions in the LNE-MVF are probably rapid events, and that magmas may ascend from the source in the upper-mantle to surface in a day. This rapid rise would produce little precursory signals that can be detected for an impending eruption. Moreover, the eruptions are probably of short-duration, which implies that they are highly energetic with sustained eruption plumes that can be deflected by the local wind conditions. Separation of ballistic ejecta and more fine-grained juvenile pyroclasts by strong cross-winds is the reason for the depositional asymmetry at Pello Hill.

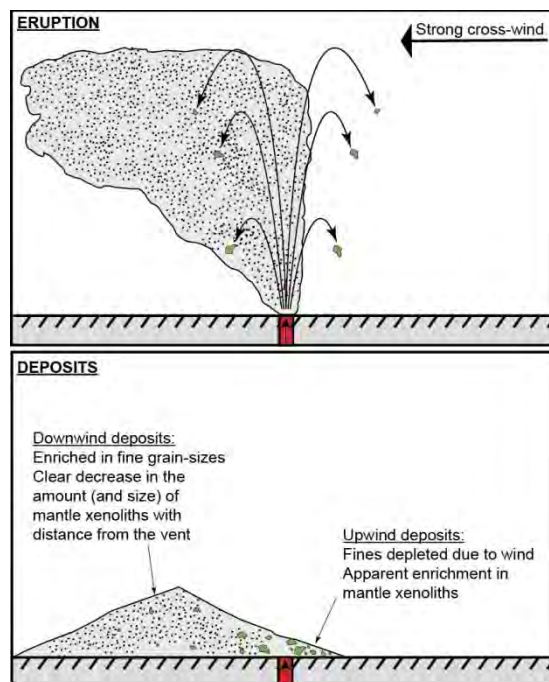


Fig. 3 – Schematic sketch showing the effect of strong cross-winds on an eruption plume and ballistic ejecta, as well as the main characteristics of the resulting deposits.

References

- Dawson, J.B., Powell, D.G. 1969. The Natron–Engaruka explosion crater area, Northern Tanzania. *Bulletin of Volcanology* 33: 761–817.
- Dawson, J.B., Smith, J.V. 1988. Metasomatised and veined upper-mantle xenoliths from Pello Hill, Tanzania: evidence for anomalously-light mantle beneath the Tanzanian sector of the East African Rift. *Contributions to Mineralogy and Petrology* 100: 510-527.
- Ebinger, C., Djomani, P., Mbede, E., Foster, A., Dawson, J.B. 1997. Rifting Archean lithosphere: the Eyasi–Manyara–Natron rifts, East Africa. *Journal of the Geological Society London* 154: 947-960.
- Mattsson, H.B., Tripoli, B.A. 2011. Depositional characteristics and volcanic landforms in the Lake Natron–Engaruka monogenetic field, northern Tanzania. *Journal of Volcanology and Geothermal Research* 203: 23-34.
- Sparks, R.S.J., Baker, L., Brown, R.J., Field, M., Schumacher, J., Stripp, G., Walters, A. 2006. Dynamical constraints on kimberlite volcanism. *Journal of Volcanology and Geothermal Research* 155: 18-48.

On the variety of root zones of monogenetic volcanoes

Károly Németh¹, Jaroslav Lexa², Vlastimil Konečný³, Zoltán Pécskay⁴ and Gábor Kereszturi¹

¹ *Volcanic Risk Solutions, Massey University, Palmerston North, New Zealand – k.nemeth@massey.ac.nz*

² *Geologický ústav SAV, Bratislava, Slovakia*

³ *Státný geologický ústav D. Stura, Mlynska dol. 1, Bratislava, Slovakia*

⁴ *Nuclear Research Centre of the Hungarian Academy of Sciences, Debrecen, Hungary*

Keywords: maar, phreatomagmatic, diatreme, alkali basalt, Hungary, Slovakia.

Older monogenetic volcanic fields that are commonly uplifted and/or have suffered advanced differential erosion can expose deeper zones of the conduits of small-volume volcanoes. One of such less-studied volcanic fields is the Nógrád-Gömör/Novohrad-Gemer Volcanic Field (NGVF) in Slovakia and Hungary (Fig. 1). It is a Late Miocene to Pleistocene (6.5–0.4 My) volcanic field (50 km across) hosting about 50 eroded volcanoes (Konečný et al. 1995; Prakfalvi 2003). The basement of the region consists of Hercynian granites and metamorphic rocks covered by autochthonous and overthrust complexes of Late Paleozoic to Early Cretaceous siliciclastic and carbonate rocks (Konečný et al. 1995). The younger underlying rocks are a succession of semi-consolidated Upper Oligocene to Lower Miocene siliciclastic and volcanoclastic rocks with sands and gravels at the base. Their thickness varies from 600 m at the NW to 1 800 m at the SE. The volcanic field evolved in a fluvio-lacustrine basin, where water-saturated siliciclastic sediments, as well as surface water, were available to interact with sporadically rising magma. There is numerous evidence to support the fact that the majority of the volcanoes went through phreatomagmatic explosive eruption phases, at least in their initial eruption stage (Konečný and Lexa, 2000). Volcanism was coeval with a gradual up-doming of the southern part of the field, creating a northward tilted relief with a relative elevation difference of nearly 300 m (Konečný et al. 1995). As a result, the southern part of the field is less preserved than the northern regions, and the southern volcanoes have deeper levels exposed than their northern counterparts.

Pyroclastic rocks of diatremes preserved in butte-like hills with cliffs show great similarities across the field; however, these features are better preserved and more abundant in the northern part than in the south. In the north, pyroclastic rocks show varieties of massive, matrix-hosted, accidental lithic-rich occurrences of tuff breccia associated with younger scoria-rich facies and sub-horizontal and/or inclined bedded lapilli tuff and tuff successions laid down in maars, commonly cut through sub-vertical irregular shape dykes and adjoining thin sill (e.g. Šurice/Sőreg) (Fig. 2). Less

voluminous pyroclastic buttes (e.g. Hajnáčka/Ajnácskő) are dominated by massive tuff breccia with lithic fragments (Fig. 3A) that host subvertical zones of scoria-rich tuff breccias and late stage thin dykes (Fig. 3B).

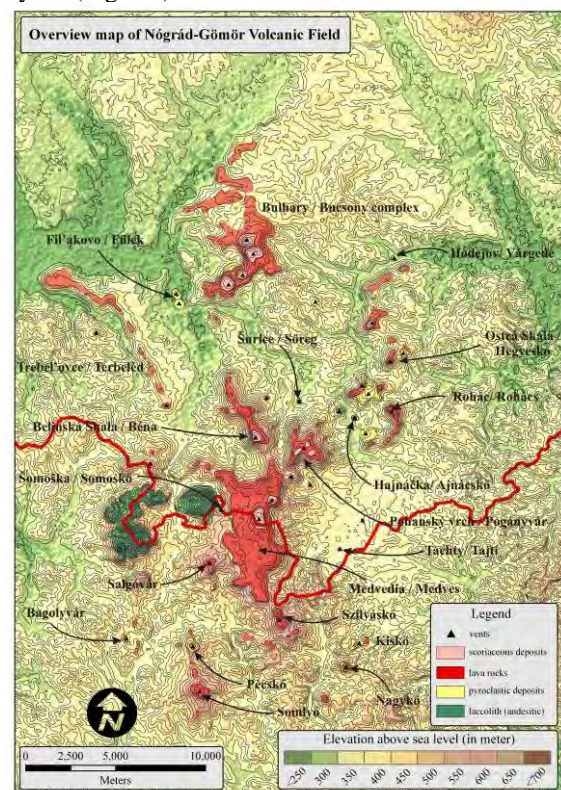


Fig. 1 – Overview of the NGVF.

These pipes are also cut through by irregular shaped chilled dykes that commonly have a peperitic margin with the silt-dominated hosts. Toward the south, the volume of pyroclastic rocks preserved in such buttes decreases and they are commonly restricted to dyke-preserved, relatively well-sorted, moderately stratified veneers of pyroclastic assemblages (Fig. 4). The common feature, however, of each of the studied pipes is that they are rich in silt and mud that is homogenized, and mixed in various ratios to glassy pyroclasts; e.g. Bagolyvár (Fig. 4B) or Boszorkánykő. Further south, along the southward-facing escarpment of the Medves basalt lava plateau (Fig. 1), only thin bodies of pyroclastic

rocks are preserved along irregular shaped dykes such as the Nagy-kő and Kis-kő (Fig. 5).



Fig. 2 – Šurice/Sőreg diatreme. Arrows show dyke.



Fig. 3 – A: overview of the massive, weakly stratified tuff breccia of the Hajnáčka/Ajnácskő diatreme. Large lithics marked in circles; B: subvertical zone of younger scoria-rich tuff breccia (dark) in massive tuff breccia (pale).



Fig. 4 – Dyke and silt matrix-rich lapilli tuff contact at Bagolyvár (Baglyas-kő) (A). Peperitic dyke margin (B) with detached chilled lava floating in silt-rich host. The pyroclastic host is a well-sorted, silt- and mud matrix hosted with lithified sediments (circle) and palagonitized lapilli (C).

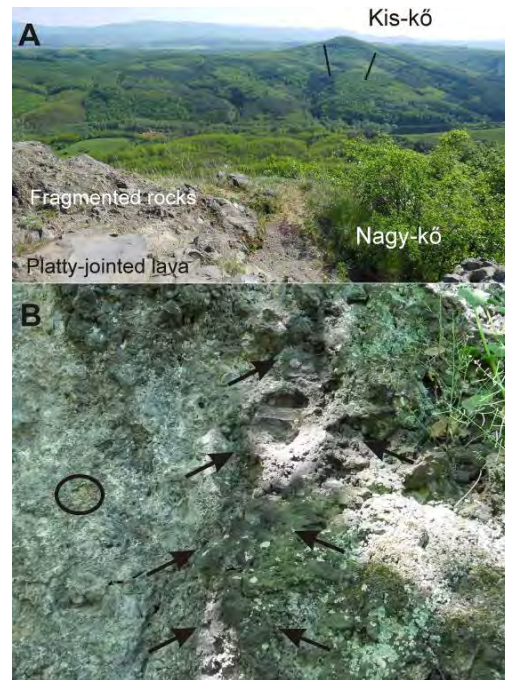


Fig. 5 – Overview of the Kis-kő diatreme looking from Nagy-kő (A). Note the pyroclast veneer preserved around coherent basalt around Nagy-kő (A). The pyroclastic rocks at Kis-kő (B) are coarse mixtures of non-vesicular, glassy lapilli hosted in a silt-rich matrix that contains large irregular shape magmatic lamps (arrows) and sedimentary clasts (circle).

These locations in addition contain a larger volume of juvenile lapilli that exhibit a broad range of vesicularities, as well as levels of palagonitization (Fig. 5B). The variation of preserved pyroclastic facies across the field is inferred to reflect either 1) the differential erosion of the field, (deeper erosion in the south) or 2) the dominance of phreatomagmatism to develop large maar/diatremes in the north against less efficient phreatomagmatic (and diatreme forming) fragmentation style eruptions in the south that produced more transitional to magmatically fragmented eruptive products in the southern part of the field.

References

- Konečný, V., Lexa, J., Balogh, K., Konečný, P. 1995. Alkali basaltic volcanism in Southern Slovakia: volcanic forms and time evolution. *Acta Vulcanologica* 7(2): 167-171.
- Konečný, V., Lexa, J. 2000: Pliocene to Pleistocene alkali basalt diatremes and maars of Southern Slovakia: a common model of their evolution. *Proceedings of the International maar conference, Daun (Germany)*. *Terra Nostra* 2000/6: 220-232.
- Prakfalvi, P. 2003. Észak-magyarországi bazaltok összefoglalása. (Summary on the North Hungarian basalts) – VII. Nemzetközi Alginít Szimpózium 2002. – *Földtani Kutatás* XL. évf. I-II: 25-31.

The Triasscholle near Greiz, E Thuringia - a volcanic based origin?

Tobias Nickschick¹, Horst Kämpf² and Thomas Jahr¹

¹ Friedrich Schiller University, Jena, Germany – tnickschick@gmx.de

² GeoForschungsZentrum, Potsdam, Germany

Keywords: maar-diatreme-volcano, geophysical survey (gravimetry, magnetics), "Triasscholle" near Greiz

The West Bohemia/Vogtland earthquake swarm region in Central Europe is characterized by seismic activity distributed over an area of at least 4.500 km². The occurrence of earthquake swarms is typically related to magmatic activity in volcanoes or rifts. From the area magmatic activity was detected only for the southernmost part of the region Bräuer et al. 2009 (Fig. 1).

The investigation area is located at the northernmost rim where seismic activity in form of earthquake swarm is known so far (Fig. 1). No quaternary volcanic activities or active fluid processes at the surface are known from the area. However, a recent geophysical survey including gravimetry, magnetics, and electromagnetics Matthes et al. 2010 revealed the existence of a diatreme near Ebersbrunn (Fig. 1). It may be indicative of a fossil fluid migration zone.

The paper's aim is to test the potential volcanogenic origin of the so called "Triasscholle" (lit. *Triassic Block*) near Greiz (Fig. 1).

The "Triasscholle" is a unique geological structure enclosed in the surrounding phyllite from the Lower Carboniferous: a stratigraphically non-coherent, steeply inclining breccia mixed with larger blocks from the Muschelkalk, which is only a few hundreds of meters in diameter Puff 1970.

Most of the information available about this structure is derived from 2 drill holes, which were sunk in the 1964 near the SW structure's border area (Fig. 2). The data collected in the past was neither enough to explain the origin of this uncommon structure, nor could it explain all the features found within the drilling cores.

The recent application of geomagnetic and gravimetric surveys offer further insight into the geometry of the structure. Although no noteworthy change in the magnetic total field can be registered, there is a laterally limited but clearly defined gravity anomaly which resembles the ones found in maar-diatreme volcano structures like e. g. the partially

eroded diatreme near Ebersbrunn found less than 20 km away Matthes et al. 2010.

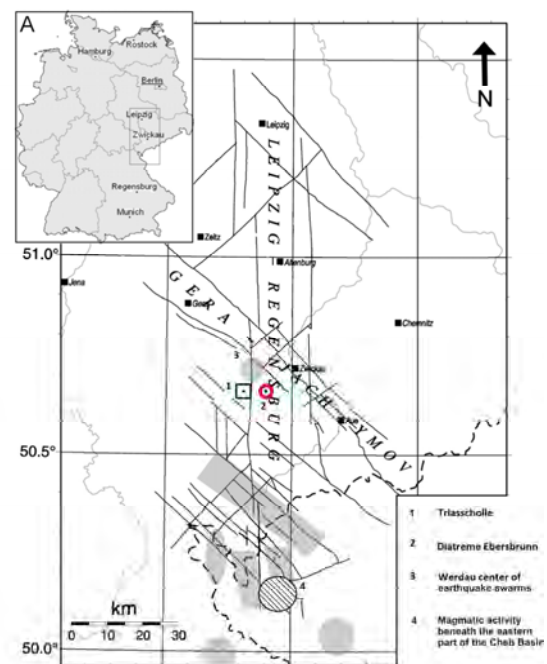


Fig. 1 – Location of the "Triasscholle" (1) in relation to the diatreme near Ebersbrunn (2) and the quake swarm area around Werdau (3). The investigation area is located at the northern rim of the West Bohemia/Vogtland earthquake swarm region (grey shaded: other earthquake swarm regions, dashed: magmatic activity) modified after Korn et al. 2008, Bräuer et al. 2009.

The small distance between these two structures and also the vicinity to the Vogtland region, characterized by recurring quake swarms, indicate a volcanic based or influenced origin of the Triasscholle Korn et al. 2008 (Fig. 1).

A simple model made with the IGMAS+ - software using recently gathered gravity data as well as yet unstudied data from the 1970s suggests a

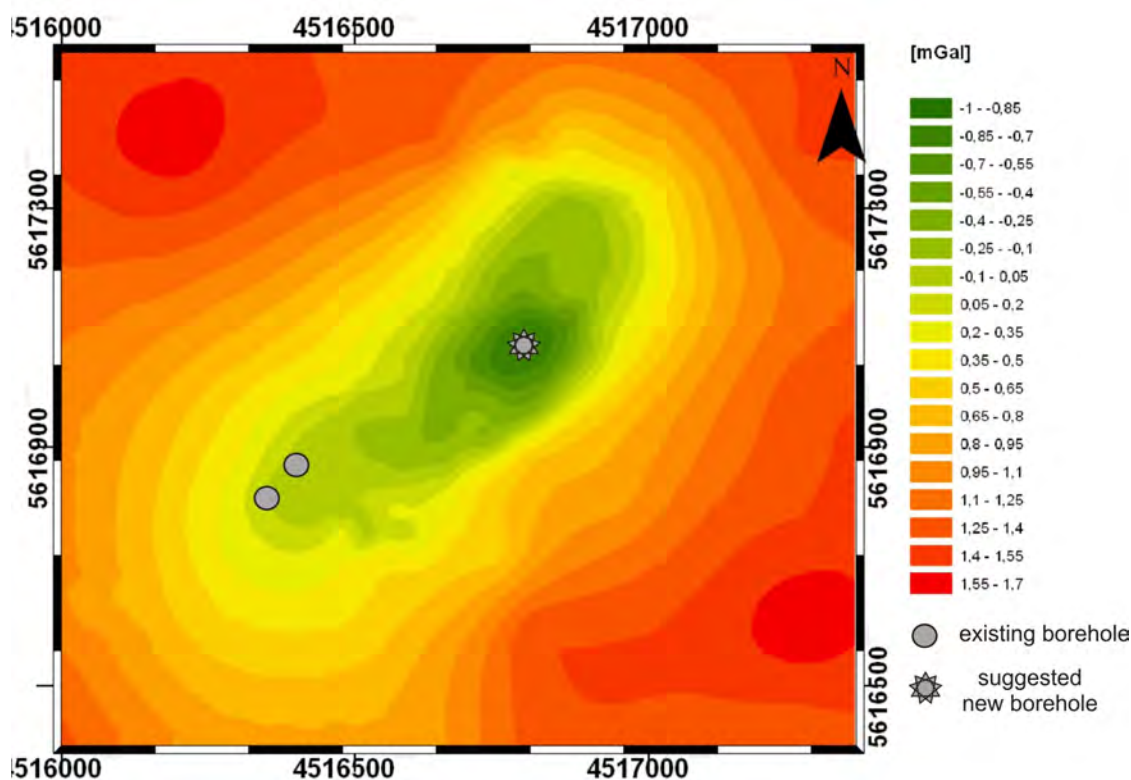


Fig. 2 – Bouguer map of the Triasscholle near Greiz, all values in mGal.

magmatic influence on the formation of the structure.

The model itself is supported by the implementation of geological investigations from the initial drilling as well as petrophysical data gathered from laboratory examinations as boundary conditions.

Although no magmatic components can be found yet in thin sections or geochemical analyses taken from the drilling core due to their distance from the gravitational anomaly, it is not unlikely to find proof for a phreatic, phreatomagmatic or even hydrothermal influence, or a carbonatitic body underneath the surface close to the gravitational low.

The latter one might be probable considering the fact that there is very little variation in the magnetic total field within the structure.

We can exclude most other breccia-generating processes like purely tectonic or impact-based events from other micro- and macroscopic properties. The new gravimetric data show that breccias formed by those processes do not result in such a gravity anomaly of 2mGal ($20\mu\text{m/s}^2$) relative to the surrounding area which is only about 200m in diameter Puff 2005 (Fig 2).

Although the final evidence for a volcanic based origin has yet to be found — considering the facts of a gravimetric minimum, the location of the

formation near an area where N-S- and NE-SW-striking fault zones cross, and the general inner structure — we suggest a series of recurring eruptions in the Upper Cretaceous with little to no ejection of younger magmatic (siliceous) material.

References

- Bräuer, K., Kämpf, H., Strauch, G. 2009. Earthquake swarms in non-volcanic regions: What fluids have to say. *Geophysical Research Letters* 36: L17309, DOI:10.1029/2009GL039615.
- Korn, M., Funke, S., Wendt, S. 2008. Seismicity and seismotectonics of West Saxony, Germany - New Insights from recent seismicity observed with the Saxonian Seismic Network. *Studia Geophysica et Geodaetica* 52: 479-492.
- Matthes, H., Kroner, C., Jahr, T., Kämpf, H. 2010. Geophysical modelling of the Ebersbrunn diatreme, western Saxony, Germany. *Near Surface Geophysics* 8: 311-319.
- Puff, P. 1970. Die Triasscholle bei Greiz - Ein Beitrag zur postvariszischen Entwicklung des Ostthüringischen Schiefergebirges. *Geologie* 19: 1135-1142, Berlin.
- Puff, P. 2005. Die Triasscholle bei Greiz - ein vulkanischer Explosionskrater? *Exkursionsführer: Geologie des Thüringischen Schiefergebirges im Gebiet von Greiz*. Thüringer Geologischer Verein, e.V., Jena, 22-24.

The ~1245 yr BP Asososca maar eruption: the youngest phreatomagmatic event on the western outskirts of Managua, Nicaragua

Natalia Pardo¹, José L. Macías², Denis R. Avellán^{2,3}, Teresa Scolamacchia⁴, Guido Giordano⁵, Paola Cianfarra⁵ and Fabio Bellatreccia⁵

¹ Volcanic Risk Solutions, Massey University, Palmerston North, New Zealand – npardov@gmail.com

² Departamento de Vulcanología, Instituto de Geofísica, Universidad Nacional Autónoma de México, Ciudad Universitaria, Coyoacán, C.P. 04510, México, D.F., Mexico

³ Centro de Investigaciones Geocientíficas (CIGEO), Managua, Nicaragua

⁴ Department of Earth and Environmental Sciences, Ludwig Maximilians Universität 80333 Muenchen, Germany

⁵ Dipartimento di Scienze Geologiche, Università Roma Tre, Largo S. Leonardo Murialdo 1, 00146 Roma, Italy

Keywords: Base surge, phreatomagmatic eruption, pyroclastic density current

The Asososca maar is one of 21 vents aligned in a N-S trend along the Nejapa Fault, located at the western outskirts of Managua, Nicaragua (Fig.1). This 15 km long fault is right-lateral, and has been active since the Pleistocene with the emission of basaltic, basaltic-andesitic and rhyolitic pyroclasts, along with basaltic and andesitic lava flows. The most prominent volcanic structures identified along this fault are from north to south the Chiltepe Volcanic Complex, Asososca, Nejapa, and Ticomo vents. In this study we present a new geological map together with the detailed stratigraphy of Holocene Asososca maar aided by radiocarbon dating of paleosols and major elements whole-rock analyses.

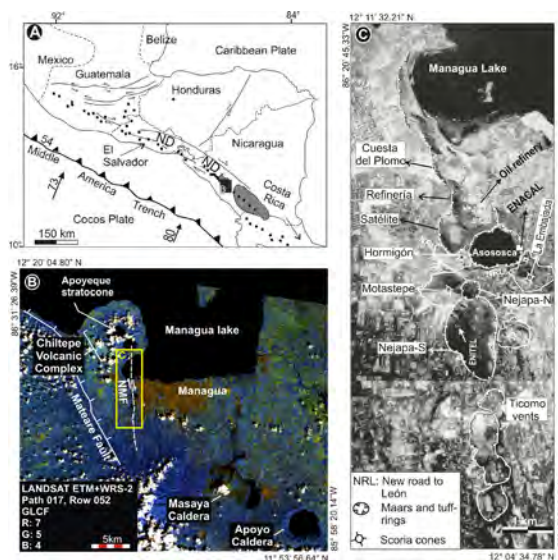


Fig. 1 - Geological framework. A. Regional tectonic regime showing the active subduction of Cocos Plate beneath the Caribbean Plate, resulting in the Middle America Volcanic Arc. In Nicaragua active volcanism is concentrated inside the Nicaragua Depression (ND). The dark gray box indicates the zoomed area shown in B, where the Nejapa-Miraflores fault (NMF) marks a right-step offset in the main arc. Along the fault recent mainly monogenetic volcanoes have been formed westward of Managua city that are shown in C

Asososca (Fig. 2) is a well preserved, East-West elongated crater filled by a lake which is currently used for supplying Managua with drinking water. Its crater is excavated through an older volcanic sequence that includes seventeen units between two paleosols dated at $12,730 \pm 255$ and < 2000 yr BP.

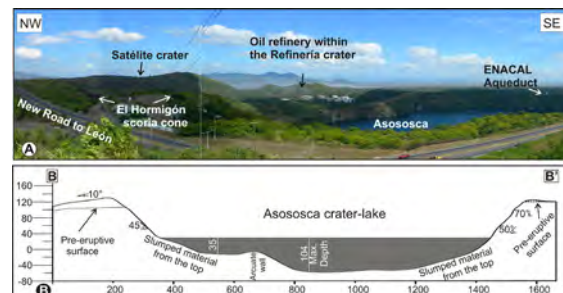


Fig. 2 - A. The Asososca Maar and volcanic structures nearby. The oil refinery of Managua is located inside one of the craters and the ENACAL aqueduct is located on the eastern Asososca crater rim. Scoria cone morphologies (e.g. El Hormigón) are modified by construction and quarrying activities. B. Profile where the morphometric parameters of the Asososca maar can be observed.

Componentry, ash morphology, and FTIR-data were obtained for the youngest eruptive unit found in the area, referred as the Asososca Tephra, which comprises the asymmetrically distributed, well-stratified phreatomagmatic products of the 1245 +125/120 yr BP Asososca maar eruption.

The Asososca Tephra (Fig. 3) dominantly consists of accidental lithics disrupted from the underlying stratigraphic units observed inside and around the maar crater. Dry base-surge bedsets are dominant throughout the eruptive unit, showing facies variation from proximal, cross-stratified beds to mid-distal plane-parallel and wavy-parallel beds. Base surges transported dominantly coarse ash particles at the bedload as traction carpets, while fine ash material in continuous suspension was minimal.

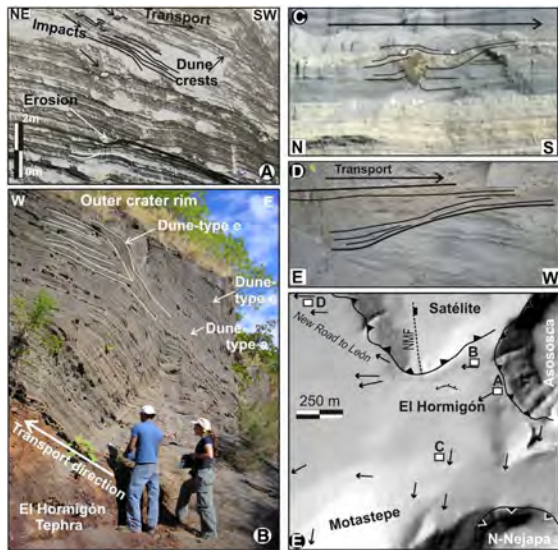


Figure 3. The Asososca Tephra showing dry base-surge facies at proximal distance exposures

Juvenile basaltic glass fragments are subordinate (< 25 vol %), fine-sized (< 2 mm), poorly vesicular clasts. SEM analyses suggest that the Asososca eruption resulted from a highly efficient fuel-coolant interaction between a tholeiitic basaltic melt and an aquifer hosted in a shallow level (between 50 and 200 m) of olivine-bearing scoria ash and lapilli beds. The explosion triggered the country-rock comminution and the production of moss-like, fused-shaped, and blocky ash-shards with stepped surfaces, quenching cracks, pitting, alteration skins, and adhered particles, all indicative of phreatomagmatic fragmentation.

The very recent age of the Asososca maar eruption confirms that the densely inhabited Managua area is volcanically active and that explosive eruptions might occur again along this fault at the western outskirts of Managua, representing a serious hazard to urban infrastructure and a population of ca. 1.3 million inhabitants.

Cyclicity in fluctuating phreatomagmatic and magmatic eruptive styles at the 35 ka Tower Hill Volcanic Complex, southeast Australia

Gemma Prata, Ray Cas and Pat Hayman

MONVOLC, School of Geosciences, Monash University, Vic, Australia – gemma.prata@monash.edu

Keywords: Markov chain, cyclicity, monogenetic.

Fluctuating styles of behaviour, from magmatic styles such as Hawaiian fire fountaining and Strombolian explosions, to intense, pulsatory phreatomagmatic eruptions are common in basaltic monogenetic volcanoes. This can be due to a number of different factors ranging from magma rise rates to inadequate aquifer recharge rate and episodic damage and occlusion of porosity and then recovery. Many phreatomagmatic eruptions appear to “dry-out” due to a decreasing supply of water as time progresses (e.g. Lorenz 1986; Németh et al. 2001), others show the reverse behaviour (e.g. Gutmann 2002) and some fluctuate between wet and dry phases (e.g. Carrasco-Núñez et al. 2007; Ort and Carrasco-Núñez 2009). Tower Hill Volcanic Complex displays many fluctuations in eruption behaviour, from phreatomagmatic maar-forming activity to explosive magmatic cone-building activity. A statistical Markov chain analysis of the most complete section in the maar rim sequence reveals a significant cyclical pattern of eruptive behaviour in the volcanic system. “Drying” cycles, from “wet” phreatomagmatic to “dry” magmatic, occur rapidly compared with “wetting” cycles which occur more gradually, from “dry” magmatic through an intermediate phase (“dry” phreatomagmatic) to “wet” phreatomagmatic. Progressive “drying” coupled with rapid onset of phreatomagmatism becomes dominant later in the eruptive history. The causes of the differing eruptive styles are associated with fluctuating water to magma mass ratios and the cyclicity observed is inferred to be either due to systematic damage and recovery of the aquifer or the result of changing magma rise rates within the

conduit, or both. Major element geochemistry reflects basanite composition and trace element signatures are remarkably similar throughout the sequence suggesting a single magmatic source.

Acknowledgements

The authors would like to acknowledge funds provided through a research grant from the Australian Institute of Geoscientists.

References

- Carrasco-Núñez, G., Ort, M.H., Romero, C. 2007. Evolution and hydrological conditions of a maar volcano (Atexcac crater, Eastern Mexico). *Journal of Volcanology and Geothermal Research* 159(1-3): 179-197.
- Gutmann, J. 2002. Strombolian and effusive activity as precursors to phreatomagmatism: eruptive sequence at maars of the Pinacate volcanic field, Sonora, Mexico. *Journal of Volcanology and Geothermal Research* 113(1-2): 345-356.
- Lorenz, V. 1986. On the growth of maars and diatremes and its relevance to the formation of tuff rings. *Bulletin of Volcanology* 48: 265-274.
- Németh, K., Martin, U., Harangi, S. 2001. Miocene phreatomagmatic volcanism at Tihany (Pannonian Basin, Hungary). *Journal of Volcanology and Geothermal Research* 111: 111-135.
- Ort, M.H., Carrasco-Núñez, G. 2009. Lateral vent migration during phreatomagmatic and magmatic eruptions at Tecuitlapa Maar, east-central Mexico. *Journal of Volcanology and Geothermal Research* 181(1-2): 67-77.

Possible causes for the magnetic anomalies in the volcanoclastic units of the Ebersbrunn diatreme (W Saxony, Germany)

Alina Schmidt¹, Norbert Nowaczyk², Horst Kämpf², Irka Schüller¹, Christina Flechsig¹ and Thomas Jahr³

¹ Universität Leipzig, Institute for Geophysics and Geology, Leipzig, Germany – alina_schmidt@gmx.net

² GFZ German Research Centre for Geosciences, Potsdam, Germany

³ Friedrich Schiller University Jena, Department of Applied Geophysics, Jena, Germany

Keywords: magmatic system, magnetic anomalies, rock magnetic studies

The Ebersbrunn diatreme is located in western Saxony, Germany, only a few kilometers southeast of the Werdau swarm earthquake region, which is the northernmost part of the NW Bohemia/Vogtland swarm earthquake region. Normally this kind of earthquakes is interpreted to be connected with magmatic activity in volcanic areas or rift systems Hill (1977). But no recent volcanic activity is known from this area so far Korn et al. (2008). The seismic activity and the location of the Ebersbrunn diatreme coincide with the intersection of the NS striking Regensburg-Leipzig-Rostock fault zone and the NW-SE striking Gera-Jachymow fault zone (Fig. 1).

The volcanic structure near Ebersbrunn was first detected as a magnetic anomaly in 1962. Closer examination of bore hole material revealed, that the magnetic anomaly is caused by volcanic breccia Jäger (1964) and later it was identified as an eroded relic of a maar diatreme volcano Kroner et al. (2006). This gives us the chance to investigate a deeper section of the diatreme what may reveal insights into processes during the maar diatreme formation.

Previous geophysical investigations detected a gravimetric minimum and a complex magnetic anomaly in the area of the Ebersbrunn diatreme. Recent and ongoing investigations include gravimetric and geoelectric measurements as well as petrographic studies Schüller, personal communication (2011). The new denser geomagnetic mapping (profile distance: 20-25m; point distance along the profiles: ~10m) of the total field intensity helped to concretize the distribution of the magnetic anomalies. Well defined positive and negative anomalies were detected. Their linear, NW-SE orientated arrangement indicates an influence of the Gera-Jachymow fault zone (Fig. 1).

To identify the possible causes for the single magnetic anomalies rock magnetic studies were performed. The sampled material derived from three half-cores of a 1964 drilling campaign. The three bore holes were drilled to one negative magnetic anomaly and two different positive anomalies. The rock magnetic studies were carried out on standard cylinders with 1-inch diameter and 2.2 cm length. In

total, 32 specimens were gained and investigated. Low and high temperature behavior of the magnetic susceptibility and scanning electron microscope investigations were performed on magnetic material, which was separated from crushed matrix material (grain size 63-500µm) with a hand-held magnet.

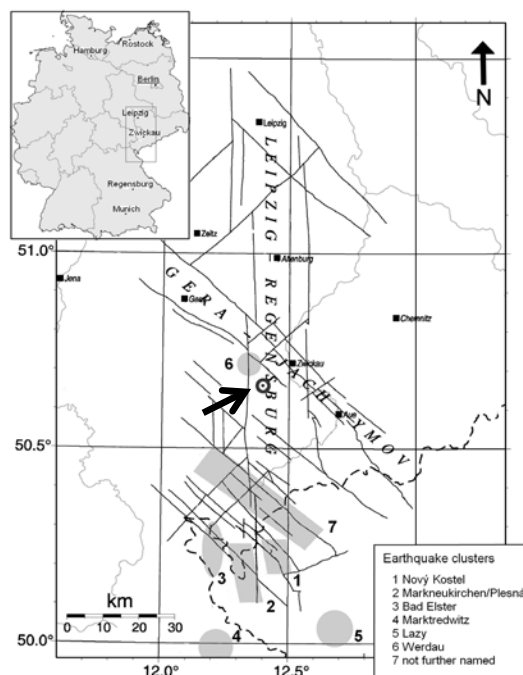


Fig. 1 – Location of the Ebersbrunn diatreme (black arrow) in the NW Bohemia/Vogtland swarm earthquake region. Modified after Korn et al. (2008); Neunhöfer and Hemmann (2005).

The magnetic anomalies can be caused by different magnetic minerals or concentration variations. The latter can be the result of the primary eruption process/conditions. Differences in the magnetic mineral content can be caused by different or more differentiated magma sources. An unequal time of weathering can also cause mineralogical differences Modalek et al. (2009).

Investigations on the magnetic mineral content show, that the magnetic information is carried by relatively coarse titanomagnetites, but with varying

proportions of titanium and slightly different grain sizes in each of the three bore holes. The magnetic minimum is characterized by the highest Ti-content in the titanomagnetites and the smallest grain size. The temperature dependant measurements of the magnetic susceptibility indicate an unequal degree of maghemitisation (= oxidation of magnetite). The material of the two magnetic maxima shows stronger influence of oxidation processes than material from the negative anomaly. This can be a sign of stronger/longer weathering.

Other differences between the magnetic anomalies could be detected in the magnetic fabric. Samples from the magnetic minimum show typical characteristics of sediments/sedimentary rocks. The results of the two positive magnetic anomalies do not have these properties.

Besides the differences in magnetomineralogy, grain size and magnetic fabric, especially between the magnetic minimum and the magnetic maxima, concentration variations of the magnetic material can be expected. Bulk susceptibility of the negative anomaly is about one order smaller than in the magnetic maxima. The remanent magnetizations (NRM, IRM) also indicate different concentrations.

From the rock magnetic point of view, the negative magnetic anomaly is caused by titanium richer titanomagnetites. The mineralogical differences were supported by differences in concentration of the magnetic minerals. But what are the processes that caused these differences? The increasing titanium content from the two magnetic maxima to magnetic minimum can display an increasing differentiation of the magmatic material. This means material derived from the positive anomalies has an older age than the material from the magnetic minimum. The results of the temperature dependant measurements support this time flow. Both positive anomalies show the strongest influence of oxidation. Based on these observations the minimum material seems to be the result of a younger reactivation of the diatreme

structure, probably caused by tectonic activity along the Gera-Jachymow zone. The first results of (U-Th)/He-dating support this interpretation. Material derived from the magnetic minimum has a younger age than material from the two positive magnetic anomalies.

One possible explanation for the magnetic minimum could be a younger intrusion/eruption of a higher differentiated magma. If that is true the smaller grain sizes and lesser juvenile material can be a hint on the water supply during the formation and therefore on the explosivity of the eruption. More explosive, water rich eruptions cause higher fragmentation of the material and therefore smaller grain sizes. Higher water to magma ratio also explains the concentration variations between the investigated anomalies.

Acknowledgements

This research is supported by the German Science Foundation (KA 902/17-1, JA 542/21-1) and the GFZ Potsdam.

References

- Hill, D.P. 1977. A model for earthquake swarms, or. *Geophysical Research* 82: 1347-1352.
- Jäger, W. 1964. *Ergebnisbericht Geologie/Erdmagnetik Ebersbrunn I. Reg.No. 209.* unpublished.
- Korn, M., Funke, S., Wendt, S. 2008. Seismicity and seismotectonics of West Saxony, Germany - New Insights from recent seismicity observed with the Saxonian Seismic Network. *Studia Geophysica et Geodaetica* 52: 479-492.
- Modalek, W., Seifert, G., Weiß, S. 2009. Die besten Funde Europas: Edle Zirkone aus dem Sächsischen Vogtland. *Lapis* 34: 13-54.
- Neunhöfer, H., Hemmann, A. 2005. Earthquake swarms in the Vogtland/ Western Bohemia region: Spatial distribution and magnitude-frequency distribution as an indication of genesis of swarms? *Journal of Geodynamics* 39: 361-385.

Petrographic and thermochronometric investigation of the diatreme breccia of the Ebersbrunn Diatreme – W Saxony, Germany

Irka Schüller¹, Horst Kämpf¹, Alina Schmidt², Christina Flechsig² and Thomas Jahr³

¹ GFZ German Research Centre for Geosciences, Potsdam, Germany – irka-schueller@t-online.de

² Universität Leipzig, Institute for Geophysics and Geology, Leipzig, Germany

³ Friedrich-Schiller-University Jena, Department of Applied Geophysics, Jena, Germany

Keywords: maar-diatreme-volcano, pelletal lapilli, (U-Th)/He thermochronometry.

The Ebersbrunn diatreme is the deep eroded residual part of a former maar-diatreme-volcano. It is located in the southwestern of Zwickau, Germany, Central Europe (location see Fig. 1).

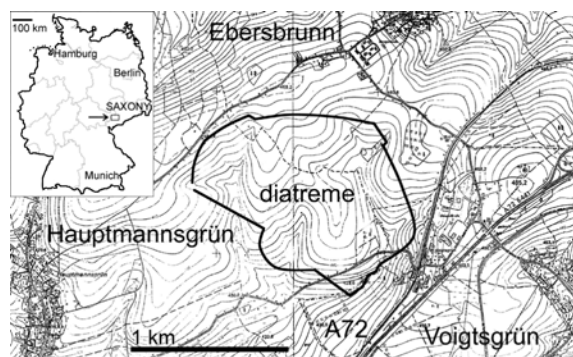


Fig. 1 – Location of the Ebersbrunn diatreme in western Saxony, Germany; see as well Fig. 1 Schmidt (2012).

Until now the age of the structure is unknown, as well as the genetic background. It is assumed that the eruption of the volcanic structure started in cretaceous or tertiary age. The crustal xenoliths included in the diatreme are sedimentary, magmatic or metamorphic Palaeozoic rocks and not clear identified in age so far Jäger (1964). According to tectonic reconstruction of the basement series surrounding the Ebersbrunn diatreme, Berger (2003) assumed that the land surface was around 1.5 to 2.0 km higher at times, when the eruption started.

Kroner et al. (2006) recognized the occurrence of pelletal lapilli inside the diatreme breccia, but did not investigate them in detail. Pelletal Lapilli are said to develop inside the magma before the eruption starts as a juvenile part of the rock melt Lloyd and Stoppa (2003).

One aim of our project was a first investigation of the pelletal lapilli, occurring at the diatreme breccia. Therefore thin sections of the rock were studied with a scanning electron microscope (SEM) at the German Research Centre for Geosciences (GFZ) in Potsdam. Most pelletal lapilli showed a very similar intern structure, illustrated in Fig. 2. The core of a lapillus mostly consists of an aggregate of mica and calcite. These minerals show

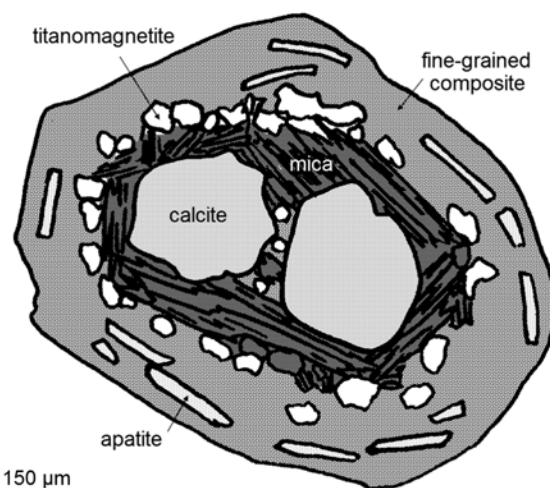


Fig. 2 – Schematic illustration of the intern structure of a pelletal lapillus; average size of these structures = 400 µm.

crystal shapes and are relatively coarse grained. So the calcite crystal sizes were around 100 - 200µm. These aggregates are always bounded by titanomagnetites, which sometimes also occur inside the aggregation, but much smaller than outside. The exterior coat is a very fine-grained composite of carbonates and silicates. Individual crystals are not visible through the SEM. There are always coarse-grained and long-shaped apatites integrated into the outer rim of this composite, which are very good arranged with the sites.

The fact that the minerals in the centre have the lowest melting temperatures indicates that a continuously crystallization of the minerals by decreasing temperature in the magma chamber is not possible. Also the circumstance of coarse-grained calcite and mica crystals in the middle show that the magma was really differentiated at the point of the crystallization, whereas the exterior coat is composed of not visible grains of a mixture of carbonates and silicates, what indicates that there was no differentiation of the magma.

Perhaps the pelletal lapilli point to a mixture of different magmas ahead of the eruption. If a hot and undifferentiated magma starts to soar, it is possible that it meets another magma chamber, which is more

cooled down with a high grade of differentiation. The magmas begin to mix incomplete without a melting of the cooler particles (calcite and mica), but with accretion of the titanomagnetites, apatites and shock-cooled and fine-grained composite of silicates and carbonates.

The real age of this volcanic structure was studied at our project by the (U-Th)/He- thermochronometry, applied at apatite and zircon crystals. All analyses were made at the laboratories of the Scottish Universities Environmental Research Centre in East Kilbride (SUERC). During the atomic decay of uranium and thorium alpha particles (in fact helium atoms) emerge and are trapped inside the crystal lattice. If the crystals are heated about the closure temperature of ~80°C (apatite) and ~120°C (zircon), the helium escapes from the crystals. After cooling down the helium trapping starts again. That means that the investigation of the U-Th/He ratio gives the age of the last heating event of the crystal about the respective closure temperature.

This thermochronometric dating of three apatites gave nearly the same dates with ages of around 105 Ma (upper cretaceous). The results of the two zircon analyses yielded more erratic ages of lower Jurassic and lowest Cretaceous.

The fact that the apatite ages are nearly the same, indicates that they give the real age of the volcano eruption, whereas the zircons (zircon xenocrysts) could be fragments of older volcanism from the lower crust or lithospheric mantle Siebel et al. (2009).

This idea is provided by the fact that the apatite crystals are part of the outer rim of the pelletal lapilli, which are said to represent the juvenile volcanic melt, whereas zircons were never noticed in the context of these aggregates. Probably they go back to the xenoliths, which became intensive shattered during the magma transport and diatreme evolution without a heavy heating about the closure temperature so that the event of the diatreme origin has not affected the zircons.

Acknowledgements

Fin Stuart and Luigia Di Nicola are kindly thanked for giving the chance to realize the apatite and zircon thermochronometry at the Scottish Universities Environmental Research Centre, East Kilbride, Glasgow University (SUERC) as well as all the staff of the GFZ Potsdam who helped for this project. Special Thanks to the German Science Foundation, who supported this research (KA 902/17-1, JA 542/21).

References

- Berger, H.J. 2008. Eruptivbrekzie von Ebersbrunn.- in: Pälchen, W., Walter, H. (ed.). Geologie von Sachsen - Geologischer Bau und Entwicklungsgeschichte, Schweizerbart'sche Verlagsbuchhandlung (Nägele u. Obermiller): 482-483.
- Jäger, W. 1964. Ergebnisbericht Ebersbrunn I, nonpublished report, VEB Geophysik Leipzig, 24 pp.
- Korn, M., Funke, S., Wendt, S. 2008. Seismicity and seismotectonics of West Saxony, Germany - New Insights from recent seismicity observed with the Saxonian Seismic Network. *Studia Geophysica et Geodaetica* 52: 479-492.
- Kroner, C., Jahr, T., Kämpf, H., Geissler, W.H. 2006. Der „Tuffschlot“ bei Ebersbrunn/ Westsachsen, der partiell erodierte Rest eines Maar-Diatrem Vulkans. *Zeitschrift für Geologische Wissenschaften* 34: 143-157.
- Lloyd, F.E., Stoppa, F. 2003. Pelletal Lapilli in Diatremes Some Inspiration from the Old Masters. *Geolines* 15(2): 65-71.
- Schmidt, A., Nowaczyk, N., Kämpf, H., Schüller, I., Flechsig, C., Jahr, T. 2012. Possible causes for the magnetic anomalies in the volcanoclastic units of the Ebersbrunn diatreme (W Saxony, Germany). IAVCEI, CMV/CVS, IAS 4IMC Conference Auckland, New Zealand
- Siebel, W., Schmitt, A.K., Danisik, M., Chen, F., Meier, S., Weiß, S., Eroglu, S. 2009. Prolonged mantle residence of zircon xenocrysts from the western Eger rift. *Nature Geoscience*, DOI: 10.1038/NGEO695.

Geophysical and volcanological investigation into subsurface morphologies of maar and nested maar-scoria cone diatremes of the Newer Volcanics Province, Southeastern Australia

Jackson van den Hove, Ray Cas and Laurent Ailleres

School of Geosciences, Monash University, Clayton, Australia – Jackson.vandenhove@monash.edu

Keywords: diatreme, geophysics, nested maar-scoria cone.

Diatreme morphologies

Maar volcanoes make up a large percentage of volcanic edifices in the southern regions of South-eastern Australia's Newer Volcanics Province (NVP), with 40 known maar eruption points (Joyce 1975). Recent studies of maar and nested maar-scoria cone volcanoes of the NVP suggest a wide variety of diatreme profiles and depths, despite having erupted through similar unconsolidated clastic and carbonate rocks (Blaikie 2009; Prata 2010; van den Hove 2010; Roche 2011; Uehara 2011). Models on how diatreme morphologies develop in relation to their host rocks are suggested in Lorenz (2003) and Auer et al. (2007). They suggest a relationship between consolidation of host rocks and the profile of the diatreme, which does not appear to be conformed to by many Maars of the NVP.

Some maars of the NVP have very large diameter craters, up to 3 km in the case of Lake Purrumbete. Though very large in diameter, current studies on Lake Purrumbete using borehole data and erupted lithics, suggests that fragmentation has only occurred to shallow depths <50 m. This implies that the profile of the diatreme is very low.

Other smaller maar and coalesced maar craters (>800 m in diameter), such as Lake Coragulac of the Red Rock Volcanic Complex and Eklin Maar have been modelled using geophysical anomalies, in conjunction with volcanological techniques. The diatremes of these maars are displayed as having fragmentation occurring to depths of >300 m, and are modelled with steeper sided diatremes, resembling idealised diatremes implied by Lorenz (1975) (Blaikie 2009; Roche 2011).

Mount Noorat Volcanic Complex and Mount Leura Volcanic Complex are both nested maar-scoria cone volcanoes that have also been modelled using geophysical anomalies. In these cases crater diameters are around 1.5 – 2 km and fragmentation depth between 240 – 350 m. Hence diatremes have been modelled with profiles that are average between that of Lake Purrumbete and those of Lake Coragulac and Eklin maar. They match the profile of

soft substrate hosted diatremes suggested by Auer et al. (2007).

Recently, several doctorate and honours projects within Monash Universities School of Geosciences have been applying geophysical and geological techniques to characterise the diatreme subsurface structure of maar and nested maar-scoria cone volcanoes of the NVP. The next section describes the work done on a single nested maar-scoria volcano.

Mount Noorat Volcanic Complex Geophysical and Volcanological Study

The Mount Noorat Volcanic Complex (MNVC) was studied as part of a 2010 honours project, which will be furthered in future research and modelling. MNVC is a monogenetic nested maar-scoria cone volcano located within the Western Plains Sub-province of the NVP, Australia. Graphic logging of deposits exposed within the many quarries surrounding the volcano suggests that MNVC experienced three distinct phases of basaltic explosive eruption style.

The initial eruption involved a subsurface phreatomagmatic eruption forming a maar crater and underlying diatreme structure. This was followed by an abrupt transition to magmatic strombolian eruptions from multiple vents within the maar crater, resulting in the formation of a scoria cone complex that has filled in and covered the maar crater. A final phase of magmatic Hawaiian fire-fountaining produced a thin veneer of welded spatter deposits and clastogenic lava flows that have flowed 5 km to the north and 3 km to the south.

In order to constrain the location of the covered maar rim and identify subsurface structures related to the maar, a detailed local gravity and magnetic geophysical survey was conducted over accessible areas of the volcano. A high resolution LiDAR DEM, made available by the Corangamite Catchment management Authority CCMA, was also applied to analyse the locality of the MNVC's maar rim. The magnetic response shows a low magnetic response halo that defines the locality of the maar

rim, which matches its location as suggested by the DEM. Results from the geophysical survey show a large gravity and magnetic high in the northern central area of the volcanic complex.

2D forward models are constructed along a single magnetic and gravity transects through the north of the complex (Figure 1). The models show three coalesced, low profile diatreme structures, based largely on visual observations and measurements of the maar rim exposed in quarry cuttings. The high gravity and magnetic responses are explained by intrusion/ponding of basaltic feeder material either within the maar crater or at the base of diatreme structures and as a dyke and sill feeder system. A detailed 2D model could not be constructed through the south of the complex, though similar subsurface structures as modelled in the north are assumed to apply.

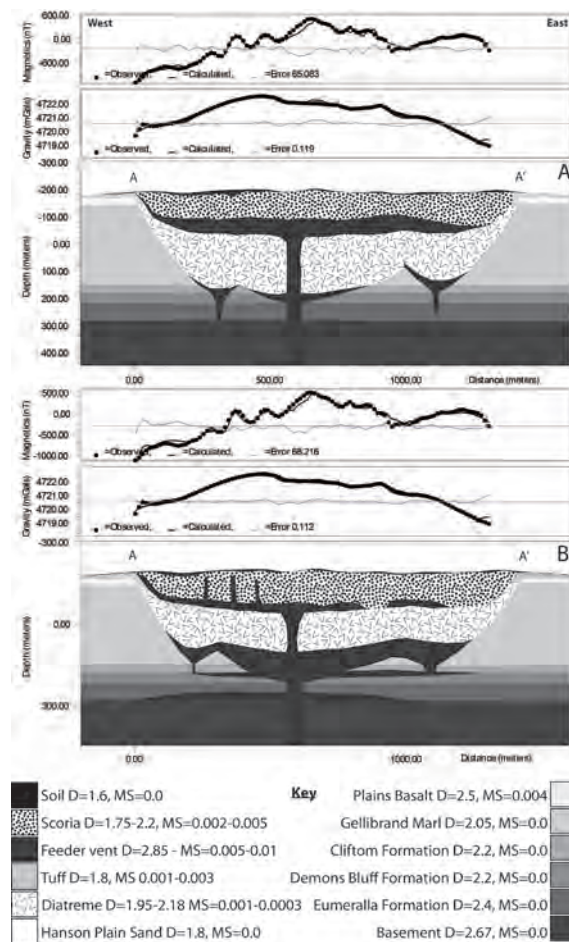


Fig. 1 - 2D forward models across the MNVC, constructed to correspond to east – west magnetic and gravity transects (transect A – A'). Model A displays ponding of rewelded spatter in the crater of the coalesced maars. Model B displays intrusion and inflation of magma along the base of the diatremes.

Acknowledgements

I wish to thank all of my fellow researchers at Monash University for their technical input and support with respect to conducting fieldwork and the use of instruments and programs. Thank you to John Black for access to his property, which makes up Mount Noorat. And thank you to the Corangamite Catchment Management Authority for the free use of their high resolution LiDAR data.

References

- Auer, A., Martin, U., Németh, K. 2007. The Fekete-hegy (Balaton Highland Hungary) "soft-substrate" and "hard-substrate" maar volcanoes in an aligned volcanic complex - Implications for vent geometry, subsurface stratigraphy and the palaeoenvironmental setting. *Journal of Volcanology and Geothermal Research* 159: 225-245.
- Blaikie, T. 2009. Determining the subsurface structure of a maar volcano using gravity and magnetic geophysical methods Lake Coragulac, Red Rock Volcanic Complex. Monash University, Clayton (unpubl.).
- Joyce, E.B. 1975. Quaternary Volcanism and Tectonics in Southeastern Australia. *Bulletin, Royal Society of New Zealand* 13: 169-176.
- Lorenz, V. 1975. Formation of phreatomagmatic maar-diatreme volcanoes and its relevance to kimberlite diatremes. *Physics and Chemistry of The Earth* 9: 17-27.
- Lorenz, V. 2003. Maar-Diatreme Volcanoes, their Formation, and their Setting in Hard-rock or Soft-rock Environments. *Geolines* 15: 72-83.
- Prata, G. 2010. Cyclicity in fluctuating phreatomagmatic and magmatic eruptive styles at Tower Hill Volcanic Complex, southeast Australia. Monash University, Melbourne (unpubl.).
- Roche, L. 2011. Volcanological evolution and subsurface structure of a maar volcano, using gravity and magnetic geophysical methods, Newer Volcanics Complex. Monash University, Melbourne (unpubl.).
- Uehara, D. 2011. Geophysical and Volcanological study on the Mount Leura Volcanic Complex of the Newer Volcanics Province, South Western Victoria. Monash University, Melbourne (unpubl.).
- van den Hove, J. 2010. Eruptive history and subsurface structure of a nested maar-scoria cone volcano, Mount Noorat Volcanic Complex, Newer Volcanics Province. Monash University, Melbourne (unpubl.).

Unraveling the eruption dynamics of the complex volcanology at the 5 ka Mt. Gambier Volcanic Complex, south-eastern Australia

Jozua van Otterloo, Ray Cas and Massimo Raveggi

MONVOLC, School of Geosciences, Monash University, Clayton, VIC 3800, Australia – jozua.vanotterloo@monash.edu

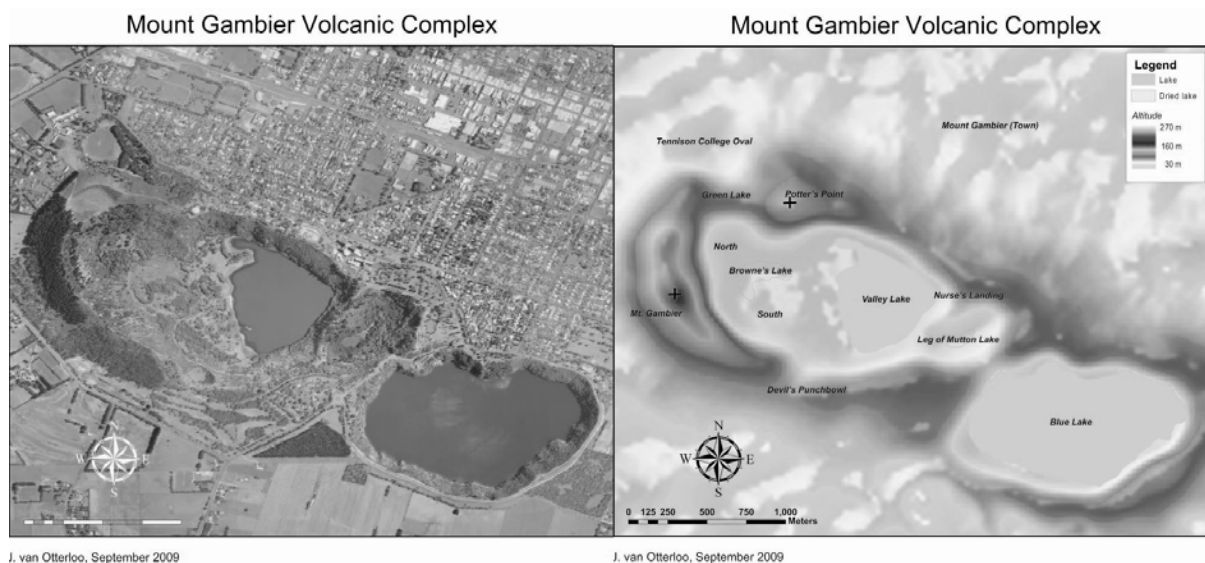
Keywords: alternating eruption styles, maars and cone complex

The monogenetic Mount Gambier Volcanic Complex (MGVC, 5 ka) is located in the western part of the intraplate basaltic Newer Volcanics Province of south-eastern Australia (4.6 Ma-Recent). This volcanic complex overlies thick carbonate and siliciclastic deposits of the Otway Basin, which was formed during the break-up between Australia and Antarctica 90 Ma. The MGVC has a complex structure of multiple craters of maars and cones, which are aligned WNW-ESE, parallel to the major Tartarup Fault System. In this presentation the different complexities are described as well as the potential factors controlling the eruption dynamics.

The stratigraphy of the MGVC shows alternating deposits of multiple alternating phreatomagmatic and magmatic eruption styles. Multiple eruption points (>12) have been identified using detailed mapping and sedimentary and stratigraphic relationships. The eruption points appear to have been active in a random manner (i.e. no migration of eruption points from one side to the other of the complex) and over a very brief period of time (i.e. days to months, possibly years).

The different magmatic facies found are massive coherent basalt associated with effusive activity, spatter and fluidal shaped bombs from Hawaiian-style fire-fountaining, and scoria with coarse ash from Strombolian activity. Phreatomagmatic facies are cross-bedded ash-rich deposits of base surges and massive block, ash and lapilli deposits interpreted as pyroclastic flow deposits. Transitional magmatic-phreatomagmatic facies occur as bedded scoriaceous tuff; these have been classified as violent Strombolian.

In addition to its structural and depositional complexity, Mount Gambier is also marked by its compositional complexity. The volcanic complex can be divided in two sectors, east and west, which are related to two different petrological suites: trachybasalt (east) and basanite (west). These magmatic suites correspond to separate magma batches coming from different depths, i.e. the western basanites originate from a depth of ~90 km with a temperature of 1200°C, whereas the eastern trachybasalts were sourced shallower at a depth of ~60 km at a temperature of 1100°C. In order to melt, the sources in both cases must have been hydrated



J. van Otterloo, September 2009

J. van Otterloo, September 2009

Fig. 1 – Aerial photograph (courtesy South Australian Government) and the digital elevation model of the Mount Gambier Volcanic Complex showing the aligned craters and cones.

for at least ~0.05 wt. %.

These two magmatic suites then rose rapidly to the surface, as evidenced from the presence of mantle xenoliths and the modeled olivine fractionation. Based on detailed stratigraphic analysis it has been made clear that the two magma batches erupted simultaneously.

However, different in composition, both magma batches produced similar depositional facies. Hence composition can be disregarded as a factor controlling the alternations in eruption styles and the associated deposits.

Other parameters which could have acted as factors controlling the complex eruption dynamics of alternating phreatomagmatic and magmatic eruption styles are either internal (magmatic) or external (hydrological). Magmatic variables are composition, crystallinity, temperature and storage pressure, but also density and viscosity. External parameters should be found in the aquifer properties and dynamics, i.e. porosity, permeability, flow and recharge rate. Another important factor is the area of hydromagmatic reactions like magmatic fuel-coolant interaction (MFCI) and quenching.

Using electron-microprobe analysis (EMPA) the composition of the groundmass glass and phenocryst phases can be analyzed and used for different geothermometers. These thermometers give a pre-eruptive temperature of 1100°C +/- 50 for all the facies of Mt. Gambier produced by explosive eruption styles. No significant temperature variation is observable between the different pyroclastic facies.

Image analyses on back-scattered SEM images of pyroclasts provide information about crystallinity and vesicularity. The modes of the different phenocryst phases appear to be similar in all the facies; however, the phreatomagmatic clasts are more micro-crystalline, though glassy

phreatomagmatic clasts do exist as well. This micro-crystallinity could relate to decreasing ascent rates and increasing viscosity, but also to cooling due to quenching. The magmatic clasts appear to be more vesicular based on volume density, however number densities of the different facies appear to be similar.

Pre- and post-eruptive volatile contents were analyzed using EMPA (F, Cl and S) and Fourier Transform IR spectroscopy (FTIR; H₂O and CO₂). The data from analyzed groundmass and olivine-hosted melt inclusions were compared. No major difference in halogens was detected between the different facies indicating similar viscosities and degassing patterns, also detectable amounts of CO₂ and S in the groundmass indicates an overall rapid magma ascent rate.

Conclusively the magmatic variables indicate largely that no variation exists between the different pyroclastic facies, hence the eruption dynamics are only dependent on the external variables.

Two main aquifers underlie the Mount Gambier Volcanic Complex: the confined Tertiary Sandstone Aquifer and the unconfined Tertiary Limestone Aquifer. Accessory lithics of both units hosting the aquifers are present in the pyroclastic facies, indicating both aquifers interacted with the rising magmas to produce the phreatomagmatic eruption styles and associated facies.

In the stratigraphy, evidence exists of trends showing deepening of the eruption focus. This evidence is found in the ratio limestone:sandstone lithics in the pyroclastic deposits from the same eruption point. This deepening could be related to depletion of the aquifers during continuous eruption as well as depressurizing of the system due to excavation. Numerical modeling can provide insight in how the aquifers were recharged. Input to these models is the measured magmatic and hydrological variables.